Optimization of RNA cancer vaccines using 3' UTR sequences selected for stabilization of RNA

Dissertation zur Erlangung des Grades
Doktor der Naturwissenschaften
im Promotionsfach Biologie

am Fachbereich Biologie der Johannes Gutenberg-Universität in Mainz

von

Alexandra Gabriela Orlandini von Niessen
geb. in Barcelona, den 20. Dezember 1979,

Mainz, September 5, 2016

Die vorliegende Arbeit wurde in der Zeit vom 01. Oktober 2009 bis 17. November 2016 an der Johannes Gutenberg-Universität Mainz unter der Anleitung von [redacted] durchgeführt.

Dekan:
1. Gutachter:
2. Gutachter:

Tag der mündlichen Prüfung:
17. November 2016

... für meinen Mann Jan und unsere Söhne Jonah und Felix.

Phantasie ist wichtiger als Wissen, denn Wissen ist begrenzt.

Albert Einstein

1 Abstract

In the last decades, *in vitro*-transcribed (IVT-)messenger (m)RNAs encoding tumor-specific antigens have emerged as a powerful new tool to deliver genetic information into human immature dendritic cells (hiDCs) to induce a specific antitumor T cell response for therapeutic cancer vaccination. However, the short half-life of mRNA is still a major challenge. This makes the pharmacologically effective dosing of IVT-mRNA difficult, resulting in a time-restricted protein expression and, thus, a limited immune response. The stability of mRNAs is mainly regulated by the 3' untranslated region (3' UTR) as exemplified by the well-characterized β-globin 3' UTR that is responsible for the high stability of globin mRNA in erythrocytes. Stability is controlled by binding of regulatory factors to respective sequence elements in the 3' UTR. While the β-globin 3' UTR also stabilizes synthetic mRNAs to some degree in other cell types, such as hiDCs, the expression of the specific regulatory factors for RNA-stability is cell-type specific. Therefore, the identification of hiDC-specific stabilizing RNA-sequence elements could further improve intracellular pharmacokinetics of mRNA cancer therapeutics.

In this work, a novel *in vitro* selection process within hiDCs was developed to find naturally occurring RNA sequence elements, which stabilize the mRNA when used as 3' UTR in preclinical and clinical studies. Instead of using a chemically synthesized library for the selection process, a self-made RNA-library was built with hiDC-specific RNA sequences cloned as 3' UTR downstream of a suitable reporter gene. Additionally, hiDCs were used as a selective environment. This ensured the selection of cell-type specific RNA sequences as the cell's inner regulatory factors [RNA-binding proteins (RBPs) and microRNAs (miRNAs)] and degradation machineries would determine the survival of the transfected RNAs. The stringency of the selection was increased with each selection round by extending the time frame, in which the transfected RNA-pool was left in the cells before purification, amplification and preparation for the next selection round. The selected 3' UTR-sequences were analyzed and characterized afterwards. New single RNA-elements were identified and analyzed individually as single 3' UTR or in combination as double 3' UTR regarding their stabilizing effect on mRNA. Differences in the stabilizing effect of the analyzed 3' UTRs were rationalized *in silico* regarding binding of RBPs and miRNAs. Results revealed less binding of miRNAs, particularly in two combinations, which also proved to be superior compared to 2hBg, the in-house *gold standard* consisting of two copies of the human β-globin 3' UTR. These combinations enhanced not only stability, but also translational efficiency of the synthetic mRNA in hiDCs yielding more protein over time. With these new potent 3' UTRs, RNA cancer immunotherapy can be further improved regarding antitumor efficacy due to a prolonged lifespan of the synthetic mRNA and an increased protein amount, thus, ultimately providing better patient care. Moreover, with this generally applicable method, cell-type specific 3' UTRs can be selected for other therapeutic fields like stem cell research or protein-replacement therapies to ensure optimal pharmacokinetics of synthetic mRNAs.

2 Kurzfassung

In den vergangenen Jahrzehnten entwickelten sich *in vitro* transkribierte (IVT)-Boten-RNAs (englisch *messenger RNA*, mRNA) zu einem neuen, wirkungsvollen Mittel tumorspezifische Antigene in humane immature dendritische Zellen (hiDCs) zu übertragen, um eine effektive und zielgerichtete Immunantwort gegen Krebs auszulösen. Jedoch bleibt hierbei die kurze Halbwertszeit der RNA weiterhin eine große Herausforderung. Die daraus resultierende zeitlich begrenzte Expression des kodierten Tumorantigens und die damit einhergehende limitierte Immunantwort, erschwert dabei eine effektive pharmakologische Dosierung von mRNA-basierten Tumorvakzinen. Die Stabilität einer mRNA wird hauptsächlich von dem 3' untranslatierten Bereich (englisch *untranslated region*, 3' UTR) beeinflusst. Dieses wird z.B. mit dem sehr gut charakterisierten β-Globin 3' UTR veranschaulicht, welches den Globin-mRNAs in den Erythrozyten eine hohe Stabilität verleiht. Die Stabilität wird dabei durch die Bindung von regulatorischen Faktoren an spezifischen Elementen in dem 3' UTR geregelt. Während das β-Globin 3' UTR auch synthetische mRNA in anderen Zelltypen wie z.B. hiDCs stabilisiert, ist die Expression der RNA-stabilisierenden Faktoren zellspezifisch. Folglich könnte die Identifizierung von hiDC-spezifischen stabilisierenden Sequenzen die intrazelluläre Pharmakokinetik von mRNA-Krebstherapeutika deutlich verbessern.
In dieser Arbeit wurde ein neuartiger Selektionsprozess innerhalb von hiDCs entwickelt und durchgeführt, um eben solche natürlich vorkommende RNA-Sequenzen zu finden, die - als 3' UTR angewandt - die für (prä)klinische Studien eingesetzte mRNA mehr stabilisieren als bisher. Anstatt eine chemisch synthetisierte Bibliothek für den Selektionsprozess zu verwenden, wurde die RNA-Bibliothek mit hiDC-spezifischen RNA-Sequenzen selbst hergestellt. Dabei wurden diese Sequenzen als 3' UTR in einen geeigneten Vektor kloniert. Der eigentliche Selektionsprozess fand zudem in hiDCs statt. Das sollte die Selektion zell-spezifischer RNA-Sequenzen sicherstellen, da die inneren regulatorischen Faktoren [RNA-binde Proteine (RBPs) und microRNAs (miRNAs)] und Degradationsproteine der Zelle das Überleben der transfizierten mRNA bestimmen würden. Die Stringenz der Selektion wurde mit jeder Selektionsrunde verstärkt, in dem die Zeitspanne zwischen der Transfektion des RNA-Pools in die Zellen und dem Aufreinigen, Vervielfältigen und Vorbereiten für die nächste Selektionsrunde verlängert wurde. Nach dem Selektionsprozess wurden die erhaltenen 3' UTR-Sequenzen untersucht und charakterisiert. Es konnten neue Sequenzen identifiziert werden, welche einzeln als einfaches 3' UTR oder in Kombination als doppeltes 3' UTR weiter untersucht wurden bezüglich ihrer stabilisierenden Eigenschaften auf die mRNA. Die ermittelten stabilisierenden Effekte der 3' UTRs wurden näher mittels bioinformatischer Analysen bezüglich der Bindung von RBPs und/ oder miRNAs rationalisiert. Die Ergebnisse zeigten eine geringere Anzahl an bindenden miRNAs, insbesondere bei den zwei 3' UTR-Kombinationen, die dem 2hBg-3' UTR überlegen waren. Diese zwei Kombinationen verbesserten nicht nur die Stabilität, sondern auch die Translationseffizienz der synthetischen mRNA in den hiDCs, was in Summe zu einer erhöhten Gesamtproteinmenge führte. Mit dieser neuen, wirkungsvolleren 3' UTR, sollte die RNA-Krebsimmuntherapie aufgrund einer verlängerten mRNA-Lebenszeit bzw. einer erhöhten -Proteinmenge, und damit einhergehend, letzten Endes das Patientenwohl, deutlich verbessert werden können. Darüber hinaus können mit der entwickelten allgemein anwendbaren Methode zellspezifische 3' UTRs für andere therapeutische Zwecke wie z.B. für die Stammzelltherapie oder Protein-Ersatz-Therapie selektiert werden, um auch für diese Anwendungen die optimale Pharmakokinetik der eingesetzten synthetischen mRNA sicherzustellen.

Contents

Abbreviations

α-CP	α-globin poly(C)-binding protein
β-S-ARCA	phosphorothioate-modified cap
βMe	β-mercaptoethanol
7-AAD	7-Aminoactinomycin D
RT-qPCR	quantitative real-time PCR
pbs	primer binding site
ddH_2O	double-distilled water
A2BP1	RNA Binding Protein, Fox-1 Homolog (C. Elegans) 1
ActD	Actinomycin D
AES	Amino-terminal enhancer of split
APC	antigen-presenting cell
ARCA	antireverse cap
ARE	AU-rich element
AUF1	AU-rich binding factor-1
BLAST	Basic Local Alignment Search Tool
BPKM	bases per kilobase of gene model per million mapped bases
C2C12	mouse myoblasts
CAF1	CCR4-associated factor
CCDC124	Coiled-coil domain containing 124
CCL22	Chemokine (C-C motif) ligand 22
CCL3	Chemokine (C-C motif) ligand 3
CCR4	carbon catabolite repression 4
CD	Cluster of differentiation
CD40L	CD40 ligand
cDNA	complementary DNA
CDS	coding DNA sequence
CEA	carcinoembryonic antigen
CIP	Calf Intestinal Alkaline Phosphatase
CPE	cytoplasmic polyadenylation element
CPEB	CPE binding protein
CTL	cytotoxic T cell
DAMP	damage-associated molecular pattern
DC	dendritic cell
DC-LAMP	DC-lysosome-associated membrane protein 1
DMSO	dimethyl sulfoxide
DNA	deoxyribonucleic acid
DNAJC4	DnaJ (Hsp40) homolog, subfamily C, member 4
dNTP	deoxynucleotide triphosphate
dsRNA	double stranded RNA
EDTA	ethylenediaminetetraacetic acid
eEF1A1	elongation factor 1 α 1
eGFP	enhanced GFP
eIF	eukaryotic translation initiation factor
ELAVL	(Embryonic Lethal, Abnormal Vision, Drosophila)-Like RNA Binding Protein; Hu-Antigen
EP	electroporation
EPO	erythropoietin
EtOH	ethanol
EU	5-ethynyl uridine
FACS	fluorescence-activated cell sorting
FCGRT	Fc fragment of IgG, receptor, transporter, alpha
FCS-HI	fetal calf serum, heat inactivated
FLT3	Fms-like tyrosine kinase 3
FUS	Fused In Sarcoma RNA Binding Protein (Heterogeneous Nuclear Ribonucleoprotein P2)
GAIT	γ-interferon-activated inhibitor of translation
GFP	green fluorescent protein
GLS	Glutaminase, nuclear gene encoding mitochondrial protein
GM-CSF	granulocyte macrophage colony-stimulating factor
GMP	good manufacturing practice
GTP	guanosine-5'-triphosphate
HFF	Human Foreskin Fibroblast cells
hiDC	human immature DC
HLA-DRB4	Major histocompatibility complex, class II, DR beta 4
hnRNP	heterogeneous nuclear ribonucleoprotein
HPRT1	Hypoxanthine-guanine phosphoribosyltransferase 1
HPV	human papilloma virus
HSA	human serum albumin
HuR	human antigen R
iDC	immature DC
IFN	interferon
Ig	immunoglobulin
IGF2BP1	Insulin-Like Growth Factor 2 mRNA Binding Protein 1
IL	interleukin
IRES	internal ribosome-entry site
IVAC®	*i*ndividual cancer *vac*cination
IVT	*in vitro* transcribed/ *in vitro*-T7-transcription
K(H)SRP	KH splicing regulatory protein
KHDRBS3	KH Domain Containing, RNA Binding, Signal Transduction Associated
LAMP1	lysosome-associated membrane protein 1
LB	Luria-Bertani
LPS	lipopolysaccharide
LSP1	Lymphocyte-specific protein 1
m5C	5-methylcytidine
m6A	N6-methyladenosine
m^7G	5' 7-methylguanosine
MDA5	melanoma differentiation-associated protein 5
mDC	mature DC

MHC	major histocompatibility complex
miRISC	miRNA-induced silencing complex
miRNA	microRNA
miRNP	micro-ribonucleoproteins
MITD	MHC class I molecule trafficking signal
mRNA	messenger RNA
MRS2	MRS2 magnesium homeostasis factor homolog (S. cerevisiae)
MT-RNR1	mitochondrially encoded 12S rRNA
MyD88	myeloid differentiation primary response gene 88
MYH9	Myosin, heavy chain 9, non-muscle
NaCl	sodium chloride
NaOAc	sodium acetate
ncRNA	non-coding RNA
NEAA	non-essential amino acids
NFκB	nuclear factor κ-light-chain-enhancer of activated B cells
NGS	next-generation sequencing
NK	natural killer
no.	number
NOVA2	Neuro-Oncological Ventral Antigen 2
NP	nucleoprotein
NP1	Nuclease P1
nts	nucleotides
ODN	oligodeoxynucleotides
ORF	open reading frame
OVA	ovalbumin
P/S	Penicillin / Streptomycin
PABP	poly(A)-binding protein
PAMP	pathogen-associated molecular pattern
PAN	poly(A) nuclease
PARN	poly(A)ribonuclease
PBMC	peripheral blood mononuclear cells
PBS	phosphate buffered saline
PBS/EDTA	PBS supplemented with 2 mM EDTA
PCR	polymerase chain reaction
pDNA	plasmid DNA
PE	phycoerythrin
PEG	polyethylene glycol
PFA	Paraformaldehyde
PKR	protein kinase R
PLD3	Phospholipase D family, member 3
polyI:C	polyinosinic:polycytidylic acid
ppp	triphsophate bridge
PRR	pattern-recognition receptor
PSA	prostate specific antigen
PSI	P-element somatic inhibitor protein
PTBP1	Polypyrimidine Tract Binding Protein 1
PTMA	Prothymosin, alpha
PTR	post-transcriptional regulator
PTRF	Polymerase I and transcript release factor
PUM2	Pumilio RNA-Binding Family Member 2
QKI	Quaking Homolog, KH Domain RNA Binding
RBP	RNA-binding protein
rel.	relative
RIG-I	retinoic acid inducible gene I
RLR	RIG-I-like receptor
Rn	round
RNA	ribonucleic acid
rRNA	ribosomal RNA
RT	room temperature
SAP-49	Splicing Factor 3b, Subunit 4, 49kDa
SBP	surfactant protein B
sec	N-terminal leader peptide
SELEX	*S*ystematic *E*volution of *L*igands by *EX*ponential Enrichment
SFM	*Scan for motifs*
SFRS2	Serine/Arginine-Rich Splicing Factor 2
SILAC	stable isotope labeling by amino acids in cell culture
SN	supernatant
SNRPA	Small Nuclear Ribonucleoprotein Polypeptide A
ssDNA	single stranded DNA
SUS	Sus scrofa pogo transposable element with ZNF domain
TAA	tumor-associated antigen
TAE	TRIS-Acetat-EDTA-Puffer
TCR	T cell receptor
TD-PCR	Touch-Down-PCR
TLR	Toll-like receptor
TNF	tumor necrosis factor
Trf4	poly(A) polymerase (in yeast)
TSA	tumor-specific antigen
TTP	tristetraprolin
uORF	upstream open reading frame
UTP	uridine-5'-triphosphate
UTR	untranslated region
VEGF	vascular endothelial growth factor
YBX1	Y Box Binding Protein 1
YBX2-a	Y Box Binding Protein 2a
ZFP36	Zinc Finger Protein 36 Homolog (TTP)

3 Introduction

3.1 mRNA-based therapies

Synthetic messenger (m)RNA-therapeutics are increasingly being exploited as a potential new class of drugs to deliver genetic information into target cells. The aim of these new therapeutics is the transient expression of the protein(s) encoded on the *in vitro* transcribed (IVT-)mRNA providing the basis for a broad range of different applications, for example vaccines against infectious diseases, protein-replacement therapies, reprogramming of cells, genome engineering or cancer immunotherapy. Most of these fields have already entered preclinical and/or clinical testing (Fig. 3.1).

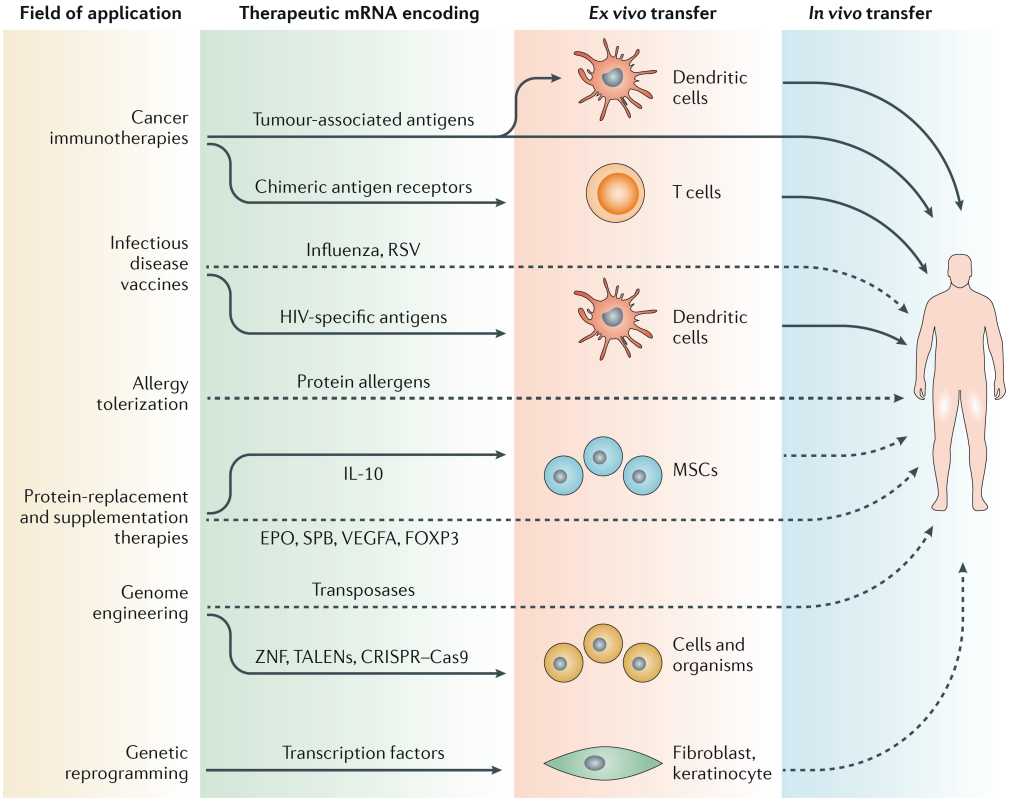

Figure 3.1: Overview of potential mRNA-based therapies. The therapeutic IVT-mRNA is either directly injected into the patient or transfected *ex vivo* before *in vivo* transfer of the cells into the patient. Details regarding preclinical (dotted arrows) or clinical (solid arrows) applications are summarized in Sahin *et al.*[1] [Cas9, CRISPR-associated protein 9; CRISPR, clustered regularly interspaced short palindromic repeat; EPO, erythropoietin; FOXP3, forkhead box P3; IL.10, interleukin.10; MSC, mesenchymal stem cell; RSV, respiratory syncytial virus; SPB, surfactant protein B; TALEN, transcription activator-like effector nuclease; VEGFA, vascular endothelial growth factor A; ZNF, zinc finger nuclease] (modified from Sahin *et al.*[1]).

Since the first discovery of the mRNA in 1961,[2] the molecular mechanisms concerning its turnover in the cell have been unveiled step by step.[1] Because of its instability, mRNA drifted out of focus for a long time - and plasmid DNA (pDNA) was preferentially used - until the early 1970s, when studies provided clear evidence of mRNA translatability and - to a certain extent - stability in mammalian cells.[3,4] Almost two decades later, Malone *et al.* and

Wolff *et al.* described two different and applicable new methods to stably transfect mammalian cells with RNA, thus paving the way for the first mRNA-based drug.[5,6] The most important advance though was the development of mRNA as a potent and effective drug in active cancer immunotherapy (see below).

Protein-replacement therapies The concept of protein-replacement therapies is based on the expression of the nucleic-acid encoded protein to either replace mal/non-functional or missing proteins. DNA-based and viral vectors were primarily used in human clinical therapy until ethical and safety concerns were raised (e.g. risk of chromosome integration). The first *in vivo* gene transfer using synthetic mRNA was demonstrated in the early 1990s by Wolff *et al.*[6] He and his colleagues directly injected naked IVT-mRNA into mouse skeletal muscle *in vivo*, which resulted in the expression of the encoded protein in the treated muscle.[6] However, the use of IVT-mRNA proved to be difficult, which could eventually be explained by the immunogenicity of unmodified IVT-mRNA (Ch. 3.4). The replacement of proteins using IVT-mRNA should ideally not activate the immune system as this could hinder the therapeutic efficacy (i) by compromising the expression of the encoded protein as the IVT-mRNA is targeted for decay due to activation of the pattern-recognition receptors (PRRs) and/or (ii) by activating immune cells (e.g. DCs and T cells) leading to cell death.[7,8] This shortcoming was overcome by using modified nucleosides and improved mRNA purification methods. By integrating different natural nucleosides (e.g. 2-thiouridine, 5-methylcytidine or pseudouridine) into IVT-mRNA, Karikó *et al.* demonstrated that the resulting modified mRNA showed a strongly reduced immunogenicity together with an increased translatability and stability.[9] The removal of double-stranded RNA (dsRNA), contaminants after synthesis of the IVT-mRNA, decreased the immunogenicity even more.[10] With these improved approaches Karikó *et al.* showed that a single injection of a synthetic pseudouridine-modified mRNA encoding for the erythropoietin (EPO) protein, led not only to increased EPO-levels in mice, but also to an EPO-protein, which was functional for four days.[11] These results were confirmed by Korman *et al.*, additionally demonstrating that the modified EPO-encoding mRNAs were not detected by the Toll-like receptors (TLRs).[12] In the same study by Korman *et al.*, mice suffering from congenital lethal lung disease, could be alleviated from respiratory failure by aerosol delivery of a modified IVT-mRNA encoding the surfactant protein B (SBP). Heart function could be improved as well in another mouse model of myocardial infarction by injecting directly the vascular endothelial growth factor A (VEGFA) modified IVT-mRNA intramyocardially.[13] The non-immunogenic properties of modified synthetic mRNAs are thus useful for protein-replacement therapies and for a targeted gene manipulation of therapeutic cells.[14]
Despite all these promising results, there are still some technical challenges, which need to be addressed such as, for example, the delivery of the IVT-mRNA in specific cells or tissues as there are cell-type specific differences regarding post-translational modifications of the protein translated from the IVT-mRNA (e.g. glycosylation, proteolytic processing or precise cleavage of the encoded protein).

Reprogramming of cells The use of modified IVT-mRNA to modulate the phenotype and function of different cells has become a promising approach, in particular in the field of regenerative medicine. In 2010 Warren *et al.* demonstrated a new and safe approach to efficiently reprogram multiple human cell types to induced pluripotent stem cells (iPSCs) by using modified IVT-mRNA encoding the so-called Yamanaka stem cell transcription factors.[15,16] Using the same technology, the iPSCs were induced to differentiate into myogenic cells to show how to direct cell fate.
The major advantage in using synthetic mRNA for the reprogramming of somatic cells compared to the original retroviral system of Takahashi *et al.*, is the avoidance of genomic integration and with this the possible risk of a permanent expression of the introduced transcription factors, which could lead to tumorigenic iPSCs.[14] Recently, this technology has been improved regarding efficacy, feasibility and costs and extended to other cell types from human skin to blood.[17]

Genome engineering This technique refers to the genetic modification of cells by using nucleic acids encoding for proteins (e.g. nucleases or transposases), which change the genome by replacing, deleting or inserting DNA-segments.[14] However, using plasmid DNA (pDNA) to introduce these editing enzymes into the cells bears the risk of off-target effects due to a nonspecific editing caused by a prolonged expression of the encoded proteins.[1] IVT-mRNA is a potential alternative to pDNA as the expression of the encoded enzymes is more limited with respect to the duration. Different IVT-mRNAs encoding for nucleases [e.g. zinc finger nucleases, transcription activator-like effector nucleases or the CRISPR (Clustered Regularly Interspaced Short Palindromic Repeats) associated protein 9] or transposases (e.g. Sleeping Beauty or piggiBac) have already been applied successfully in different species providing, for example, the opportunity to create human disease models.[1]

Vaccines against diseases and allergy alleviation The first success of mRNA-based vaccines was reported in the early 1990s, where a nucleoprotein (NP) specific T cell immune response was induced upon injection of lipoplexed mRNA encoding the NP of the influenza virus.[18] This facilitated the development of vaccines against infectious diseases. Since then, different approaches have been described using, for example, (i) self-amplifying IVT-mRNA formulated with synthetic lipid nanoparticles against the H7N9 influenza virus[19] or the respiratory syncytial virus[20] or (ii) dendritic cells (DCs) transfected with synthetic mRNA encoding proteins of the human immunodeficiency virus (HIV).[21,22] The latter entered clinical testing demonstrating not only its efficacy in preclinical models but also its safety in humans. Protective vaccines against the influenza virus are on the advance and are also preclinically tested, where the vaccine is either combined with RNA adjuvants[23] or by using the recombinant RNA replicon system.[24] All of these approaches elicited a strong and specific immune response in different animal models.[25–27] This not only facilitated the development of vaccines against viruses, but also for active cancer immunotherapy (Ch. 3.2).

In the field of allergy therapy, synthetic mRNA-based approaches have shown first promising results. A long-lasting and allergen-specific immune response was induced after injection of IVT-mRNA in a murine model of allergic rhinitis, inhibiting the induction of an allergic reaction after exposure to the allergen.[1] Moreover, by using IVT-mRNA, the potential risks as seen with DNA-based vaccines (e.g. anaphylactic shock) can be circumvented.

mRNA-based cancer immunotherapeutics The most important advance was the development of the IVT-mRNA as a potent and effective drug in active cancer immunotherapy, which is why this part is described in more detail in the next chapter(s).

3.2 mRNA-based cancer immunotherapeutics

Nucleic-acid based vaccines have been shown to be more efficient compared to peptides or proteins in activating tumor specific cytotoxic T cells (CTLs).[28,29] However, among other reasons described in Ch. 3.4, plasmid DNA (pDNA) is not very efficient in promoting a strong antitumor response[30] and - due to ubiquitous ribonucleases (RNases)[31] - mRNA was assumed to be too unstable for a long time until its translatability and sufficient stability in mammalian cells was demonstrated.[3,4] With the promising results of Malone *et al.*[5] and Wolff *et al.*[6] the way was paved for IVT-mRNA to be used as therapeutic drug.

In the context of cancer immunotherapy, Conry *et al.* presented in 1995 the first results of an induced specific immune response in mice vaccinated with naked mRNA encoding the carcinoembryonic antigen (CEA), followed by a challenge with CEA-expressing tumor cells.[32] Only shortly thereafter Boczkowski *et al.* used a completely different approach for an effective anticancer therapy.[33] He and his colleagues demonstrated the feasibility of using mRNA-transfected DCs in cancer therapy. DCs were pulsed with chicken ovalbumin (OVA) RNA to activate *in vitro* OVA-specific CTLs. *In vivo*, mice vaccinated with DCs loaded with tumor RNA of OVA-expressing EL-4 tumor cells showed protection after EL-4 tumor challenge. Moreover, reduction of lung metastasis was observed after vaccination of mice with B16 tumor RNA-pulsed DCs.[33] Positive results obtained with animal models were further demonstrated *in vitro* with human monocyte-derived DCs loaded with naked or lipoplexed IVT-mRNAs encoding for CEA or human papilloma virus (HPV) E6 protein.[30] Since then IVT-mRNAs have emerged as a powerful new tool to deliver genetic information into DCs for active cancer immunotherapy.[1,34,35]

Administration of RNA-based vaccines that have been used for clinical applications includes *ex vivo* transfected autologous DC and the direct injection of the naked RNA into the patient (Ch. 3.3). In the first approach, autologous DCs are isolated from a cancer patient and transfected *ex vivo* with RNA from whole tumor cells or encoding a specific tumor-associated antigen (TAA) or tumor-specific antigen (TSA) before being re-administered into the patient.[36] However, this method is expensive and time-consuming. Currently the direct and local injection of naked RNA is the method of choice, which had already been shown in the early 1990s by Wolff *et al.*[6] Wolff and his colleagues demonstrated at that time the effi-

cient uptake of naked pDNA or mRNA via direct injection into murine skeletal muscle cells. The local administration route of RNA includes the intradermal, subcutaneous, intramuscular, or intranodal application of the naked nucleic acid therapeutic into the patient. From these different administration routes, the direct intranodal injection has been proven to be superior for the induction of strong antigen-specific CTL-responses.[37] In another study an alternative to intranodal injection was presented. Based on results by Hoerr *et al.*,[38] a strong immunization of mice could successfully be reached by intradermal injection using naked mRNA combined with protamine-formulated mRNA as a two-component vaccine.[39] While the naked RNA promotes optimal antigen expression, the protamine-complex mediates a strong immunostimulatory response.[40] Together these examples demonstrate the efficacy and potency of RNA-based cancer vaccines for active cancer immunotherapy.

IVT-mRNA based drugs are particularly suitable due to their characteristics, i.e. no risk of genomic integration, easy and reproducible synthesis and most important, transient activity and value of an adjuvant (for details see Ch. 3.4). To develop full impact, mRNA must be delivered into the cytoplasm of the DCs, so that it can be translated into the desired encoded protein (Ch. 3.3). A spontaneous uptake of nucleic acids by target cells *in vitro* (pulsing) has been observed to be inefficient, compared to other viral and non-viral nucleic acid delivery systems such as electroporation or lipo-/polyplexing.[41–43] Unlike the *in vitro* pulsing approach, Wolff *et al.* demonstrated the efficient uptake of naked pDNA or mRNA via direct injection into murine skeletal muscle cells.[6] Uptake of the RNA therapeutic *in vivo* is thereby mediated by receptor-mediated endocytosis involving macropinocytosis in immature DCs (iDCs) or the scavenger receptor in fibroblasts.[44,45] Since then, several studies followed to not only understand mechanisms of mRNA-based vaccine deliveries, but to improve outcome as well. Viral and non-viral delivery approaches were compared, demonstrating different transfection efficiencies of DCs. For example, Grünebach *et al.* compared different delivery systems including electroporation and lipofection and analyzed efficacy of specific CTL-induction.[46] Although electroporation was shown to be the most effective approach, similar inductions of tumor-specific CTLs could be achieved. This suggested that even low levels of gene expression can mediate an antigen-specific CTL-response showing high efficacy of DCs. These results were later confirmed and analyzed in more detail by other studies.[47–50] The most recent development regarding delivery of the mRNA therapeutic is an intravenously administered lipoplexed mRNA formulated with optimized lipid carriers to direct the IVT-mRNA specifically to DCs and macrophages residing in lymphoid compartments, thus yielding a strong antitumor effector and memory T cell response.[51]

The development and clinical translation in the field of cancer immunotherapy has additionally been boosted with the improved identification of new tumor targets.[30,39,52–66] As cancer is mainly induced by DNA aberrations,[67] mutations facilitate the discrimination of normal and tumor cells. Next-generation sequencing (NGS) proved to be a highly efficient and reproducible method to quickly identify these somatic mutations in tumors. This

technology is able to provide a complete map of the so-called *mutanome* of each individual patient, paving the way for personalized vaccination in cancer immunotherapy.[68–71]
In 2012 Castle *et al.* reported the identification of non-synonymous somatic point mutations in B16F10 murine tumors by NGS.[69] The authors could demonstrate the immunogenicity of the neoepitopes defined by selected mutations as well as antitumoral activity of vaccines directed against such neoepitopes. Based on these results, a short time later Kreiter *et al.* presented the further development of a new messenger (m)RNA-based vaccine using poly-neo-epitope *in vitro* transcribed (IVT)-RNAs, derived from targets prioritized by bioinformatic analysis of their expression levels and major histocompatibility complex (MHC) class II-binding capacity.[72] These new vaccines induce a potent antitumor activity, resulting in tumor control and complete rejection in mice. Kreiter and colleagues proposed to employ the same predictive algorithm on human cancers, to be able to produce individual mRNA-based vaccines in a quick and safe manner. This concept for *i*ndividual cancer *vac*cination (IVAC®) has successfully entered clinical trials [ClinicalTrials.gov identifier: NCT02035956, NCT02316457]. To date, many companies have been founded that are dedicated to developing suitable RNA-based vaccines, such as Argos Therapeutic, BioNTech AG, CureVac GmbH, eTheRNA and Moderna Therapeutics. In summary, mRNA-based immunotherapeutics have been proven to be safe and efficacious,[63,73–75] and moreover, not only customizable for each patient, but also a potential off-the-shelf therapeutic of the future.[76]

3.3 Mode of action of mRNA-based immunotherapeutics

The mode of action of RNA cancer vaccines is based on the translation of the encoded specific tumor antigen(s) in DCs, followed by processing, and presentation of epitopes on MHC class I and II complexes for recognition by T cells (Fig. 3.3). DCs were first described in the early 1970s by Ralph M. Steinman.[47] These cells are an important link between the innate and adaptive immune system due to their characteristic features.[34] They are able to control immune tolerance as well as cellular and humoral immunity, by activating and interacting with naïve T lymphocytes, B cells and cells of the innate immune system such as natural killer (NK) cells, phagocytes and mast cells.[34,49,77] Further understanding of DC biology as well as how they promote immune responses particularly along with the tumor microenvironment[35] improved outcome of mRNA-based vaccines.

Immature cells (iDCs) mainly reside in tissues, but migrate partially through the blood and lymph streams as well. There iDCs may possibly encounter antigens and injected naked mRNA therapeutics (Ch. 3.2) as well. These antigens or RNA are internalized through receptor-mediated endocytosis, phagocytosis or macropinocytosis.[44,78,79] During antigen processing, iDCs differentiate into mature DCs (mDCs) and travel to the lymphoid organs, where they encounter naïve or memory T cells. Migration is mediated by chemokines such as CCL19 and CCL21 that are highly expressed in lymph nodes[80] and bind to the DC-receptor CCR7 (see below). The maturation process involves phenotypic and functional changes.

iDCs mainly express MHC class II and fewer co-stimulatory molecules such as CD80 and CD86. Upon maturation, expression of MHC class I and II is upregulated, together with an increased expression of the CCR7 chemokine receptor, co-stimulatory (CD80, CD86, OX40L and CD40) and adhesion molecules (CD54, CD102, CD11a, CD58 and CD209). Phagocytic ability is thereby decreased. Moreover, mDCs have an enhanced secretion of cytokines [interleukin (IL)-6, IL-12, IL-23, tumor necrosis factor (TNF)α] and chemokines (CCL18), which attract naïve T cells to their location (Fig. 3.2).[36,81]

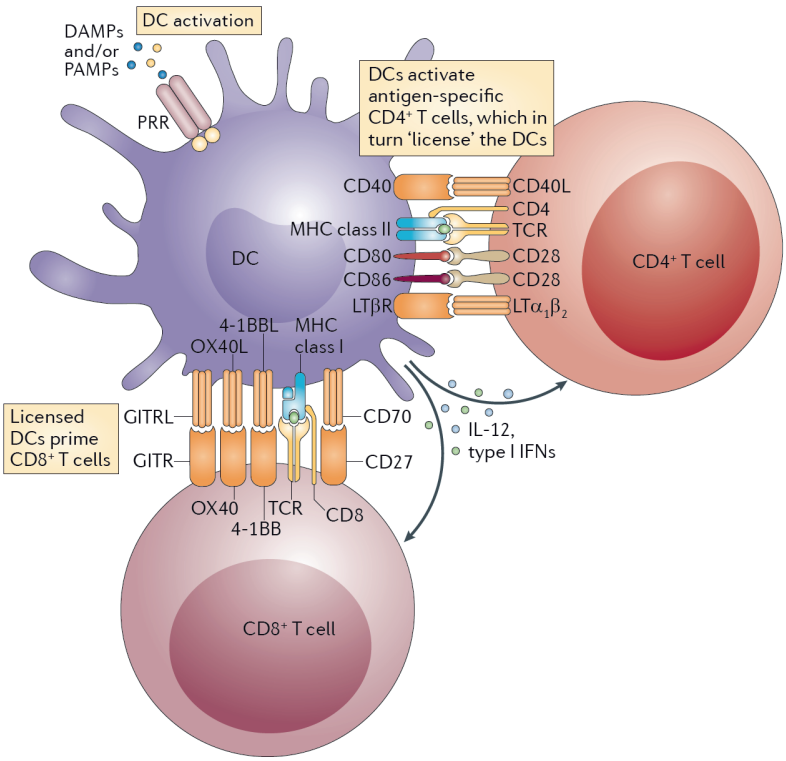

Figure 3.2: Crosstalk between DCs and T cells upon DC activation. Activation of iDCs by pathogen-associated molecular patterns (PAMPs) or damage-associated molecular patterns (DAMPs) mediate down- and upregulation of receptors resulting in optimal antigen presentation to T lymphocytes. $CD4^+$ T cells are primed by recognition of the antigen presented on MHC class II molecules of DCs with their T cell receptor (TCR) and additional interaction with co-stimulatory receptors with respective ligands (L) as CD40-CD40L, CD80/CD86-CD28 and LTβR-LT$\alpha_1\beta_2$. Priming of $CD8^+$ T cells occurs by MHC-class I restricted peptides. Co-stimulatory interaction takes place between CD70-CD27, OX40L-OX40, GITR-GITRL and 4-1BB-41-BBL. Stimulation of the receptors CD40 and LTβR leads to secretion of IL-12 and type I IFN, which additionally boost $CD8^+$ T cells activation and proliferation, as well as effector function and formation of $CD8^+$ T cells memory. [IFN: interferon; LTβR: lymphotoxin-ß receptor; LT: lymphotoxin; GITR: Glucocorticoid-induced TNF-receptor-related protein] (by Deluca *et al.*[82]).

Depending on the antigen's origin, antigens are presented via MHC class I or II molecules (Fig. 3.3).[82] Antigens of endogenous origin, for instance after bacterial or viral infection, are degraded via the proteasome. The resulting peptides are loaded onto MHC class I within the endoplasmatic reticulum and presented on the cell surface to $CD8^+$ T cells. In contrast, exogenous antigens are taken up as described above and processed in endosomal-lysosomal compartments. Peptides are loaded onto MHC class II molecules, which present then the peptides on the DC surface to $CD4^+$ T cells. However, exogenous antigens can also be

presented via MHC class I molecules due to a process called *cross-priming*.[83] Internalized antigens are thereby shuttled back from lysosomal compartments into the cytosol, entering the MHC class I pathway. Princiotta *et al.* and Holtkamp *et al.* both observed a direct dose-response relationship between the antigen level produced by DCs and the density of peptide/MHC-molecule complexes displayed on the cell surface for stimulation and activation of T cells.[84,85] That is, the longer the exogenous administered RNA is present in the cell, the more protein is translated from the RNA, which in turn promotes a stronger antigen-specific and sustained immune response. Thus, antigen abundance and exposure duration affect the speed and type of the T cell response.[86]

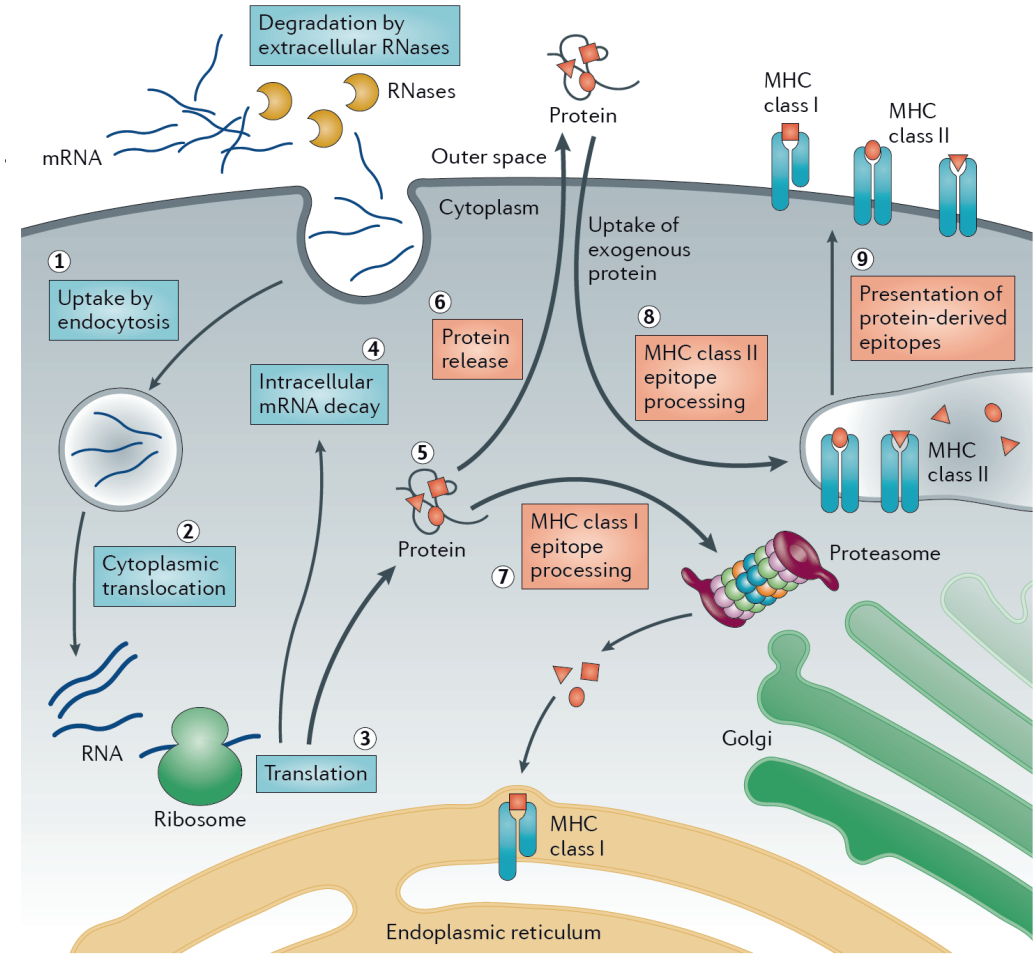

Figure 3.3: Mode of action of antigen-encoding mRNA as immunotherapeutic. ① Synthetic mRNA is endocytosed by the target cell and ② translocated into the cytoplasm, where it is immediately ③ translated, but also ④ degraded by the inner cell degradation machinery. The resulting protein product is ⑤ post-transcriptionally modified depending on the cell proteome. For the use of mRNA as immunotherapeutic, protein needs to be degraded into antigenic peptide epitopes. This is mediated ⑦ by the proteasome. Peptides are next loaded on MHC class I molecules, which then present the epitopes to $CD8^+$ T cells. To activate $CD4^+$ T cells as well, ⑥ proteins released from the target cell ⑧ can be internalized again due to signals routing the protein to MHC class II compartments.[87] These signals can be encoded in the mRNA as well and enable ⑨ the presentation of epitopes to $CD4^+$ T cells (by Sahin *et al.*[1]).

DCs do not only present (tumor) antigens to naïve $CD4^+$ helper and cytotoxic $CD8^+$ T lymphocytes.[88–90] Several signals and interactions must take place to successfully prime

these lymphocytes, thereby influencing the T cells function and fate as well. T cell activation can only occur upon interaction between CD28 on the T cell surface with the co-stimulatory molecules CD80/CD86 on the DC surface. Signaling failure due to antigen presentation without positive co-stimulation can, for instance, lead to T cell anergy or tolerance.[91] In addition, while naïve $CD8^+$ T cells proliferate into CTLs and expand clonally upon induction, activation of naïve $CD4^+$ T cells forms different helper effector cells - T_H1, T_H2, T_H17 or T follicular helper cells - depending on the secreted cytokines such as interferon (IFN)γ or IL-4.[77,92,93] Primed $CD4^+$ T cells then produce IL-2, which in turn enhances T cell proliferation and clonal expansion.

Loading of DCs with RNA-based cancer vaccines *ex vivo*, involves isolation of DC precursor cells from the patient, loading of the RNA tumor antigen and re-administration into the patient.[94] Although an antitumor response is observed using this approach for mRNA-based cancer vaccines, there are still many question unanswered regarding the best (i) transfection approach; (ii) delivery route and (iii) DC-type to use. Direct transfection approaches into the cytosol of the DC, such as electroporation or lipofection, have been proven to be more feasible compared to passive pulsing.[33,94] And though all tested delivery routes proved to be immunogenic by inducing T cell responses, not all of them ensure a high migration capacity of the DCs to the lymph nodes;[95] this being a crucial step using *ex vivo* autologous DCs loaded with tumor-specific RNA. This problem can be circumvented, for example, by culturing DCs *in vitro* with special maturation cocktails[96,97] before injecting them into the patient intranodally or intralymphatically. This way, migration is no longer necessary and DCs can directly interact with T cells,[98] as described above in this section.

3.4 Advantages of IVT-mRNA for immunotherapy

There are several advantages in using mRNAs for immunotherapy, due to their specific characteristics, which are described in the following paragraphs.

Non-genomic integration Compared to pDNA or viral vectors the IVT-mRNA does not integrate into the genome to risk insertional mutagenesis, which can result in the deregulation or destruction of genes and open reading frames (ORFs), respectively, up- or downstream of the insertion site.[99] This in turn often mediates a perturbation of the cellular phenotype, possibly leading to aberrant cell transformation, and thus, cancer.

Easy synthesis of the IVT-mRNA The IVT-reaction is carried out in cell-free systems, which makes the synthesis of IVT-mRNAs easy for basically all sequences and for lengths of several thousands nucleotides.[1] A template DNA - linearized pDNA, complementary DNA (cDNA) or polymerase chain reaction (PCR) product - encoding the (whole) gene of interest, together with characteristical structural elements of naturally occurring mRNAs (Ch. 3.5) is used as starting material. The synthesis of RNA is enzymatically carried out

in the presence of nucleotides by the well-characterized T7 or SP6 bacteriophage RNA polymerases.[100,101] The corresponding promoter should, thereby, be encoded upstream of the 5' untranslated region (5' UTR)-region on the template DNA. After the IVT reaction and subsequent removal of the DNA, the IVT-mRNA can easily be purified via bead-based methods, precipitation or chromatography. The IVT-mRNA is usually resuspended in RNase-free water and stored until use. IVT-mRNAs used for clinical studies must be produced under good manufacturing practice (GMP) conditions. This involves not only up-scaling and optimization of the standard protocol, but also an extensive characterization of the RNA regarding purity, quantification and functionality.[1]

Easy translation of the IVT-mRNA The IVT-mRNA is translated immediately, as soon as it has entered the cytoplasm of the cell. In contrast, DNA needs to enter the nucleus to be transcribed first into RNA, which has then to be transported into the cytoplasm, where in eukaryotic cells translation takes place. Transfection of target cells with pDNA is best achieved during cell division, where the nuclear envelope is temporarily lost. Nevertheless, transfection efficacy with pDNA is very low and depends on mitotic cell activity.[43] Functionality of DNA based therapeutics is therefore unpredictable.[1,102]

Transient activity of the IVT-mRNA The IVT-mRNA is only temporary active and is completely degraded by the cell's own degradation machinery. Therefore, the production of the encoded protein is timely confined.[43] This characteristic is useful in the context of cancer immunotherapy, where only a transient expression is desired.

Immunstimulatory capacity Upon internalization of the RNA cancer vaccine by DCs (Ch. 3.3), the unmodified IVT-mRNA is recognized by intracellular receptors, which activate the cells by inducing the expression of pro-inflammatory cytokines (Ch. 3.1, *Protein-replacement therapies*). Thus, the IVT-mRNA does not only encode for a specific tumor antigen, but also functions as an adjuvant by enhancing the immune response. This is favorable in the context of cancer immunotherapy.
These intracellular - so-called - PRRs are part of the innate immune system. They originally protected the host from bacterial or viral invasion by binding of conserved foreign structures known as pathogen-associated molecular patterns (PAMPs). These structures are either associated with microbial envelopes [e.g. bacterial lipopolysaccharide (LPS), flagellin and lipoproteins] or nucleic acids.[103,104] In contrast, endogenous signals derived from damaged host's molecules, which could harm cells and tissues, are termed damage-associated molecular patterns (DAMPs). Both PAMPs and DAMPs are able to stimulate the innate immune system by activating the PRRs, which then induce the expression of pro-inflammatory cytokines (Fig.3.4).[105]

Foreign nucleic acids - either derived from pathogens or exogenously administered nucleic acid based vaccines - can be recognized by three different groups of PRRs (Fig.3.4). The membrane-bound Toll-like receptors TLR3, TLR7, TLR8 and TLR9 control the con-

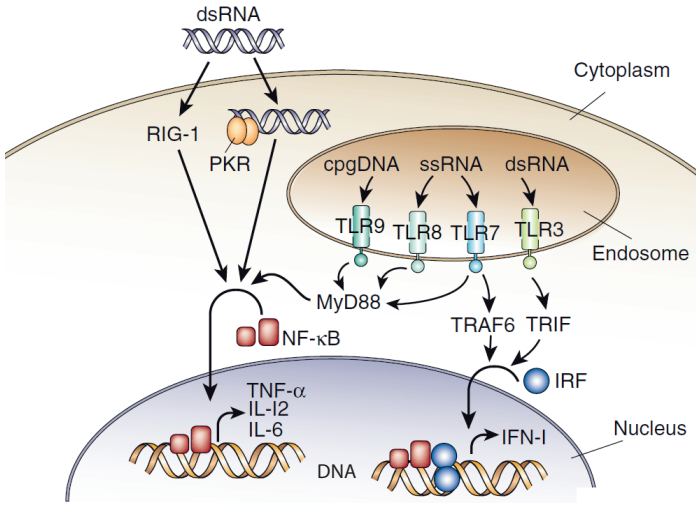

Figure 3.4: Sensing of (foreign) nucleic acids by the immune system. Activation of TLRs and RLRs results in activation of NFκB via the adaptor molecule MyD88 and/or translocation of the IRF into the nucleus via the adaptor molecules TRAF6 and TRIF. NFκB and IRF induce the production of pro-inflammatory cytokines and the TLR-independent type I interferons (IFN-I) in the nucleus. [IRF: IFN regulatory factor; MyD88: myeloid differentiation primary response gene 88; NFκB: nuclear factor κ-light-chain-enhancer of activated B cells; RLR: retinoic acid inducible gene I (RIG-I)-like receptors; TRAF6: TNF receptor-associated factor 6, TRIF: Toll/IL-1 receptor domain-containing adaptor inducing IFNβ] (by Robbins *et al.*[106]).

tents of endolysosomal compartments and the cytoplasm is monitored by retinoic acid inducible gene I (RIG-I)-like receptors (RLRs) and the double stranded RNA (dsRNA)-activated protein kinase (PKR).[105,107,108] While RLRs are widely expressed by somatic cells, TLRs are mainly expressed by a variety of immune cells, such as DCs, macrophages and B cells.[104] Signals derived from PRRs are thus integrated at an antigen-presenting cell (APC)-level, which also induces an adaptive immune response.[105] Owing to this potent immunstimulatory capacity, several studies demonstrated the feasibility of synthetic nucleic acids to function as an adjuvant in, for example, so-called nanovaccines.[109] For instance, the unmethylated CpG DNA, typically characteristic for prokaryotic DNA, is recognized by TLR9. Vaccines containing CpG synthetic oligodeoxynucleotides (ODNs) have been demonstrated to improve functional activity of APCs and enhance humoral and cellular immune responses.[110–112] They have successfully reached clinical trials [ClinicalTrials.org identifier: NCT00043407, NCT00292045, NCT00031278]. Furthermore, small 5' triphosphate-containing double stranded RNAs - artifacts arising from *in vitro* transcription reactions - are able to activate RIG-I inducing an immune response.[113–116] Another example describes the activation of the TLR3-signaling pathway in human HEK293 after transfection with IVT-mRNA resulting in NFκB-production.[117]

A different approach to use nucleic acid sensors for improvement of RNA-based immunotherapeutics is the use of TLR and RLR agonists. For instance, polyinosinic:polycytidylic acid (polyI:C) activates TLR3 and the RLR melanoma differentiation-associated protein 5 (MDA5) in DCs and stromal cells inducing a potent type I IFN production, which mediates activation of T_H1 and $CD8^+$ T cells.[118,119] Stabilization of polyI:C with a poly-L-lysine and

carboxymethylcellulose (polyICLC) resulted in an even faster immune response.[120] These examples demonstrate the feasibility of using different nucleic acids as adjuvants for induction of a strong immune response; at least as co-administered antigens in RNA vaccine formulations.

3.5 Structure of the IVT-mRNA

A typical mRNA is composed of (i) a cap; (ii) a UTR up- (5' UTR) and downstream (3' UTR) of the ORF; (iii) an ORF encoding the desired tumor antigen; and (iv) the poly(A)-tail (Fig. 3.5), all of which are required for its functionality. Thus, the synthetic mRNA is designed accordingly.

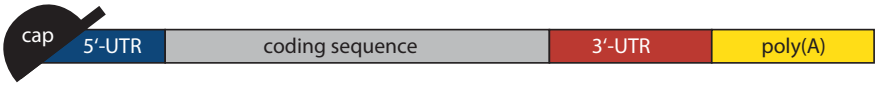

Figure 3.5: IVT-mRNA and its structural elements: cap, untranslated regions (5′ UTR, 3′ UTR), coding sequence and poly(A)-tail.

The RNA cap-structure The 5'-end of all endogenous eukaryotic mRNA is comprised of a 5' 7-methylguanosine (m^7G) cap attached during transcription to the first nucleotide through a 5' to 5' triphosphate bridge (ppp).[121] The cap is - along with the poly(A)-tail (see below) - an essential element for exonuclease protection and full functionality of mature mRNA with regards to efficient translation and stability (Ch. 3.6 and 3.7).[122–124] Thus, capping of the synthetic mRNA-therapeutic is essential. It can be done during transcription by adding a corresponding cap analogue to the *in vitro* reaction or post-transcriptionally with capping enzymes e.g. derived from the *vaccinia* virus.[125] Co-transcriptional capping is thereby more feasible, as the cap-analog can easily be added to the IVT reaction. However, for technical reasons a part of the IVT-mRNA remains uncapped. In addition, it was recognized that the plain cap dinucleotide m^7GpppG is integrated in two orientations by phage RNA polymerases (Fig. 3.6).[126] Only one of them is functional, i.e. about half of the capped RNA is non-functional. To circumvent this, so-called anti-reverse cap analogs (ARCAs) were developed, which can only be incorporated in the correct orientation due to modifications at the 2' or 3' position of the m^7guanosine (Fig. 3.6).[127]

These new ARCA-caps mediated an enhanced translational efficiency of the IVT-mRNA in rabbit reticulocyte lysates[128] and in DCs.[129,130] Nevertheless, the caps were further improved to increase RNA-stability even more by impeding cap-mediated RNA-decay (Ch. 3.7). The phosphorothioate-modified cap analog (β-S-ARCA) D1 (Fig. 3.6) has been shown to substantially improve stability and -at the same time - translational efficiency of RNA-based vaccines *in vitro* and *in vivo*. This yielded a significantly higher *de novo* priming of naïve T cells after immunization with antigen-encoding IVT-mRNA.[130] Moreover, IVT-mRNAs with β-S-ARCA modified cap-analogs showed a higher stability and translational efficiency compared to post-transcriptionally capped mRNA. Altogether this demonstrates

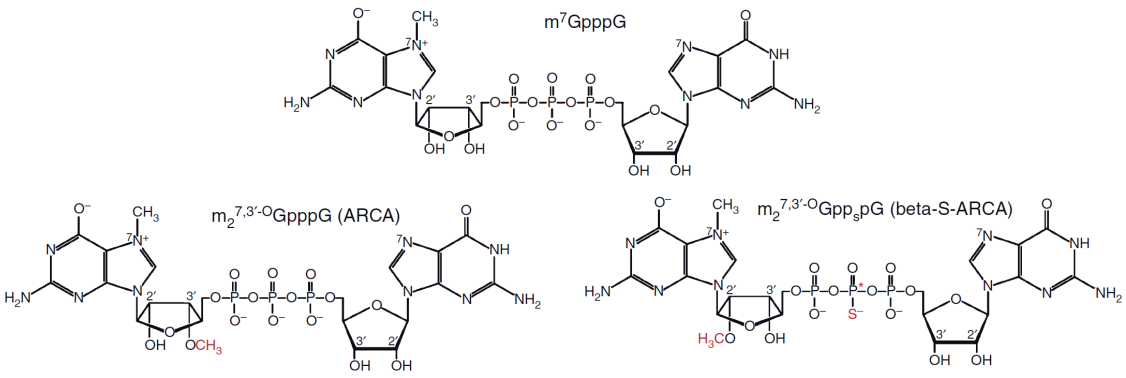

Figure 3.6: Cap analogs used for *in vitro* transcription of the mRNA. Details are described in the text (modified from Vallazza *et al.*[14]).

that RNA drugs that are used for pharmaceutical applications can be significantly improved by modified cap structures.

The poly(A)-tail As mentioned above, the poly(A)-tail is an essential determinant of a fully functional IVT-mRNA. The length of the poly(A)-tail thereby influences stability and translational efficiency (see also Ch.3.6 and 3.7). The poly(A)-tail of synthetic IVT-mRNAs can be generated in two ways. It can be added post-transcriptionally using recombinant poly(A)-polymerase derived from *Escherichia coli* or yeast.[131,132] However, this does not produce RNAs with one well defined poly(A)-tail, but rather a population of RNAs with a poly(A) size range that can cover from only few to several hundreds of adenosines. In addition, the reaction is difficult to control, giving batch to batch variation. In contrast, when the poly(A)-tail is encoded on the DNA template, reproducible mRNA batches with defined poly(A)-tail lengths are obtained. In order to obtain *unmasked* poly(A)-tails (i.e. not flanked by other nucleotides), which is important for maximal translational efficiency, the template DNA can be linearized downstream of the poly(dA:dT)-sequence using type IIs restriction enzymes.[121] In this way, poly(A)-tails with 120 consecutive adenosines can be obtained, which have been demonstrated to give maximal activity in DCs.[85]

The coding sequence Due to the redundancy in the genetic code, most amino acids are encoded by more than one codon.[133] This means, that the nucleotide sequence can be changed - at least to some degree - without altering the protein sequence. Based on different mechanisms, e.g. transfer (t)RNA availability in a target cell, codon usage can significantly affect the expression of the encoded proteins.[134] Therefore, it is generally aimed to optimize the codon usage for therapeutic synthetic RNAs. For example, codon optimization of T cell receptors (TCRs) showed an improved functional expression in transgenic human T cells.[135] However, due to the complexity of influencing factors, the optimal codon usage usually has to be verified experimentally for each case.[14]

In addition to the described codon adaptation within the ORF, the efficacy of the IVT-mRNA can also be improved by adding N- and/or C-terminal extensions up-/downstream of the encoded protein. For example, the potency of the vaccine can be further increased by

ensuring presentation of the encoded tumor antigen to both $CD8^+$ and $CD4^+$ T cells through the MHC class I and II molecules, respectively. Several groups reported a significant higher stimulatory capacity of DCs transfected with RNA encoding not only for the tumor antigen, but also for a sorting signal upstream of the ORF. This can be either the lysosome-associated membrane protein 1 (LAMP1), the DC-lysosome-associated membrane protein 1 (DC-LAMP) or a combination of an N-terminal leader peptide (sec) with an MHC class I molecule trafficking signal (MITD).[87,136,137] Using these signals mediates trafficking of the translated protein to the correct endolysosomal compartments thereby entering the MHC pathways.

The 5′ and 3′ untranslated regions (UTRs) The UTRs significantly influence mRNA turnover and translatability (Ch. 3.6 and 3.7). An optimal Kozak sequence element, composed of the nucleotides GCCRCCAUGG for vertebrates (with AUG being the start codon for translation),[138] within the 5' UTR of the IVT-mRNA should be included for an optimal translation initiation. Moreover, the 5' UTR should be unstructured and not include upstream open reading frames (uORFs), which impede or induce incorrect translation initiation (Ch. 3.6).
The 3' UTR has a strong influence on RNA-stability.[139–142] This is mediated through sequence elements such as AU- or GU-rich elements, where destabilizing RNA-binding proteins (RBPs) can bind.[142] In addition, binding sites for microRNAs (miRNAs) are generally located in the 3' UTR. Often, binding of these *trans*-factors to the *cis*-elements leads to degradation of the RNA. Accordingly, shorter 3' UTRs, which statistically have fewer binding sites for *trans*-acting factors, have been shown to correlate with higher stability of RNAs.[143,144] Thus, destabilizing motifs within the 3' UTR of synthetic IVT-mRNAs should be avoided, and ideally replaced by stabilizing sequences (see also Ch. 3.7).

Modification of the mRNA-nucleoside composition The mRNA is usually built out of four different nucleosides: uridine, adenosine, guanine and cytidine. Nevertheless, mammalian mRNAs contain modified nucleosides as well, such as 5-methylcytidine (m5C), N6-methyladenosine (m6A) or inosine.[145] As nucleoside modifications differ between bacterial and mammalian RNA, it helps immune cells to discriminate between foreign and host RNA. Thus, use of modified nucleosides is the goal in therapeutic IVT-mRNA, where low or even no immunogenicity is desired (Ch. 3.1, Protein-replacement therapies). The RNA-composition can easily be modified during *in vitro* transcription by using natural nucleosides such as 2-thiouridine, 5-methyluridine, m5C or pseudouridine, which are successfully incorporated into RNA during *in vitro* transcription.[146]

3.6 Translation of the (m)RNA

Although located at opposite ends of the RNA, the cap and the poly(A)-tail act synergistically for translation initiation and efficiency.[147,148] Moreover, they are both essential in

mediating mRNA protection and turnover as well (Ch. 3.7).[121] The cap is recognized by the eukaryotic translation initiation factor 4E (eIF4E), which is part of the cap-binding protein complex eIF4F (Fig. 3.7).[14,149] The poly(A)-binding protein (PABP) interacts not only with the poly(A)-tail, but also with other translation factors such as eIF4G, which is also part of the eIF4F complex. This interaction results in circularization of the mRNA (so-called *closed-loop* formation).[150] This not only stabilizes the mRNA by impeding binding of deadenylating and decapping enzymes (Ch. 3.7), but also promotes translation initiation through the recruitment of the small (40S) ribosomal subunit as part of the 43S pre-initiation complex.[150,151] The 43S initiation complex scans the mRNA in a 3'-end direction and binds to the first encountered AUG (start codon). There, the 40S ribosomal subunit is joined by the large 60S subunit to form the 80S ribosome, which starts the translation of the protein-encoded gene (Fig. 3.7).

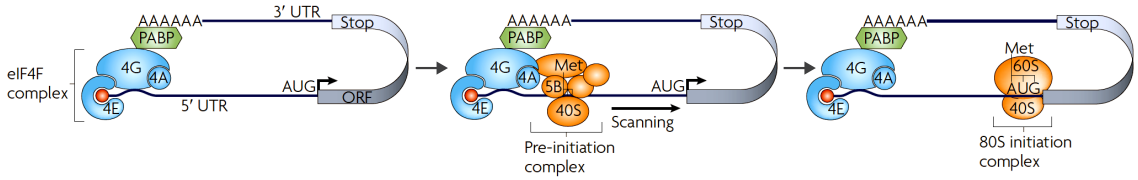

Figure 3.7: Translation initiation. Details are described in the text (modified from Besse *et al.*[152]).

In addition to affecting RNA stability (Ch. 3.5, Ch. 3.7), 3' UTRs contain regulatory elements influencing translation (Fig. 3.8). For instance, several RBPs impede the circularization of the mRNA - such as the *Drosophila* Bicoid or Bruno and *Xenopus* cytoplasmic polyadenylation element (CPE) binding proteins (CPEB) - thus repressing mRNA translation.[153–155] Another example is the γ-interferon-activated inhibitor of translation (GAIT) complex, which represses translation initiation without disturbing the closed-loop formation.[156] This complex binds to a specific secondary structure located within the 3' UTR of ceruloplasmin mRNA inhibiting ribosome recruitment.

Translational repression is also mediated by miRNAs in the form of ribonucleoprotein complexes, the so-called miRNA-induced silencing complexes (miRISCs).[157] These complexes bind to complementary sequences located within the 3' UTR. Base-pairing of the miRNAs with their targets often occurs imperfectly, often due to mismatches or bulged nucleotides.[158,159] Only binding of the seed-region (5' nucleotides 2 to 8) requires a perfect Watson-Crick base-pairing. The 3' region of the miRNA stabilizes the (suboptimal) miRNA-mRNA interaction. Multiple miRNA sites within the 3' UTR were observed to act cooperatively, thus mediating an effective translational repression at the initiation or postinitiation block.[160]

3.7 Lifetime of the (m)RNA

mRNAs in eukaryotes are typically degraded via the deadenylation-dependent mRNA-decay pathway (Fig. 3.9). The decay is thereby initiated by the enzymatic removal of the poly(A)-

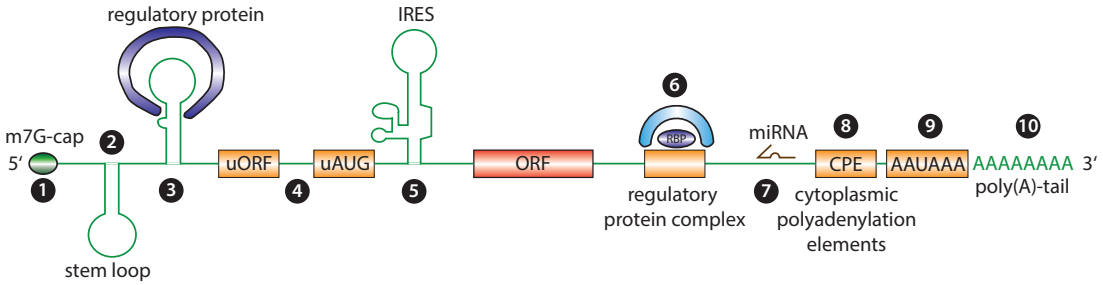

Figure 3.8: Elements of the mRNA influencing translation of the mRNA. Elements, which can be located within the 5′ UTR regulating translation, are for example the ❶ 5′ cap which is essential for translation initiation and efficiency; ❷ secondary structures (e.g. stem-loops), which impede binding and/or migration of the 40S ribosomal subunit; ❸ motifs for regulatory proteins; or ❹ upstream ORFs (uORFs) or AUGs (uAUGs), which provide an alternative start site, which lead to down-regulation of the main ORF. A cap-independent translation is mediated by ❺ the internal ribosome-entry sites (IRES). Different binding sites for ❻ regulatory protein (complexes) and ❼ miRNAs can be located within the 3′ UTR-region next to the ❽ CPE and the ❾ hexanucleotide AAUAAA, which are both required for lengthening of the ❿ poly(A)-tail, essential for translation initiation (modified from Wilkie *et al.*[149]).

tail via (i) the PABP-dependent poly(A) nucleases PAN2/PAN3; (ii) the CCR4-NOT complex, which include the transcriptional regulators carbon catabolite repression 4 (CCR4) and CCR4-associated factor (CAF1); and (iii) the poly(A)ribonuclease (PARN).[161–166] As soon as the poly(A)-tail reaches a critical length,[167,168] decapping at the 5'-end of the mRNA occurs via the Dcp1-Dcp2 complex together with the Lsm proteins and its associated enzymes, which are recruited to the deadenylated 3'-end. The transcript body is then digested in the 5'⟶3' direction by the exonuclease Xrn1.[169] The capped but deadenylated mRNA can also be degraded by the so-called exosome, a complex of 3'⟶5' exonucleases.[170] The remaining cap-structure is thereby removed by the scavenger-decapping enzyme DcpS.[171] Intriguingly, the deadenylation process has been shown to be inhibited by PABP, and activity of PARN to be cap-dependent (Ch. 3.5).[162,164]

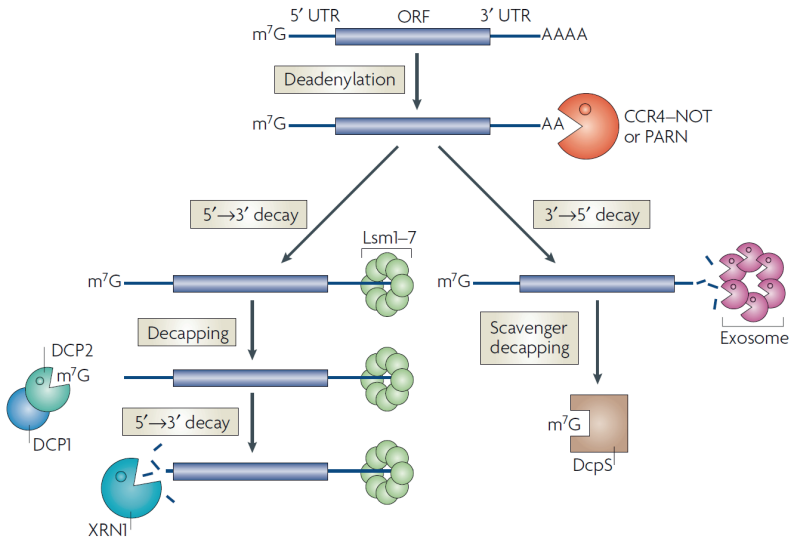

Figure 3.9: Deadenylation-dependent mRNA decay. Details are described in the text (modified from Garneau *et al.*[123]).

Different signals have been described, which control degradation of a specific mRNA. Determinants mediating RNA-stability are mainly found in the 3' UTR, but also in the 5' UTR and coding region (Ch. 3.5).[123] Different regulatory motifs and their respective RBPs have been described. Most prominent are the AU-rich elements (AREs) often found within the 3' UTR of short-lived mRNAs such as cytokines, proto-oncogenes and transcription factors.[172–174] The AUUUA pentamer represents the basic sequence element of the AREs and is bound, for instance, by the AU-rich binding factor-1 (AUF1), tristetraprolin (TTP) or the KH splicing regulatory protein (KSRP).[175–178] However, binding of the protein human antigen R (HuR) to ARE mediates stability of the RNA instead of its degradation.[179,180] Moreover, it was shown that sequences up- and downstream of the AREs influence the overall effect on RNA-stability. This was demonstrated, for example, with the 3' UTR of the TNFα transcript.[181] Furthermore, degradation of TNFα was observed to be mediated by miRNAs interacting with RBPs (Fig. 3.10).[182]

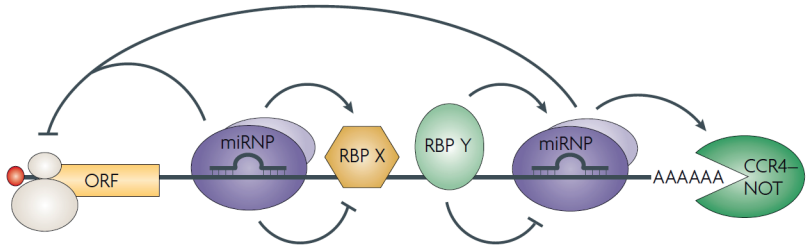

Figure 3.10: Interplay between RBPs and miRNAs for mRNA-regulation. *Cis*-acting elements recruit *trans*-acting factors such as RBPs and/or miRNAs to the mRNA. Both of them can recruit more factors and interact with each other to form so-called micro-ribonucleoproteins (miRNPs), thereby influencing - negatively or positively - translational efficiency and stability of the mRNA. Details are described in the text (by Filipowicz *et al.*[183]).

This interplay between miRNAs and RBPs was confirmed by other studies as well.[184–187] In contrast, there are stabilizing elements within transcripts encoding for proteins with housekeeping functions. The most prominent and well-characterized examples are the α-globin and β-globin,[188–191] , whose respective mRNAs have half-lives of more than one day.[192] Their stabilizing effect is promoted by a phylogenetically conserved pyrimidine-rich sequence element within both 3' UTRs.[189,190,193] RBPs of the α-CP/hnRNP-E family [α-globin poly(C)-binding protein/ heterogeneous nuclear ribonucleoprotein E] bind to this motif together with other *trans*-acting factors forming a multimeric complex and thus, hindering RNA-decay. Furthermore, a motif for the nucleolin-binding protein was found within the β-globin-3' UTR, which is known to stabilize the mRNA as well.[189,194] However, stability mediated by RBPs of the α-CP/hnRNP-E family is not limited to the globin-UTRs.[195] Investigations of the minimal β-globin-element, led to the identification of the characterized pyrimidine-rich sequence in other stable RNAs.[140]

Selected regions of viral RNAs of the semliki forest virus and sindbis virus have also been described to influence stability and translational efficiency of RNAs.[121] However, viral motifs often function only in the context of viral infection, as seen with the translational enhancer of the semliki forest virus capsid RNA.[196] Other stabilizing 3' UTRs were detected via

identification of stable cellular RNAs such as the elongation factor 1 α1 (eEF1A1) mRNA using bioinformatic analysis on housekeeping genes.[197] Another recent approach described the labeling of nascent RNA with 4-thiouridine[198] combined with the *stable isotope labeling by amino acids in cell culture* (SILAC) method.[199] This allowed the simultaneous measurement of RNA turnover and their respective proteins identifying, for instance, collagen α chain mRNAs, as stable RNAs in NIH3T3 mouse fibroblasts.[144] As a result, the thereby generated mouse model was proposed to be useful in predicting mRNA and protein abundance in other cell types as was shown with the MCF7 human breast cancer cell line. However, whether the stability of these stable mRNAs is mediated through the respective 3' UTRs must still be determined.

An interesting approach for the identification of new stabilizing mRNA elements was demonstrated by Chrzanowska *et al.*[200] Their approach is based on the *S*ystematic *E*volution of *L*igands by *EX*ponential Enrichment (SELEX)-process developed by Tuerk *et al.* and Ellington *et al.* in the early 1990s.[201,202] Selection of the new stabilizing elements was thereby accomplished under physiological conditions *in vivo* in human liver Hep G2 cells. Intriguingly, Chrzanowska and colleagues identified specific GU-rich elements, which, instead of promoting decay as commonly observed for GU containing RNA,[142] increased functional RNA half-life from 55 to 140 min.

However, despite of these identified stable mRNAs and 3' UTRs, the β-globin-3' UTR has been used widely in immunotherapy since its use in one of the first studies by Malone *et al.* demonstrating a 1,000 fold increase of protein production with capped mRNAs and β-globin as 3' UTR[5] (Ch. 3.2). Further improvement of the β-globin 3' UTR was achieved by Holtkamp *et al.* in 2006.[85] Higher levels and a prolonged persistence of the protein were observed using IVT-mRNAs containing two reiterated β-globin-3' UTR sequence elements - 2hBg - in human iDCs (hiDCs). This was mediated due to an enhanced stability and translational efficiency. Since then, this 3' UTR is not only used for further improvement of RNA vaccines in research and development, but also in clinical trials as well [ClinicalTrials.gov identifier: NCT02035956, NCT02316457].

However, there is one major drawback using two identical sequences in tandem as 3' UTR. They are prone to recombination during cloning and PCR amplification procedures, leading to undesired by-products lacking one element.[203,204] Thus, handling is aggravated, which impedes quick cloning and thus, timely preparation of (personalized) cancer vaccines.[72] Furthermore, on average RNAs with shorter 3' UTRs (below 100 nts) have been proven to increase translational efficiency and functional mRNA half-life compared to RNAs with longer 3' UTRs.[144,205] As the two reiterated β-globin-sequence elements have a total length of 284 nts, shortening of the 3' UTR could therefore potentially improve turnover of IVT-mRNA. In conclusion, a further optimization of the immunobioavailability of RNA-based immunotherapeutics is still required and would most likely improve antitumor efficacy and patient care.

Another intriguing aspect is the link between mRNA decay and translation (Ch. 3.6), which facilitates changes in gene expression.[123] Inhibition of translation initiation results in mRNA decay, but inhibition of translation elongation stabilizes the transcript. Several

proteins have been described that act both in RNA turnover and translation such as αCP or HuR.[195,206] Moreover, as deadenlyation results typically first in mRNA decay, the poly(A) is a determinant for both events as well (Ch. 3.6).[147,148]
In summary, these examples demonstrate that the cell must be able to respond quickly to external or internal stimuli by changing gene expression. This includes, not only modulation of RBPs, but also coordination of RNA turnover involving processes starting from its birth to death.

3.8 Aim of the thesis

In the last decades, much effort has been made to improve IVT-mRNAs for active cancer immunotherapy as a high stability ensures a high efficacy of the therapeutic. Nevertheless, not many 3' UTRs, which are the main determinant for RNA stabilization, have been tested and analyzed so far. Thus, the current choice of the 3' UTR, e.g. the 2hBg (two consecutive β-globin-3' UTRs), used now in RNAs for immunotherapy is more historically and practically justified, rather than based on rational design. Thus, the aim of this thesis was to develop a novel *in vitro* selection process within hiDCs to find new naturally occurring RNA sequence elements, which stabilize as 3' UTR the generic RNA backbone structure as used for preclinical and clinical studies in our group. Based on the rationale that each cell type has its individual transcriptome, a self-made library should be build with mRNA sequences derived from hiDCs. This in turn should limit complexity of the library as well, which could impede the selection process carried out in hiDCs as selective environment. At the end, individual 3' UTRs should be characterized and compared to the internal reference β-globin 3' UTR to elucidate improvement of intracellular pharmacokinetics regarding stability and also translational efficiency of the IVT-mRNA.

4 Materials

If not mentioned otherwise, materials were purchased from the corresponding manufacturer and suppliers as described in this Chapter.

4.1 Hardware

Table 4.1: Hardware.

Hardware	Manufacturer
ABI Prism 7300 Real Time PCR System	Applied Biosystems, Thermo Fisher Scientific, Darmstadt, Germany
Bioanalyzer 2100	Agilent Technologies, Waldbronn, Germany
Centrifuge 5810, Multifuge-X1R,-X3R	Heraeus Instruments, Hanau, Germany
Centrifuge Mikro 22R	Hettich, Tuttlingen, Germany
Clean bench Bio wizard Golden GL-200	Kojair, Vilppula, Finland
CO_2 Incubator	Binder, Tuttlingen, Germany
Duo Cycler	VWR International, Darmstadt, Germany
Electrophoresis power supply ST 606	Gibco, Life Technologies, Darmstadt, Germany
Electro Square Porator ECM 830	BTX Instrument Division, Harvard Apparatus, Inc. Holliston ,USA
FACS Canto II flow cytometer	BD Biosciences, Heidelberg, Germany
Fragment Analyzer	Advanced Analytical, Ames, USA
Gel documentation system Gel Jet Imager	Intas, Göttingen, Germany
Gene Pulser® II	Bio-Rad, München, Germany
HiSeq™ 2000 Sequencing System	Illumina, San Diego, USA
ImageQuant™ LAS 4000	GE Healthcare, München, Germany
Laminar flow bench herasafe	Heraeus Instruments, Hanau, Germany
MACS Magnet	Miltenyi Biotec, Bergisch Gladbach, Germany
Microscope Wilovert S	Hund, Wetzlar, Germany
Microscope DM2000	Leica, Wetzlar, Germany
Multifuge X1	Heraeus Instruments, Hanau, Germany
Multifuge X3R	Heraeus Instruments, Hanau, Germany
Multipette® plus	Eppendorf, Hamburg, Germany
NanoDrop 1000 UV-Vis Spectrophotometer	Thermo Scientific, St. Leon-Rot, Germany
NanoDrop 2000 UV-Vis Spectrophotometer	Thermo Scientific, St. Leon-Rot, Germany
Neubauer Chamber	Carl Roth GmbH, Karlsruhe, Germany
NucleoVac 96 Vacuum Manifold	Macherey-Nagel, Düren, Germany
PerfectSpinP	Peqlab, VWR International, Erlangen, Germany
Power supply Power Pac HC	Bio-Rad, München, Germany
Qubit® 2.0 Fluorometer	Invitrogen, Life Technologies, Darmstadt, Germany
Table centrifuge mikro 22R	Hettich, Tuttlingen, Germany
Thermocycler T3	Biometra, Göttingen, Germany
Thermomixer compact/comfort	Eppendorf, Hamburg, Germany
Tecan Infinite® M1000 Multimode Reader	Tecan, Crailsheim, Germany
TruSeq DNA Sample Preparation Kit	Illumina, San Diego, USA
Vortex-Genie 2	Scientific Industries, New York, USA
Vortexer VF2	IKA, Staufen, Germany
Vortex Wizard	VELP Scientifica, Usmate, Italy

4.2 Consumables

Consumables were mainly used from the following manufacturers: Becton Dickinson (Heidelberg, Germany), Greiner Bio-One (Essen, Germany), Life Technologies GmbH (Darmstadt, Germany), Miltenyi Biotec (Bergisch Gladbach, Germany), Nunc (Wiesbaden, Germany), Sarstedt AG & Co. KG (Nümbrecht, Germany), Thermo Scientific (Bonn, Germany) and Qiagen (Hilden, Germany).

4.3 Kits

Table 4.2: Kits.

Kit	Manufacturer
Agilent DNA 1000 Kit	Agilent Technologies, Waldbronn, Germany
Agilent High Sensitivity DNA Kit	Agilent Technologies, Waldbronn, Germany
Agilent RNA 6000 Nano Kit	Agilent Technologies, Waldbronn, Germany
Agilent RNA 6000 Pico Kit	Agilent Technologies, Waldbronn, Germany
Click-iT®Nascent RNA Capture Kit	Invitrogen, Life Technologies, Darmstadt, Germany
Cold Fusion Cloning Kit	System Biosciences, Inc., California, USA
Fast DNA End Repair Kit	Fermentas, Thermo Scientific, St. Leon-Rot, Germany
MinElute® Reaction Cleanup Kit	Qiagen, Hilden, Germany
MinElute® PCR Purification/Gel Extraction Kit	Qiagen, Hilden, Germany
NucleoBond® Xtra Midi/Maxi Plasmid DNA Purification Kit	Macherey-Nagel, Düren, Germany
NucleoSpin 8® Plasmid DNA Purification Kit	Macherey-Nagel, Düren, Germany
NucleoSpin® Plasmid DNA Purification Kit	Macherey-Nagel, Düren, Germany
Poly(A) Purist Kit	Ambion, Life Technologies, Darmstadt, Germany
QIAquick® PCR Purification/Gel Extraction Kit	Qiagen, Hilden, Germany
QuantiTect SYBR green Kit	Qiagen, Hilden, Germany
RiboZero rRNA Removal Kit	Epicentre Biotechnologies, Wisconsin, USA
RevertAid™ Premium First Strand cDNA Synthesis Kit	Fermentas, Thermo Scientific, St. Leon-Rot, Germany
RNA 6000 LabChip® Kit	Agilent Technologies, Waldbronn, Germany
RNase free DNAse Kit	Qiagen, Hilden, Germany
RNeasy® MinElute® Cleanup Kit	Qiagen, Hilden, Germany
RNeasy® Mini/Midi Kit	Qiagen, Hilden, Germany
ScriptSeq mRNA-Seq Library Preparation Kit	Epicentre Biotechnologies, Wisconsin, USA

4.4 Chemicals and reagents

Chemicals and reagents not listed in Tab. 4.3 such as anorganic salts, HEPES (4-(2-hydroxyethyl)-1-piperazineethanesulfonic acid) and ethanol were mainly purchased from AppliChem (Darmstadt, Germany), Becton Dickinson (Heidelberg, Germany), Merck (Darmstadt, Germany), Roth (Karlsruhe, Germany) and Sigma-Aldrich (München, Germany). Antibodies (Tab. 4.4) were always kept between 2 °C and 8 °C or on ice and opened in shaded working benches.

Table 4.3: Reagents.

Reagent	Manufacturer
2'deoxy-5-methylcytidine 5'-triphosphate, sodium salt (dm^5CTP)	Fermentas, Thermo Scientific, St. Leon-Rot, Germany
5-ethynyl uridine (EU)	Invitrogen, Life Technologies, Darmstadt, Germany
7-Aminoactinomycin D (7-AAD) Viability Dye	BD Biosciences, Heidelberg, Germany
Actinomycin D from *Streptomyces* sp.	Sigma-Aldrich, München, Germany
Advantage® UltraPure PCR Deoxynucleotide Mix	Clontech, Saint-Germain-en-Laye, France
Agencourt® AMPure® XP	Beckman Coulter, Krefeld, Germany
CD14 MicroBeads, human	Miltenyi Biotec, Bergisch Gladbach, Germany
Dynabeads® MyOneTM Carboxylic Acid	Invitrogen, Life Technologies, Darmstadt, Germany
Fetal calf serum	Gibco, Life Technologies, Darmstadt, Germany
Human serum albumin (HSA)	Invitrogen, Life Technologies, Darmstadt, Germany
Human GM-CSF, premium grade	Miltenyi Biotec, Bergisch Gladbach, Germany
Human IL-4, premium grade	Miltenyi Biotec, Bergisch Gladbach, Germany
Human IL-6, premium grade	Miltenyi Biotec, Bergisch Gladbach, Germany
Non-essential amino acids (NEAA)	Invitrogen, Life Technologies, Darmstadt, Germany
One Shot® OmniMAX™ 2 $T1^R$	Invitrogen, Life Technologies, Darmstadt, Germany
Penicillin / Streptomycin	Invitrogen, Life Technologies, Darmstadt, Germany
RPMI 1640-Glutamax Medium	Invitrogen, Life Technologies, Darmstadt, Germany
Sodium acetate (3 M ; pH 4.5)	Ambion, Life Technologies, Darmstadt, Germany
Sodium pyruvate	Invitrogen, Life Technologies, Darmstadt, Germany
SYBR®Gold Nucleic Acid Gel Stain	Invitrogen, Life Technologies, Darmstadt, Germany
Triton-X100	Applichem, Darmstadt, Germany
X-Vivo	Bio Whittaker Europe, Verviers, Belgium

Table 4.4: Antibodies used for fluorescence-activated cell sorting (FACS)- and fluorescence staining.

Antibody	Manufacturer
Alexa Fluor® 488 Mouse anti-human CD14	BD Biosciences, Heidelberg, Germany
Allophycocyanin (APC) Mouse anti-human CD83	BD Biosciences, Heidelberg, Germany
Anti-Mouse immunglobulin (Ig), κ/Negative Control Compensation Particles Set	BD Biosciences, Heidelberg, Germany
Phycoerythrin (PE) Mouse Anti-Human CD209	BD Biosciences, Heidelberg, Germany

4.5 Buffers, solutions and cell culture media

Buffers, solutions and media used in this work were autoclaved or sterile-filtered with the exception of products purchased directly from the manufacturer.

Table 4.5: Buffers, media and solutions for molecular biology methods.

Buffer	Composition
Blue marker and loading buffer for agarose gels	0.25 % Bromphenol blue [v/v], 0.25 % Xylene cynole FF [v/v], 0.25 % Orange G [v/v], 1 mM ethylenediaminetetraacetic acid (EDTA), 40 % Sucrose
Click-Chemistry Wash-solution	2 % fetal calf serum, heat inactivated (FCS-HI), phosphate buffered saline (PBS)
diethyl dicarbonate (DEPC) water	1 mL DEPC, 1 L double-distilled water (ddH_2O)
Luria-Bertani (LB)-agar	15 g Agar, 1 L LB-medium
LB-medium	1 % Trypton [w/v], 0.5 % yeast extract [w/v], 1 % sodium chloride NaCl [w/v]
Luciferin-solution	1 mg mL^{-1} Luciferin, 50 mM HEPES, 1 mL ddH_2O
Paraformaldehyde (PFA), 1 %	540 µL 37 % PFA, 19.45 mL PBS
Tris-Acetat-EDTA (TAE) gel (x %)	x % agarose [w/v], 100 mL 1x TAE-buffer, 75 µL 0.05 % ethidium bromide
Triton-X, 0.5 %	250 µL Triton-X, 49.75 mL PBS

Table 4.6: Buffers, media and solutions for cell culture.

Buffer	Composition
Freezing medium	10 % dimethyl sulfoxide (DMSO) in FCS-HI [v/v]
hiDC-medium	10 % FCS-HI [v/v], 1 % 100 mM Sodium pyruvate [v/v], 1 % 100x NEAA [v/v], 0.5 % 100 U mL^{-1} Penicillin/ 100 µg mL^{-1} Streptomycin (P/S) [v/v], 500 mL RPMI-medium containing Glutamax
PBS/EDTA	5 % EDTA [v/v], 500 mL PBS

Table 4.7: Buffers and solutions for flow cytometry, MACS^{TM} technology and fluorescence stainings.

Buffer	Composition
FACS-buffer	5 % FCS-HI [v/v], 5 mM EDTA
Fixation buffer (FACS)	1 % PFA in PBS
MACS-buffer	5 % FCS-HI [v/v], 20 % Human serum albumin (HSA) [v/v], 1 % EDTA [v/v], 500 mL PBS
PFA, 4 %	540 µL 37 % PFA, 4.46 mL PBS

Table 4.8: Purchased solutions and media.

Solutions/ media	Manufacturer
S.O.C. (Super Optimal broth with Catabolite repression) Medium	Invitrogen, Life Technologies, Darmstadt, Germany
Sodium Acetate, 3 M, pH 5.5	Ambion, Life Technologies, Darmstadt, Germany
Tris, 1 M, pH 7.0/ pH 8.0	Ambion, Life Technologies, Darmstadt, Germany

4.6 Enzymes

Enzymes (Tab. 4.9) were purchased with reaction buffers mainly from Fermentas (Thermo Scientific, St. Leon-Rot, Germany) and NEB (Frankfurt a.M., Germany).

Table 4.9: List of enzymes and their suppliers.

Enzyme	Manufacturer
Bright-Glo™ Luciferase Assay System	Promega, Madison, WI, USA
EcoRV-HF™	New England Biolabs, Frankfurt a.M., Germany
FastAP™ Thermosensitive Alkaline Phosphatase	Fermentas, Thermo Scientific, St. Leon-Rot, Germany
NotI-HF™	New England Biolabs, Frankfurt a.M., Germany
Nuclease P1	Sigma-Aldrich, München, Germany
RevertAid™ Premium Reverse Transcriptase	Fermentas, Thermo Scientific, St. Leon-Rot, Germany
RiboLock™ RNase Inhibitor	Fermentas, Thermo Scientific, St. Leon-Rot, Germany
PfuUltra Hotstart DNA Polymerase	Agilent Technologies, Waldbronn, Germany
Phusion® Hot Start Flex DNA Polymerase	New England Biolabs, Frankfurt a.M., Germany
RNase H	Fermentas, Thermo Scientific, St. Leon-Rot, Germany
SuperScript™ II Reverse Transcriptase	Invitrogen, Life Technologies, Darmstadt, Germany
TURBO™ DNase	Ambion, Life Technologies, Darmstadt, Germany

4.7 Ladders

Table 4.10: Ladders.

Ladder	Manufacturer
GeneRuler™ 1 kb DNA Ladder	Fermentas, Thermo Scientific, St. Leon-Rot, Germany
GeneRuler™ 50 bp DNA Ladder	Fermentas, Thermo Scientific, St. Leon-Rot, Germany
QuickLoad 2-log DNA	New England Biolabs, Frankfurt a.M., Germany
QuickLoad 50bp DNA	New England Biolabs, Frankfurt a.M., Germany
RiboRuler™ Low Range RNA Ladder	Fermentas, Thermo Scientific, St. Leon-Rot, Germany

4.8 Nucleotide sequences

Primers <50 nts were synthesized by Eurofins Genomics GmbH (Ebersberg, Germany). Primers and single stranded (ss)DNA >50 nts were mainly ordered at IDT (Integrated DNA Technologies, Leuven, Belgium). Primers used for cold fusion cloning technology are depicted separately in Supplementary Tab. A.1.

Table 4.11: Primers. The binding region of the PCR-primers is underlined.

Primer	Sequence (5′ ⟶ 3′)
Sequencing	
3UTR-check-d2eGFPmut	GAT GAT GGC ACG CTG CCC ATG
3UTR-check-luc2mut	GAA GGA GAT CGT GGA CTA TGT GG
3UTR-check-luc2CPmut	CCA GGA GAG CGG CAT GGA TAG
d2eGFP-ende2	GAT GAT GGC ACG CTG CCC ATG
d2eGFP-For2	CGC ACC ATC TTC TTC AAG GAC
T7up	CTC ACA TGT TCT TTC CTG CG
PCR	
bGlo-deltaL-FW	TAA GTA AGC TCG AGG AGA GCT CGC TTT CTT GCT G
bGlo-deltaL-REV	TTT AGA GCT AGC GAC GCA GCA ATG AAA ATA AAT G
d2eGFP-FW-T7p	CGC CTC GAG AAT TAA TAC GAC TCA CTA TAG GGC GAA CTA GTA CTC TTC TGG TCC CCA CAG ACT C
d2eGFP-noUTR-REV-T60	T60-GAT CCT TAC ACA TTG ATC CTA GCA GAA GCA CAG G
LIB-Cloning-FW	GGA TCA ATG TGT AAG GAT CCG
LIB-Cloning-REV	CTC AAT GCC GTA TCC CAT CTT AGC GGC CGC
LIB-FW-T7-2	CGC CTC GAG AAT TAA TAC GAC TCA CTA TAG GGC GAA CTA GTA CTC TTC TGG TCC CCA CAG ACT C
LIB-REV-T60	T60-CTC TTT GCC GTA TCC CAT CTT AGC
LUC2-FW-T7p	CGC CTC GAG AAT TAA TAC GAC TCA CTA TAG GGC GAA CTA GTA TTC TTC TGG TCC CCA CAG ACT C
LUC2CP-FW-T7p	CGC CTC GAG AAT TAA TAC GAC TCA CTA TAG GGC GAA TAG TAC TCT TCT GGT CCC CAC AGA CTC
LUC2-noUTR-REV-T60	T60-CTC GAG TTA CAC GGC GAT CTT GC
LUC2CP-noUTR-REV-T60	T60-AGT TAG ACG TTG ATC CTG GCG CTG G
negCtrl-REV-T60	T60-CCG ATA TCG GAT CCT TAC ACA TTG ATC C
NGS-FW-BpmI	CCT GCA GCC TGT GCT TCT GCT AGC TGG AGT GTG TAA GGA TCC G
NGS-REV-BpmI	T24-CTC AAT GCC TGG AGC CAT CTT AGC GGC CGC
RT-qPCR and cDNA-synthesis	
dT18	TTT TTT TTT TTT TTT TTT
d2eGFP-sense	CAC ATG AAG CAG CAC GAC TTC
d2eGFP-antisense	CAC CTT GAT GCC GTT CTT CTG
hPRT1-sense	TGA CAC TGG CAA AAC AAT GCA
hPRT1-antisense	GGT CCT TTT CAC CAG CAA GCT
LIB-cDNA-REV-RandomHexamer	CGT ATC CCA TCT TAG CGG CCG C NNNNNN

Table 4.12: ssDNA used for modification of vector backbones.

Name	Sequence (5′ ⟶ 3′)
UTR-Adap-FW1	GATCCGATAT CGGATCACTC TCTCGCCGAA ACTACAAGAG ACAAGCAGAC ACAAGTTCAC AACGTCTAGC GGCCGCTAAG ATGGGATACG GCAAAGAGCT
UTR-Adap-REV1	CTTTGCCGTA TCCCATCTTA GCGGCCGCTA GACGTTGTTG AACTTGTGTC TGCTTGTCTC TTGTAGTTTC GGCGAGAGAG TGATCCGATA TCG
UTR-Adap-FW1-GFP	GATCCGATAT CGGATCACTC TCTCGCCGAA ACTACAAGAG ACAAGCAGAC ACAAGTTCAA CAACGTCTAG CGGCCGCTAA GATGGGATAC GGCATTGAGC T
UTR-Adap-REV1-GFP	CAATGCCGTA TCCCATCTTA GCGGCCGCTA GACGTTGTTG AACTTGTGTC TGCTTGTCTC TTGTAGTTTC GGCGAGAGAG TGATCCGATA TCG
A60-Linker sense	GTAAGTAAGC TCGAGGTAAC ATATGGTGAG CTAGCTCTAA AAAAAAAAAA AAAAAAAAAA AAAAAAAAAA AAAAAAAAAA AAAAAAAAAA AAAAAAAAGA AGAGCT
A60-Linker antisense	CTTCTTTTTT TTTTTTTTTT TTTTTTTTTT TTTTTTTTTT TTTTTTTTTT TTTTTTTTTT TTTAGAGCT AGCTCACCAT ATGTTACCTC GAGCTTACTT ACTGCA

4.9 Software

Table 4.13: Software.

Software	Manufacturer
Agilent 2100 Bioanalyzer	Agilent Technologies, Waldbronn, Germany
Clone Manager Professional	Sci-Ed Software, North Carolina, USA
FACSDiva Software 6.0	BD Biosciences, Heidelberg, Germany
FlowJo 7.6.5.	FlowJo, Oregon, USA
GraphPad 5.5	GraphPad Software, San Diego, USA
ImageJ	Wayne Rasband, Research Services Branch, National Institute of Mental Health, Bethesda, MD, USA
Matlab 16	The MathWorks GmbH, Ismaning, Germany
R	The R Foundation for Statistical Computing, Vienna, Austria

5 Methods

5.1 Molecular biological methods

If not otherwise stated, bacterial cells, DNA and consumables were handled as follows. Bacterial cells were incubated at 37 °C. Consumables were autoclaved and kept sterile prior use. Solutions and buffers were kept between 2 °C and 8 °C or on ice during pipetting and preparation of reaction mixtures. Reaction mixtures such as enzyme digests, ligations or PCRs were prepared according to the manufacturer's recommendations. DNA was purified from reaction mixtures using the NucleoSpin® Plasmid and eluted twice with ddH_2O according to the manufacturer's protocol. Concentration of the DNA was measured using the NanoDrop 1000/2000 UV-Vis Spectrophotometer (Ch. 5.1.10). Purity and appearance were monitored with the Bioanalyzer 2100 (Ch. 5.1.11) or via analytical agarose gel. If not directly used for further experiments, the DNA was kept between -15 °C and -25 °C and for long-term storage between -65 °C and -85 °C.

5.1.1 Plasmid vector constructs

The plasmid vector constructs used in this work are based on the pST1-A120 vectors described in Holtkamp *et al.*[85] The pST1-A120 features a T7-promoter, a human α-globin-Kozak region as 5' UTR (hAg-Kozak), two consecutive human β-globin-3' UTR regions as 3' UTR, a 120 bps long poly(A) tail and a Neomycin resistance gene (Fig. 5.1).
For library build up (Ch. 5.4) and analysis of newly selected 3' UTRs (Ch. 5.5) the vector backbones with d2eGFPmut and luc2CPmut as reporter genes (Ch. 5.1.2) were modified by removing the T7-promoter and the poly(A)-tail. This was done enzymatically using class II restriction enzymes in a double digest reaction as recommended by the manufacturer. PacI and SpeI were used to remove the T7-promoter. The linearized plasmid was purified via agarose gel preparation and overhangs were then blunted via the T4 DNA polymerase and ligated with the T4 DNA ligase. After verification of the plasmid sequence (Ch. 5.1.9), the poly(A)-tail was removed with BamHI and SacI and ligated (Ch. 5.1.6) back via insertion of a *UTR-adapter* (Ch. 5.1.4). This *UTR-adapter* (Fig. 5.1) allowed the introduction of the EcoRV and NotI restriction sites and a primer binding site (*pbs*) needed for cloning of the library sequences (Ch. 5.4.5) and PCR amplification (Ch. 5.5) respectively. The DNA was purified and verified by sequencing (Ch. 5.1.9).

5.1.2 Reporter genes

Different reporter genes were used throughout this work depending on the experimental setup and read-out (Tab. 5.1). The destabilized luciferase luc2CPmut has a lower protein half-life compared to luc2mut, facilitating analysis of RNA-stability by measuring its activity.[207]

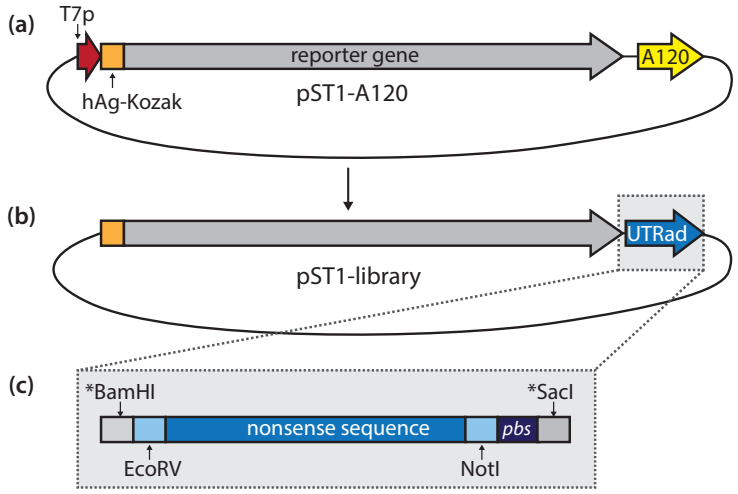

Figure 5.1: Plasmid vector constructs. **(a)** pST1-A120 vector used as starting plasmid for optimization of vector backbone for cloning of library sequences. **(b)** Plasmid for cloning of library sequences - pST1-library - without T7-promoter and poly(A)-tail, but featuring a UTR-adapter (103 bps). **(c)** UTR-adapter featuring a NotI- and EcoRV-restriction site separated by a nonsense sequence (58 bps) and a primer binding site (*pbs*; 17 bps) for cDNA-synthesis and PCRs. *BamHI and *SacI: correct overhangs respectively for easy ligation into linearized plasmid.

Table 5.1: Reporter genes used in this work for *in vitro* selection and analysis of 3′ UTRs. [eGFP: enhanced green fluorescent protein; FACS: fluorescence-activated cell sorting; RT-qPCR: quantitative real-time PCR]

Reporter gene	Background	Read-out	Experiments
d2eGFPmut	GFP	FACS (Ch. 5.2.7), RT-qPCR (Ch. 5.3.3)	*in vitro* selection (Ch. 5.5)
luc2CPmut	destabilized luciferase	bioluminescence	analysis of 3′ UTRs (Ch. 5.6)
luc2mut	luciferase	bioluminescence	analysis of 3′ UTRs (Ch. 5.6)

5.1.3 3′ UTR used as controls for analysis of newly selected 3′ UTRs

Control RNAs used in this work differed in their 3' UTRs. The internal reference *2hBg* (284 nts/bps), previously identified as optimal for RNA stabilization,[85] contains two consecutive human β-Globin 3' UTRs; *hBg* (142 nts/bps) has only one single human β-Globin 3' UTR-element; *UTRad* (103 nts/bps) refers to the UTR-adapter used for cloning of the library (Ch. 5.1.4 and 5.4.5); and *noUTR* served as negative control, as this RNA did not contain any 3' UTR, but only 3 nts/bps between the reporter gene and poly(A)-tail.

5.1.4 Hybridization of ssDNA fragments for insertion into vector backbones

Sense and corresponding antisense sequence were pipetted in equimolar amounts (5 µM, total volume 40 µL) and hybridized according to the protocol described in Tab. 5.2. The success of hybridization was monitored via a 10 % polyacrylamid gel and via sequencing (Ch. 5.1.6) after ligation into the vector backbone (Ch. 5.1.6).

Table 5.2: Protocol for hybridization of sense and antisense sequence of UTR-adapter.

Time	Temp.
10 min	95 °C
each step 3 min	stepwise reduction of temperature by 5 °C starting at 90 °C, down to 50 °C
10 min	22 °C
hold	between 2 °C and 8 °C

5.1.5 Purification of nucleic acids via magnetic beads

Paramagnetic beads (Agencourt® AMPure® XP) are widely used for purification of single (ss) or double stranded (ds) DNA to remove salts, enzymes, primers and other contaminants from any reaction mixture. Furthermore, the beads can be used for size-selection of DNA-fragments.[208,209]

Each bead consists of a polystyrene core surrounded by a magnetite layer. This layer is coated with carboxyl molecules groups. The reversible binding of the DNA is mediated by the presence of polyethylene glycol (PEG) and salt, which are contained in the bead solution (20 % PEG, 2.5 M NaCl). Thus, the immobilization depends on the concentration of both substances. Therefore, the volumetric ratio of beads and DNA can be used to efficiently size select DNA fragments. As the total charge per DNA molecule is larger with longer DNA-fragments, the electrostatic interaction with the beads is higher, so that smaller fragments are displaced. Thus, the lower the ratio between beads and DNA, the larger the eluted fragments and vice versa.

The magnetic beads were equilibrated to room temperature (RT) for at least 30 min before starting with the size-selection and purification of DNA-samples. The beads were thoroughly homogenized and mixed with the DNA reaction mixture at the desired volumetric ratio (Fig. 5.2). The samples were next incubated for 15 min at RT and another 5 min on a magnetic rack to separate both beads and bound DNA from contaminants. To discard contaminants, supernatant (SN) was aspirated carefully and the beads were washed twice with 70 % ethanol (EtOH) - EtOH covering both beads and bound DNA completely for at least 30 s, thereby leaving the samples on the magnetic rack. The beads and the bound DNA were next dried for at least 30 min at RT. To elute the DNA, ddH_2O was mixed with the beads and left for 5 min at RT on the tube rack. The DNA-bead-mixture was bound for 5 min on the magnetic rack and the eluate containing the dissolved DNA was transferred into a new tube. The DNA fragments expected to be in the SN, were purified by transferring the SN to a new tube before adding the correct volume of magnetic beads and continuing with the protocol as described above.

5.1.6 Ligation of fragments into vector backbones

The fragments were enzymatically ligated into the vector backbones via the T4 DNA ligase according to manufacturer's recommendations with the following changes. Ligation of

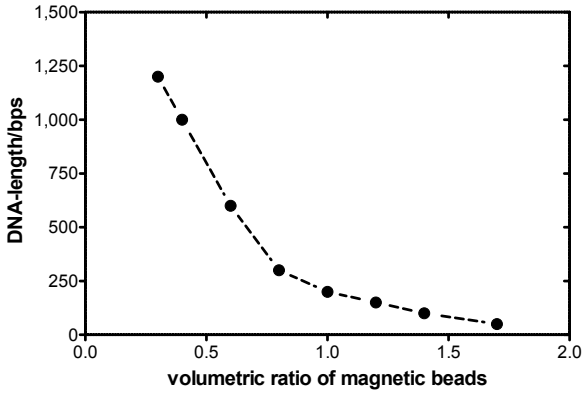

Figure 5.2: Volumetric ratio of magnetic beads for size-selection of DNA-fragments. The cut-off depends on the volumetric ratio between the DNA and the magnetic beads. For example, a ratio of 1.0 volume purifies DNA fragments > 200 bps.

inserts with blunt and sticky ends was optimized as described by Lund *et al.*. For this, temperature cycling between 4 and 30 °C - each temperature for 30 s - was applied to meet the requirements of blunt and sticky DNA-ends. A low temperature reduces ligase activity, thus allowing the enzyme to ligate blunt DNA-ends more efficiently. In contrast, a higher temperature increases overall molecular motion, which improves ligation of sticky ends.[210] Ligation of inserts with sticky ends at both 5' and 3' DNA-ends was done by increasing the temperature slowly from 4, up to 16 and finally 22 °C, each temperature for 2 h.

5.1.7 Transformation

The transformation was done via chemically competent *E. coli* (One Shot® TOP10/ One Shot® OmniMAX™ 2 T1 Phage-Resistant Cells, Invitrogen, Life Technologies, Darmstadt, Germany) and DNA in a ratio of 10:1 respectively. The protocol was followed according to manufacturer's recommendation with the following changes. After adding the DNA to the bacterial cells, mixture was left for 15 min on ice. The cells were heat-shocked and 500 µL of pre-warmed S.O.C. medium was added. If necessary, the bacterial cells were diluted with LB-medium before spreading on a pre-warmed selective plate.

5.1.8 Plasmid DNA purification from bacterial cultures

The plasmid DNA was purified using the NucleoBond® Xtra Mini, Midi or Maxi kit, depending on the starter culture volume prepared according to manufacturer's protocol. The DNA was eluted from the NucleoBond® Xtra Column using the NucleoBond® Finalizer according to manufacturer's protocol.

5.1.9 Sequencing

To verify the sequence of the plasmid DNA, inserts or PCR-products, samples were prepared and shipped according to protocol of Eurofins Genomics GmbH (Ebersberg, Germany).

5.1.10 Spectralphotometric analysis of nucleic acids

The concentration and purity of nucleic acids was measured using the NanoDrop 1000/2000 UV-Vis Spectrophotometers according to manufacturer's recommendations.

5.1.11 Analysis of nucleic acids via 2100 Bioanalyzer

The Agilent 2100 Bioanalyzer is based on capillary electrophoresis by using Lab-on-a-Chip technology. It allows the accurate analysis of quality and integrity of nucleic acids.[211] Nucleic acids were mainly analyzed by the 2100 Bioanalyzer according to manufacturer's recommendations. The lower and - in case of the High Sensitivity DNA Kit - upper marker peak (25 nts and 10,380 bps, respectively) are used as internal standards to align the data of both ladder and samples. The peak sizes of the ladder (nts/bps) were calculated from the migration time.

5.2 Cell biological and immunological methods

If not otherwise stated, the centrifugation of cells was done for 8 min at 311 x g.

5.2.1 Cultivation of cells

The cells were handled by using aseptic cell culture techniques and cultivated in sterile incubators with 5 % CO_2 at 37 °C.

5.2.2 Determination of cell density

The cell density was determined by using the Neubauer hemocytometer counting chambers. For this, a 30 µL cell suspension and Trypan Blue[212] was prepared in a ratio of 1:2. For higher dilutions the cell suspension was first diluted with PBS. A minimum of three quadrants were counted (Eq.5.1). The cell density and the total cell number (Eq.5.2) were calculated as follows:

$$\text{Cell density } [\text{mL}^{-1}] = \frac{\text{counted cells}}{\text{number of counted quadrants}} \cdot \text{dilution factor} \cdot 10^4 \tag{5.1}$$

$$\text{Total cell number} = \text{cell density} \cdot \text{volume of cell suspension } [\text{mL}] \tag{5.2}$$

5.2.3 Extraction of peripheral blood mononuclear cells using ficoll

Peripheral blood mononuclear cells (PBMC) were isolated from blood provided by the Blood Bank of University Medical Center Mainz using Ficoll density gradient centrifugation. The blood was filled up with PBS up to approx. 150 mL and carefully layered on Ficoll. The density gradient centrifugation was carried out for 25 min at RT and 779 x g with deceleration set on 3 to inhibit phase separation. After centrifugation, the plasma and buffy coat layer were carefully transferred into new tubes and centrifugated. The SN was transferred into new tubes and filled up with cold PBS containing 2 mM EDTA (PBS/EDTA). The pellet was resuspended and the tube was filled up as well with PBS/EDTA. Two washing

steps were carried out by discarding the SN after each centrifugation step, resuspension and filling up of pellet with PBS/EDTA. The pellets were then combined through a cell strainer (70 µm filter mesh size) and filled up to 50 mL with cold PBS/EDTA. For determination of the cell density and total cell number, 30 µL of cell suspension were used in a 1:10 dilution with PBS and Trypan blue (Ch. 5.2.2). The PBMC were next used for isolation of $CD14^+$ monocytes (Ch. 5.2.4) or frozen between -65 °C and -85 °C (Ch. 5.2.6).

5.2.4 Generation of human immature dendritic cells (hiDCs)

For the generation of hiDCs $CD14^+$ monocytes were enriched from fresh PBMC by using anti-CD14 microbeads and MACS™ technology according to the kit's protocol with the following changes. Twelve µL of beads were used per 1×10^7 cells and were washed by filling the tube up to 50 mL with fridge cold MACS buffer. After centrifugation the cell pellets were resuspended in 2 mL MACS buffer before proceeding with the magnetic separation. The elution of labeled cells was done twice with each 5 mL cold hiDC-medium.
After determination of the cell number of the eluted fraction (Ch. 5.2.2) the $CD14^+$ monocytes were seeded in cell culture flasks with a density of approx. 1×10^6 cells per mL hiDC-medium supplemented with human (h)IL-4 (1,000 U/mL) and hGM-CSF (1,000 $U mL^{-1}$). The aliquots of the effluent (approx. 100 µL) and the eluted fraction ($0.75 - 1.25 \times 10^6$) were used for further analysis via flow cytometry to confirm the success of magnetic separation and purity of isolated $CD14^+$ monocytes.
On day two or three appearance of the cells was monitored microscopically and the cells were fed with fresh hiDC-medium supplemented with hIL-4 (1,000 $U mL^{-1}$) and hGM-CSF (1,000 $U mL^{-1}$). The hiDCs were harvested at day four (Ch. 5.2.5) and quality and purity was monitored by flow cytometry (Ch. 5.2.7).

5.2.5 Harvesting of hiDCs

The whole cell suspension was transferred to a 50 mL tube. To detach the remaining cells, 10 mL of cold PBS/EDTA was added to the cell culture flask. After a 10 min incubation at 37 °C, the flask was tapped carefully on the side and cells were thoroughly resuspended before transferring them to the cell suspension. After centrifugation the cell pellet was resuspended in an appropriate amount of PBS/EDTA. The cell density and total cell number were determined (Ch. 5.2.2) and an aliquot was prepared for flow cytometric analysis (Ch. 5.2.7). The hiDCs were used directly for experiments or frozen between -65 °C and -85 °C (Ch. 5.2.6).

5.2.6 Freezing and thawing of hiDCs

The hiDCs were pelleted after harvesting (Ch. 5.2.5) and resuspended in cold freezing medium. A maximum of 3.0×10^7 cells mL^{-1} were frozen per cryogenic vial. The cells were quickly transferred into an appropriate freezing container (Mr. Frosty™ Freezing Container) and stored between -65 °C and -85 °C. After 24 h the cryogenic vials were transferred into liquid nitrogen.

For thawing, the hiDCs frozen in cryogenic vials were defrosted at 37 °C in a pre-warmed water bath and carefully pipetted into pre-warmed PBS/EDTA. The cells were washed twice with PBS/EDTA and the cell density and total cell number were determined (Ch. 5.2.2).

5.2.7 Flow cytometric analysis of cells

The centrifugation of cells during preparation for flow cytometric analysis was done for 6 min at 486 x g. For each sample, an aliquot of $0.75-1.0\times10^6$ cells was transferred to round-bottom tubes, 12 x 75 mm. The control samples included one unstained sample (prepared without antibodies) and compensation controls stained each with only one antibody.
During the centrifugation of the cells, master mix was prepared containing FACS-buffer and respective antibodies (Tab. 5.3) calculating 50 µL of total volume for each sample tube. 7-AAD was used to determine cell viability as this fluorescent intercalator is generally excluded from live cells.[213]

Table 5.3: Master-mix for staining of samples to be measured by flow cytometry. Volume of each sample was filled up to 50 µL with FACS-buffer after addition of antibodies and/or 7-AAD.

Analysis of hiDC purity[85]	Volume	Specificity
α-CD83-APC	14 µL	Maturation marker
α-DC-Sign/CD209-PE	12 µL	hiDC-cell specific marker
7-AAD	2.5 µL	Control of viability
Analysis of MACS outcome		
α-CD14-PE	2 µL	Marker specific for $CD14^+$ monocytes
7-AAD	2.5 µL	Control of viability
Analysis of eGFP expression		
7-AAD	2.5 µL	Control of viability

The mastermix was added to the cell pellets. The tubes were carefully vortexed before incubation for 10-20 min on ice in the dark. Next, 3 mL FACS-buffer were added to each tube and the samples were centrifuged. For fixation, the cell pellets were resuspended in 150 µL freshly prepared 1 % PFA solution. The samples were kept between 2 °C and 8 °C until acquisition of 1.0×10^5 events per sample via BD FACS Canto II within the next 24 h according to manufacturer's recommendation. To remove the effects of spillover emission, the compensation was done according to protocol of BD FACS Diva software. The raw data was analyzed with the FlowJo-software (Ch. 5.2.8).

5.2.8 Analysis of flow cytometric raw data

The raw data of the flow cytometric measurements was analyzed by using FlowJo-software as exemplarily shown in Fig. 5.3.

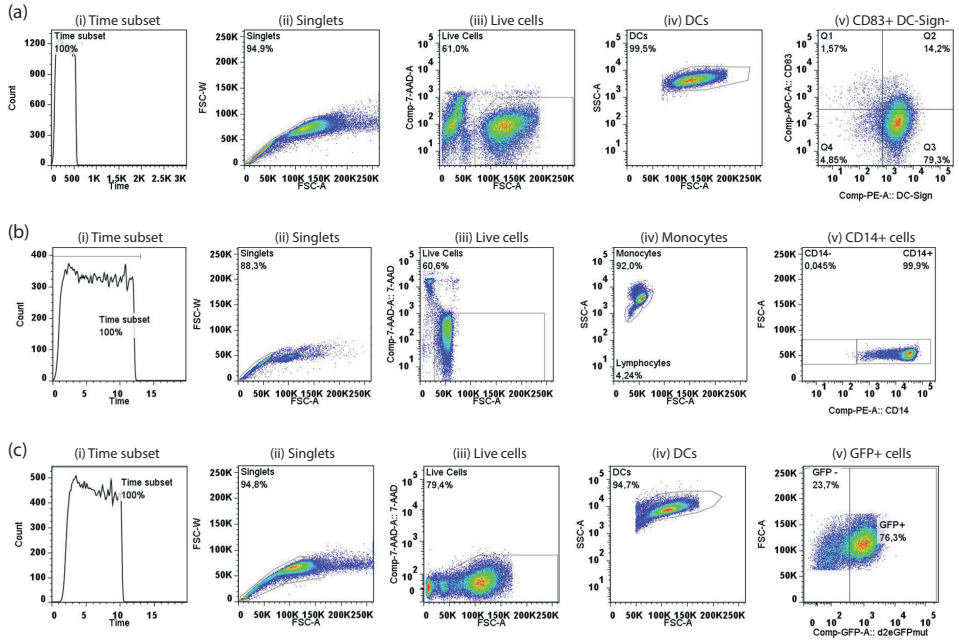

Figure 5.3: Analysis of flow cytometric raw data from (a) analysis of hiDC-purity, (b) enrichment of $CD14^+$ monocytes and (c) $eGFP^+$ cells. (i) Setting of measurement time. (ii) Exclusion of doublets by gating singlets. (iii) Gating of live cells. (iv) Gating of DC (a,c) and monocytes (b) respectively. (v) Gating of (a) $CD83^-$DC-$Sign^+$, (b) $CD14^+$ and (c) $eGFP^+$ cells, respectively.

5.2.9 Electroporation of IVT-mRNA into hiDCs

The handling of RNA is described in detail in Ch. 5.3. Depending on the gene encoded in the IVT-mRNA - either luciferase or eGFP - RNA concentration and volumes of media and cells differed in the protocol (Tab. 5.4).

hiDCs were harvested (Ch. 5.2.5) and washed with PBS/EDTA, pelleted again and resuspended in RNAse free X-Vivo-15. The cell suspension (220 µL) was filled into ice pre-cooled electroporation cuvettes (4 mm gap). The IVT-mRNA (30 µL) was added to the cells and carefully mixed before electroporation at 300 V and 150 µF with the Electro Square Porator ECM 830. After electroporation, the hiDC-medium was added to the cells and mixed. The cuvette was stored on ice until all samples were electroporated.

One plate was prepared for each time point, in which the cells were plated equally; one well per sample. Medium supplemented with hIL-4 (2000 U/mL) and hGM-CSF (2000 U/mL) was added to the wells, and cells were cultivated at 37 °C until harvesting. Plates with later time points (over 24 h) were wrapped in cling film to avoid loss of media due to evaporation.

5.2.10 Analysis of luciferase expression

The firefly luciferase expression in hiDCs was monitored with the Bright-Glo™ Luciferase Assay System according to manufacturer's protocol. After addition of the Bright-Glo™ reagent, a 3 min incubation time at RT was done before measuring the luminescence via the Tecan Infinite® M1000 Multimode Reader. Tab. 5.5 shows the parameters set for measuring luciferase expression.

Table 5.4: Electroporation overview. Differences in RNA concentration and volume of media and cells depending on the read-out.

Read-out	Luciferase assay	eGFP assay
Cells per cuvette	1×10^6 cells in 220 µL X-Vivo-15	5×10^6 cells in 220 µL X-Vivo-15
RNA-concentration	10 pmol	30 pmol
hiDC-medium after electroporation	750 µL	350 µL
Time points	up to 8	up to 6
Cell suspension per well	50 µL	95 µL
Media with cytokines	50 µL	1.9 mL, pre-layed in each well

Table 5.5: Parameters set on Tecan Infinite® M1000 Multimode Reader to measure luciferase expression. For further details of parameters see manufacturer's hardware description.

Parameter	Setting	Parameter	Setting
Target Temperature	22 °C to 8 °C	Kinetic Cycles	4
Shaking (Orbital) Duration	5 s	Shaking (Orbital) Amplitude	3 mm
Interval time	70 s	Attenuation	None
Integration time	1000 ms	Settle time	0 ms

5.2.11 Analysis of eGFP-expression

Analysis of eGFP-expression was done via flow cytometry (Ch. 5.2.7) and quantitative real-time PCR (RT-qPCR, Ch. 5.3.3). The flow cytometric analysis allows the monitoring of eGFP-protein expression, while RT-qPCR enables the monitoring of RNA decay. Both parameters are important to determine RNA turnover on protein and RNA level.
Depending on the time point, the cell suspension was transferred to a tube. To detach remaining cells, the well was thoroughly washed with 1 mL of cold PBS and added to the tube as well. A cell suspension of 1.3 mL (approx. 0.75×10^6 cells per mL) was transferred to a round-bottom tube, 12 x 75 mm, and the sample was prepared for flow cytometric analysis (Ch. 5.2.7). The remaining cell suspension was pelleted and prepared for RNA extraction by resuspending pellet with RLT/βMercaptoethanol (βMe)-buffer (Ch. 5.3.1).

5.2.12 RNA-stability in CD4$^+$ T cells mediated by newly selected 3′ UTRs

CD4$^+$ T cells were freshly isolated from PBMC (Ch. 5.2.3) by MACS^{TM} technology according to kit's protocol with the following change. T cells were eluted with X-Vivo-15. Ten pM IVT-mRNA was electroporated each in 3.0×10^6 cells. The cells were transfered to 500 µL hiDC-medium, and 50 µL of the cell suspension were each plated to a cell culture well (12 well, flat bottom). The wells were filled up with 50 µL hiDC-medium supplemented with 20 U mL^{-1} IL-2. The luciferase expression was measured as described in Ch. 5.2.9 and Ch. 5.2.10.

5.2.13 RNA-stability in fibroblasts (HFF and C2C12) mediated by newly selected 3′ UTRs

Human Foreskin Fibroblast cells (HFF, System Bioscience) and mouse myoblasts (C2C12) cells were cultured and electroporated with 2 µg IVT-mRNA and 1 µg GFP-RNA (spike-in control) as described previously.[214]

5.3 RNA methods

The RNA was kept at all times on ice or stored between -15 °C and -25 °C to minimize RNase activity to avoid its degradation by ubiquitous RNases.[31] The working place and pipettes were kept sterile and cleaned regularly with the RNase inhibitor RNase Zap®. All consumables were free of RNases, DNases or endotoxins. The solutions and buffers were kept on ice during pipetting and preparation of the reaction mixtures. If not otherwise stated, the RNA samples were purified with the RNeasy® Mini Kit (Qiagen) according to manufacturer's protocol. The elution of the RNA was done twice with each 30 µL ddH_2O. The concentration of the RNA was measured using the NanoDrop 1000/2000 UV-Vis Spectrophotometer (Ch. 5.1.10). Both purity and appearance were monitored with the Bioanalyzer 2100 (Ch. 5.1.11). If not directly used for further experiments, the RNA was kept between -15 °C and -25 °C and for long-term storage between -65 °C and -85 °C.

5.3.1 Purification of total RNA from hiDCs

Total RNA was purified with the RNeasy® Mini Kit according to manufacturer's protocol using spin technology with the following changes and optional steps. The hiDCs were pelleted after harvesting, resuspended with RLT supplemented with β-mercaptoethanol (βMe) according to manufacturer (RLT/βMe-buffer), 600 µL per 0.5-1 $\times 10^7$ cells, and frozen between -65 °C and -85 °C to improve the lysis of cells. To homogenize the lysate a blunt 20-gauge needle fitted to an RNase-free syringe was used. An on-column DNase digestion was performed with each sample using the RNase-free DNase Set (Qiagen), as DNA contamination could falsify the RT-qPCR outcome.[215,216] The RNA was eluted twice with each 30 µL ddH_2O.

5.3.2 Purification of mRNA from total RNA

The Poly(A)Purist™ Kit was used for mRNA purification out of total RNA (Ch. 5.3.1) according to manufacturer's protocol starting with the total RNA resuspended in ddH_2O.

5.3.3 Quantification of d2eGFP-encoding RNA levels by RT-qPCR

Total RNA (Ch. 5.3.1) was reverse transcribed with a dT18-primer using the SuperScript™ II Kit according to manufacturer's protocol. The cDNA was analyzed via real-time quantitative analysis ABI PRISM 7700 Sequence Detection System and software in a 40 PCR cycle using the QuantiTect SYBR Green PCR Kit according to manufacturer's protocol. The reactions were prepared in duplicates with primers amplifying the reporter gene d2eGFPmut

and for RNA encoding for Hypoxanthine-guanine phosphoribosyltransferase (HPRT1). This housekeeping gene is used as internal standard for normalization of variances in RNA-quality and input amount of cDNA. The PCR reaction conditions are described in Kuhn *et al.*[130] The relative expression of d2eGFPmut was quantified and analyzed via ΔC_t-calculation relative to HPRT1.

5.3.4 Generation of IVT-mRNA

In vitro-T7-transcription (IVT) of DNA allows the specific production of the RNA of interest. The DNA-templates for IVT-synthesis were either a plasmid - linearized downstream of the poly(A) tail[85] and purified with the NucleoSpin® Plasmid DNA Purification Kit - or a PCR-product (described in detail in Ch. 5.4.5 and Ch. 5.5) purified and eluted in RNase-free ddH_2O (Fig. 5.4). The IVT-synthesis was carried out for 2.5 h at 37 °C.

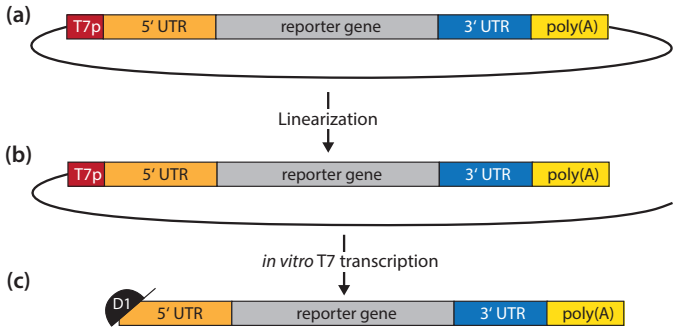

Figure 5.4: Generation of IVT-mRNA. (a) A plasmid - featuring basically a T7-promoter (T7p), a 5′ UTR (hAg-Kozak), a reporter gene and a 3′ UTR and poly(A)-tail - is (b) linearized downstream of the poly(A) tail and used (c) as template for *in vitro* T7-transcription.

To obtain maximum yield of RNA, 0.75 µL of 100 mM guanosine-5'-triphosphate (GTP) was added every 30 min to the reaction mixture (Tab. 5.6). The IVT-synthesis was stopped by adding 1 µL TURBO™ DNase (2 U µL^{-1}) and incubated for another 15 min at 37 °C. After addition of each component - GTP and DNase - the tubes were vortexed for 5 s and spun down shortly before continuing the incubation in the thermo block. Tab. 5.6 shows the reagents for a 50 µL IVT-reaction.

Table 5.6: Reaction mixture for a 50 µL *in vitro*-T7-transcription. [A/ C/ U/ GTP: adenosine/ cytidine/ uridine/ guanosine triphosphate]

Reagent	$c_{reaction}$
ddH_2O	n/a
cap stock solution	6.0 mM
A/C/UTP	7.5 mM
GTP	1.5 mM
10x T7 buffer	1x
Template DNA	0.05 µg µL^{-1}
T7 enzyme mix HC	1x

As shown by Kuhn *et al.*, the *cap* structures modified from the 7-methylguanosine (m^7G) influenced stability and translational efficiency of the RNAs. The phosphorothioate-modified cap β-S-ARCA has two diastereoisomers designated D1 and D2, from which D1 showed the highest and longest lasting protein expression in hiDCs.[130] If not otherwise stated, the D1-β-S-ARCA was used in this work.

5.4 Build up of library

The 3' UTR-RNA-library used for the *in vitro* selection process was build from mRNA derived from hiDCs. Before purifying the mRNA from these cells, the transcription process was inhibited by addition of Actinomycin D (ActD), a substance which binds to the transcription initiation complex and prevents elongation by RNA polymerases[217] (Ch. 5.4.1). This allowed the degradation of short-living mRNAs, so that the library was mainly built with more stable RNA and used in a selection process by amplifying the RNA and electroporating it into new hiDCs. After six rounds of selection, the mRNA was further characterized and analyzed by sequencing.

5.4.1 Actinomycin D treatment of hiDCs

ActD was solubilized in ddH_2O and DMSO (25 % [v/v]) with a final concentration of $1.25\,g\,L^{-1}$. mRNA, which was used to build up the library, was purified from hiDCs treated with 3 µM ActD for 3 h using the Poly(A)Purist™ Kit according to manufacturer's protocol.

5.4.2 Monitoring of transcription inhibition in hiDCs via click-chemistry

5-ethynyl uridine (EU) is an analog of uridine (see Fig. 5.5), which is taken up by the cells and incorporated into nascent RNA.[218] EU can easily be detected with fluorescent azides via the Sharpless–Meldal copper (I)-catalyzed Huisgen cycloaddition reaction, often referred to as click-chemistry (Fig. 5.5). This method, which is highly efficient and selective, allows the quick detection of EU with high sensitivity.[218] Transcription inhibition was monitored via click-chemistry using the Click-iT® RNA Imaging Kit. This allowed the determination of the minimum ActD-concentration needed to inhibit the transcription in hiDCs, without stressing the cells too much.

To monitor transcription inhibition in hiDCs, the cells - harvested at day 4 (Ch. 5.2.4; 5.2.5) and resuspended in hiDC-medium supplemented with hIL-4 and hGM-CSF at a cell density of $0.5 \times 10^6\,mL^{-1}$ - were fed with ActD in concentrations with a range from 3 pM to 3 µM for a total time of 5 h. After 3 h, 8 mM EU was added to the medium. The cells were harvested (Ch. 5.2.5) and prepared for viability staining with 7-AAD (Ch. 5.2.7) before continuing with the click-chemistry reaction according to manufacturer's protocol with the following changes. The click-chemistry reaction was performed in round-bottom tubes. For removal of solutions and buffers, the cells were centrifugated at RT for 6 min at 600 x g. After the click-chemistry reaction, the cells were fixed with 1 % PFA and analyzed via flow cytometry analysis (Ch. 5.2.7).

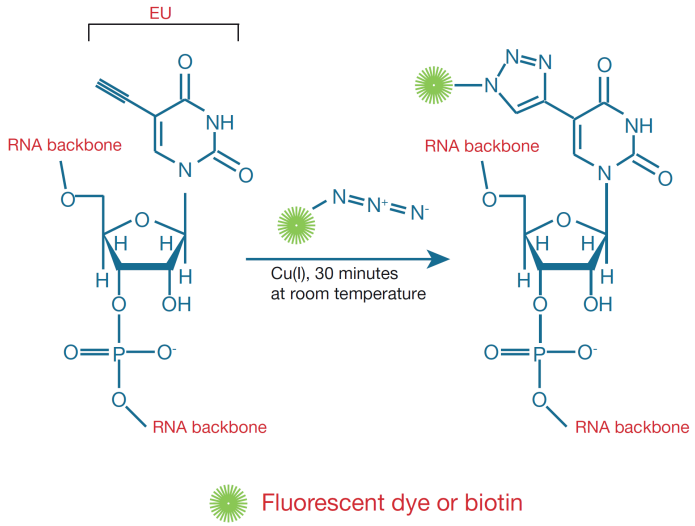

Figure 5.5: Click-chemistry reaction:[219] into RNA incorporated 5-ethynyl uridine (EU) reacts within 30 min at RT with a fluorescent dye or biotin containing an azide group. Reaction is catalyzed by copper Cu(I).

5.4.3 Fragmentation of mRNA

mRNA from ActD-treated hiDCs was reduced to fragments of 200 to 1,000 nts prior to being cloned into the library vector backbone with d2eGFPmut as reporter gene (Ch. 5.1.2). The fragmentation was done with Nuclease P1 (NP1), an enzyme able to completely degrade the RNA producing 5'-mononucleotides.[220–224] As no suitable protocol was available, both buffer and parameters were adjusted for an optimal reaction based on the work of Shimelis *et al.*[225] The IVT-mRNAs with different sizes (746, 1294 and 2472 nts) were treated with NP1 under different conditions to obtain fragments with the desired length. The optimization was done by adjusting temperature, incubation time and enzyme concentration using first IVT-mRNA and second mRNA of untreated hiDCs to confirm optimized protocol.
It was expected, that NP1 would hydrolyze the RNA quickly,[220] so a high dilution of the enzyme would be necessary to avoid complete degradation. As the pH seems also to play an important role in stabilizing the enzyme,[226] NP1 was solubilized in 30 mM Tris-HCl (pH 7.9) with a final concentration of 30 U/mL.[225] The aliquots were kept between -65 °C and -85 °C for a maximum of 6 months. Sodium acetate (NaOAc, 50 mM, pH 5.5) was chosen as buffer in the reaction mixture (Tab. 5.7). The RNA designated for the library was incubated for 55 min at 20 °C with NP1 at a ratio of 0.075 U NP1 per µg mRNA to obtain fragments with a main size of 200 to 800 nts. To inhibit NP1, the samples were heated for 5 min at 95 °C and quickly cooled down on ice. The RNA was purified and stored between -15 °C and -25 °C before continuing with the first-strand cDNA-synthesis (Ch. 5.4.4). The correct size of the fragments was monitored via the Agilent 2100 Bioanalyzer (Ch. 5.1.11).

Table 5.7: Reaction mixture for incubation of RNA with Nuclease P1.

Component	c_{stock}	c_{end}
RNA	10 µg	0.42 µg
NaOAc, pH 5.5	50 mM	2.08 mM
NP1, 1:100 dilution	0.3 U/mL	0.075 UmL^{-1}
ad 24 µL ddH_2O		

5.4.4 Library cDNA-synthesis

The fragmented mRNA (Ch. 5.4.3) was used as template for cDNA-synthesis using the Revert Aid™ Premium First Strand cDNA Synthesis Kit following the protocol for *cDNA synthesis for cloning* including the protocol for second strand cDNA synthesis with the following changes and optional steps. All steps recommended for the random hexamer primers including optional ones were done. The hexamer primer (*LIB-cDNA-REV-Random Hexamer*) had a random sequence of 6 nts and an overhang with a defined sequence and NotI-restriction site. The deoxynucleotide triphosphate (dNTP)-mix with 10 mM of each dNTP was added to the reaction mixture for second strand cDNA synthesis. For proofreading (3'⟶5' exonuclease activity) of the double-stranded cDNA, 3 µL Pfu Polymerase was pipetted to the reaction mixture after the cDNA-synthesis and incubated for another 30 min at 72 °C. The cDNA was purified using the MinElute® Kit following manufacturer's instructions. The elution was done twice with each 10 µL ddH_2O and the appearance was monitored via Agilent 2100 Bioanalyzer (Ch. 5.1.11).

5.4.5 Cloning and amplification of 3′ UTR-library into vector backbone

The cDNA-ends were blunted and phosphorylated via the Fast DNA End Repair Kit according to manufacturer's protocol. The samples were purified via the MinElute® Kit following manufacturer's instructions, but were eluted twice each with 10 µL ddH_2O. To clone the library-cDNA into the prepared vector backbone (Ch. 5.1.6), the cDNA was digested using 40 U NotI-HF enzyme per reaction mixture of 50 µL. The correct in size cDNAs (between 200 and 1,000 bps) were purified by agarose gel preparation and magnetic beads (Ch. 5.1.5) to ensure removal of all fragments smaller than 150 bps.
The ligation was prepared according to manufacturer's recommendations for the T4 DNA Ligase. The loss of library sequences during transformation into chemically competent *E. coli* was avoided by using the ligation reaction mixture directly as a PCR template.[227] To allow for subsequent IVT-mRNA-synthesis (Ch. 5.4.6) and to avoid the amplification of non-desired DNA-sequences - in particular during the selection process, where the cDNA of the total RNA is used as PCR-template - special primers (*LIB-FW-T7-2* and *LIB-REV-T60*) were designed (Fig. 5.6). Both primers only partially bind to the DNA. *LIB-FW-T7-2* hybridizes to the hAg-Kozak region and is elongated with a T7 promoter overhang needed for the T7 polymerase to bind. In contrast, *LIB-REV-T60* hybridizes to the primer binding

site (Ch. 5.1.1) and is elongated with a 60 bps long poly(A)-tail. Tab. 5.8 and 5.9 shows the reaction mixture components and adjusted PCR-conditions. The PCR-samples were purified via preparative agarose gel and additionally via magnetic beads (Ch. 5.1.5). Half of the library was stored as backup between -65 °C and -85 °C and the other half was used for subsequent IVT-synthesis (Ch. 5.4.6).

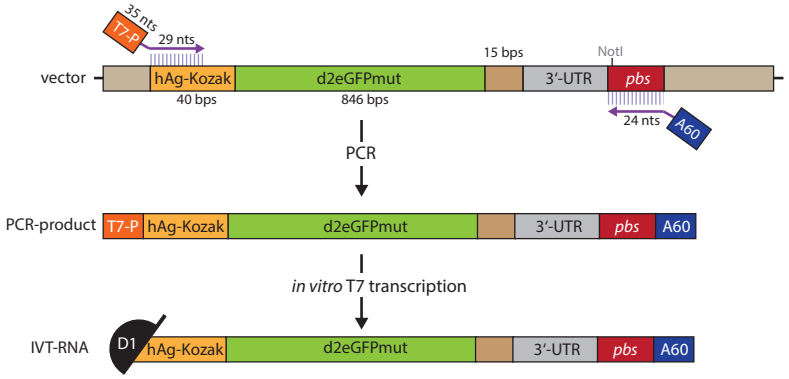

Figure 5.6: From DNA- to RNA-library. D2eGFPmut vector serves as template of PCR-reaction with primers, elongated at their 5′ end with the T7-promoter (T7-P) and 60 nts-long poly(T)-tail (A60). PCR-product is used as template for *in vitro* T7 transcription to produce IVT-mRNA capped with D1 (β-S-ARCA). *pbs*: primer binding site with NotI as restriction site.

Table 5.8: PCR-reaction mixture components for amplification of library. Two µL were used for the ligation reaction mixture, and 4 µL for cDNA synthesized from selection rounds.

Component	c_{stock}	c_{end}	Vol./ µL
DNA-template	-	-	2-4
Phusion Buffer	5x	1x	20
dNTPs	10 mM	0.2 mM	2
Forward Primer *LIB-FW-T7-2*	10 µM	0.5 µM	5
Reverse Primer *LIB-REV-T60*	10 µM	0.5 µM	5
DMSO	100 %	3 %	3
Phusion Polymerase	2 U/µL	0.02 U/µL	1
ad ddH_2O			100

Table 5.9: PCR-reaction conditions for amplification of library.

Duration	Temp./ °C	Step
1 min 30 s	98	Initial denaturation
20 s	98	Denaturation
30 s	65	Annealing
45 s	72	Extension
5 min	72	Final extension
hold	4	

5.4.6 *In vitro*-T7-transcription of library

The IVT-synthesis of the DNA-library was done as described in Ch. 5.3.4. The RNA-library was split. One half was stored as backup between -15 °C and -25 °C and the second half was used for subsequent *in vitro* selection of new 3' UTR sequences (Ch. 5.5).

5.4.7 Sequence variability determined by next generation sequencing (NGS)

The sequence variability of the library and also of later selection rounds was determined by NGS, as shown in Fig. 5.7. To increase the specificity and sensitivity, a Touch-Down-PCR (TD-PCR)[228] was done to amplify unknown 3' UTR-regions using primers with a BpmI restriction site. The cDNA of the library and selection rounds were used as templates (Ch. 5.4.4; 5.5). The PCR-products were digested with BpmI and purified with magnetic beads (Ch. 5.1.5). Only the 3' UTR-regions should be left over for NGS to reduce sequencing bias.[229,230] Tab. 5.10 and 5.11 show PCR conditions and the reaction mixture respectively.

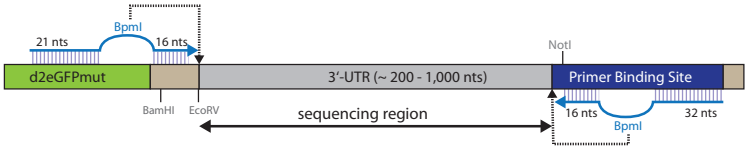

Figure 5.7: Sequence variability determined by NGS of unknown 3' UTR-regions was done with primers having both a BpmI-restriction site encoded. After BpmI-digest only unknown regions were left over for sequencing.

Table 5.10: PCR-reaction mixture components for amplification of library and selection round DNA for NGS.

Component	c_{stock}	c_{end}	Amount
DNA-template	-	-	50 ng or 1 µL
Phusion Buffer	5x	1x	10 µL
dNTPs	10 mM	0.2 mM	1 µL
Forward Primer *NGS-UTR-FW-BpmI*	10 µM	0.2 µM	1 µL
Reverse Primer *NGS-UTR-REV-BpmI*	10 µM	0.2 µM	1 µL
DMSO	100 %	6 %	3 µL
Phusion Polymerase	2 U/µL	0.02 U/µL	1 µL
ad ddH_2O			50 µL

The 3' UTR-PCR-products were further prepared with the TruSeq DNA Sample Preparation Kit with the following changes. The fragmentation and size selection steps were omitted. The samples were quantified via the Qubit according to manufacturer's protocol. The quality of the library was analyzed via Agilent 2100 Bioanalyzer using the DNA High Sensitivity Chip (5.1.11). NGS was performed on a HiSeq 2000. The sequence alignment of the reads were analyzed with STAR (version 2.3.0e)[231] using the human reference genome (version hg19). The coordinates of the read-alignments were compared with the UTR and coding DNA sequence (CDS)-region coordinates of *UCSC known genes*. The read bases,

Table 5.11: Touch-Down-PCR-reaction conditions for amplification of library and selection round DNA for NGS.

Duration	Temp./°C	Step
1 min 30 s	98	Initial denaturation
Step 1: 10 cycles		
20 s	98	Denaturation
30 s	82-64	Annealing
45 s	72	Extension
Step 2: 20 cycles		
1 min 30 s	98	Denaturation
30 s	64	Annealing
45 s	72	Extension
5 min	72	Final extension
hold	4	

which overlapped with the respective transcript coordinates, were counted and normalized to bases per kilobase of gene model per million mapped bases (BPKM).

5.5 *In vitro* selection of new 3′ UTR sequences

The *in vitro* selection process comprised several rounds starting with the transcription of the library (Ch. 5.4.6), the electroporation of 10 µg RNA into 1×10^7 hiDCs following the protocol for the eGFP assay as described in Ch. 5.2.9, the extraction (Ch. 5.3.1) and the amplification of stable sequences (Ch. 5.5) after defined time points (see also Fig. 6.1). During the last selection round, cells were split for three differently length time points. For the *in vitro*-selection hiDCs generated from 10 different blood donors (Ch. 5.2.4), were pooled after harvesting at day 4 (Ch. 5.2.5) to ensure the same cell composition throughout the selection process.

The total RNA was purified (Ch. 5.3.1) after defined time points and used as template for first-strand cDNA-synthesis as described in Ch. 5.3.3 with the following changes. After denaturation of the Reverse Trancriptase at 70 °C, 0.5 µL RNase H was added to each sample followed by a 20 min incubation at 37 °C. The RNase H was heat-inactivated according to manufacturer's recommendation. The synthesized cDNA served next as template for PCR (Ch. 5.5) using *LIB-FW-T7-2* and *LIB-REV-T60* as primers. Experimental bias, which can occur during PCR,[232,233] was reduced by following recommendations reviewed in detail by Polz *et al.*: (i) PCR reactions were prepared in replicates and mixed afterwards, (ii) minimum cycle number was used for amplification and (iii) unique primers were used.[234] The optimal cycle number was thereby determined after a test-PCR with cycles between 6 and 15 to avoid byproducts, which often arise from too many cycles.[234]
The PCR reaction mixture was purified first via agarose gel preparation and second via magnetic beads (0.5 volumes), to not only remove contaminants, but to also discard aborted frag-

ments smaller 700 bps, which could disturb subsequent IVT-mRNA-synthesis (Ch. 5.1.5). The elution was done twice with each 30 µL ddH_2O. The quality of DNA was checked via 1.5 % agarose gel and the PCR-product was next used as template for IVT-mRNA-synthesis (Ch. 5.4.6) to continue with the next selection round.

5.6 Analysis of selected 3′ UTRs

Samples and consumables were handled as described in Ch. 5.1.

5.6.1 Cloning of selected 3′ UTRs for sequencing analysis

The selected 3' UTRs of selection rounds 5 and 6 were cloned into a vector backbone with luc2CPmut as reporter gene (Ch. 5.1.2). For this, a PCR was done using primers (*LIB-Cloning-FW/REV*), which bind to the 3' end of the d2eGFPmut reporter gene (Ch. 5.1.1) and the primer binding site respectively (see Fig. 5.6). The PCR-reaction mixture was prepared as described in Tab. 5.5 with the following changes. The total volume was 50 µL. 20 ng of the purified PCR-products obtained during the *in vitro* selection were used as DNA template. The reaction conditions are shown in Tab. 5.12.

Table 5.12: PCR-reaction conditions for amplification of PCR-products obtained during *in vitro* selection.

Duration	Temp./ °C	Step
1 min 30 s	98	Initial denaturation
15 s	98	Denaturation
30 s	65	Annealing
25 s	72	Extension
5 min	72	Final extension
hold	4	

The PCR-products obtained for cloning into the luc2CPmut backbone were purified via magnetic beads (Ch. 5.1.5) and were next subjected to end repair via Fast End Repair as described in Ch. 5.5 prior to NotI-digestion. The luc2CPmut vector backbone was linearized with NotI and EcoRV and dephosphorylated with FastAP™ Thermosensitive Alkaline Phosphatase. The ligation was done by using the T4 DNA ligase (Ch. 5.1.6). After transformation into One Shot® OmniMAX™ 2 T1 Phage-Resistant Cells, 100 clones of the selection rounds 5 and 6 were picked and prepared for plasmid DNA purification as described in NucleoSpin® 8 Plasmid Kit protocol. The sequencing results (Ch. 5.1.9) were analyzed via CloneManager software.

5.6.2 Analysis of 3′ UTR-similarity and gene origin with Clone Manager and BLAST

To analyze unknown 3' UTR sequences, a genealogical tree was drawn using Clone Manager software. Multi-way DNA alignment was applied with the following parameters. The

scoring matrix was chosen as adjusted per default. In general, the branch length indicates the family relationship between the sequences.[235] The shorter the branch length, the more similar the sequences are. Thus, sequences could be grouped and analyzed separately regarding similarity within the group, origin, average length, GC-amount of each sequence and similarity between the groups. The origin of the sequences and alignment region within the origin mRNA (5' UTR, CDS or 3' UTR) was verified via Basic Local Alignment Search Tool (BLAST, National Center for Biotechnology Information).

5.6.3 Cloning of selected 3′ UTRs to analyze their effect on IVT-mRNA

Stabilizing effects of the selected 3' UTRs were analyzed on protein level by measuring luciferase activity (Ch. 5.2.10) from sequences cloned into luc2CPmut (Ch. 5.6.1). Promising candidates were further cloned in pair-wise combinations to analyze stabilizing effects (i) on protein level by measuring luciferase activity (Ch. 5.2.10) using luc2CPmut as reporter gene (Ch. 5.1.2) and (ii) on RNA level by RT-qPCR (see Ch. 5.3.3) using d2eGFPmut as reporter gene (Ch. 5.1.2). The selected 3' UTRs were cloned into a luc2mut vector backbone (Ch. 5.1.2) for further analysis of the translational efficiency and total protein over time. Cloning of the sequence elements into the vector backbones was done via cold fusion cloning technology (Fig. 5.8) according to manufacturer's protocol with the following changes. The ligation mix was transformed as described in Ch. 5.1.7. Obtained DNA was verified via sequencing (Ch. 5.1.9).

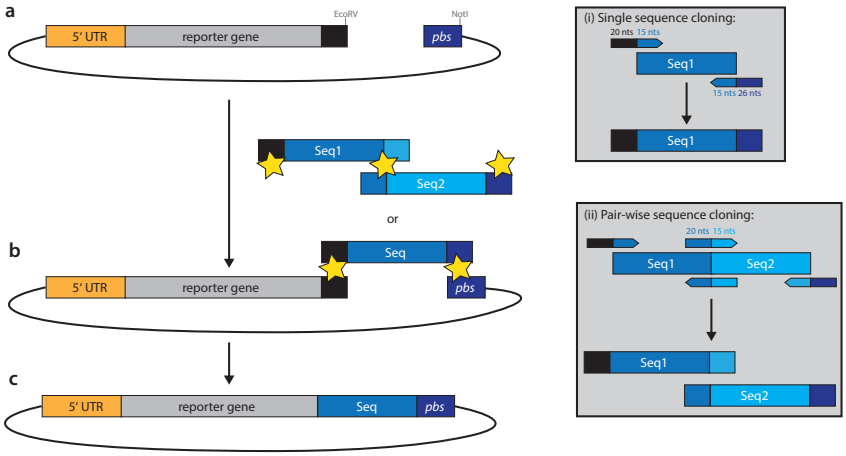

Figure 5.8: Cold Fusion reaction. (a) Plasmid with corresponding reporter gene (luc2CPmut, luc2CP or d2eGFPmut) was linearized with EcoRV and NotI and dephosphorylated via FastAP. Corresponding primer pairs for (i) single or (ii) pair-wise sequence cloning were used for amplification of selected 3′ UTR-elements (Seq1 and/or Seq2). (b) Cold Fusion reaction was prepared with linearized plasmid and PCR-products according to manufacturer's protocol. Insertion location of sequence elements (Seq1/2) are marked with the yellow star symbol. (c) Plasmid DNA with new 3′ UTR-sequences.

The plasmids containing chosen sequence elements were double digested with EcoRV and SfoI for 3 h at 37 °C. Calf Intestinal Alkaline Phosphatase (CIP) was added to dephosphorylate digested sequences for another 15 min. The success of the digest was analyzed by agarose gel. To introduce homologue sequences at the 5' and 3' end of each sequence,

a PCR was done (Tab. 5.13; Tab. 5.14) with primers elongated as depicted in Fig. 5.8. A complete list of primers are depicted in Supplementary Tab. A.1.

Table 5.13: PCR-reaction conditions for amplification of sequence elements as preparation for cold fusion reaction. X refers to annealing temperature of used primer pairs (Supplementary Tab. A.1).

Duration	Temp./°C	Step
1 min	98	Initial denaturation
Step 1: 5 cycles		
10 s	98	Denaturation
30 s	X	Annealing
30 s	72	Extension
Step 2: 25 cycles		
10 s	98	Denaturation
1 min	72	Annealing and Elongation
10 min	72	Final extension
hold	2 °C to 8 °C	

Table 5.14: PCR-reaction mixture components for amplification of sequence elements as preparation for cold fusion reaction.

Component	c_{stock}	c_{end}	Amount
DNA-template	-	-	10 ng
Phusion Buffer	5x	1x	10 µL
dNTPs	10 mM	0.2 mM	1 µL
Forward Primer	10 µM	0.5 µM	2.5 µL
Reverse Primer	10 µM	0.5 µM	2.5 µL
DMSO	100 %	2 %	1 µL
Phusion Polymerase	2 U/µL	0.02 U/µL	0.5 µL
ad ddH_2O			50 µL

5.7 Analysis of binding sites for RNA-binding proteins (RBPs)

Potential RNA-binding sites located on newly selected 3' UTRs were analyzed via *Scan for motifs* (SFM).[236] For this, the sequence in FASTA format was analyzed using the default setting (E-value ≤ 0.175 for regulatory elements and E-value ≤ 0.1 for protein binding sites). As an output, all regulatory elements - except for the Plant Polyadenylation Element - and protein binding sites were chosen.

RBPs and their respective number of binding sites located on the single 3' UTR were compared with the internal reference 2hBg (Ch. 5.1.3). The results obtained from a single 3' UTR were extrapolated for the pair-wise combinations and verified using IF, FI, IhBg and hBgI. Number of binding sites for each found RBP was analyzed via Matlab V.16 (analysis of variance function, general linear model) regarding their correlation to RNA half-life and their stabilizing or destabilizing effect on the IVT-mRNA.

5.8 Analysis of microRNAs (miRNAs) binding sites

Potential miRNA-binding sites located on newly selected 3' UTRs were analyzed via IntaRNA, a program for fast and accurate prediction of RNA-RNA-interaction.[237–240] The interactions are predicted by an energy-based approach, based on (i) accessibility of the interaction site calculated from all possible thermodynamic stable structures formed by the RNA sequence and (ii) the seed region of the miRNA.[241–243] Two miRNA-sets with miRNAs, which are found typically in unstimulated and LPS-stimulated DCs, were used for the prediction of miRNA-binding sites. These miRNA-sets were combined from published data by Hashimi *et al.*[244] and Landgraf *et al.*[245] taking into account hiDC-specificity by using determined copy number and p-value (Supplemetary Tab. A.2 and Tab. A.3). Each single 3' UTR and pair-wise combination was analyzed using both miRNA-sets. Default settings were used.

5.9 Statistical methods

If applicable, statistical methods of data results were applied using Graph Pad Prism 5 software except for results obtained for RNA-binding proteins (Ch. 5.7). The employed tests are described in the respective figure captions. P-values below 0.05 were considered to be statistically significant. The RNA turnover was analyzed via R computational software using internal script codes.

6 Results

In the following section results will be presented in the order as depicted in Fig. 6.1.

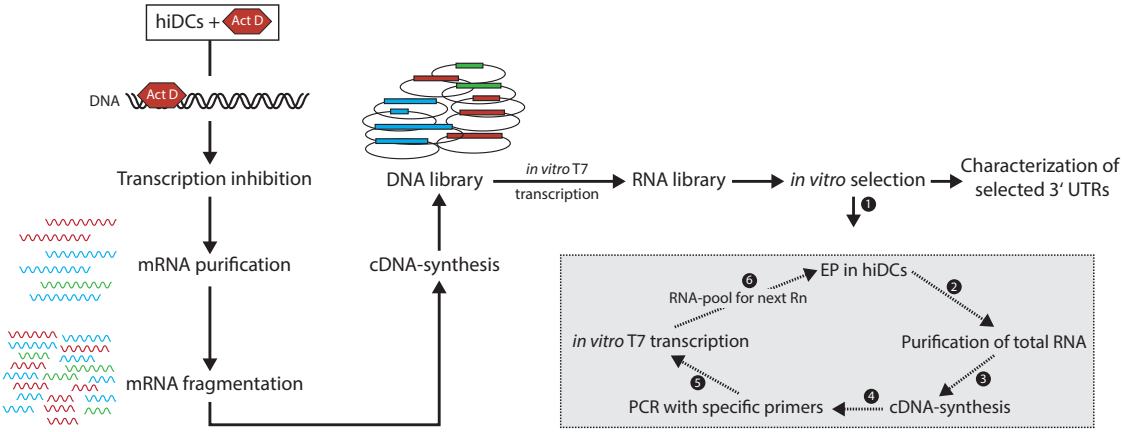

Figure 6.1: Overview of library build up and *in vitro* selection process. mRNA of Actinomycin D (ActD)-treated hiDCs was purified, fragmented and used as template for cDNA-synthesis. cDNA was cloned into linearized plasmid and DNA-library was used as template for *in vitro* T7 transcription. *In vitro*-selection comprised several rounds (Rn) of ❶ electroporation (EP) in hiDCs, ❷ purification of total RNA, ❸ cDNA-synthesis, ❹ PCR with specific primers, ❺ *in vitro* T7 transcription and thus, ❻ generation of an RNA-pool for the next selection round starting with EP in hiDCs. At the end of the selection, selected sequences were characterized.

6.1 Library build up for *in vitro* selection

To perform the selection with RNA-sequences, which are naturally occurring in human immature dendritic cells (hiDCs), the initial mRNA-pool was generated directly from these cells, instead of using a chemically synthesized random cDNA-library for the *in vitro* selection. Moreover, the mRNA was already preselected by treating the cells with Actinomycin D (ActD), a substance which binds to the transcription initiation complex and prevents elongation by RNA polymerases.[217,246,247] As a consequence of blocking new RNA synthesis, short-living mRNA was degraded, while only stable mRNA was purified and used for library build up.

6.1.1 Treatment of hiDCs with ActD

ActD is lethal within several hours as the cell metabolism is arrested due to transcription inhibition.[248] Therefore, toxicity was assessed first by treating hiDCs with different concentrations for up to 24 h (Fig. 6.2). Compared to untreated cells, ActD-treated hiDCs were unaffected within the first 5 h. However, after 24 h only approx. 15 % were alive. This can be attributed to the transcription inhibition, because control cells treated with DMSO - the solvent DMSO used for ActD, which has been reported to be toxic at high concentrations[249] - showed similar viability as untreated cells.

Effective transcription inhibition was verified by treating the cells with 5-ethynyl uridine (EU) and following incorporation into RNA by coupling a fluorescent dye to the modified

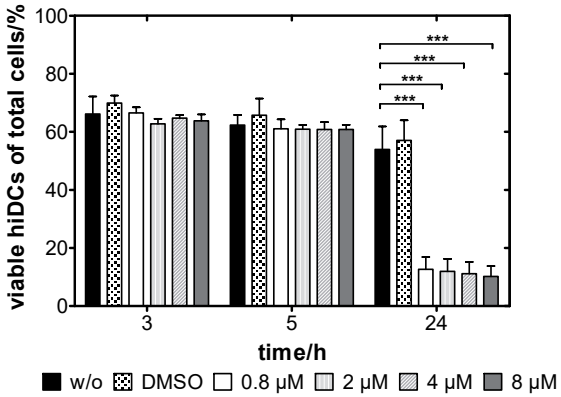

Figure 6.2: Viability of hiDCs after ActD-treatment with different concentrations (0.8-8 µM) for 3, 5 and 24 h to determine toxicity via flow cytometric analysis. Non-treated (w/o) and DMSO-treated hiDCs were used as control samples. Shown is the viability of hiDCs from total cells in %. Values are mean±SD of 3 independent experiments; ***: p<0.001, Two-way ANOVA, Bonferroni post-test.

nucleoside using click-chemistry. The protocol was adapted for hiDCs by identifying the optimal concentration of EU in the medium. Cells were treated with increasing concentrations of EU for up to 3 h (Fig. 6.3a). After a 2 h treatment, maximal labeling of the nascent RNA with over 80 % of Alexa Fluor 488 positive cells was yielded, which was sufficient to verify transcription inhibition. Eight mM EU was therefore still better than 4 mM, thereby not affecting marker expression (Fig. 6.3b) or cell viability (data not shown) indicating that such a high EU-concentration is non-toxic for hiDCs.

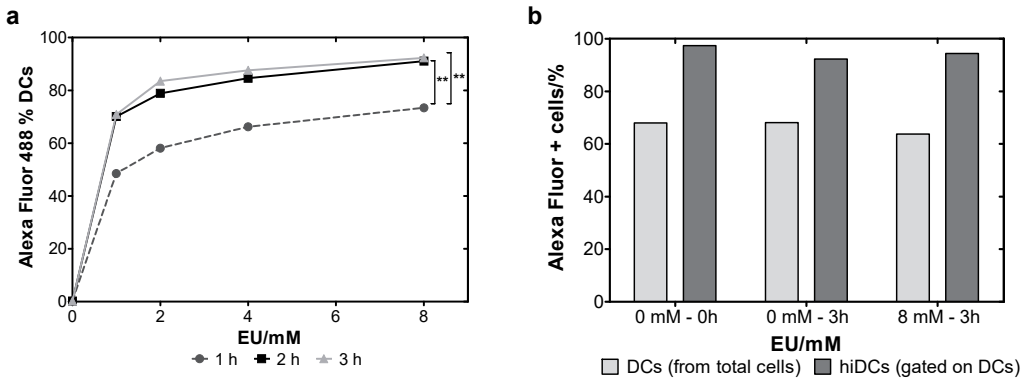

Figure 6.3: Optimization of click-chemistry reaction. (a) hiDCs were treated with 5-ethynyl uridine (EU) at different concentrations to determine its uptake and incorporation into nascent RNA for 1, 2 and 3 h. EU incorporated into nascent RNA was detected by click-chemistry reaction using Alexa Fluor 488 azide. **: p<0.01 (One-way ANOVA, Bonferroni post-test). (b) Viability and marker expression of hiDCs after treatment with 8 mM EU for 3 h (8 mM – 3 h). Non-treated hiDC at time point 0 h (0 mM – 0 h) and 3 h (0 mM – 3 h) were used as control samples. Shown is the percentage of Alexa Fluor 488-positive cell populations: DCs from total acquired cells and hiDCs gated on DCs (DC-Sign$^+$ CD83$^-$).

Optimized conditions - i.e. incubation of hiDCs with 8 mM EU for 2 h - were applied to verify transcription inhibition upon ActD-treatment. Transcription was successfully inhibited after a 3 h-treatment with at least 1 µM ActD (Fig. 6.4). Based on these results, mRNA to be used to build the library for the selection was purified after a 3 h-treatment with 3 µM ActD.

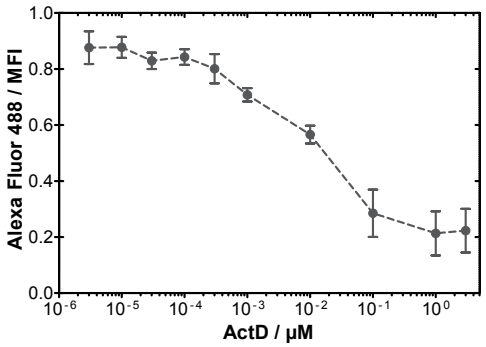

Figure 6.4: Efficiency of transcription inhibition in ActD treated hiDCs. hiDCs were treated with ActD at different concentrations (3.0 pM to 3.0 µM) for 5 h. After 3 h 8 mM EU was added to the cells for 2 h to determine efficiency of transcription inhibition by visualization of nascent RNA via click-chemistry reaction with Alexa Fluor 488 azide. Shown is the mean fluorescence intensity (MFI) of Alexa Fluor 488 positive DCs after ActD incubation. Values are mean±SD of 4 independent experiments.

6.1.2 Fragmentation of mRNA from ActD-treated hiDCs with Nuclease P1 (NP1) and final preparation of the library

mRNA has an average length of 1,400 nts.[250] Based on the rationale that shorter 3' UTRs (i) usually have better translational efficiencies[205] and (ii) are more cost-efficient for production of respective IVT-mRNAs as fewer reagents are needed, the purified mRNA from ActD-treated hiDCs was fragmented down to 200-1,000 nts for further build up of the library. The initially applied reaction conditions demonstrated a high enzymatic activity of NP1 (Fig. 6.5a). Within 5 min a 2,472 nts long IVT-mRNA was degraded down to approx. 50-200 nts. Dilution of the enzyme and reduction of the reaction temperature down to 20 °C yielded more controllable reaction conditions (Fig. 6.5b). RNA-fragments showed the desired range of between 200 and 1,000 nts after a 55 min incubation with 0.075 U mL^{-1} NP1.

Applying these conditions for fragmentation with NP1 yielded the expected lengths of the mRNA from ActD-treated hiDCs (mRNA-NP1), namely between approx. 200 and 1,000 nts (Fig. 6.6a). Quality and size distribution of the double strand (ds) cDNA obtained from the fragmented mRNA also confirmed the correct size for the final library build up (Fig. 6.6b). Moreover, no secondary peaks were visible after cDNA-synthesis, indicating success of the reaction.

cDNA-fragments were cloned downstream of the d2eGFPmut reporter gene in a suitable vector backbone (Fig. 6.7a, lower panel) to function as 3' UTR after IVT-synthesis. The quality of the DNA-library (Fig. 6.7a, upper panel) and its derived RNA-library (Fig. 6.7b) were analyzed via agarose gel and capillary electrophoresis, respectively. The expected size of the DNA-library of between 1,100 and 2,000 bps after PCR could be confirmed. There was a slight smear visible above 3,000 bps. However, this seemed not to disturb subsequent IVT-synthesis, as no corresponding longer RNAs could be detected. In addition to RNAs in the expected size range, which for unknown reasons migrated as a double peak, some smaller RNAs below 500 nts could be detected. These might represent products

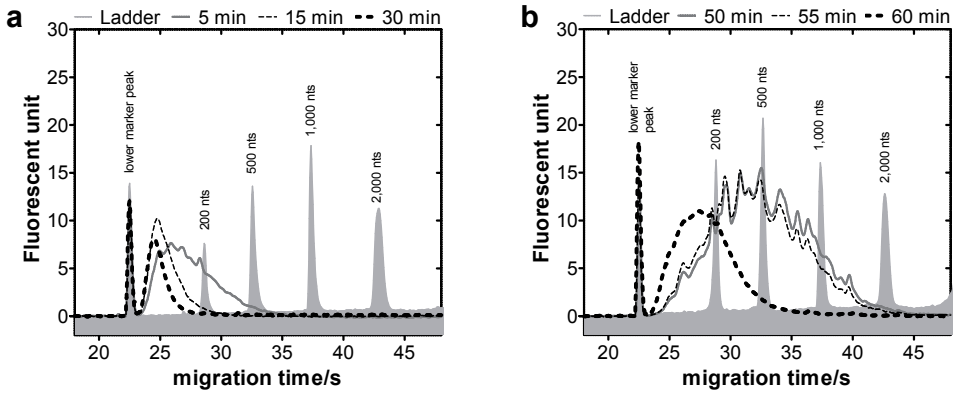

Figure 6.5: Optimization of reaction conditions for fragmentation of RNA down to 200-700 nts length with NP1. Reaction conditions were optimized by incubating 10 µg of *in vitro* transcribed (IVT)-mRNA with (a) 3.0 or (b) 0.075 U mL^{-1} NP1 in a 24 µL reaction mixture at (a) 25 or (b) 20 °C for the times as indicated. The RNA template was (a) a 2,472 nts RNA or (b) an equimolar mixture of three RNAs with 746, 1,294 and 2,472 nts length. Length of fragmented RNA was analyzed on an Agilent 2100 Bioanalyzer. Shown are representative electropherograms with the corresponding ladder (gray). The lower marker peak (25 nts) is used as internal standard to align data of ladder and samples. Peak sizes of the ladder (nts) were calculated from the migration time.

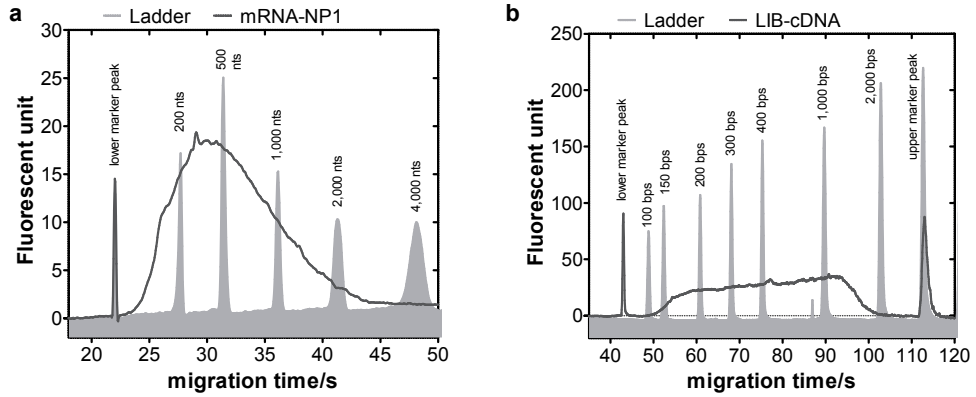

Figure 6.6: Quality control of mRNA and corresponding cDNA used for library buildup. (a) mRNA from ActD treated hiDCs was fragmented down with 0.075 U mL^{-1} NP1 at 20 °C for 55 min in a 24 µL reaction mixture. Length of fragmented mRNA was analyzed on an Agilent 2100 Bioanalyzer using the RNA 6000 pico kit. (b) Fragmented mRNA was used as template for first strand cDNA-synthesis using the Revert Aid Premium Enzyme Mix and DNA polymerase I with RNase H for second strand synthesis. Appearance of cDNA was analyzed on an Agilent 2100 Bioanalyzer using the High Sensitivity DNA Kit.

from degraded DNA templates, because the DNA library was exposed to UV-light during purification. In any case, these RNAs are not expected to affect the selection process. Accordingly, after verification of a suitable variability of the DNA library (see next section) the *in vitro* selection was started with this RNA-library.

6.1.3 Variability of the DNA-library

To determine the variability of the DNA-template pool used for synthesis of the RNA-library, DNA was analyzed via next generation sequencing (NGS). 1.39×10^8 sequences

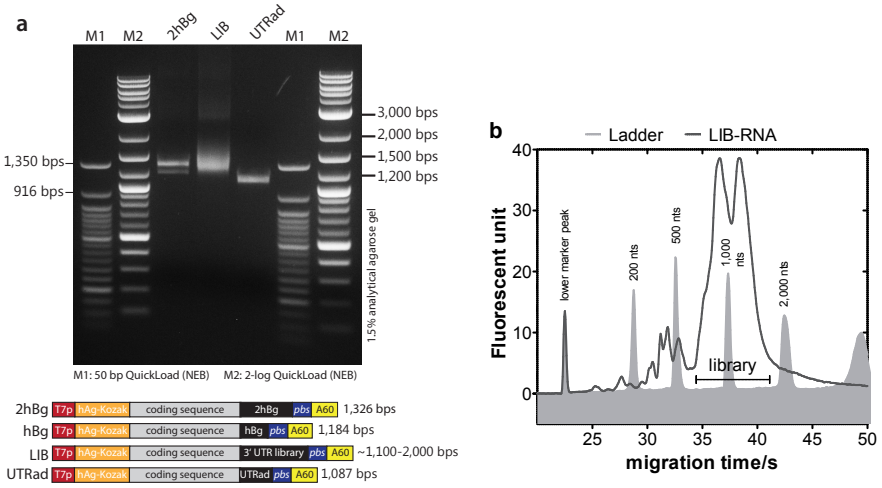

Figure 6.7: Quality control of the library after ligation into vector backbone (DNA) and after *in vitro* T7-transcription (RNA). (a) Agarose gel of the DNA-library (LIB) is shown with control samples containing 2hBg and UTRad as 3′ UTRs. Sequence appearance is depicted in the lower panel. (b) Quality of RNA-library (LIB-RNA) was analyzed on an Agilent 2100 Bioanalyzer.

could be aligned and assigned to human transcripts (65 %) divided in coding and non-coding RNA. 51 % corresponded to the 3' UTR, 27 % to the 5' UTR and 77 % to the CDS-region of coding RNAs, indicating a high complexity as desired as a starting library for the *in vitro* selection process. Approximately 9 % (1.25×10^7 reads) of the aligned reads mapped to the mitochondrial genome.

6.2 *In vitro* selection process in hiDCs

The conditions that are applied to enrich for the sequences of interest are an important factor for any selection approach. In the case of selecting stabilizing RNA sequences, the time after which the selection is stopped is most critical. It should be avoided that due to a too short incubation time in hiDCs too many unstable sequences are present. At the same time it should also be avoided to lose too many sequences due to degradation of the RNA-pool as a consequence of a too long chosen time point. Thus, to get an understanding about the average half-life of the starting pool, an aliquot of a test-RNA-library - derived from optimization of library build up - was electroporated into hiDCs. RNA stability was monitored for 48 h via RT-qPCR. As control, an RNA with just a short linker sequence between the coding region and the poly(A)-tail was applied. In addition, an RNA containing two consecutive copies of the human β-globin 3' UTR (called 2hBg), which have been previously shown to increase the RNA stability in DCs,[85] was used. As expected, the latter RNA was more stable than the RNA without the UTR (data not shown). The average half-life of the RNA pool was similar to the RNA without a UTR, indicating that most of the sequences do not stabilize the RNA. Still, about 20 % of the RNA was present after 24 h. This time point was thus chosen as the duration for the first selection round.
For each selection round, the RNA was electroporated into hiDCs, extracted after defined time points and then reverse transcribed, amplified by PCR and transcribed into RNA

before starting a new round (Fig. 6.1). Proceeding of the selection process was monitored by analyzing the average stability of the selected RNA pool by RT-qPCR for rounds (Rn) 1 to 5 in comparison to internal reference 2hBg. As depicted in Fig. 6.8b, there is a continuous increase in the average stability of the RNA pool up to Rn3, indicating an enrichment of stabilizing 3' UTR-sequences. Thus, stringency was increased during the selection process by choosing longer incubation times for later rounds (Fig. 6.8a). The stabilizing effect was less pronounced for Rn4 and Rn5 (Fig. 6.8c), indicating that selection process was reaching a plateau. Nevertheless, a last selection round was done (Rn6), for which the stringency was increased once more by prolonging cell incubation after electroporation up to two weeks.

a

Sample	TP	Half-life (rel. to 2hBg)
2hBg	-	1.00
LIB	-	0.59
Rn1	24h	0.63
Rn2	48h	0.89
Rn3	48h	1.00
Rn4#	72h	1.01
Rn5#	72h	1.11
Rn6	96h/1wk/2wk	n.a.

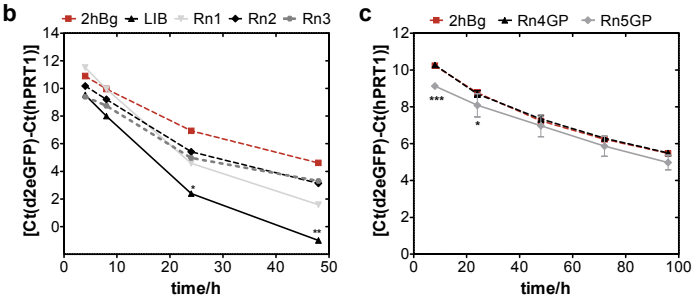

Figure 6.8: Progress of selection process (a) monitored by real-time reverse transcriptase-PCR (RT-PCR) after selection rounds (Rn) (b) 3 and (c) 5. hiDCs were electroporated in equal amounts with RNA of the starting library (LIB) and with RNA of Rn1 to Rn5. From Rn3 on PCR-templates for RT-PCR and next Rn were purified by preparative agarose gel electrophoresis prior to RNA-synthesis (GP). RNA with 2hBg as 3′ UTR was electroporated in equal amount as control sample. hiDCs were harvested at different time points up to 72 h and total RNA was isolated and prepared for RT-PCR. Transcript levels of samples were determined by calculation of the difference between the threshold cycles (Ct) of RNAs encoding for d2eGFPmut and HPRT1 as internal control. (a) Table shows calculated half-lives relative (rel.) to 2hBg for each selection round and their time points (TP) respectively; n.a.: not analyzed. (b) Values from a one time experiment (2way ANOVA, Bonferroni post-test). (c) Values are mean±SD of 3 independent experiments (2way ANOVA, Bonferroni post-test). *: $p<0.05$; **: $p<0.01$; ***: $p<0.001$.

6.3 Sequence analysis of newly selected 3′ UTRs

After the *in vitro* selection process, more than 350 individual clones from Rn5 and Rn6 (divided in the three selection times of 96 h, 1 wk and 2 wk) were sequenced to identify the selected 3' UTRs (Tab. 6.1). First, overall median lengths of the sequence elements obtained were compared. These were similar throughout Rn5 and Rn6 with approx. 180 nts. The minimum and maximum lengths were 77 and 581 nts respectively. Overall GC-content varied throughout all analyzed groups by around 60±6 % (median±SD).

To identify similar or even identical sequences, a genealogical tree was drawn. Fifteen main groups, named A to O, consisting of at least four individual clones (Tab. 6.2) could be identified. In total, these 15 groups cover more than 200 of the sequenced clones (Tab. 6.1). Within each group, a minimal core sequence could be identified with rare base substitutions - arising probably from PCR bias during amplification as part of the *in vitro* selection process[251,252] - and extensions of different lengths up- and downstream of the core area (as shown in Fig. 6.9 and calculated as non-match mean or median percentage in Tab. 6.2).

Table 6.1: Distribution of sequence length in each analyzed selection round. Sequence length varied between 77 and 581 nts for Rn5 (time point: 72 h) and Rn6 (time points: 96 h, 1 wk and 2 wk), respectively. Number (no.) of sequences analyzed varied between 88 and 110 sequences.

	Rn5 – 72h	Rn6 – 96h	Rn6 – 1wk	Rn6 – 2wk
mean±SD length/nts	192±50	189±58	191±59	207±92
median length/nts	181	172	176	181
max. length/nts	346	402	429	581
min. length/nts	77	94	109	79
no. of sequences analyzed	108	88	110	96
no. of sequences grouped	60	42	64	51

From each group, a representative sequence covering the core area (Fig. 6.9, red highlighted sequence) was further analyzed regarding gene origin and its mapping position within the corresponding gene [5' UTR, coding DNA sequence (CDS) or 3' UTR]. Interestingly, most sequences mapped - at least partially - to the 5' or 3' UTR regions of their respective coding genes. As on average, the gene encoding region usually makes up the majority of the transcribed region, this result indicates an enrichment of 5' and 3' UTR-elements during the selection process. Strikingly, one group is derived from a non-coding (nc)RNA, the mitochondrially encoded 12S ribosomal (r)RNA (MT-RNR1; Tab. 6.2). Although this RNA was not expected to be in the starting pool, verification of the sequencing data obtained to determine variability of the library (Ch. 6.1.3) revealed, that MT-RNR1 was represented by approximately 741,441 reads (0.5 % of all alignments). Its selection indicates a strong stabilizing effect (see also *Discussion*, Ch. 7.2).
With regard to the expression of the identified sequences, the genes were not only found to be overexpressed in hiDCs (NextBio® by Illumina), but five of the groups (over 50 %) are also immune cell specific (groups B, D, E, J, N). This is to be expected when using mRNA derived from hiDCs as a starting material for the library.

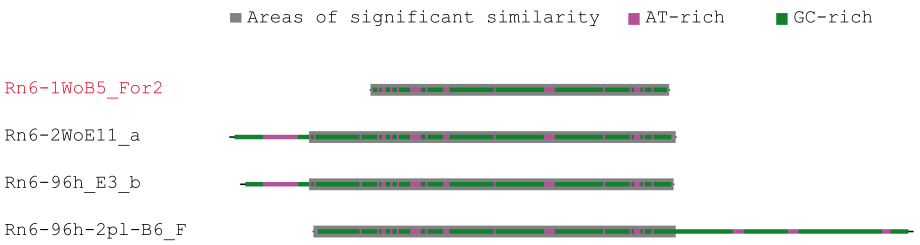

Figure 6.9: Example group F exported from Clone Manager software. Shown are core areas shared by all sequences of one group (solid block) and AT- and GC-rich regions (pink and green respectively). Sequence depicted in red was used for further analysis.

Table 6.2: Overview of analyzed groups and their origin. Genealogical analysis of the selected sequences identified 15 main groups named A to O. For each group the number of unique sequences that were identified (no.), gene origin, its abbreviation (abbr.), mapping region (MR), median and core sequence length (CSL) in nts are shown. Non-matching areas (non-match) describe percentage of nts, which differ between the sequences within the same group outside of the core area. [ncRNA: non-coding RNA]

Group	no.	BLAST-result with representative sequence of each group, Homo Sapiens	abbr.	MR	CSL [nts]	median length [nts]	non-match % mean	non-match % median
A	13	DnaJ (Hsp40) homolog, subfamily C, member 4, mRNA	DNAJC4	5′ UTR+CDS	170	216	13	7
B	50	Fc fragment of immunglobulin (Ig)G, receptor, transporter, alpha, mRNA (cDNA clone)	FCGRT	3′ UTR	143	189.5	22	22
C	11	MRS2 magnesium homeostasis factor homolog, mRNA (S. cerevisiae)	MRS2	5′ UTR+CDS	142	142	7	1
D	22	Lymphocyte-specific protein 1, mRNA	LSP1	3′ UTR	149	156.5	21	19
E	13	Chemokine (C-C motif) ligand 22, mRNA	CCL22	3′ UTR	155	191	28	21
F	4	Amino-terminal enhancer of split, mRNA	AES	3′ UTR	136	200	30	27
G	15	Phospholipase D family, member 3, mRNA	PLD3	CDS+3′ UTR	190	191	17	20
H	8	Polymerase I and transcript release factor, mRNA	PTRF	5′ UTR+CDS	172	172	4	1
I	17	Mitochondrially encoded 12S RNA	MT-RNR1	ncRNA	142	154	12	10
J	22	Major histocompatibility complex, class II, DR beta 4, mRNA	HLA-DRB4	3′ UTR	233	249.5	15	13
K	16	Coiled-coil domain containing 124, mRNA	CCDC124	CDS	170	175	16	3
L	8	Prothymosin, alpha, mRNA	PTMA	5′ UTR	142	152.5	6	4
M	5	Myosin, heavy chain 9, non-muscle, mRNA	MYH9	CDS	167	167	27	17
N	4	Chemokine (C-C motif) ligand 3, mRNA	CCL3	5′ UTR+CDS	109	161	43	42
O	8	Glutaminase, nuclear gene encoding mitochondrial protein, mRNA	GLS	5′ UTR	126	145	57	55

6.4 Functional analysis of newly selected 3′ UTRs

To analyze whether the selected sequence elements indeed stabilize the mRNA when used as 3' UTR, a representative sequence of each group, covering the core area, was cloned as 3' UTR of an RNA coding for luc2CPmut. This reporter gene was chosen, as its low protein half-life facilitates analysis of the RNA stability via measurement of the luciferase activity.[207] Moreover, it allows verification of the stabilizing properties of the selected sequence elements in a different reporter gene context compared to the selection process, where an RNA encoding d2eGFPmut has been used.

After the electroporation of the respective IVT-mRNAs into hiDCs, luciferase activity was monitored for 72 h and compared to cells electroporated with an RNA containing the 2hBg 3' UTR (see above; for simplicity, this RNA is called *2hBg* from now on) as internal reference (Fig. 6.10). Strikingly, stability of most IVT-mRNAs, as deduced from the protein expression profile, was very similar to 2hBg. Thus, with this newly developed *in vitro* selection process new single RNA sequence elements with stabilizing properties comparable to 2hBg, consisting of two copies of the human β-globin 3' UTR, could be identified. This is in line with the results from the RT-qPCR analysis of the stability of the selected RNA pools as shown in Fig. 6.8 and further demonstrates that the *in vitro* selection process has been successful.

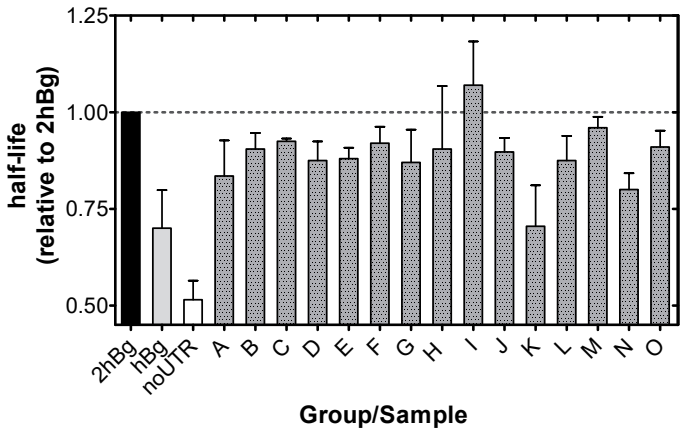

Figure 6.10: RNA half-life of groups compared to control samples. Of each group a reference RNA was electroporated into hiDCs. Luciferase activity was monitored over 72 h and half-life was calculated using R. Relative half-life of groups in comparison to 2hBg, hBg and noUTR. Values are mean of 2-4 independent experiments (Mean±SD).

Next, the pair-wise combinations of seven selected sequences and the single hBg element were used to test whether further improvement of RNA stability could be reached as had been observed for 2hBg.[85] For this, the sequence elements B, D, E, F, G, and J were chosen, along with hBg, as they all derive from 3' UTR sequences of the corresponding genes (Tab. 6.2). As the single I-element, which originates from the non-coding MT-RNR1 RNA, showed the best stabilizing properties, it was also included in this analysis. In total 64 combinations were cloned as 3' UTR of an RNA with luc2CPmut as a reporter gene, either as an up- or downstream element (Tab. 6.3), and were analyzed as described above.

Unexpectedly, several combinations and even reiterations of several single elements such as G, B, J and E actually decreased RNA stability compared to single elements (Tab. 6.3, indicated with red background). The most stabilizing effect (Tab. 6.3, blue background) was found for combinations containing the I-element. Still the half-life of these RNAs was - if at all - only slightly enhanced compared to just one single I-element (Fig. 6.10) and thus was similar to 2hBg (depicted as hBg-hBg in Tab. 6.3).

Table 6.3: Stability of analyzed 3′ UTR-combinations relative to internal reference 2hBg. Each upstream element was combined with one downstream element and cloned as 3′ UTR with luc2CPmut as reporter gene. Luciferase activity was measured over 72 h and half-life was calculated using R. Dark red color shadings show low half-lives (<0.65) and dark blue high half-lives (>0.90) relative to the internal reference (2hBg, indicated here as hBg-hBg).

downstream element (■) \ upstream element (■)	I	G	B	D	J	E	F	hBg
I	1.08	0.94	0.97	0.98	0.93	0.90	1.08	1.10
G	0.99	0.58	0.83	0.75	0.60	0.74	0.88	0.76
B	1.03	0.58	0.62	0.69	0.60	0.67	0.85	0.69
D	1.06	0.68	0.76	0.76	0.62	0.74	0.64	0.85
J	1.00	0.59	0.73	0.68	0.63	0.68	0.81	0.81
E	0.96	0.62	0.76	0.77	0.58	0.74	0.82	0.84
F	1.08	0.68	0.81	0.83	0.71	0.78	0.92	0.97
hBg	1.10	0.78	0.93	0.88	0.81	0.76	1.03	1.00

3′ UTR: 5′ — upstream — downstream — 3′

Using the data obtained from the experiments described above (Fig. 6.10 and Tab. 6.3), the correlation of 3' UTR-length and RNA-stability was analyzed (Fig. 6.11). Interestingly, the longer the 3' UTR, the less stabilizing it is for the corresponding RNA, with a statistical significance of $p<0.0001$. This supports the decision to use mRNA-fragments of between 200 and 1,000 nts length for cloning of the library and is in agreement with published data.[205,253]

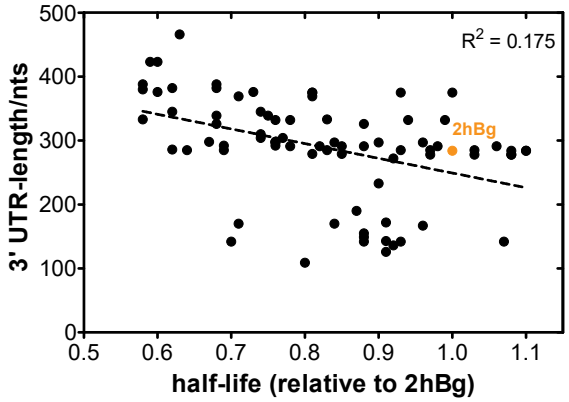

Figure 6.11: Correlation of 3′ UTR-length in nts vs relative half-life of RNA. Linear regression with coefficient of determination $R^2 = 0.175$. 2hBg is highlighted. Correlation is significant (***) with $p<0.0001$ (Pearson, two-tailed).

The most promising candidates, as judged by the results obtained so far and confirmed by replicate experiments (data not shown) - IF, FI, IhBg and hBgI - were analyzed more extensively, and thus cloned as 3' UTRs in luc2mut (standard luciferase). This reporter

allows for a more detailed analysis of not only the RNA stability, but also of the protein expression divided in (i) translational efficiency [the maximal slope of the curve], (ii) relative functional mRNA stability [time point of the maximal protein expression] and (iii) total protein expression over time [integral under the curve].[121] Analysis of the corresponding RNAs in hiDCs showed that an RNA with the IF as 3' UTR has a significantly higher maximal protein expression ($p<0.01$ after 8 h and $p<0.001$ after 24 h post electroporation) indicating a higher functional mRNA stability compared to the internal reference 2hBg (Fig. 6.12a). While RNA-stability with IF as a 3' UTR was again comparable to 2hBg (Fig. 6.12b), the effect can be attributed to an enhanced translational efficiency (up about 1.2-fold; Fig. 6.12c), giving a 1.3-fold increased total protein expression over time (Fig. 6.12d). FI also had a slightly higher maximal protein expression, though it was not statistically significant (Fig. 6.12a). The same could be observed for its half-life, translational efficiency and total protein over time (Fig. 6.12b-d). Combinations of I with hBg did not improve any of the examined parameters. For the single I-element half-life, translational efficiency and total protein over time were comparable to 2hBg, which is consistent with the data shown above (Fig. 6.10). This indicates promising qualities of I as a single 3' UTR-element.

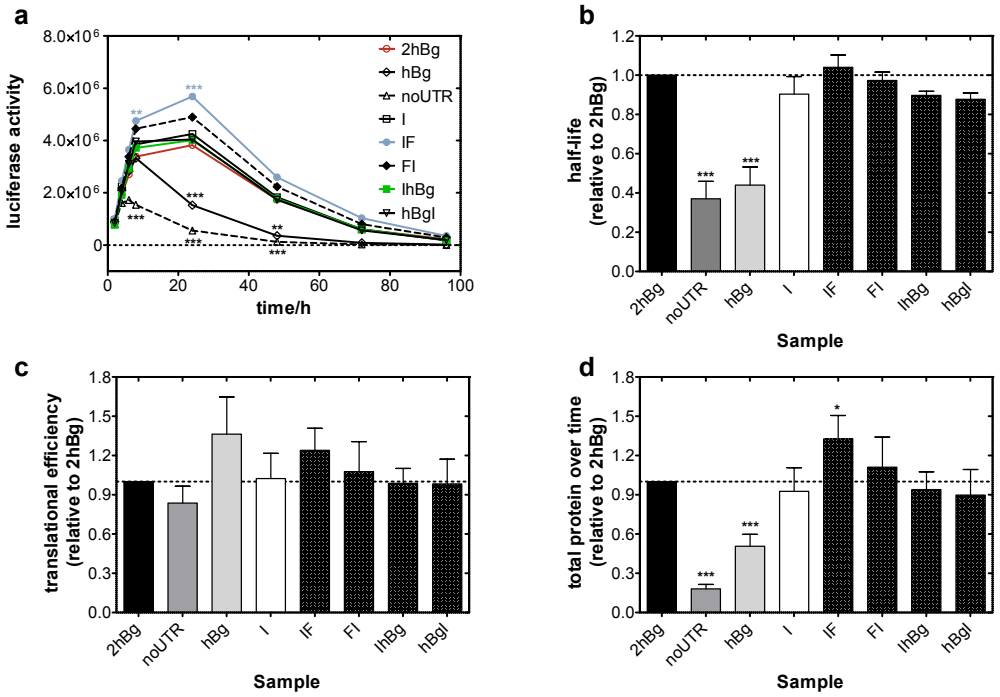

Figure 6.12: RNA turnover with newly selected 3′ UTRs. Sequences were cloned as 3′ UTRs with luc2mut as reporter gene. Luciferase activity was measured (a) over 96 h and (b) half-life, (c) translational efficiency (d) and total protein over time were calculated using R. Shown are results relative to internal reference 2hBg. noUTR: negative control RNA without 3′ UTR; hBg: RNA with one human β-globin 3′ UTR as 3′ UTR; I: RNA with one single I-element as 3′ UTR. (a) Representative curve diagram. ***: $p< 0.001$, **: $p< 0.01$ (2way ANOVA, Bonferroni post-test) (b-d) Values are mean±SD of 3 independent experiments. ***: $p< 0.001$, *: $p< 0.05$ (One-way ANOVA, Dunnett post-test).

By measuring luciferase activity, RNA stability is only deduced from the protein expression pattern, thus limiting detailed and direct analysis of RNA turnover. Therefore, selected sequence elements I, IF, FI, IhBg and hBgI were cloned as 3' UTRs downstream of d2eGFPmut to analyze their stabilizing properties via RT-qPCR. By choosing d2eGFPmut as the reporter gene, both RNA turnover and protein expression of eGFP can be analyzed at the same time by RT-qPCR and FACS-measurement, respectively. Expression of eGFP could be demonstrated in all samples (data not shown). Unfortunately, due to technical difficulties during electroporation of the noUTR-sample[a], the results obtained with this RNA had to be excluded (Fig. 6.13). Nevertheless, analysis of the stabilizing properties of selected 3' UTRs by RT-qPCR in comparison to 2hBg confirmed the previous results obtained from the protein expression profiles with luc2CPmut (Fig. 6.10; Tab. 6.3) and luc2mut (Fig. 6.12). All RNA half-lives are in the same range as 2hBg, which has been shown to be at least up to 2.5-fold more stable compared to noUTR in previous studies (own data). While IF looked slightly better than FI with the luciferase constructs, this time both UTRs were about equal. Apparently, both 3' UTRs have overall similar stabilizing properties.

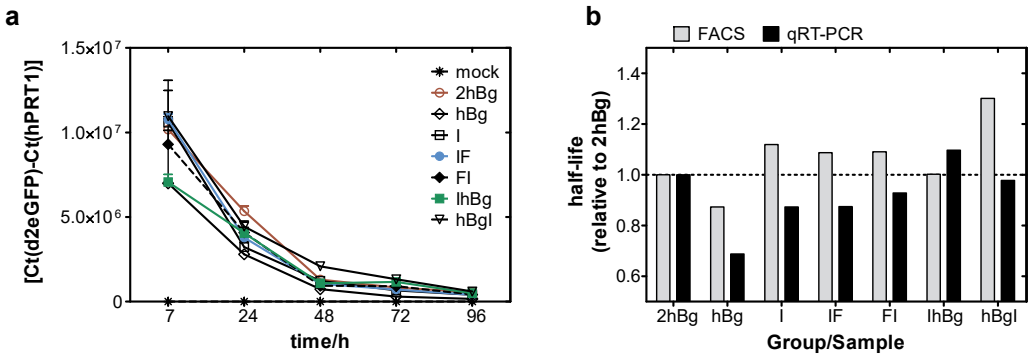

Figure 6.13: RNA turnover with newly selected 3′ UTRs by RT-qPCR and FACS-analysis. Sequences were cloned as 3′ UTRs with d2eGFPmut as reporter gene. GFP-expression on protein- and RNA-level via FACS (data not shown) and (a) RT-qPCR was monitored over 96 h. Shown are (a) transcript levels of samples determined by calculation of the difference between the threshold cycles (Ct) of RNAs encoding for d2eGFPmut and HPRT1. Values are mean±SD of 3 measured samples. (b) Respective half-lives were calculated using R. Shown are results relative to internal reference 2hBg.

Although the focus of the *in vivo* selection process was to find RNA-elements, which stabilize the exogenous administered IVT-mRNA explicitly in hiDCs, IVT-mRNAs encoding for luc2CPmut or luc2mut and I, IF, FI, IhBg or hBgI as 3' UTRs were electroporated into C2C12 (mouse myoblast cell line), HFF (Human Foreskin Fibroblast cells) and $CD4^+$ T cells, to analyze if the stabilizing properties of selected 3' UTRs are hiDC-specific or not. C2C12 and HFF are two cell lines used in-house for stem cell research.[17,214] Intriguingly, stabilization of the mRNA could also be observed in these cells (Supplementary Fig. A.1 to A.3). However, the extent of stabilization and the detailed effect of each 3' UTR on RNA stability and translation efficiency was different in each of these cells compared to hiDCs. This is in agreement with the reported cell-type specificities for UTR elements.[187,254]

[a]The experimental setup did not allow repetition of failed electroporated samples. Once the RNA is thawed and the cells are harvested, a quick electroporation must follow to hinder degradation of the RNA and to ensure same treatment of all samples.

6.5 Analysis of RNA-binding proteins (RBPs) and binding miRNAs

As mentioned above, *trans*-acting factors that bind to *cis*-acting elements are the main mechanism of regulating mRNA turnover within the cell. Thus, bioinformatical identification of putative binding sites for RBPs (Ch. 6.5.1) and miRNAs (Ch. 6.5.2) was attempted to better understand the potential causes of the observed differences in the effects of the 3' UTR(-combinations) on the RNAs in the cell.

6.5.1 Predicted binding sites for RNA-binding proteins (RBPs)

Types of RBPs and their respective number of putative binding sites located on selected 3' UTRs were analyzed via *Scan for motifs* (SFM).[236] Results are summarized in Tab. 6.4 for single 3' UTRs and in Tab. 6.5 for pair-wise combinations (for full names of RBPs see Tab. 6.6). Possible binding sites for well-known RBPs with stabilizing or destabilizing effects on the mRNA were found, such as ELAVL1[255] or PUM2[256] respectively. The most abundant or lowest putative binding sites (Tab. 6.4 and 6.5, dark blue or red background, respectively) were found for YBX1 and PSI or IGF2BP1 and YBX2-a, respectively.

Table 6.4: Number of putative binding RNA-binding proteins on newly selected single 3′ UTRs. Binding was analyzed via *Scan for motifs*[236] for each representative sequence of selected groups and for 2hBg (internal reference) and hBg. Binding number is color-coded with dark blue as high (>15) and dark red (<3) as low numbers.

RNA-binding proteins (RBPs) / 3'-UTRs	A	B	C	D	E	F	G	H	I	J	K	L	M	N	O	hBg	2hBg
YBX1	11	14	15	11	15	12	13	11	2	17	13	7	15	12	21	6	12
ELAVL1	5	4	6	7	4	2	2	3	6	14	14	7	15	4	3	13	26
ELAVL2						1		1	3	3	1	5	3			8	16
SNRPA		3		2	1	2	1	2	4	6	4	1	3	4	1	1	2
FUS	3	1	1		1	4	3	4	2	2	1		1		2	1	2
PUM2	2	1	3	1	4	1	3	1		4	2	1	2	1		2	4
SUS	1	5	3			4	1	2	2	4	6	4	6	1	2	3	7
PSI	6	6	8	9	6	6	5	4	12	17	19	10	18	5	8	10	21
SAP-49		1	1				2		1	1			1				
KHSRP	2	1	1		3	3	4	3	2		6	1	3	1		3	6
NOVA2									1	1	1		2			1	2
QKI									2							1	2
ZFP36									1							1	2
KHDRBS3									2							3	6
A2BP1				1	1	1				2		1		1		1	2
SFRS2			1			2	2	1			4						
NCL								1					1				
PTBP1				1						1						1	2
IGF2BP1										1							
YBX2-a				1													
Sum of binding RBPs	30	36	39	33	35	38	36	33	40	73	71	37	70	29	37	55	112

The I-element with its most promising stabilizing properties, as shown in the obtained results, was the only sequence, next to hBg, with putative binding sites for QKI, ZFP36 and KHDRBS3. However, total predicted number of binding sites for each single 3' UTR varied between 29 and 73 (Tab. 6.4) and for pair-wise 3' UTR-combinations between 66 and 146 (Tab. 6.5). As this was a large variance, the number of putative binding sites was analyzed further regarding their overall effect on RNA stability (Fig. 6.14).

Unfortunately, the direct correlation between RNA-stability and the total number of possible RBP-binding sites was not significant (Fig. 6.14). However, the analysis of variance for each RBP - that is comparison between number of putative binding sites and average half-life for each UTR per number of putative binding sites (Fig. 6.15) - revealed possible significant (de)stabilizing effects mediated through binding of for example YBX1, ELAVL1, PUM2, QKI or ZPF36 on the 3' UTR (Tab. 6.6). The positive or negative stabilizing effect is thereby represented by the slope from the corresponding curve chart and exemplarily shown for PUM2, KHSRP, QKI and ELAVL2 in Fig. 6.15. Although these results suggest that stability of the IVT-mRNA is mediated through the binding of certain RBPs at different extents, predictions must be taken into account carefully. Several calculations are based on only three degrees of freedom (DF), which does not support ideal statistical remarks and moreover, (de)stabilizing effects were partially contradictory to the literature (see Discussion, Ch. 7.3).

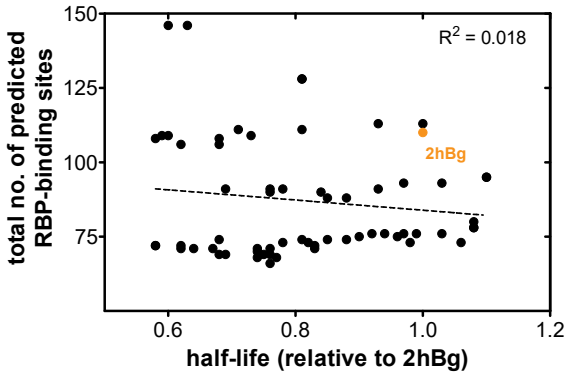

Figure 6.14: Correlation between RNA-stability and number of binding RBPs. Linear regression with coefficient of determination $R^2 = 0.018$. 2hBg is highlighted. Correlation is not significant ($p>0.05$; Pearson, two-tailed).

Table 6.5: Number of putative binding RNA-binding proteins on pair-wise combinations. Binding was analyzed via *Scan for motifs*[236] for each 3′ UTR pair-wise combination. Binding number is color-coded with dark blue as high (>15) and red as low dark red (<3) numbers.

RNA-binding proteins (RBPs) \ 3'-UTRs	I								G								B								D							
	II	IG	IB	ID	IJ	IE	IF	IhBg	GI	GG	GB	GD	GJ	GE	GF	GhBg	BI	BG	BB	BD	BJ	BE	BF	BhBg	DI	DG	DB	DD	DJ	DE	DF	DhBg
YBX1	4	15	16	13	19	17	14	8	15	26	27	24	30	28	25	19	16	27	28	25	31	29	26	20	13	24	25	22	28	26	23	17
ELAVL1	12	8	10	13	20	10	8	19	8	4	6	9	16	6	4	15	10	6	8	11	18	8	6	17	13	9	11	14	21	11	9	20
ELAVL2	6	3	3	3	6	3	4	11	3				3		1	8	3				3		1	8	3				3		1	8
SNRPA	8	5	7	6	10	5	6	5	5	2	4	3	7	2	3	2	7	4	6	5	9	4	5	4	6	3	5	4	8	3	4	3
FUS	4	5	3	2	4	3	6	3	5	6	4	3	5	4	7	4	3	4	2	1	3	2	5	2	2	3	1		2	1	4	1
PUM2		3	1	1	4	4	1	2	3	6	4	4	7	7	4	5	1	4	2	2	5	5	2	3	1	4	2	2	5	5	2	3
SUS	4	3	7	2	6	2	6	5	3	2	6	1	5	1	5	4	7	6	10	5	9	5	9	8	2	1	5		4		4	3
PSI	24	17	18	21	29	18	18	22	17	10	11	14	22	11	11	15	18	11	12	15	23	12	12	16	21	14	15	18	26	15	15	19
SAP-49	2	3	2	1	2	1	1	1	3	4	3	2	3	2	2	2	2	3	2	1	2	1	1	1	1	2	1		1			
KHSRP	4	6	3	2	2	5	5	5	6	8	5	4	4	7	7	7	3	5	2	1	1	4	4	4	2	4	1			3	3	3
NOVA2	2	1	1	1	2	1	1	2	1				1			1	1				1			1	1				1			1
QKI	4	2	2	2	2	2	2	3	2							1	2							1	2							1
ZFP36	2	1	1	1	1	1	1	2	1							1	1							1	1							1
KHDRBS3	4	2	2	2	2	2	2	5	2							3	2							3	2							3
A2BP1				1	2	1	1	1				1	2	1	1	1				1	2	1	1	1	1	1	1	2	3	2	2	2
SFRS2		2					2		2	4	2	2	2	2	4	2		2					2			2					2	
PTBP1				1	1			1				1	1			1				1	1			1	1	1	1	2	2	1	1	2
IGF2BP1					1								1								1								1			
YBX2-a				1								1								1					1	1	1	2	1	1	1	1
sum of binding RBPs	80	76	76	73	113	75	78	95	76	72	72	69	109	71	74	91	76	72	72	69	109	71	74	91	73	69	69	66	106	68	71	88

RNA-binding proteins (RBPs) \ 3'-UTRs	J								E								F								hBg							
	JI	JG	JB	JD	JJ	JE	JF	JhBg	EI	EG	EB	ED	EJ	EE	EF	EhBg	FI	FG	FB	FD	FJ	FE	FF	FhBg	hBgI	hBgG	hBgB	hBgD	hBgJ	hBgE	hBgF	2hBg
YBX1	19	34	31	28	34	32	29	23	17	28	29	26	32	30	27	21	14	25	26	23	29	27	24	18	8	19	20	17	23	21	18	12
ELAVL1	20	28	18	21	28	18	16	27	10	6	8	11	18	8	6	17	8	4	6	9	16	6	4	15	19	15	17	20	27	17	15	26
ELAVL2	6	6	3	3	6	3	4	11	3				3		1	8	4	1	1	1	4	1	2	9	11	8	8	8	11	8	9	16
SNRPA	10	12	9	8	12	7	8	7	5	2	4	3	7	2	3	2	6	3	5	4	8	3	4	3	5	2	4	3	7	2	3	2
FUS	4	4	3	2	4	3	6	3	3	4	2	1	3	2	5	2	6	7	5	4	6	5	8	5	3	4	2	1	3	2	5	2
PUM2	4	8	5	5	8	8	5	6	4	7	5	5	8	8	5	6	1	4	2	2	5	5	2	3	2	5	3	3	6	6	3	4
SUS	6	8	9	4	8	4	8	7	2	1	5		4		4	3	6	5	9	4	8	4	8	7	5	4	8	3	7	3	7	6
PSI	29	34	23	26	34	23	23	27	18	11	12	15	23	12	12	16	18	11	12	15	23	12	12	16	22	15	16	19	27	16	16	20
SAP-49	2	2	2	1	2	1	1	1	1	2	1		1				1	2	1		1				1	2	1		1			
KHSRP	2		1			3	3	3	5	7	4	3	3	6	6	6	5	7	4	3	3	6	6	6	5	7	4	3	3	6	6	6
NOVA2	2	2	1	1	2	1	1	2	1				1			1	1				1			1	2	1	1	1	2	1	1	2
QKI	2							1	2							1	2							1	3	1	1	1	1	1	1	2
ZFP36	1							1	1							1	1							1	2	1	1	1	1	1	1	2
KHDRBS3	2							3	2							3	2							3	5	3	3	3	3	3	3	6
A2BP1	2	4	2	3	4	3	3	3	1	1	1	2	3	2	2	2	1	1	1	2	3	2	2	2	1	1	1	2	3	2	2	2
SFRS2							2			2					2		2	4	2	2	2	2	4	2		2					2	
PTBP1	1	2	1	2	2	1	1	2				1	1			1				1	1			1	1	1	1	2	2	1	1	2
IGF2BP1	1	2	1	1	2	1	1	1					1								1								1			
YBX2-a				1								1								1								1				
sum of binding RBPs	113	146	109	106	146	108	111	128	75	71	71	68	108	70	73	90	78	74	74	71	111	73	76	93	95	91	91	88	128	90	93	110

Table 6.6: Putative binding of RBPs and their overall stabilization effect. P-value of (de)stabilizing effect in relation to determined RNA half-lives calculated via Anova. Slope of corresponding curve indicates if effect is stabilizing (+) or destabilizing (-) (see also examples in Fig. 6.15). R^2 (coefficient of determination) describes curve charts between average half-life relative to 2hBg per number of RBP-binding sites (Fig. 6.15). Expression of each RBP in hiDCs was determined via NextBio® (by Illumina). Over- or underexpression refers to median expression of all tested cell lines. n.s.: not specified.

RBP	symbol	Significance of (de)stabilizing effect (p-value)	DF	expression of RBP in hiDCs	Slope	R^2
Y Box Binding Protein 1	YBX1	0	28	over	-0.013	0.641
(Embryonic Lethal, Abnormal Vision, Drosophila)-Like RNA Binding Protein 1 (Hu-Antigen R)	ELAVL1	0.001	23	over	-0.003	0.028
(Embryonic Lethal, Abnormal Vision, Drosophila)-Like RNA Binding Protein 2 (Hu-Antigen B)	ELAVL2	0.101	11	over	0.012	0.494
Small Nuclear Ribonucleoprotein Polypeptide A	SNRPA	0.031	12	under	-0.011	0.158
Fused In Sarcoma RNA Binding Protein (Heterogeneous Nuclear Ribonucleoprotein P2)	FUS	0.965	9	under	0.006	0.132
Pumilio RNA-Binding Family Member 2	PUM2	0	9	over	-0.045	0.892
Sus scrofa pogo transposable element with ZNF domain	SUS	0.031	11	n.s.	-0.01	0.132
P-element somatic inhibitor protein	PSI	0	22	under	-0.002	0.014
Splicing Factor 3b, Subunit 4, 49kDa	SAP-49	0.176	5	n.s.	-0.059	0.702
KH-Type Splicing Regulatory Protein	KHSRP	0.006	9	under	0.005	0.028
Neuro-Oncological Ventral Antigen 2	NOVA2	0.023	3	under	0.063	0.999
Quaking Homolog, KH Domain RNA Binding	QKI	0	5	over	0.091	0.898
Zinc Finger Protein 36 Homolog	ZFP36 (TTP)	0	3	under	0.155	1
KH Domain Containing, RNA Binding, Signal Transduction Associated	KHDRBS3	0	6	under	0.046	0.531
RNA Binding Protein, Fox-1 Homolog (C. Elegans) 1	A2BP1	0.015	5	over	-0.065	0.912
Serine/Arginine-Rich Splicing Factor 2	SFRS2	0.516	4	over	-0.028	0.504
Polypyrimidine Tract Binding Protein 1	PTBP1	0.155	3	under	-0.046	0.999
Insulin-Like Growth Factor 2 mRNA Binding Protein 1	IGF2BP1	0.004	3	over	-0.118	0.996
Y Box Binding Protein 2	YBX2-a	0.447	3	under	-0.038	0.973

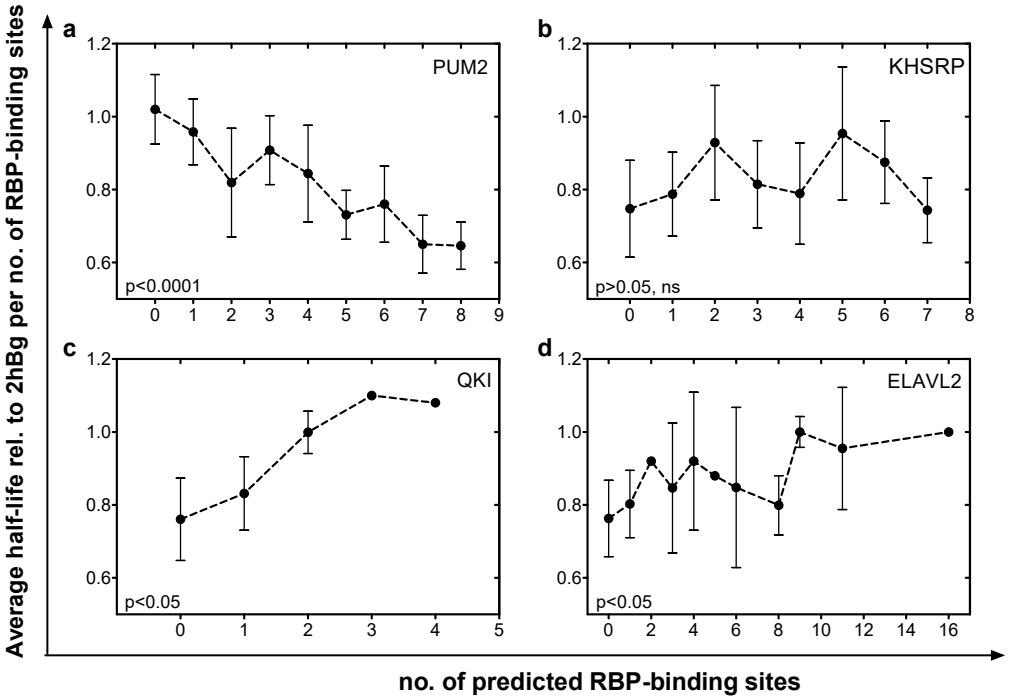

Figure 6.15: Examples of RBPs binding to newly selected 3′ UTRs. Shown are correlations between average half-life per no. of RBP-binding sites and no. of RBP-binding sites and their significances (Pearson correlation, two tailed) for (a) PUM2, (b) KHSRP, (c) QKI and (d) ELAVL2. [rel.: relative]

6.5.2 Predicted miRNA binding sites

miRNAs bind to their target RNAs via sequence complementarity, and lead to translational arrest and ultimately RNA degradation. To obtain an miRNA expression profile typical for unstimulated and stimulated DCs, published data of Hashimi *et al.*[244] and Landgraf *et al.*,[245] who both described miRNA expression patterns for different cell lines and tissues via microarray and NGS, respectively, was combined discriminating between unstimulated and LPS-stimulated DCs (Supplementary Tab. A.2 and A.3). Putative miRNA binding sites in the selected UTRs were identified using IntaRNA.[237–240] Interestingly, there was a significant correlation between RNA-stability and total number of putative miRNA binding sites in unstimulated and LPS-stimulated DCs ($p<0.001$; Fig. 6.16a,c). This was also seen for the sum of miRNA hybridization energy among analyzed 3' UTR-sequences ($p<0.0001$; Fig. 6.16b,d).

Analyzing these results in more detail, it was remarkable that pair-wise combinations with B and J and partially with G, D and E - i.e. the single UTR elements which in combination were less efficient in RNA stabilization - showed the highest sum of total binding miRNAs (Tab. 6.7a,c) and also lowest sum of hybridization energy (Tab. 6.7b,d). Supplementary Tab. A.4 and A.5 give a detailed overview of all binding miRNAs and their corresponding hybridization energies.

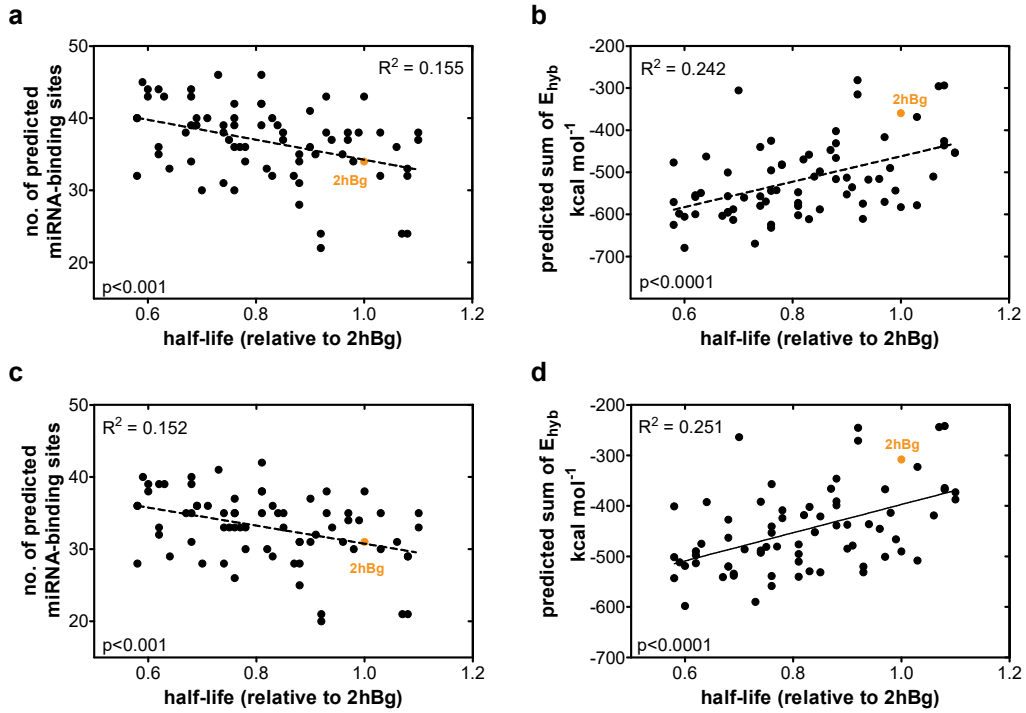

Figure 6.16: Correlation of no. of putative binding miRNAs and sum of hybridization energy vs RNA-stability. Linear regression with coefficient of determination R^2. 2hBg is highlighted. Correlation is significant with p<0.0001 and p<0.001 (Pearson, two tailed).

Table 6.7: Sum of putative binding miRNAs and hybridization energies in unstimulated and LPS-stimulated DCs. Tables are color-coded according to Tab. 6.3. (a, c) Sum of binding miRNAs and (b, d) sum of hybridization energies in kcal/mol of all binding miRNAs for each combination in unstimulated (a, b) and LPS-stimulated DCs (c, d).

a

sum of binding miRNAs (DC)	upstream element (■) I	G	B	D	J	E	F	hBg
downstream element (■) I	21	33	35	30	38	31	29	35
G	34	28	36	33	38	33	31	35
B	35	36	32	36	39	35	35	36
D	31	35	37	26	39	35	29	33
J	38	40	41	40	39	39	38	42
E	31	33	35	33	36	28	30	35
F	29	31	35	29	36	30	21	34
hBg	33	33	35	31	38	33	30	31

b

sum of hybridization energies (DC)	upstream element (■) I	G	B	D	J	E	F	hBg
downstream element (■) I	-224	-427	-483	-378	-532	-411	-356	-361
G	-457	-383	-521	-463	-501	-475	-430	-444
B	-481	-534	-435	-493	-589	-505	-522	-507
D	-374	-427	-485	-321	-451	-435	-348	-358
J	-454	-476	-554	-466	-439	-484	-450	-465
E	-383	-445	-487	-436	-456	-365	-409	-425
F	-350	-418	-513	-384	-450	-415	-253	-331
hBg	-337	-391	-484	-345	-422	-414	-278	-272

c

sum of binding miRNAs (LPS-DC)	upstream element (■) I	G	B	D	J	E	F	hBg
downstream element (■) I	24	37	38	34	43	36	32	38
G	38	32	40	37	43	38	35	39
B	38	40	35	40	44	38	38	39
D	36	39	42	30	44	39	33	37
J	43	45	46	44	43	43	42	46
E	35	36	40	36	40	31	33	39
F	33	34	39	32	40	34	24	37
hBg	37	36	38	34	42	36	32	34

d

sum of hybridization energies (LPS-DC)	upstream element (■) I	G	B	D	J	E	F	hBg
downstream element (■) I	-276	-490	-552	-454	-611	-486	-417	-436
G	-517	-441	-602	-533	-597	-544	-489	-535
B	-551	-616	-492	-568	-652	-567	-579	-561
D	-465	-494	-570	-380	-528	-494	-417	-444
J	-556	-571	-615	-549	-522	-551	-519	-544
E	-453	-496	-560	-498	-517	-413	-461	-483
F	-418	-473	-575	-440	-515	-473	-297	-381
hBg	-417	-447	-539	-421	-503	-468	-333	-333

Stabilizing properties of each selected 3' UTR (single or combined) were further analyzed by comparing results - number of putative binding miRNA and respective hybridization energy - of each 3' UTR with each other in unstimulated (Supplementary Tab. A.6) and LPS-stimulated DC (Supplementary Tab. A.7). The outcome was not only in line with previously obtained results (Ch. 6.4), but affirmed the decision to analyze IF and FI further, as both combinations and as single - I and F - or reiterated versions - II and FF - were significantly different in stabilizing the IVT-mRNA compared to all other selected 3' UTRs. Single hBg as well as 2hBg (hBg-hBg) also showed significant differences to most 3' UTRs, but combinations with I (IhBg, hBgI) did not have the same effect. These results suggest, that binding of miRNAs to selected 3' UTRs with different hybridization energy strengths, promote destabilization of IVT-mRNA at different extents and thus, can potentially explain why several pair-wise combinations decreased the half-life of IVT-mRNA by almost half (Tab. 6.3). Respective results obtained for hiDCs and other cell types/lines regarding stability, translational efficiency and putative miRNA binding sites are summarized in Tab. 6.8.

Table 6.8: Summary of most promising new 3′ UTR candidates compared to 2hBg. miRNA: miRNAs in unstimulated DC; miRNA-LPS: miRNAs in LPS-stimulated DCs; HL: half-life; TE: translational efficiency; $\sum$: total protein over time; no.: number of miRNAs; Δ: sum of hybridization energy in kcal mol^{-1}. Reporter genes: *luc2CPmut, **luc2mut.

	hiDCs			miRNA		miRNA-LPS		other cell types		
3′ UTR	HL*	TE**	$\sum$**	no.	Δ	no.	Δ	HFF*	C2C12*	CD4+**
2hBg	1.00	1.00	1.00	31	-272	34	-333	1.00	1.00	1.00
I	1.07	1.02	0.93	21	-217	24	-269	0.97	1.15	1.08
IF	1.12	1.24	1.33	29	-350	33	-418	1.73	1.33	1.00
FI	1.02	1.08	1.11	29	-356	32	-417	1.61	1.19	1.02
IhBg	1.16	0.99	0.94	33	-337	37	-417	1.19	1.36	1.07
hBgI	1.09	0.98	0.90	35	-361	38	-436	1.00	1.25	1.04

7 Discussion

Since the mid-1990s, mRNA-based therapeutics have emerged as a powerful new drug tool for active immunotherapy of cancer by using synthetic mRNA coding for one or more specific tumor antigens.[1] By loading hiDCs *ex vivo* with RNA or after targeted delivery into hiDCs *in vivo*, translation takes place in the cell, so that the entirety of epitopes encoded on the tumor antigen(s) are processed and presented on MHC class I and II complexes to $CD4^+$ and $CD8^+$ T cells. Hence, these cells are activated and able to induce an effective and powerful antitumor response.[28,33–35,109]

However, a major challenge of using synthetic RNA is its limited intracellular stability, which is essential for an effective and sustained immune response, because this defines the time span during which the antigenic epitopes are generated.[121] In addition, a high translational efficiency, i.e. high amounts of protein made from one RNA molecule, is desired, because this determines the absolute level of antigens at a given time. As RNA-based therapeutics structurally mimic naturally occurring mRNA, modifications of the 5' cap structure, the 3' poly(A)-tail, as well as the 5' and 3' UTR of the exogenous mRNA can improve stability and translational efficiency in hiDCs. For example, not only protein expression, but also priming and expansion of naïve T cells is enhanced *in vivo* by using β-S-ARCA (D1) as a 5' cap and two reiterated human β-globin 3' UTRs as 3' UTR.[85,130]

The β-globin 3' UTR confers a high stability to the β-globin mRNA in erythrocytes in line with the fact that these enucleated cells have no active RNA synthesis.[257] The stabilizing effect can be principally transferred to mRNAs in other cell types including hiDCs.[85] However, from literature it is known that mammalian transcriptomes are dynamic, varying with each cell type, tissue or organ system.[187,254] Thus, the identification of stabilizing and hiDC-specific RNA sequence elements could improve intracellular pharmacokinetics of the mRNA-based therapeutic in these cells. Therefore, an *in vitro* selection process was developed partially based on the studies of Chrzanowska-Lightowlers *et al.*[200] and Yuhashi *et al.*[258] by using not only a self-made library derived from hiDC-specific mRNA, but also hiDCs as a selective environment. This allowed the identification of novel sequence elements that improve RNA stability and translational efficiency, when used as 3' UTRs. Moreover, using single RNA elements as 3' UTR would also circumvent the disadvantages coming from using two reiterated copies, which are prone to recombination, leading to undesired by-products lacking one β-globin-element during PCR or cloning procedures. This would ensure a time and cost efficient preparation of personalized cancer vaccines.[72]

7.1 Library used for *in vitro* selection process

Cells and tissues do not only have different transcriptomes,[187,254] the stability of each mRNA also differs depending on the physiological/developmental state of the cell and the presence or absence of distinct structural motifs on the mRNA.[259] This means, that an RNA, which is stable in one cell type, is not necessarily stable in another cell type. To take this into

account for the selection process applied here, the starting mRNA-library was generated directly from hiDCs to ensure selection of hiDC-specific RNA-sequences. Moreover, before isolating the mRNA, the cells were cultured in the presence of the transcription inhibitor Actinomycin D (ActD) to preselect stable RNAs.[260,261]
Unfortunately, ActD is known to profoundly change the cellular physiology, including splicing events, polyadenylation of the mRNA and even increased destabilization of distinct transcripts[262,263] as has been shown with HeLa cells,[264,265] Jurkat and human T cells[261,266] as well as fibroblasts.[267] However, ActD was still used for transcription inhibition in hiDCs and the resulting possible changes in the transcriptome were accepted. This was based on the rationale to start the selection process with a library preselected for stability, to avoid dragging along RNA-sequence elements that do not have stabilizing properties. Fortunately, transcription was efficiently inhibited within the first 3 h, so that toxicity could be kept to a minimum. Furthermore, as most short-living mRNAs have a half-life in the range of minutes, not hours,[265,268,269] they should be efficiently degraded during the treatment of cells with ActD.[259,264] Thus, the library could be build with RNA-sequences derived mostly from long-lasting mRNAs.

The variability of the self-made library was low with only 56,539 identified unique human transcripts compared to chemically synthesized libraries. The maximum complexity of such a synthetic library depends on the length of the variable region.[270] For example, a 20 nucleotides (nts) long variable region yields a sequence complexity of 10^{12}, and a region twice the length 10^{24}. With respect to the number of different transcripts that are present in a cell, the obtained complexity is in the expected range, especially when taking into account that the library had undergone several steps, which decreased not only total mRNA amount, but also diminished samples prior NGS-analysis. For example, PCRs were done during the library build up and preparation for NGS-analysis to determine library key characteristics. Each of these PCRs can introduce sequence artifacts due to PCR selection and drift,[232,234] especially in multitemplate PCRs as was the case here.[251] Another explanation are the enzyme digests also done during library and NGS-preparation. A digest in the unknown sequence area is likely to happen and thus, bears the risk to lose sequence fragments.
Importantly, a library with a smaller variability compared to chemically synthesized sequence libraries was not only expected, but also intended, as it has been shown, that mammalian cells take up only approximately 10^4 to 10^5 of electroporated molecules (corresponding to <5 % of external concentration) with one pulse and field strength below $1\,\mathrm{kV\,cm^{-1}}$ depending on the molecule size.[271–275] Tested were molecules between 623 Da (calcein) up to 71 kDa (dextran). The heavier the molecule, the less could be transfected into the cells. In another study, Javorovic and colleagues aimed to determine the exact amount of electroporated tyrosinase encoding RNA - with a length of about 2,000 nts - in DCs.[276] They could detect less than 0.1 % of the total electroporated RNA molecules via RT-qPCR. Based on their results, they calculated an average of 3,364±1,139 electroporated molecules per cell.

The RNA-library used in this work has an estimated weight of between 300 and 700 kDa (corresponds to approx. 1,100-2,000 nts) per molecule. Ten µg of this library were electroporated into 1×10^7 hiDCs, which corresponds to a median number of 1.1×10^{13} RNA-molecules, respectively. In this context and based on the literature (see above), these numbers led to the assumption, that less than 1 % of RNA molecules could be electroporated into hiDCs. As a consequence, more than 9.9×10^{23} sequences would be lost, when using, for example, a synthetic library with a complexity of up to 10^{24} sequences.[270] Moreover, as reported by Velculescu *et al.* the average expression levels of genes in different tissues varied between 0.3 and 9,417 transcript copies per mRNA type per cell,[277] suggesting that the physiological range of mRNA molecules per cell of a specific cell type can't be overstrained. Therefore, using RNA directly derived from hiDCs, not only allowed for the performing of *in vitro* selection with RNA naturally preselected and optimized for hiDCs, but also the possibility to reduce loss of putative stabilizing sequence elements at the limiting step, i.e. electroporation into cells,[208,209] and in this context, avoid overuse of the cell.

7.2 Progress of the *in vitro* selection process

The progress of the selection process was followed by determining the average stability of the library at the beginning of the process and after each selection round. As expected, the stability of the RNA pool increased during the first four rounds of the selection process. Thereafter no further improvement was observed, i.e. the average stability remained constant. Accordingly, the selection was stopped so as not to lose sequence divergence due to overrepresentation of single sequences, due to e.g. because of better amplification by PCR. In addition, a comparison of the sequencing result of the library prior to selection with the sequences of the selected clones also gives insight into the selection process. The selection process was started with sequences mapping one-to-one to the UTRs compared to the CDS-region of a coding RNA (51 %vs. 50 % respectively of aligned sequences; Ch. 6.1.3). Intriguingly, more than half of the sequences map to 3' UTRs after the selection process (Tab. 6.2). This is in agreement with the fact that RNA stability is mainly determined by sequences in the 3' UTR.[278] The main reason for this is most likely the limitation of the coding region, which can only be adapted for RNA stability to a certain degree, because its main function is to code for a specific protein sequence. Therefore, the enrichment of endogenous 3' UTRs during the selection process verifies its progress.
Finally, sequencing of the selected sequences revealed several groups, each with multiple members characterized by a core sequence, but different 5' and/or 3'-ends. This indicates that the same core sequences were selected starting from independent RNAs. Altogether, these results not only confirmed that a real selection of individual stabilizing sequences took place, but also that the measures taken to avoid experimental bias as described in Ch. 5.5 were successfully applied.

7.3 Characteristics of selected 3′ UTRs

7.3.1 Selected 3′ UTR sequences

By developing a novel *in vitro* selection process, new candidate sequences, which can enhance the half-life of IVT-mRNA, were identified. One third of the in total 15 defined groups (A to O) were immune cell specific: group B, D, E, J and N (Tab. 6.2). Two of these selected sequence groups mapped against chemokines: group E (CCL22) and N (CCL3). This was surprising, because chemokines like cytokines are generally encoded on RNAs with short half-lives. Their translation needs to be monitored closely as aberrant expression has been linked with cancer, autoimmune disorders and inflammatory diseases.[279–284] Apparently, the selected sequence parts from these mRNAs do not contain any strong destabilizing elements [like AU-rich elements (AREs)], by which the instability of such RNAs is controlled. Recently, Schwanhausser *et al.* published mRNA and protein half-lives of more than 5,000 genes of mammalian cells.[144] Genes of group F, G, H, K, L and M were not only found within the data, but were also found to be above the median mRNA half-life (9.9 h), namely between 15.7 and 29.7 h. This is in line with the obtained stability results. As single elements, these groups - except for group K - stabilize the IVT-mRNA similarly to 2hBg.
The identification of sequence elements mapping to the mitochondrially encoded 12S rRNA (group I; MT-RNR1) was surprising. These sequences should actually not be included in the library in the first place, as a poly(A)+ RNA purification step was involved in the build up of the library.[285] In any case, group I derived from MT-RNR1 is the fourth largest group with 17 members identified after the selection (Tab. 6.2). MT-RNR1 is the smaller ribosomal RNA (rRNA) encoded on the mitochondrial genome (mtDNA).[286,287] The complete MT-RNR1 has a length of almost 1,000 nts, but only fragments mapping to the 5' domain of the 12S MT-RNR1 were selected.[288] This suggests a strong stabilizing potential for the selected sequences derived from MT-RNR1 (group I) and also demonstrates the success of the *in vitro* selection process.

7.3.2 Factors that contribute to RNA-stability

In an attempt to understand the underlying mechanism by which the selected sequences stabilize mRNAs, the presence of putative binding sites for RBPs and miRNAs was analyzed bioinformatically. RBPs bind to their respective RNA-sequence motifs with different specificities and affinities, thereby - depending on the specific protein - either stabilizing or destabilizing the mRNA. The minimal consensus sequence is often only a few nucleotides long (approx. 4 nts).[289]
However, the fate of mature mRNAs is also influenced by miRNAs. These are small endogenous 21 nts long non-coding RNAs, which regulate gene expression post-transcriptionally. In mammalian cells, they form imperfect hybrids with their target sequences mostly in the 3' UTR of the mRNA, inhibiting protein synthesis by repression of translation and/or promoting deadenylation; and thus inducing subsequent mRNA degradation.[157,183,290]

RBPs and their influence on RNA-stability Putative binding sites for RBPs and motifs for regulatory elements were identified on newly selected 3' UTRs by *Scan for motifs* (SFM).[236] Regulatory motifs located on the 3' UTR, such as AREs often promote destabilization of the mRNA.[178,291] Interestingly, no such ARE-motifs could be found in any of the newly selected 3' UTRs, consistent with a selection for stabilizing sequences, which should be devoid of such elements. ARE-motifs could not even be detected within sequences of group N (CCL3), D (LSP1) or J (HLA-DRB4), where the corresponding natural occurring mRNAs are known to be regulated by the Zinc Finger Protein Tristetraprolin (TTP; also known as ZFP36) to limit inflammatory responses by destabilizing its mRNA targets.[282,292–294] This suggests that the RNA elements responsible for promoting RNA decay, were probably excluded - as intended - during the *in vitro* selection. Intriguingly, RNA-sequences of group I (MT-RNR1) and hBg have each - as predicted by SFM - one binding site for ZFP36 (TTP). However, with respect to the I-3' UTR, this element showed a strong stabilizing effect on the IVT-mRNA. Thus, the predicted ZFP36-binding site and possible influence on RNA-stability can only be confirmed experimentally (see below).
Other than the destabilizing ZPF36 (TTP), putative binding sites of its counterpart, the stabilizing ARE-binding proteins, such as ELAVL1 (also known as HuR)[255,295] or YBX1,[296] were also predicted in every newly selected 3' UTR. The ELAV family (ELAV like RNA binding protein) plays a role in stabilizing its target mRNAs by binding to the same ARE-motif as its destabilizing counterpart.[295] Instead, YBX1 is not only able to bind to the ARE-motif, but also to the JNK response element to mediate stability of IL-2.[297] Other putative binding sites concerned RBPs mainly involved in splicing activities (NOVA2, SNRPA, FUS, SAP-49, SFRS2 or PSI).[298–304]

SFM predicted binding sites on every 3' UTR for stabilizing and destabilizing RBPs. However, how these putative binding sites mediate RNA stability or decay through binding of respective RBPs, could not be elucidated using this data. Thus, to identify potential correlations between predicted binding sites, number of binding sites for each RBP in a given element were plotted against the stabilizing effect. Intriguingly, for some RBPs a correlation in line with the reported activity of the protein could be observed. For example, high numbers of binding sites (up to 8) for PUM2 correlate - according to the analysis of variance - significantly with a higher RNA destabilization. This result is consistent with the literature. To date, PUM2 is known to promote deadenylation of its target[256,305] and hence, mRNA decay (Ch. 3.7). However, some of the predicted significant correlations are controversial regarding the literature. For example, it seems that the more YBX1 binding sites (up to 34) the RNA has, the less stable the mRNA. Yet, YBX1 is known to stabilize RNAs. It is not only able to bind to specific motifs (see above), but also to interact with other proteins to form a multiprotein complex thereby mediating stability of the target mRNA.[306] Other binding sites predicted by SFM did not show any clear correlation between number of binding sites and RNA stability (e.g. binding sites for ZFP36, IGF2BP1 or PTBP1) or did not have any clear trend in promoting stabilization or destabilization of the RNA (e.g. binding sites for SUS, FUS or PSI).

As RBPs do not always bind to their respective consensus sequence motifs, other factors must contribute to their binding specificity.[289] In this context, to affirm the binding of RBPs to the selected 3' UTRs, proteins could be cross-linked with UV-light followed by immunoprecipitation (CLIP-technique) and NGS.[307–311] Moreover, as RBPs bound to their target RNA interact with other proteins or RNAs to form multifunctional complexes, *trans*-acting factors should be analyzed further as well. This has been already reported for α- and β-globin mRNAs[189,190] and could help understand regulation of the IVT-mRNAs by RBPs, when using newly selected sequences as 3' UTRs.

miRNAs and their influence on RNA-stability Putative binding sites for miRNAs expressed in hiDCs in the newly selected 3' UTRs were analyzed using IntaRNA, a web server which allows a fast and accurate prediction of RNA-RNA-interaction by taking into account secondary structure of the entered target RNA sequence and with this, miRNA accessibility.[237–240] Using this program, 42 and 48 different miRNAs expressed in unstimulated and stimulated DCs, respectively, were predicted to bind to the newly selected 3' UTR-sequences. However, the predicted number of binding miRNAs differed between the analyzed single 3' UTR-elements with F and I as the lowest (20 an 21, respectively) and D, E, G, B and J as the highest (25, 28, 28, 32 and 37, respectively). The single β-globin 3' UTR hBg was predicted to have 28 miRNA binding sites as well. The putative number of binding sites increased in each sequence element by two to four in LPS-stimulated DCs. In this context, it was reported that repression strength increases with the number of miRNAs binding to the 3' UTR-region.[312] Therefore, a possible correlation between number of predicted miRNA binding sites and the stabilizing effect of the 3' UTRs - individually and as combinations as tested experimentally - was determined. A significant correlation was revealed, which demonstrated that 3' UTRs comprised of two sequence elements were more prone to RNA decay; in particular combinations with B, G, E and J.
However, the putative number of miRNA binding sites in combined 3' UTRs rarely increased compared to the respective single elements (e.g. F with 20 and FF with 21 predicted and accessible miRNA binding sites; see also Fig. 6.16). Yet, the RNA was stabilized less by most of the combined 3' UTRs, suggesting that not only the predicted number of binding miRNAs is responsible for the low RNA half-life, but probably the sum of the hybridization energy as well. Thus, the predicted sum of hybridization energy, as a measure of binding strengths, was also taken into account. This energy differed significantly among all analyzed sequences; between -652 and -269 $\mathrm{kcal\,mol^{-1}}$ for stimulated and -589 and -217 $\mathrm{kcal\,mol^{-1}}$ for unstimulated DCs. Combined 3' UTRs with B, E, G and J as adjacent element had significantly ($p<0.05$) lower single miRNA hybridization energies (mainly between -25,1 and -15 $\mathrm{kcal\,mol^{-1}}$) compared with combinations with I, F or hBg (mainly between -15 and -4 $\mathrm{kcal\,mol^{-1}}$). Combined 3' UTRs with one D-sequence element seem to fold unfavorably, so that miRNA binding sites could be more accessible leading to faster RNA decay.

Overall, there was the same predicted distribution of binding sites and hybridization energies for stimulated DCs. The main difference between unstimulated and stimulated

DCs was the predicted miRNA expression pattern. Several putative miRNA-binding sites were only found in stimulated (hsa-mir-19a; hsa-miR-222; hsa-miR-30e; hsa-miR-320; hsa-miR-423-3p; hsa-miR-423-5p; hsa-miR-92a) and others only in unstimulated DCs (hsa-miR-17); but, as the hybridization energy pattern does not change between stimulated and unstimulated DCs, the overall effect on RNA stability should be the same.
These results suggest that the fewer miRNA binding sites are located on the 3' UTR, and the weaker the RNA-RNA-interaction is, the more stable the target mRNA is. This is particularly true for the selected I- and F-element. When used as 3' UTR, both sequences showed higher or similar stabilizing properties than 2hBg, respectively. Although their combinations, IF and FI, have lower hybridization energies and only two predicted miRNA-binding sites less compared to 2hBg, their overall improvement of RNA turnover regarding RNA half-life and translational efficiency was shown to be significant in hiDCs and other cell types (see below). In this context, a detailed analysis of the secondary structure of the 3' UTR and respective mRNA should be carried out, as it is known that the RNA structure determines which regions are accessible to miRNAs and RBPs as well.[313,314]

Improvement of selected 3′ UTRs Despite these positive results, newly selected 3' UTRs - including the most promising IF and FI - can still be improved in their mode of action by analyzing mutations on specific predicted miRNA-binding sites or by introducing recognition motifs of certain RBPs known to enhance RNA stability and translational efficiency. The single I-element should be analyzed further as well, as this 3' UTR had identical properties compared to 2hBg regarding translational efficiency and total protein over time, but with enhanced RNA-stability. Interestingly, this single element shows characteristics with a high potential compared to 2hBg: (i) the sum of miRNA-hybridization energy is much higher; (ii) the number of miRNA-binding sites is much lower; (iii) as predicted it has no PUM2-, but does have QKI-binding sites, which are destabilizing[256] and stabilizing[315] RBPs, respectively; and (iv) is much shorter in length (142 vs 284 nts), which could additionally contribute to an enhanced translational efficiency.[205]
Furthermore, differences in the complex network of RNA-protein interactions were already observed between human immature and mature DCs regarding stability and decay kinetics of different IVT-mRNAs.[85] Thus, further studies should be done to elucidate crosstalk between RBPs and miRNAs, and overall RNA competition effects as well.[187] Recently, Goodarzi *et al.* presented a computational framework, which allowed a systematic exploration of small structural sequence elements in human mRNA stability data, revealing new specific RNA motifs and HNRPA2B1 (heterogeneous nuclear ribonucleoprotein A2/B1) as key regulator of stabilizing its target genes.[316] Therefore, a systematic discovery of RNA specific structural motifs, which determine stability of the IVT-mRNA in hiDCs is a difficult, but not impossible task.

7.3.3 Translational efficiency of IVT-mRNAs with different 3′ UTRs

Generally translational efficiency is not influenced that much by the 3' UTR-region of the RNA.[124] However, stability of an antigen-encoding IVT-mRNA is not the only factor that is important for a sustained and strong immune response in RNA-based immunotherapeutics.[121] A stable, but non-translatable RNA would not be of use for active cancer therapy. Efficiency and duration of translation plays a central role as well, as it ensures a high amount of available antigen for processing and presentation. Thus, the most promising 3' UTR-combinations IF, FI, IhBg and hBgI were analyzed further regarding their effect on translational efficiency, relative functional mRNA stability and total protein expression over time. The rationale for this prioritization was (i) best stabilizing effects on the IVT-mRNAs; (ii) highest predicted miRNA hybridization energies; (iii) lowest predicted number of binding sites; and (iv) RBP-binding sites predicted to be similar to 2hBg, particularly in respect of QKI, ZFP36 and KHDRBS3. For the detailed analysis of translational efficiency a more suitable reporter was chosen (Ch. 6.4).

Intriguingly, the newly selected 3' UTRs IF and FI significantly improved translational efficiency ($p<0.001$ and $p<0.05$, respectively), while providing similar RNA stability compared to 2hBg. One can only speculate why RNAs with IF and FI are more translatable than 2hBg. Several factors are known to influence translatability of an mRNA, e.g. the 5' cap, the ORF or RBP and the miRNA binding sites located in the UTR-regions of the mRNA.[149,317] The analyzed RNAs only differ in their 3' UTRs and hence, their binding sites for *trans*-acting factors, which most often repress translation by binding to the 3' UTR.[318] SFM predicted 5 and 6 binding sites for KHSRP in 2hBg and IF/FI, respectively. This RBP is known to repress translation of the RNA.[175] However, a difference by one KHSRP-binding site is not expected to explain significantly enhanced translatability of the RNA with IF or FI as 3' UTR. Additional factors must be responsible. In this context, miRNAs could be taken into account. These small regulatory RNAs are known to not only repress translation,[157] which often leads to subsequent mRNA decay,[123] but to also upregulate translation of the RNA.[319,320] However, this seems to be restricted to cells having left the cell cycle and remaining in the G0 (quiescent) state. As hiDCs are still able to be activated by external stimuli (e.g. antigens),[321] the possibility of a translation activated by miRNAs seems highly unlikely.
Only further detailed studies can reveal complex interrelationship between mRNA translation and decay for the used RNA therapeutic, as both mechanisms are inevitably linked together to regulate the correct protein expression in the cell.[322] In this context, these results underline the importance that both RNA characteristics - stability and translational efficiency - should always be analyzed to ensure a continuous and lasting protein production to sustain a strong immune response mediated by the RNA-based cancer vaccine. Moreover, it could be beneficial to add the *translational efficiency* as parameter to the *in vitro* selection process. This could increase the selective pressure from the beginning. Sequences,

which might have strong stabilizing effects when used as 3' UTR, but inhibit partially translation of the RNA, could be cleared within the first selection rounds, making room to other RNA-sequence elements, which improve the overall characteristics of the RNA therapeutic from the start.

7.3.4 RNA-stability in other cell types and lines

Although newly selected 3' UTRs were not only derived from hiDCs, but also specifically selected in these cells for RNA vaccine optimization, stabilizing effects of the most promising candidates (IF, FI, IhBg and hBgI) were further analyzed in $CD4^+$ T cells, HFF and C2C12 cells. These cells and cell lines are used in-house for TCR-engineering and stem cell research, respectively.[17,214,323,324] Optimization of the IVT-mRNA could also improve functionality and outcome in targeted therapies using these cell types.
RNA turnover was significantly improved in HFF and C2C12 cells. The stabilizing effect of newly selected 3' UTRs and translational efficiency of the IVT-mRNA was up to 2-fold better than 2hBg in HFF and C2C12. As expression profiles for miRNAs and RBPs were not analyzed further in HFF and C2C12, it can only be speculated, that expression of respective miRNAs and RBPs favors RNA stability and turnover in these cells. These results could not be yielded in $CD4^+$ T cells demonstrating here hiDC-specificity of the selected 3' UTRs. Although, these sequences improve RNA turnover in HFF and C2C12 cells, cell-type specific 3' UTRs should be identified to ensure the best results regarding intracellular pharmacokinetics of the IVT-mRNA.

7.4 Selected 3′ UTRs I, IF and FI

In vitro results clearly demonstrated enhanced stability and translational efficiency of the newly selected 3' UTRs I, IF and FI in hiDCs and in other cell types/lines (Ch. 7.3.4). However, functional activity *in vivo* is also crucial for a specific antitumor response. In-house data demonstrated a similar and even slightly enhanced immunstimulatory capacity of FI compared to 2hBg (data not shown, internal communication).[325] The immunstimulatory capacity is desired as the exogenous administered RNA-vaccine does not only provide encoded tumor-antigens, but also acts as adjuvant by binding to membrane-bound (e.g. TLRs) and cytosolic receptors (e.g. RIG-I) on APCs, thus activating them and inducing the desired and aimed antitumor response (Ch. 3.4).[121,326]
To sum up, with the *in vitro* selection process using a cell-type specific self-made RNA library and hiDCs as selective environment, new stabilizing RNA-sequences were discovered. In particular, the IF-sequence showed best overall properties, when used as a 3' UTR: (i) a 1.12 to 1.73-fold higher stabilizing effect not only in hiDCs, but also in HFF and C2C12; (ii) an up to 1.24-fold better translational efficiency; (iii) a 1.33-fold higher protein over time; and (iv) less putative miRNA-binding sites, which prevents possible degradation mediated by miRNAs. Furthermore, technical difficulties as seen with 2hBg, can now be circumvented, when using a 3' UTR with two different sequence elements. Lastly, FI and IF are a promising new candidates to replace 2hBg as 3' UTR in future RNA cancer vaccines.

8 Conclusion and Outlook

In this work, a novel *in vitro* selection process, carried out within hiDCs as a selective environment, was developed to identify naturally occurring RNA sequence elements that stabilize exogenously administered IVT-mRNA for (pre)clinical studies. This should help to further increase the efficacy of RNA-based cancer immunotherapies. The selection process was started with a library comprised of RNA-sequences preselected from hiDCs, in which transcription was inhibited for several hours. Thereby, it was expected that the starting library would already be enriched for sequences derived from stable RNAs, because instable RNAs would degrade during that time. After up to six rounds of selection, sequencing of the selected clones demonstrated that a set of new RNA sequence elements, each contained in several independent clones, could be identified.

Functional characterization of the newly selected RNA-sequences showed that when used as single 3' UTR-element, the stability of the corresponding IVT-mRNA was at least as good and in some cases even better than of an RNA with the 2hBg 3' UTR, the in-house *gold standard* consisting of two copies of the human β-globin 3' UTR. As for 2hBg, pair-wise combinations of the newly selected sequences could in some instances further improve the stabilizing effect. However, other combinations actually diminished RNA half-life compared to single elements. Importantly, the selected sequences generally had no diminishing effect on RNA translation. Some elements actually increased the translational efficiency compared to 2hBg. Furthermore, 3' UTRs with two different single elements are advantageous compared to 2hBg, because PCR amplification of the 2hBg 3' UTR have proved to be difficult in handling with the two identical β-globin sequences in tandem. These are prone to recombination and lead to undesired by-products, e.g. lacking one β-globin-element.

In an attempt to elucidate the mechanisms behind the stabilizing properties, bioinformatical analysis was carried out by searching for *cis*-acting elements located on the selected sequences, which possibly recruit specific *trans*-acting factors, such as RBPs and miRNAs (also called post-transcriptional regulators or PTRs), thereby determining the fate of the IVT-mRNA. These PTRs are able to regulate mRNAs by influencing their stability and translational efficiency.

While the analysis revealed several putative binding sites for RBPs known to accelerate or inhibit mRNA decay, no clear trend indicative of one or more of these proteins to be the determining factor for RNA stability could be identified. In contrast, a significant correlation was found between the stabilizing effect of the newly selected 3' UTRs and the number of putative binding sites for miRNAs, as well as their respective hybridization energies. The better a sequence is with respect to RNA stability, the lower the number and the higher the hybridization energies of the miRNA binding sites in this UTR. If this holds true, it might be possible to further improve 3' UTR-sequences by removal of the still present miRNA binding sites, for example, by introducing suitable mutations.

Surprisingly, one of the identified sequences, namely I, is derived from the mitochondrially encoded 12S rRNA (MT-RNR1). Together and in combination with F, derived from the

amino-terminal enhancer of split mRNA (AES), this element shows a very strong effect on RNA stability not only in hiDCs, but also in HFF and C2C12 cells. However, as for hiDCs, a new selection performed in these cells might identify even better elements for HFF and C2C12.

In conclusion, it could be demonstrated that sequence elements that cell-specifically stabilize exogenously introduced RNAs are selected with a newly developed selection procedure. In the context of RNA-based cancer immunotherapy, where RNA is delivered into hiDCs, these elements further increase the efficacy of the RNA. RNA is especially suited for a personalized vaccine approach, where the specific mutation profile of an individual tumor is targeted. Every improvement of the RNA platform technology will help in the further development of this innovative approach.

References

[1] Sahin, U., Kariko, K. and Türeci, Ö., mRNA-based therapeutics–developing a new class of drugs, *Nature reviews. Drug discovery* **2014**, *13*, 759–780.

[2] Brenner, S., Jacob, F. and Meselson, M., An Unstable Intermediate Carrying Information from Genes to Ribosomes for Protein Synthesis, *Nature* **1961**, *190*, 576–581.

[3] Grafi, G., Galili, G., Gurdon, J.B. *et al.*, Induction of cytoplasmic factors that bind to the 3' au-rich region of human interferon beta mrna during early development of xenopus laevis: Use of frog eggs and oocytes for the study of messenger rna and its translation in living cells, *Nature* **1971**, *233*, 177–182.

[4] Laskey, R.A., Gurdon, J.B. and Crawford, L.V., Translation of encephalomyocarditis viral rna in oocytes of xenopus laevis, *Proceedings of the National Academy of Sciences of the United States of America* **1972**, *69*, 3665–3669.

[5] Malone, R.W., Felgner, P.L. and Verma, I.M., Cationic liposome-mediated RNA transfection, *Proc Natl Acad Sci U S A* **1989**, *86*, 6077–6081.

[6] Wolff, J.A., Malone, R.W., Williams, P. *et al.*, Direct gene transfer into mouse muscle in vivo, *Science* **1990**, *247*, 1465–1468.

[7] Kariko, K. and Weissman, D., Naturally occurring nucleoside modifications suppress the immunostimulatory activity of RNA: implication for therapeutic RNA development, *Current opinion in drug discovery & development* **2007**, *10*, 523–532.

[8] Devoldere, J., Dewitte, H., de Smedt, S.C. and Remaut, K., Evading innate immunity in nonviral mrna delivery: don't shoot the messenger, *Drug discovery today* **2016**, *21*, 11–25.

[9] Kariko, K., Muramatsu, H., Welsh, F.A. *et al.*, Incorporation of pseudouridine into mRNA yields superior nonimmunogenic vector with increased translational capacity and biological stability, *Molecular therapy* **2008**, *16*, 1833–1840.

[10] Kariko, K., Muramatsu, H., Ludwig, J. and Weissman, D., Generating the optimal mRNA for therapy: HPLC purification eliminates immune activation and improves translation of nucleoside-modified, protein-encoding mRNA, *Nucleic acids research* **2011**, *39*, e142.

[11] Kariko, K., Muramatsu, H., Keller, J.M. and Weissman, D., Increased erythropoiesis in mice injected with submicrogram quantities of pseudouridine-containing mRNA encoding erythropoietin, *Molecular therapy* **2012**, *20*, 948–953.

[12] Kormann, M., Hasenpusch, G., Aneja, M. *et al.*, Expression of therapeutic proteins after delivery of chemically modified mRNA in mice, *Nature biotechnology* **2011**, *29*, 154–157.

[13] Zangi, L., Lui, K.O., von Gise, A. *et al.*, Modified mrna directs the fate of heart progenitor cells and induces vascular regeneration after myocardial infarction, *Nature biotechnology* **2013**, *31*, 898–907.

[14] Vallazza, B., Petri, S., Poleganov, M.A. *et al.*, Recombinant messenger RNA technology and its application in cancer immunotherapy, transcript replacement therapies, pluripotent stem cell induction, and beyond, *Wiley interdisciplinary reviews. RNA* **2015**, *6*, 471–499.

[15] Takahashi, K. and Yamanaka, S., Induction of pluripotent stem cells from mouse embryonic and adult fibroblast cultures by defined factors, *Cell* **2006**, *126*, 663–676.

[16] Warren, L., Manos, P., Ahfeldt, T. *et al.*, Highly efficient reprogramming to pluripotency and directed differentiation of human cells with synthetic modified mRNA, *Cell stem cell* **2010**, *7*, 618–630.

[17] Poleganov, M.A., Eminli, S., Beissert, T. *et al.*, Efficient Reprogramming of Human Fibroblasts and Blood-Derived Endothelial Progenitor Cells Using Nonmodified RNA for Reprogramming and Immune Evasion, *Human gene therapy* **2015**.

[18] Martinon, F., Krishnan, S., Lenzen, G. *et al.*, Induction of virus-specific cytotoxic T lymphocytes in vivo by liposome-entrapped mRNA, *European journal of immunology* **1993**, *23*, 1719–1722.

[19] Hekele, A., Bertholet, S., Archer, J. *et al.*, Rapidly produced sam((r)) vaccine against h7n9 influenza is immunogenic in mice, *Emerging microbes & infections* **2013**, *2*, e52.

[20] Geall, A.J., Verma, A., Otten, G.R. *et al.*, Nonviral delivery of self-amplifying rna vaccines, *Proceedings of the National Academy of Sciences of the United States of America* **2012**, *109*, 14604–14609.

[21] Routy, J.P., Boulassel, M.R., Yassine-Diab, B. *et al.*, Immunologic activity and safety of autologous hiv rna-electroporated dendritic cells in hiv-1 infected patients receiving antiretroviral therapy, *Clinical immunology (Orlando, Fla.)* **2010**, *134*, 140–147.

[22] van Gulck, E., Vlieghe, E., Vekemans, M. *et al.*, mrna-based dendritic cell vaccination induces potent antiviral t-cell responses in hiv-1-infected patients, *AIDS (London, England)* **2012**, *26*, F1–12.

[23] Petsch, B., Schnee, M., Vogel, A.B. *et al.*, Protective efficacy of in vitro synthesized, specific mrna vaccines against influenza a virus infection, *Nature biotechnology* **2012**, *30*, 1210–1216.

[24] Liljestrom, P. and Garoff, H., A new generation of animal cell expression vectors based on the semliki forest virus replicon, *Bio/technology (Nature Publishing Company)* **1991**, *9*, 1356–1361.

[25] Fleeton, M.N., Chen, M., Berglund, P. *et al.*, Self-replicative rna vaccines elicit protection against influenza a virus, respiratory syncytial virus, and a tickborne encephalitis virus, *The Journal of infectious diseases* **2001**, *183*, 1395–1398.

[26] Anraku, I., Harvey, T.J., Linedale, R. *et al.*, Kunjin virus replicon vaccine vectors induce protective cd8+ t-cell immunity, *Journal of virology* **2002**, *76*, 3791–3799.

[27] Greer, C.E., Zhou, F., Legg, H.S. *et al.*, A chimeric alphavirus rna replicon gene-based vaccine for human parainfluenza virus type 3 induces protective immunity against intranasal virus challenge, *Vaccine* **2007**, *25*, 481–489.

[28] Gilboa, E. and Vieweg, J., Cancer immunotherapy with mRNA-transfected dendritic cells, *Immunological reviews* **2004**, *199*, 251–263.

[29] Parvanova, I., Rettig, L., Knuth, A. and Pascolo, S., The form of NY-ESO-1 antigen has an impact on the clinical efficacy of anti-tumor vaccination, *Vaccine* **2011**, *29*, 3832–3836.

[30] Nair, S.K., Boczkowski, D., Morse, M. *et al.*, Induction of primary carcinoembryonic antigen (CEA)-specific cytotoxic T lymphocytes in vitro using human dendritic cells transfected with RNA, *Nature biotechnology* **1998**, *16*, 364–369.

[31] Sorrentino, S., Human extracellular ribonucleases: multiplicity, molecular diversity and catalytic properties of the major RNase types, *Cell Mol Life Sci* **1998**, *54*, 785–794.

[32] Conry, R.M., LoBuglio, A.F., Wright, M. *et al.*, Characterization of a messenger RNA polynucleotide vaccine vector, *Cancer research* **1995**, *55*, 1397–1400.

[33] Boczkowski, D., Nair, S.K., Snyder, D. and Gilboa, E., Dendritic cells pulsed with RNA are potent antigen-presenting cells in vitro and in vivo, *The Journal of experimental medicine* **1996**, *184*, 465–472.

[34] Steinman, R.M. and Banchereau, J., Taking dendritic cells into medicine, *Nature* **2007**, *449*, 419–426.

[35] Palucka, K. and Banchereau, J., Cancer immunotherapy via dendritic cells, *Nature reviews* **2012**, *12*, 265–277.

[36] Bringmann, A., Held, S.A.E., Heine, A. and Brossart, P., RNA vaccines in cancer treatment, *Journal of biomedicine & biotechnology* **2010**, *2010*, 623687.

[37] Kreiter, S., Selmi, A., Diken, M. *et al.*, Intranodal vaccination with naked antigen-encoding RNA elicits potent prophylactic and therapeutic antitumoral immunity, *Cancer research* **2010**, *70*, 9031–9040.

[38] Hoerr, I., Obst, R., Rammensee, H.G. and Jung, G., In vivo application of RNA leads to induction of specific cytotoxic T lymphocytes and antibodies, *European journal of immunology* **2000**, *30*, 1–7.

[39] Fotin-Mleczek, M., Duchardt, K., Lorenz, C. *et al.*, Messenger RNA-based vaccines with dual activity induce balanced TLR-7 dependent adaptive immune responses and provide antitumor activity, *J Immunother* **2011**, *34*, 1–15.

[40] Schlake, T., Thess, A., Fotin-Mleczek, M. and Kallen, K.J., Developing mRNA-vaccine technologies, *RNA biology* **2012**, *9*, 1319–1330.

[41] Neumann, E., Schaefer-Ridder, M., Wang, Y. and Hofschneider, P.H., Gene transfer into mouse lyoma cells by electroporation in high electric fields, *The EMBO journal* **1982**, *1*, 841–845.

[42] Van Driessche, A., Ponsaerts, P., Van Bockstaele, D.R., Van Tendeloo, V.F I and Berneman, Z.N., Messenger RNA electroporation: an efficient tool in immunotherapy and stem cell research, *Folia Histochem Cytobiol* **2005**, *43*, 213–216.

[43] Tavernier, G., Andries, O., Demeester, J. *et al.*, mRNA as gene therapeutic: how to control protein expression, *J Control Release* **2011**, *150*, 238–247.

[44] Diken, M., Kreiter, S., Selmi, A. *et al.*, Selective uptake of naked vaccine RNA by dendritic cells is driven by macropinocytosis and abrogated upon DC maturation, *Gene therapy* **2011**, *18*, 702–708.

[45] Lorenz, C., Fotin-Mleczek, M., Roth, G. *et al.*, Protein expression from exogenous mRNA: uptake by receptor-mediated endocytosis and trafficking via the lysosomal pathway, *RNA biology* **2011**, *8*, 627–636.

[46] Grunebach, F., Muller, M.R., Nencioni, A. and Brossart, P., Delivery of tumor-derived RNA for the induction of cytotoxic T-lymphocytes, *Gene therapy* **2003**, *10*, 367–374.

[47] Steinman, R.M., Identification of a novel cell type in peripheral lymphoid organs of mice: I. Morphology, Quantitation, Tissue distribution, *Journal of Experimental Medicine* **1973**, *137*, 1142–1162.

[48] Bousso, P. and Robey, E., Dynamics of CD8+ T cell priming by dendritic cells in intact lymph nodes, *Nature immunology* **2003**, *4*, 579–585.

[49] Steinman, R.M., Decisions About Dendritic Cells: Past, Present, and Future, *Annual review of immunology* **2011**.

[50] Celli, S., Day, M., Muller, A.J. *et al.*, How many dendritic cells are required to initiate a T cell response?, *Blood* **2012**.

[51] Kranz, L.M., Diken, M., Haas, H. *et al.*, Systemic rna delivery to dendritic cells exploits antiviral defence for cancer immunotherapy, *Nature* **2016**, *534*, 396–401.

[52] van der Bruggen, P., Traversari, C., Chomez, P. *et al.*, A gene encoding an antigen recognized by cytolytic T lymphocytes on a human melanoma, *Science* **1991**, *254*, 1643–1647.

[53] Sahin, U., Türeci, Ö., Schmitt, H. *et al.*, Human neoplasms elicit multiple specific immune responses in the autologous host, *Proc Natl Acad Sci U S A* **1995**, *92*, 11810–11813.

[54] Morse, M.A., Deng, Y., Coleman, D. *et al.*, A Phase I study of active immunotherapy with carcinoembryonic antigen peptide (CAP-1)-pulsed, autologous human cultured dendritic cells in patients with metastatic malignancies expressing carcinoembryonic antigen, *Clin Cancer Res* **1999**, *5*, 1331–1338.

[55] Nair, S.K., Heiser, A., Boczkowski, D. *et al.*, Induction of cytotoxic T cell responses and tumor immunity against unrelated tumors using telomerase reverse transcriptase RNA transfected dendritic cells, *Nature medicine* **2000**, *6*, 1011–1017.

[56] Heiser, A., Coleman, D., Dannull, J. *et al.*, Autologous dendritic cells transfected with prostate-specific antigen RNA stimulate CTL responses against metastatic prostate tumors, *The Journal of clinical investigation* **2002**, *109*, 409–417.

[57] Jarnjak-Jankovic, S., Pettersen, R.D., Saeboe-Larssen, S. *et al.*, Preclinical evaluation of autologous dendritic cells transfected with mRNA or loaded with apoptotic cells for immunotherapy of high-risk neuroblastoma, *Cancer gene therapy* **2005**, *12*, 699–707.

[58] Kyte, J.A., Kvalheim, G., Lislerud, K. *et al.*, T cell responses in melanoma patients after vaccination with tumor-mRNA transfected dendritic cells, *Cancer immunology, immunotherapy : CII* **2007**, *56*, 659–675.

[59] Bonehill, A., van Nuffel, M.T.a., Corthals, J. *et al.*, Single-step antigen loading and activation of dendritic cells by mRNA electroporation for the purpose of therapeutic vaccination in melanoma patients, *Clin Cancer Res* **2009**, *15*, 3366–3375.

[60] Aarntzen, E.H.J.G., Schreibelt, G., Bol, K. *et al.*, Vaccination with mRNA-electroporated dendritic cells induces robust tumor antigen-specific CD4+ and CD8+ T cells responses in stage III and IV melanoma patients, *Clin Cancer Res* **2012**, *18*, 5460–5470.

[61] Fotin-Mleczek, M., Zanzinger, K., Heidenreich, R. *et al.*, Highly potent mRNA based cancer vaccines represent an attractive platform for combination therapies supporting an improved therapeutic effect, *The journal of gene medicine* **2012**.

[62] Bregy, A., Wong, T.M., Shah, A.H., Goldberg, J.M. and Komotar, R.J., Active immunotherapy using dendritic cells in the treatment of glioblastoma multiforme, *Cancer treatment reviews* **2013**, *39*, 891–907.

[63] Coosemans, A., Vanderstraeten, A., Tuyaerts, S. *et al.*, Immunological response after WT1 mRNA-loaded dendritic cell immunotherapy in ovarian carcinoma and carcinosarcoma, *Anticancer research* **2013**, *33*, 3855–3859.

[64] Vik-Mo, E.O., Nyakas, M., Mikkelsen, B.V. *et al.*, Therapeutic vaccination against autologous cancer stem cells with mRNA-transfected dendritic cells in patients with glioblastoma, *Cancer Immunol Immunother* **2013**, *62*, 1499–1509.

[65] Li, J., Sun, Y., Jia, T. *et al.*, Messenger RNA vaccine based on recombinant MS2 virus-like particles against prostate cancer, *International journal of cancer. Journal international du cancer* **2014**, *134*, 1683–1694.

[66] Shindo, Y., Hazama, S., Maeda, Y. *et al.*, Adoptive immunotherapy with MUC1-mRNA transfected dendritic cells and cytotoxic lymphocytes plus gemcitabine for unresectable pancreatic cancer, *Journal of translational medicine* **2014**, *12*, 175.

[67] Hanahan, D. and Weinberg, R.A., Hallmarks of cancer: the next generation, *Cell* **2011**, *144*, 646–674.

[68] Besaratinia, A., Li, H., Yoon, J.I. *et al.*, A high-throughput next-generation sequencing-based method for detecting the mutational fingerprint of carcinogens, *Nucleic Acids Research* **2012**.

[69] Castle, J.C., Kreiter, S., Diekmann, J. *et al.*, Exploiting the mutanome for tumor vaccination, *Cancer research* **2012**.

[70] Kreiter, S., Castle, J.C., Türeci, Ö. and Sahin, U., Targeting the tumor mutanome for personalized vaccination therapy, *Oncoimmunology* **2012**, *1*, 768–769.

[71] Boisguerin, V., Castle, J.C., Loewer, M. *et al.*, Translation of genomics-guided RNA-based personalised cancer vaccines: towards the bedside, *British journal of cancer* **2014**, *111*, 1469–1475.

[72] Kreiter, S., Vormehr, M., van de Roemer, N. *et al.*, Mutant MHC class II epitopes drive therapeutic immune responses to cancer, *Nature* **2015**, *520*, 692–696.

[73] Wilgenhof, S., van Nuffel, A., Benteyn, D. *et al.*, A phase IB study on intravenous synthetic mRNA electroporated dendritic cell immunotherapy in pretreated advanced melanoma patients, *Ann Oncol* **2013**, *24*, 2686–2693.

[74] Hunyadi, J., Andras, C., Szabo, I. *et al.*, Autologous Dendritic Cell Based Adoptive Immunotherapy of Patients with Colorectal Cancer-A Phase I-II Study, *Pathol Oncol Res* **2014**, *20*, 357–365.

[75] Amin, A., Dudek, A.Z., Logan, T.F. *et al.*, Survival with AGS-003, an autologous dendritic cell-based immunotherapy, in combination with sunitinib in unfavorable risk patients with advanced renal cell carcinoma (RCC): Phase 2 study results, *J Immunother Cancer* **2015**, *3*, 14.

[76] Pascolo, S., The messenger's great message for vaccination, *Expert Rev Vaccines* **2015**, *14*, 153–156.

[77] Banchereau, J. and Steinman, R.M., Dendritic cells and the control of immunity, *Nature* **1998**, *392*, 245–252.

[78] Cella, M., Sallusto, F. and Lanzavecchia, A., Origin, maturation and antigen presenting function of dendritic cells, *Current opinion in immunology* **1997**, *9*, 10–16.

[79] Savina, A. and Amigorena, S., Phagocytosis and antigen presentation in dendritic cells, *Immunological reviews* **2007**, *219*, 143–156.

[80] Sanchez-Sanchez, N., Riol-Blanco, L., La Rosa, G.d. *et al.*, Chemokine receptor CCR7 induces intracellular signaling that inhibits apoptosis of mature dendritic cells, *Blood* **2004**, *104*, 619–625.

[81] Benencia, F., Sprague, L., McGinty, J., Pate, M. and Muccioli, M., Dendritic cells the tumor microenvironment and the challenges for an effective antitumor vaccination, *Journal of biomedicine & biotechnology* **2012**.

[82] Deluca, L.S. and Gommerman, J.L., Fine-tuning of dendritic cell biology by the TNF superfamily, *Nature reviews* **2012**, *12*, 339–351.

[83] Bevan, M.J., Cross-priming, *Nature immunology* **2006**, *7*, 363–365.

[84] Princiotta, M.F., Finzi, D., Qian, S.B. *et al.*, Quantitating protein synthesis, degradation, and endogenous antigen processing, *Immunity* **2003**, *18*, 343–354.

[85] Holtkamp, S., Kreiter, S., Selmi, A. *et al.*, Modification of antigen-encoding RNA increases stability, translational efficacy, and T-cell stimulatory capacity of dendritic cells, *Blood* **2006**, *108*, 4009–4017.

[86] Kaech, S.M., Wherry, E.J. and Ahmed, R., Vaccines: effector and memory T-cell differentiation: Implications for vaccine development, *Nature Reviews Immunology* **2002**, *2*, 251–262.

[87] Kreiter, S., Selmi, A., Diken, M. *et al.*, Increased antigen presentation efficiency by coupling antigens to MHC class I trafficking signals, *Journal of immunology* **2008**, *180*, 309–318.

[88] Kapsenberg, M.L., Dendritic-cell control of pathogen-driven T-cell polarization, *Nat Rev Immunol* **2003**, *3*, 984–993.

[89] Cahalan, M.D. and Parker, I., Close encounters of the first and second kind: T-DC and T-B interactions in the lymph node, *Seminars in immunology* **2005**, *17*, 442–451.

[90] Kadowaki, N., Dendritic cells: a conductor of T cell differentiation, *Allergology international* **2007**, *56*, 193–199.

[91] Lutz, M.B. and Schuler, G., Immature, semi-mature and fully mature dendritic cells: which signals induce tolerance or immunity?, *Trends in immunology* **2002**, *23*, 445–449.

[92] Langenkamp, A., Messi, M., Lanzavecchia, A. and Sallusto, F., Kinetics of dendritic cell activation: impact on priming of TH1, TH2 and nonpolarized T cells, *Nature immunology* **2000**, *1*, 311–316.

[93] Iezzi, G., Scheidegger, D. and Lanzavecchia, A., Migration and function of antigen-primed nonpolarized T lymphocytes in vivo, *The Journal of experimental medicine* **2001**, *193*, 987–993.

[94] Benteyn, D., Heirman, C., Bonehill, A., Thielemans, K. and Breckpot, K., mRNA-based dendritic cell vaccines, *Expert review of vaccines* **2015**, *14*, 161–176.

[95] Butterfield, L.H., Dendritic Cells in Cancer Immunotherapy Clinical Trials: Are We Making Progress?, *Frontiers in immunology* **2013**, *4*, 454.

[96] Han, T.H., Jin, P., Ren, J. *et al.*, Evaluation of 3 clinical dendritic cell maturation protocols containing lipopolysaccharide and interferon-gamma, *Journal of immunotherapy* **2009**, *32*, 399–407.

[97] Gustafsson, K., Junevik, K., Werlenius, O. *et al.*, Tumour-loaded a-type 1-polarized dendritic cells from patients with chronic lymphocytic leukaemia produce a superior NK-, NKT- and CD8+ T cell-attracting chemokine profile, *Scandinavian journal of immunology* **2011**, *74*, 318–326.

[98] Quillien, V., Moisan, A., Carsin, A. *et al.*, Biodistribution of radiolabelled human dendritic cells injected by various routes, *European journal of nuclear medicine and molecular imaging* **2005**, *32*, 731–741.

[99] Ranzani, M., Annunziato, S., Adams, D.J. and Montini, E., Cancer gene discovery: exploiting insertional mutagenesis, *Mol Cancer Res* **2013**, *11*, 1141–1158.

[100] Krieg, P.A. and Melton, D.A., Functional messenger RNAs are produced by SP6 in vitro transcription of cloned cDNAs, *Nucleic acids research* **1984**, *12*, 7057–7070.

[101] Nielsen, D.A. and Shapiro, D.J., Preparation of capped RNA transcripts using T7 RNA polymerase, *Nucleic acids research* **1986**, *14*, 5936.

[102] Kuhn, A.N., Beissert, T., Simon, P. *et al.*, mRNA as a versatile tool for exogenous protein expression, *Current gene therapy* **2012**, *12*, 347–361.

[103] Takeuchi, O. and Akira, S., Pattern recognition receptors and inflammation, *Cell* **2010**, *140*, 805–820.

[104] Barbalat, R., Ewald, S., Mouchess, M. and Barton, G., Nucleic acid recognition by the innate immune system, *Annual review of immunology* **2011**, *29*, 185–214.

[105] Desmet, C.J. and Ishii, K.J., Nucleic acid sensing at the interface between innate and adaptive immunity in vaccination, *Nature Reviews Immunology* **2012**, *12*, 479–491.

[106] Robbins, M.A. and Rossi, J.J., Sensing the danger in RNA, *Nature medicine* **2005**, *11*, 250–251.

[107] Robertson, H.D. and Mathews, M.B., The regulation of the protein kinase PKR by RNA, *Biochimie* **1996**, *78*, 909–914.

[108] Cole, J., Activation of PKR: an open and shut case?, *Trends in biochemical sciences* **2007**, *32*, 57–62.

[109] Paulis, L.E., Mandal, S., Kreutz, M. and Figdor, C.G., Dendritic cell-based nanovaccines for cancer immunotherapy, *Current opinion in immunology* **2013**.

[110] Cho, H.C., Kim, B.H., Kim, K. *et al.*, Cancer immunotherapeutic effects of novel CpG ODN in murine tumor model, *International immunopharmacology* **2008**, *8*, 1401–1407.

[111] Jahrsdorfer, B. and Weiner, G.J., CpG oligodeoxynucleotides as immunotherapy in cancer, *Update on cancer therapeutics* **2008**, *3*, 27–32.

[112] Olbert, P.J., Schrader, A.J., Simon, C. *et al.*, In vitro and in vivo effects of CpG-Oligodeoxynucleotides (CpG-ODN) on murine transitional cell carcinoma and on the native murine urinary bladder wall, *Anticancer research* **2009**, *29*, 2067–2076.

[113] Schlee, M., Roth, A., Hornung, V. *et al.*, Recognition of 5' triphosphate by RIG-I helicase requires short blunt double-stranded RNA as contained in panhandle of negative-strand virus, *Immunity* **2009**, *31*, 25–34.

[114] Schmidt, A., Schwerd, T., Hamm, W. *et al.*, 5'-triphosphate RNA requires base-paired structures to activate antiviral signaling via RIG-I, *Proc Natl Acad Sci U S A* **2009**, *106*, 12067–12072.

[115] Duewell, P., Steger, A., Lohr, H. *et al.*, RIG-I-like helicases induce immunogenic cell death of pancreatic cancer cells and sensitize tumors toward killing by CD8(+) T cells, *Cell death and differentiation* **2014**, *21*, 1825–1837.

[116] Yuan, D., Xia, M., Meng, G. *et al.*, Anti-angiogenic efficacy of 5'-triphosphate siRNA combining VEGF silencing and RIG-I activation in NSCLCs, *Oncotarget* **2015**.

[117] Kariko, K., Ni, H., Capodici, J., Lamphier, M. and Weissman, D., mRNA is an endogenous ligand for Toll-like receptor 3, *The Journal of biological chemistry* **2004**, *279*, 12542–12550.

[118] Longhi, M.P., Trumpfheller, C., Idoyaga, J. *et al.*, Dendritic cells require a systemic type I interferon response to mature and induce CD4+ Th1 immunity with poly IC as adjuvant, *The Journal of experimental medicine* **2009**, *206*, 1589–1602.

[119] Wang, Y., Cella, M., Gilfillan, S. and Colonna, M., Cutting edge: polyinosinic:polycytidylic acid boosts the generation of memory CD8 T cells through melanoma differentiation-associated protein 5 expressed in stromal cells, *Journal of immunology* **2010**, *184*, 2751–2755.

[120] Caskey, M., Lefebvre, F., Filali-Mouhim, A. *et al.*, Synthetic double-stranded RNA induces innate immune responses similar to a live viral vaccine in humans, *The Journal of experimental medicine* **2011**, *208*, 2357–2366.

[121] Kuhn, A., Diken, M., Kreiter, S. *et al.*, Determinants of intracellular RNA pharmacokinetics: Implications for RNA-based immunotherapeutics, *RNA biology* **2011**, *8*, 35–43.

[122] Wilusz, C., Wormington, M. and Peltz, S., The cap-to-tail guide to mRNA turnover, *Nat Rev Mol Cell Biol* **2001**, *2*, 237–246.

[123] Garneau, N., Wilusz, J. and Wilusz, C., The highways and byways of mRNA decay, *Nat Rev Mol Cell Biol* **2007**, *8*, 113–126.

[124] Szostak, E. and Gebauer, F., Translational control by 3'-UTR-binding proteins, *Briefings in functional genomics* **2012**.

[125] Cong, P. and Shuman, S., Methyltransferase and subunit association domains of vaccinia virus mRNA capping enzyme, *The Journal of biological chemistry* **1992**, *267*, 16424–16429.

[126] Pasquinelli, A.E., Dahlberg, J.E. and Lund, E., Reverse 5' caps in rnas made in vitro by phage rna polymerases, *RNA* **1995**, *1*, 957–967.

[127] Jemielity, J., Fowler, T., Zuberek, J. *et al.*, Novel 'anti-reverse' cap analogs with superior translational properties, *RNA* **2003**, *9*, 1108–1122.

[128] Stepinski, J., Waddell, C., Stolarski, R., Darzynkiewicz, E. and Rhoads, R.E., Synthesis and properties of mrnas containing the novel 'anti-reverse' cap analogs 7-methyl(3'-o-methyl)gpppg and 7-methyl (3'-deoxy)gpppg, *RNA* **2001**, *7*, 1486–1495.

[129] Michael Mockey, Cristine GonÃ§alves, Franck P Dupuy *et al.*, mRNA transfection of dendritic cells: synergistic effect of ARCA mRNA capping with Poly(A) chains in cis and in trans for a high protein expression level, *Biochem Biophys Res Commun* **2006**, *340*, 1062–1068.

[130] Kuhn, A.N., Diken, M., Kreiter, S. *et al.*, Phosphorothioate cap analogs increase stability and translational efficiency of RNA vaccines in immature dendritic cells and induce superior immune responses in vivo, *Gene therapy* **2010**, *17*, 961–971.

[131] Cao, G.J. and Sarkar, N., Identification of the gene for an Escherichia coli poly(A) polymerase, *Proc Natl Acad Sci U S A* **1992**, *89*, 10380–10384.

[132] Martin, G. and Keller, W., Tailing and 3'-end labeling of RNA with yeast poly(A) polymerase and various nucleotides, *RNA* **1998**, *4*, 226–230.

[133] Lagerkvist, U., 'Two out of three': an alternative method for codon reading, *Proc Natl Acad Sci U S A* **1978**, *75*, 1759–1762.

[134] Plotkin, J.B. and Kudla, G., Synonymous but not the same: the causes and consequences of codon bias, *Nature reviews. Genetics* **2011**, *12*, 32–42.

[135] Scholten, K.B.J., Kramer, D., Kueter, E.W.M. *et al.*, Codon modification of T cell receptors allows enhanced functional expression in transgenic human T cells, *Clinical immunology (Orlando, Fla.)* **2006**, *119*, 135–145.

[136] Su, Z., Vieweg, J., Weizer, A.Z. *et al.*, Enhanced induction of telomerase-specific CD4(+) T cells using dendritic cells transfected with RNA encoding a chimeric gene product, *Cancer research* **2002**, *62*, 5041–5048.

[137] Bonehill, A., Heirman, C., Tuyaerts, S. *et al.*, Messenger RNA-electroporated dendritic cells presenting MAGE-A3 simultaneously in HLA class I and class II molecules, *Journal of immunology* **2004**, *172*, 6649–6657.

[138] Kozak, M., At least six nucleotides preceding the AUG initiator codon enhance translation in mammalian cells, *Journal of molecular biology* **1987**, *196*, 947–950.

[139] Shaw, G. and Kamen, R., A conserved AU sequence from the 3' untranslated region of GM-CSF mRNA mediates selective mRNA degradation, *Cell* **1986**, *46*, 659–667.

[140] Holcik, M. and Liebhaber, S., Four highly stable eukaryotic mRNAs assemble 3‘ untranslated region RNA-protein complexes sharing cis and trans components, *Proc Natl Acad Sci U S A* **1997**, *94*, 2410–2414.

[141] Andreassi, C. and Riccio, A., To localize or not to localize: mRNA fate is in 3‘UTR ends, *Trends Cell Biol* **2009**, *19*, 465–474.

[142] Matoulkova, E., Michalova, E., Vojtesek, B. and Hrstka, R., The role of the 3' untranslated region in post-transcriptional regulation of protein expression in mammalian cells, *RNA biology* **2012**, *9*, 563–576.

[143] Mayr, C. and Bartel, D.P., Widespread shortening of 3'UTRs by alternative cleavage and polyadenylation activates oncogenes in cancer cells, *Cell* **2009**, *138*, 673–684.

[144] Schwanhäusser, B., Busse, D., Li, N. *et al.*, Global quantification of mammalian gene expression control, *Nature* **2011**, *473*, 337–342.

[145] Grosjean, H. and Benne, R. (Hrsg.), *Modification and Editing of RNA*, American Society of Microbiology **1998**.

[146] Kariko, K., Buckstein, M., Ni, H. and Weissman, D., Suppression of RNA recognition by Toll-like receptors: the impact of nucleoside modification and the evolutionary origin of RNA, *Immunity* **2005**, *23*, 165–175.

[147] Munroe, D. and Jacobson, A., mRNA poly(A) tail, a 3' enhancer of translational initiation, *Molecular and cellular biology* **1990**, *10*, 3441–3455.

[148] Gallie, D.R., A tale of two termini: a functional interaction between the termini of an mRNA is a prerequisite for efficient translation initiation, *Gene* **1998**, *216*, 1–11.

[149] Wilkie, G., Dickson, K. and Gray, N., Regulation of mRNA translation by 5‘- and 3‘-UTR-binding factors, *Trends Biochem Sci* **2003**, *28*, 182–188.

[150] Kahvejian, A., Roy, G. and Sonenberg, N., The mRNA closed-loop model: the function of PABP and PABP-interacting proteins in mRNA translation, *Cold Spring Harbor symposia on quantitative biology* **2001**, *66*, 293–300.

[151] Amrani, N., Ghosh, S., Mangus, D.A. and Jacobson, A., Translation factors promote the formation of two states of the closed-loop mRNP, *Nature* **2008**, *453*, 1276–1280.

[152] Besse, F. and Ephrussi, A., Translational control of localized mRNAs: restricting protein synthesis in space and time, *Nat Rev Mol Cell Biol* **2008**, *9*, 971–980.

[153] Stebbins-Boaz, B., Cao, Q., Moor, C.H.d., Mendez, R. and Richter, J.D., Maskin is a CPEB-associated factor that transiently interacts with elF-4E, *Molecular cell* **1999**, *4*, 1017–1027.

[154] Nakamura, A., Sato, K. and Hanyu-Nakamura, K., Drosophila cup is an eIF4E binding protein that associates with Bruno and regulates oskar mRNA translation in oogenesis, *Developmental cell* **2004**, *6*, 69–78.

[155] Cho, P.F., Poulin, F., Cho-Park, Y.A. *et al.*, A new paradigm for translational control: inhibition via 5'-3' mRNA tethering by Bicoid and the eIF4E cognate 4EHP, *Cell* **2005**, *121*, 411–423.

[156] Kapasi, P., Chaudhuri, S., Vyas, K. *et al.*, L13a blocks 48S assembly: role of a general initiation factor in mRNA-specific translational control, *Molecular cell* **2007**, *25*, 113–126.

[157] Fabian, M., Sonenberg, N. and Filipowicz, W., Regulation of mRNA translation and stability by microRNAs, *Annual review of biochemistry* **2010**, *79*, 351–379.

[158] Bartel, D.P., MicroRNAs: target recognition and regulatory functions, *Cell* **2009**, *136*, 215–233.

[159] Friedman, R.C., Farh, K.K.H., Burge, C.B. and Bartel, D.P., Most mammalian mRNAs are conserved targets of microRNAs, *Genome research* **2009**, *19*, 92–105.

[160] Grimson, A., Farh, K.K.H., Johnston, W.K. *et al.*, MicroRNA targeting specificity in mammals: determinants beyond seed pairing, *Molecular cell* **2007**, *27*, 91–105.

[161] Sachs, A.B. and Davis, R.W., The poly(A) binding protein is required for poly(A) shortening and 60S ribosomal subunit-dependent translation initiation, *Cell* **1989**, *58*, 857–867.

[162] Gao, M., Fritz, D.T., Ford, L.P. and Wilusz, J., Interaction between a poly(A)-specific ribonuclease and the 5' cap influences mRNA deadenylation rates in vitro, *Molecular cell* **2000**, *5*, 479–488.

[163] Dehlin, E., Wormington, M., Korner, C.G. and Wahle, E., Cap-dependent deadenylation of mRNA, *The EMBO journal* **2000**, *19*, 1079–1086.

[164] Martinez, J., Ren, Y.G., Nilsson, P., Ehrenberg, M. and Virtanen, A., The mRNA cap structure stimulates rate of poly(A) removal and amplifies processivity of degradation, *The Journal of biological chemistry* **2001**, *276*, 27923–27929.

[165] Tucker, M., Staples, R.R., Valencia-Sanchez, M.A., Muhlrad, D. and Parker, R., Ccr4p is the catalytic subunit of a Ccr4p/Pop2p/Notp mRNA deadenylase complex in Saccharomyces cerevisiae, *The EMBO journal* **2002**, *21*, 1427–1436.

[166] Yamashita, A., Chang, T.C., Yamashita, Y. *et al.*, Concerted action of poly(A) nucleases and decapping enzyme in mammalian mRNA turnover, *Nature structural & molecular biology* **2005**, *12*, 1054–1063.

[167] Sheiness, D., Puckett, L. and Darnell, J.E., Possible relationship of poly(A) shortening to mRNA turnover, *Proc Natl Acad Sci U S A* **1975**, *72*, 1077–1081.

[168] Traude H Beilharz and Thomas Preiss, Transcriptome-wide measurement of mRNA polyadenylation state, *Methods* **2009**, *48*, 294–300.

[169] Nagarajan, V.K., Jones, C.I., Newbury, S.F. and Green, P.J., XRN 5'–3' exoribonucleases: structure, mechanisms and functions, *Biochimica et biophysica acta* **2013**, *1829*, 590–603.

[170] Lykke-Andersen, S., Tomecki, R., Jensen, T.H. and Dziembowski, A., The eukaryotic RNA exosome: same scaffold but variable catalytic subunits, *RNA biology* **2011**, *8*, 61–66.

[171] Wang, Z., Jiao, X., Carr-Schmid, A. and Kiledjian, M., The hDcp2 protein is a mammalian mRNA decapping enzyme, *Proc Natl Acad Sci U S A* **2002**, *99*, 12663–12668.

[172] Dean, J.L.E., Sarsfield, S.J., Tsounakou, E. and Saklatvala, J., p38 Mitogen-activated protein kinase stabilizes mRNAs that contain cyclooxygenase-2 and tumor necrosis factor AU-rich elements by inhibiting deadenylation, *The Journal of biological chemistry* **2003**, *278*, 39470–39476.

[173] Gingerich, T.J., Feige, J.J. and LaMarre, J., AU-rich elements and the control of gene expression through regulated mRNA stability, *Anim Health Res Rev* **2004**, *5*, 49–63.

[174] Khabar, K.S.A., The AU-rich transcriptome: more than interferons and cytokines, and its role in disease, *J Interferon Cytokine Res* **2005**, *25*, 1–10.

[175] Gherzi, R., Lee, K.Y., Briata, P. *et al.*, A KH domain RNA binding protein, KSRP, promotes ARE-directed mRNA turnover by recruiting the degradation machinery, *Molecular cell* **2004**, *14*, 571–583.

[176] Linker, K., Pautz, A., Fechir, M. *et al.*, Involvement of KSRP in the post-transcriptional regulation of human iNOS expression-complex interplay of KSRP with TTP and HuR, *Nucleic acids research* **2005**, *33*, 4813–4827.

[177] Brooks, S.A. and Blackshear, P.J., Tristetraprolin (TTP): interactions with mRNA and proteins, and current thoughts on mechanisms of action, *Biochimica et biophysica acta* **2013**, *1829*, 666–679.

[178] White, E.J.F., Brewer, G. and Wilson, G.M., Post-transcriptional control of gene expression by AUF1: mechanisms, physiological targets, and regulation, *Biochimica et biophysica acta* **2013**, *1829*, 680–688.

[179] Brennan, C.M. and Steitz, J.A., HuR and mRNA stability, *Cellular and molecular life sciences : CMLS* **2001**, *58*, 266–277.

[180] Al-Ahmadi, W., Al-Ghamdi, M., Al-Souhibani, N. and Khabar, K.S.A., miR-29a inhibition normalizes HuR over-expression and aberrant AU-rich mRNA stability in invasive cancer, *The Journal of pathology* **2013**, *230*, 28–38.

[181] Stoecklin, G., Lu, M., Rattenbacher, B. and Moroni, C., A constitutive decay element promotes tumor necrosis factor alpha mRNA degradation via an AU-rich element-independent pathway, *Molecular and cellular biology* **2003**, *23*, 3506–3515.

[182] Mols, J., van den Berg, A., Otsuka, M. *et al.*, TNF-alpha stimulation inhibits siRNA-mediated RNA interference through a mechanism involving poly-(A) tail stabilization, *Biochimica et biophysica acta* **2008**, *1779*, 712–719.

[183] Filipowicz, W., Bhattacharyya, S. and Sonenberg, N., Mechanisms of post-transcriptional regulation by microRNAs: are the answers in sight?, *Nat Rev Genet* **2008**, *9*, 102–114.

[184] van Kouwenhove, M., Kedde, M. and Agami, R., MicroRNA regulation by RNA-binding proteins and its implications for cancer, *Nature Reviews Cancer* **2011**, *11*, 644–656.

[185] Srikantan, S., Tominaga, K. and Gorospe, M., Functional interplay between RNA-binding protein HuR and microRNAs, *Current protein & peptide science* **2012**, *13*, 372–379.

[186] Lu, Y.C., Chang, S.H., Hafner, M. *et al.*, ELAVL1 modulates transcriptome-wide miRNA binding in murine macrophages, *Cell reports* **2014**, *9*, 2330–2343.

[187] Jens, M. and Rajewsky, N., Competition between target sites of regulators shapes post-transcriptional gene regulation, *Nature Reviews Genetics* **2015**, *16*, 113–126.

[188] Kiledjian, M., Wang, X. and Liebhaber, S.A., Identification of two KH domain proteins in the alpha-globin mRNP stability complex, *The EMBO journal* **1995**, *14*, 4357–4364.

[189] Yu, J. and Russell, J.E., Structural and functional analysis of an mRNP complex that mediates the high stability of human beta-globin mRNA, *Molecular and cellular biology* **2001**, *21*, 5879–5888.

[190] Waggoner, S.A. and Liebhaber, S.A., Regulation of alpha-globin mRNA stability, *Exp Biol Med* **2003**, *228*, 387–395.

[191] Peixeiro, I., Silva, A. and Romao, L., Control of human beta-globin mRNA stability and its impact on beta-thalassemia phenotype, *Haematologica* **2011**, *96*, 905–913.

[192] Ross, J. and Sullivan, T.D., Half-lives of beta and gamma globin messenger RNAs and of protein synthetic capacity in cultured human reticulocytes, *Blood* **1985**, *66*, 1149–1154.

[193] Waggoner, S.A. and Liebhaber, S.A., Identification of mRNAs associated with alphaCP2-containing RNP complexes, *Molecular and cellular biology* **2003**, *23*, 7055–7067.

[194] Russell, J. and Liebhaber, S., The stability of human beta-globin mRNA is dependent on structural determinants positioned within its 3‘ untranslated region, *Blood* **1996**, *87*, 5314–5323.

[195] Lindquist, J.N., Parsons, C.J., Stefanovic, B. and Brenner, D.A., Regulation of alpha1(I) collagen messenger RNA decay by interactions with alphaCP at the 3’-untranslated region, *The Journal of biological chemistry* **2004**, *279*, 23822–23829.

[196] Sjoberg, E.M., Suomalainen, M. and Garoff, H., A significantly improved Semliki Forest virus expression system based on translation enhancer segments from the viral capsid gene, *Bio/technology (Nature Publishing Company)* **1994**, *12*, 1127–1131.

[197] Al-Zoghaibi, F., Ashour, T., Al-Ahmadi, W. *et al.*, Bioinformatics and experimental derivation of an efficient hybrid 3’ untranslated region and use in expression active linear DNA with minimum poly(A) region, *Gene* **2007**, *391*, 130–139.

[198] Friedel, C.C., Dolken, L., Ruzsics, Z., Koszinowski, U.H. and Zimmer, R., Conserved principles of mammalian transcriptional regulation revealed by RNA half-life, *Nucleic acids research* **2009**, *37*, e115.

[199] Mann, M., Functional and quantitative proteomics using SILAC, *Nature reviews* **2006**, *7*, 952–958.

[200] Chrzanowska-Lightowlers, Z. and Lightowlers, R. **2001**.

[201] Tuerk, C. and Gold, L., Systematic evolution of ligands by exponential enrichment: RNA ligands to bacteriophage T4 DNA polymerase, *Science* **1990**, *249*, 505–510.

[202] Ellington, A.D. and Szostak, J.W., In vitro selection of RNA molecules that bind specific ligands, *Nature* **1990**, *346*, 818–822.

[203] Bradley, R.D. and Hillis, D.M., Recombinant DNA sequences generated by PCR amplification, *Molecular biology and evolution* **1997**, *14*, 592–593.

[204] Orpana, A.K., Ho, T.H. and Stenman, J., Multiple heat pulses during PCR extension enabling amplification of GC-rich sequences and reducing amplification bias, *Analytical chemistry* **2012**, *84*, 2081–2087.

[205] Tanguay, R.L. and Gallie, D.R., Translational efficiency is regulated by the length of the 3' untranslated region, *Molecular and cellular biology* **1996**, *16*, 146–156.

[206] Vo, D., Abdelmohsen, K., Martindale, J. *et al.*, The oncogenic RNA-binding protein Musashi1 is regulated by HuR via mRNA translation and stability in glioblastoma cells, *Molecular cancer research : MCR* **2012**, *10*, 143–155.

[207] Leclerc, G.M., Boockfor, F.R., Faught, W.J. and Frawley, L.S., Development of a destabilized firefly luciferase enzyme for measurement of gene expression, *BioTechniques* **2000**, *29*, 590–1, 594–6, 598 passim.

[208] Hawkins, T.L., O'Connor-Morin, T., Roy, A. and Santillan, C., DNA purification and isolation using a solid-phase, *Nucleic acids research* **1994**, *22*, 4543–4544.

[209] DeAngelis, M.M., Wang, D.G. and Hawkins, T.L., Solid-phase reversible immobilization for the isolation of PCR products, *Nucleic acids research* **1995**, *23*, 4742–4743.

[210] Lund, A.H., Duch, M. and Pedersen, F.S., Increased cloning efficiency by temperature-cycle ligation, *Nucleic acids research* **1996**, *24*, 800–801.

[211] Hawtin, P., Hardern, I., Wittig, R. *et al.*, Utility of lab-on-a-chip technology for high-throughput nucleic acid and protein analysis, *Electrophoresis* **2005**, *26*, 3674–3681.

[212] Tennant, J.R., Evaluation of the Trypan Blue technique for the determination of cell viability, *Transplantation* **1964**, *2*, 685–694.

[213] Schmid, I., Krall, W.J., Uittenbogaart, C.H., Braun, J. and Giorgi, J.V., Dead cell discrimination with 7-amino-actinomycin D in combination with dual color immunofluorescence in single laser flow cytometry, *Cytometry* **1992**, *13*, 204–208.

[214] Sahin, U., Beissert, T., Poleganov, M., Herz, S. and Koste, L., Method for cellular rna expression, *Patent* **2014**.

[215] Bustin, S.A., Quantification of mRNA using real-time reverse transcription PCR (RT-PCR): trends and problems, *Journal of molecular endocrinology* **2002**, *29*, 23–39.

[216] Udvardi, M.K., Czechowski, T. and Scheible, W.R., Eleven golden rules of quantitative RT-PCR, *The Plant cell* **2008**, *20*, 1736–1737.

[217] Sobell, H.M., Actinomycin and DNA transcription, *Proc Natl Acad Sci U S A* **1985**, *82*, 5328–5331.

[218] Jao, C.Y. and Salic, A., Exploring RNA transcription and turnover in vivo by using click chemistry, *Proc Natl Acad Sci U S A* **2008**, *105*, 15779–15784.

[219] invitrogen, Click-iT RNA Imaging Kits **2009**.

[220] Fujimoto, M., Fujiyama, K., Kuninaka, A. and Yoshino, H., Mode of action of nuclease P1 on nucleic acids and its specificity for synthetic phosphodiesters, *Agricultural and Biological Chemistry* **1974**, *38*, 2141–2147.

[221] Fujimoto, M., Kuninaka, A. and Yoshino, H., Identity of Phosphodiesterase and Phosphomonoesterase Activities with Nuclease P1 (a Nuclease from Penicillium citrinum), *Agricultural and Biological Chemistry* **1974**, *38*, 785–790.

[222] Fujimoto, M., Kuninaka, A. and Yoshino, H., Purification of a Nuclease from Penicillium citrinum, *Agricultural and Biological Chemistry* **1974**, *38*, 777–783.

[223] Fujimoto, M., Kuninaka, A. and Yoshino, H., Substrate Specificity of Nuclease P1, *Agricultural and Biological Chemistry* **1974**, *38*, 1555–1561.

[224] Fujimoto, M., Kuninaka, A. and Yoshino, H., Studies on a nuclease from Penicillium citrinum. V. Some physical and chemical properties of nuclease P1, *Agricultural and Biological Chemistry* **1975**, *39*, 1991–1997.

[225] Shimelis, O. and Giese, R.W., Nuclease P1 digestion/high-performance liquid chromatography, a practical method for DNA quantitation, *Journal of chromatography* **2006**, *1117*, 132–136.

[226] Desai, N. and Shankar, V., Single-strand-specific nucleases, *FEMS microbiology reviews* **2003**, *26*, 457–491.

[227] An, Y., Wu, W. and Lv, A., A PCR-after-ligation method for cloning of multiple DNA inserts, *Analytical biochemistry* **2010**, *402*, 203–205.

[228] Korbie, D.J. and Mattick, J.S., Touchdown PCR for increased specificity and sensitivity in PCR amplification, *Nature protocols* **2008**, *3*, 1452–1456.

[229] Krueger, F., Andrews, S.R. and Osborne, C.S., Large scale loss of data in low-diversity illumina sequencing libraries can be recovered by deferred cluster calling, *PloS one* **2011**, *6*, e16607.

[230] Mitra, A., Skrzypczak, M., Ginalski, K. and Rowicka, M., Strategies for achieving high sequencing accuracy for low diversity samples and avoiding sample bleeding using illumina platform, *PloS one* **2015**, *10*, e0120520.

[231] Dobin, A., Davis, C.A., Schlesinger, F. *et al.*, STAR: ultrafast universal RNA-seq aligner, *Bioinformatics* **2013**, *29*, 15–21.

[232] Acinas, S.G., Sarma-Rupavtarm, R., Klepac-Ceraj, V. and Polz, M.F., PCR-induced sequence artifacts and bias: insights from comparison of two 16S rRNA clone libraries constructed from the same sample, *Applied and environmental microbiology* **2005**, *71*, 8966–8969.

[233] Aird, D., Ross, M.G., Chen, W.S. *et al.*, Analyzing and minimizing PCR amplification bias in Illumina sequencing libraries, *Genome biology* **2011**, *12*, R18.

[234] Polz, M.F. and Cavanaugh, C.M., Bias in template-to-product ratios in multitemplate PCR, *Applied and environmental microbiology* **1998**, *64*, 3724–3730.

[235] Saitou, N. and Nei, M., The neighbor-joining method: a new method for reconstructing phylogenetic trees, *Molecular biology and evolution* **1987**, *4*, 406–425.

[236] Biswas, A. and Brown, C.M., Scan for Motifs: a webserver for the analysis of post-transcriptional regulatory elements in the 3' untranslated regions (3' UTRs) of mRNAs, *BMC bioinformatics* **2014**, *15*, 174.

[237] Busch, A., Richter, A.S. and Backofen, R., IntaRNA: efficient prediction of bacterial sRNA targets incorporating target site accessibility and seed regions, *Bioinformatics* **2008**, *24*, 2849–2856.

[238] Richter, A.S., Schleberger, C., Backofen, R. and Steglich, C., Seed-based INTARNA prediction combined with GFP-reporter system identifies mRNA targets of the small RNA Yfr1, *Bioinformatics* **2010**, *26*, 1–5.

[239] Wright, P.R., Georg, J., Mann, M. *et al.*, CopraRNA and IntaRNA: predicting small RNA targets, networks and interaction domains, *Nucleic acids research* **2014**, *42*, W119–23.

[240] Smith, C., Heyne, S., Richter, A.S., Will, S. and Backofen, R., Freiburg RNA Tools: a web server integrating INTARNA, EXPARNA and LOCARNA, *Nucleic acids research* **2010**, *38*, W373–7.

[241] Schuster, P., Fontana, W., Stadler, P.F. and Hofacker, I.L., From sequences to shapes and back: a case study in RNA secondary structures, *Proc Biol Sci* **1994**, *255*, 279–284.

[242] Gruber, A.R., Neubock, R., Hofacker, I.L. and Washietl, S., The RNAz web server: prediction of thermodynamically stable and evolutionarily conserved RNA structures, *Nucleic acids research* **2007**, *35*, W335–8.

[243] Lorenz, R., Bernhart, S.H., Honer Zu Siederdissen, C. *et al.*, ViennaRNA Package 2.0, *Algorithms for molecular biology : AMB* **2011**, *6*, 26.

[244] Hashimi, S.T., Fulcher, J.A., Chang, M.H. *et al.*, MicroRNA profiling identifies miR-34a and miR-21 and their target genes JAG1 and WNT1 in the coordinate regulation of dendritic cell differentiation, *Blood* **2009**, *114*, 404–414.

[245] Landgraf, P., Rusu, M., Sheridan, R. *et al.*, A mammalian microRNA expression atlas based on small RNA library sequencing, *Cell* **2007**, *129*, 1401–1414.

[246] Goldberg, I.H., The interaction of actinomycin with DNA, *Antibiotics and chemotherapy* **1971**, *17*, 67–86.

[247] Goldberg, I.H. and Friedman, P.A., Antibiotics and nucleic acids, *Annual review of biochemistry* **1971**, *40*, 775–810.

[248] Sawicki, S.G. and Godman, G.C., On the differential cytotoxicity of actinomycin D, *The Journal of cell biology* **1971**, *50*, 746–761.

[249] Hanslick, J.L., Lau, K., Noguchi, K.K. *et al.*, Dimethyl sulfoxide (DMSO) produces widespread apoptosis in the developing central nervous system, *Neurobiology of disease* **2009**, *34*, 1–10.

[250] S. S. Sommer and J. E. Cohen, The size distributions of proteins, mRNA, and nuclear RNA, *J Mol Evol* **1980**, *15*, 37–57.

[251] Kanagawa, T., Bias and artifacts in multitemplate polymerase chain reactions (PCR), *Journal of bioscience and bioengineering* **2003**, *96*, 317–323.

[252] McInerney, P., Adams, P. and Hadi, M.Z., Error Rate Comparison during Polymerase Chain Reaction by DNA Polymerase, *Molecular biology international* **2014**, *2014*, 287430.

[253] Mignone, F., Gissi, C., Liuni, S. and Pesole, G., Untranslated regions of mRNAs, *Genome biology* **2002**, *3*.

[254] Brown, J.B., Boley, N., Eisman, R. *et al.*, Diversity and dynamics of the Drosophila transcriptome, *Nature* **2014**, *512*, 393–399.

[255] Herdy, B., Karonitsch, T., Vladimer, G.I. *et al.*, The RNA-binding protein HuR/ELAVL1 regulates IFN-beta mRNA abundance and the type I IFN response, *European journal of immunology* **2015**, *45*, 1500–1511.

[256] Weidmann, C.A., Raynard, N.A., Blewett, N.H., van Etten, J. and Goldstrohm, A.C., The RNA binding domain of Pumilio antagonizes poly-adenosine binding protein and accelerates deadenylation, *RNA* **2014**, *20*, 1298–1319.

[257] Grasso, J.A., Chromey, N.C. and Moxey, C.F., Biochemical characterization of RNA and protein synthesis in erythrocyte development, *The Journal of cell biology* **1977**, *73*, 206–222.

[258] Yuhashi, K., Ohnishi, S., Kodama, T., Koike, K. and Kanamori, H., In vitro selection of the 3'-untranslated regions of the human liver mRNA that bind to the HCV nonstructural protein 5B, *Virology* **2014**, *450-451*, 13–23.

[259] Harrold, S., Genovese, C., Kobrin, B., Morrison, S.L. and Milcarek, C., A comparison of apparent mRNA half-life using kinetic labeling techniques vs decay following administration of transcriptional inhibitors, *Analytical biochemistry* **1991**, *198*, 19–29.

[260] Sobell, H.M., Actinomycin and DNA transcription, *Proc Natl Acad Sci U S A* **1985**, *82*, 5328–5331.

[261] Raghavan, A., Ogilvie, R.L., Reilly, C. *et al.*, Genome-wide analysis of mRNA decay in resting and activated primary human T lymphocytes, *Nucleic Acids Res* **2002**, *30*, 5529–5538.

[262] Cheadle, C., Fan, J., Cho-Chung, Y.S. *et al.*, Stability regulation of mRNA and the control of gene expression, *Annals of the New York Academy of Sciences* **2005**, *1058*, 196–204.

[263] Tani, H. and Akimitsu, N., Genome-wide technology for determining RNA stability in mammalian cells: historical perspective and recent advantages based on modified nucleotide labeling, *RNA biology* **2012**, *9*, 1233–1238.

[264] Singer, R.H. and Penman, S., Stability of HeLa cell mRNA in actinomycin, *Nature* **1972**, *240*, 100–102.

[265] Singer, R.H. and Penman, S., Messenger RNA in HeLa cells: kinetics of formation and decay, *J Mol Biol* **1973**, *78*, 321–334.

[266] Cheadle, C., Fan, J., Cho-Chung, Y.S. *et al.*, Control of gene expression during T cell activation: alternate regulation of mRNA transcription and mRNA stability, *BMC Genomics* **2005**, *6*, 75.

[267] Shyu, A.B., Greenberg, M.E. and Belasco, J.G., The c-fos transcript is targeted for rapid decay by two distinct mRNA degradation pathways, *Genes & development* **1989**, *3*, 60–72.

[268] Harpold, M.M., Wilson, M.C. and Darnell, J.E.J., Chinese hamster polyadenylated messenger ribonucleic acid: relationship to non-polyadenylated sequences and relative conservation during messenger ribonucleic acid processing, *Molecular and cellular biology* **1981**, *1*, 188–198.

[269] Yang, E., van Nimwegen, E., Zavolan, M. *et al.*, Decay rates of human mRNAs: correlation with functional characteristics and sequence attributes, *Genome Res* **2003**, *13*, 1863–1872.

[270] Thiel, W.H., Bair, T., Wyatt, T. *et al.*, Nucleotide Bias Observed with a Short SELEX RNA Aptamer Library, *Nucleic acid therapeutics* **2011**.

[271] Bartoletti, D.C., Harrison, G.I. and Weaver, J.C., The number of molecules taken up by electroporated cells: quantitative determination, *FEBS letters* **1989**, *256*, 4–10.

[272] Prausnitz, M.R., Lau, B.S., Milano, C.D. *et al.*, A quantitative study of electroporation showing a plateau in net molecular transport, *Biophysical journal* **1993**, *65*, 414–422.

[273] Prausnitz, M.R., Milano, C.D., Gimm, J.A., Langer, R. and Weaver, J.C., Quantitative study of molecular transport due to electroporation: uptake of bovine serum albumin by erythrocyte ghosts, *Biophysical journal* **1994**, *66*, 1522–1530.

[274] Gift, E.A. and Weaver, J.C., Observation of extremely heterogeneous electroporative molecular uptake by Saccharomyces cerevisiae which changes with electric field pulse amplitude, *Biochimica et biophysica acta* **1995**, *1234*, 52–62.

[275] Canatella, P.J., Karr, J.F., Petros, J.A. and Prausnitz, M.R., Quantitative study of electroporation-mediated molecular uptake and cell viability, *Biophysical journal* **2001**, *80*, 755–764.

[276] Javorovic, M., Pohla, H., Frankenberger, B., Wolfel, T. and Schendel, D.J., RNA transfer by electroporation into mature dendritic cells leading to reactivation of effector-memory cytotoxic T lymphocytes: a quantitative analysis, *Molecular therapy* **2005**, *12*, 734–743.

[277] Velculescu, V.E., Madden, S.L., Zhang, L. *et al.*, Analysis of human transcriptomes, *Nature genetics* **1999**, *23*, 387–388.

[278] J. Guhaniyogi and G. Brewer, Regulation of mRNA stability in mammalian cells, *Gene* **2001**, *265*, 11–23.

[279] Akashi, M., Shaw, G., Hachiya, M. *et al.*, Number and location of AUUUA motifs: role in regulating transiently expressed RNAs, *Blood* **1994**, *83*, 3182–3187.

[280] Fan, J., Heller, N.M., Gorospe, M., Atasoy, U. and Stellato, C., The role of post-transcriptional regulation in chemokine gene expression in inflammation and allergy, *The European respiratory journal* **2005**, *26*, 933–947.

[281] Schott, J. and Stoecklin, G., Networks controlling mRNA decay in the immune system, *Wiley interdisciplinary reviews* **2010**, *1*, 432–456.

[282] Kang, J.G., Amar, M.J., Remaley, A.T. *et al.*, Zinc finger protein tristetraprolin interacts with CCL3 mRNA and regulates tissue inflammation, *J Immunol* **2011**, *187*, 2696–2701.

[283] Palanisamy, V., Jakymiw, A., Van, T., D'Silva, N.J. and Kirkwood, K.L., Control of Cytokine mRNA Expression by RNA-binding Proteins and microRNAs, *Journal of dental research* **2012**.

[284] Ivanov, P. and Anderson, P., Post-transcriptional regulatory networks in immunity, *Immunological reviews* **2013**, *253*, 253–272.

[285] Ambion, Poly(A)Purist™ Kit **2008**.

[286] Chinnery, P.F. and Hudson, G., Mitochondrial genetics, *British medical bulletin* **2013**, *106*, 135–159.

[287] Nicholls, T.J., Rorbach, J. and Minczuk, M., Mitochondria: mitochondrial RNA metabolism and human disease, *The international journal of biochemistry & cell biology* **2013**, *45*, 845–849.

[288] Suzuki, T., Terasaki, M., Takemoto-Hori, C. *et al.*, Proteomic analysis of the mammalian mitochondrial ribosome. Identification of protein components in the 28 S small subunit, *The Journal of biological chemistry* **2001**, *276*, 33181–33195.

[289] Anko, M.L. and Neugebauer, K.M., RNA-protein interactions in vivo: global gets specific, *Trends in biochemical sciences* **2012**, *37*, 255–262.

[290] Brodersen, P. and Voinnet, O., Revisiting the principles of microRNA target recognition and mode of action, *Nature reviews* **2009**, *10*, 141–148.

[291] Chen, J.M., Ferec, C. and Cooper, D.N., A systematic analysis of disease-associated variants in the 3' regulatory regions of human protein-coding genes II: the importance of mRNA secondary structure in assessing the functionality of 3' UTR variants, *Human genetics* **2006**, *120*, 301–333.

[292] Lai, W.S., Parker, J.S., Grissom, S.F., Stumpo, D.J. and Blackshear, P.J., Novel mRNA targets for tristetraprolin (TTP) identified by global analysis of stabilized transcripts in TTP-deficient fibroblasts, *Molecular and cellular biology* **2006**, *26*, 9196–9208.

[293] Sauer, I., Schaljo, B., Vogl, C. *et al.*, Interferons limit inflammatory responses by induction of tristetraprolin, *Blood* **2006**, *107*, 4790–4797.

[294] Emmons, J., Townley-Tilson, W.H.D., Deleault, K.M. *et al.*, Identification of TTP mRNA targets in human dendritic cells reveals TTP as a critical regulator of dendritic cell maturation, *RNA* **2008**, *14*, 888–902.

[295] Ratti, A., Fallini, C., Cova, L. *et al.*, A role for the ELAV RNA-binding proteins in neural stem cells: stabilization of Msi1 mRNA, *Journal of cell science* **2006**, *119*, 1442–1452.

[296] Capowski, E.E., Esnault, S., Bhattacharya, S. and Malter, J.S., Y box-binding factor promotes eosinophil survival by stabilizing granulocyte-macrophage colony-stimulating factor mRNA, *Journal of immunology* **2001**, *167*, 5970–5976.

[297] Chen, C.Y., Gherzi, R., Andersen, J.S. *et al.*, Nucleolin and YB-1 are required for JNK-mediated interleukin-2 mRNA stabilization during T-cell activation, *Genes & Development* **2000**, *14*, 1236–1248.

[298] Fu, X.D. and Maniatis, T., Isolation of a complementary DNA that encodes the mammalian splicing factor SC35, *Science* **1992**, *256*, 535–538.

[299] Siebel, C.W., Fresco, L.D. and Rio, D.C., The mechanism of somatic inhibition of Drosophila P-element pre-mRNA splicing: multiprotein complexes at an exon pseudo-5' splice site control U1 snRNP binding, *Genes & Development* **1992**, *6*, 1386–1401.

[300] Champion-Arnaud, P. and Reed, R., The prespliceosome components SAP 49 and SAP 145 interact in a complex implicated in tethering U2 snRNP to the branch site, *Genes & Development* **1994**, *8*, 1974–1983.

[301] Flickinger, T.W. and Salz, H.K., The Drosophila sex determination gene snf encodes a nuclear protein with sequence and functional similarity to the mammalian U1A snRNP protein, *Genes & Development* **1994**, *8*, 914–925.

[302] Musunuru, K. and Darnell, R.B., Determination and augmentation of RNA sequence specificity of the Nova K-homology domains, *Nucleic acids research* **2004**, *32*, 4852–4861.

[303] Vance, C., Rogelj, B., Hortobagyi, T. *et al.*, Mutations in FUS, an RNA processing protein, cause familial amyotrophic lateral sclerosis type 6, *Science* **2009**, *323*, 1208–1211.

[304] Racca, C., Gardiol, A., Eom, T. *et al.*, The Neuronal Splicing Factor Nova Co-Localizes with Target RNAs in the Dendrite, *Frontiers in neural circuits* **2010**, *4*, 5.

[305] van Etten, J., Schagat, T.L., Hrit, J. *et al.*, Human Pumilio proteins recruit multiple deadenylases to efficiently repress messenger RNAs, *The Journal of biological chemistry* **2012**, *287*, 36370–36383.

[306] Weidensdorfer, D., Stohr, N., Baude, A. *et al.*, Control of c-myc mRNA stability by IGF2BP1-associated cytoplasmic RNPs, *RNA* **2009**, *15*, 104–115.

[307] Ule, J., Jensen, K., Mele, A. and Darnell, R.B., CLIP: a method for identifying protein-RNA interaction sites in living cells, *Methods* **2005**, *37*, 376–386.

[308] Licatalosi, D.D., Mele, A., Fak, J.J. *et al.*, HITS-CLIP yields genome-wide insights into brain alternative RNA processing, *Nature* **2008**, *456*, 464–469.

[309] Konig, J., Zarnack, K., Rot, G. *et al.*, iCLIP reveals the function of hnRNP particles in splicing at individual nucleotide resolution, *Nature structural & molecular biology* **2010**, *17*, 909–915.

[310] Hafner, M., Landthaler, M., Burger, L. *et al.*, Transcriptome-wide identification of RNA-binding protein and microRNA target sites by PAR-CLIP, *Cell* **2010**, *141*, 129–141.

[311] Cook, K.B., Hughes, T.R. and Morris, Q.D., High-throughput characterization of protein-RNA interactions, *Briefings in functional genomics* **2015**, *14*, 74–89.

[312] Jackson, R.J., Hellen, C.U. and Pestova, T.V., The mechanism of eukaryotic translation initiation and principles of its regulation, *Nat Rev Mol Cell Biol* **2010**, *11*, 113–127.

[313] Mahen, E.M., Watson, P.Y., Cottrell, J.W. and Fedor, M.J., mRNA secondary structures fold sequentially but exchange rapidly in vivo, *PLoS biology* **2010**, *8*, e1000307.

[314] Wan, Y., Kertesz, M., Spitale, R., Segal, E. and Chang, H., Understanding the transcriptome through RNA structure, *Nature reviews* **2011**, *12*, 641–655.

[315] Larocque, D., Galarneau, A., Liu, H.N. *et al.*, Protection of p27(Kip1) mRNA by quaking RNA binding proteins promotes oligodendrocyte differentiation, *Nature neuroscience* **2005**, *8*, 27–33.

[316] Goodarzi, H., Najafabadi, H.S., Oikonomou, P. *et al.*, Systematic discovery of structural elements governing stability of mammalian messenger RNAs, *Nature* **2012**.

[317] Gebauer, F. and Hentze, M.W., Molecular mechanisms of translational control, *Nat Rev Mol Cell Biol* **2004**, *5*, 827–835.

[318] Abaza, I. and Gebauer, F., Trading translation with RNA-binding proteins, *RNA* **2008**, *14*, 404–409.

[319] Vasudevan, S., Tong, Y. and Steitz, J.A., Switching from repression to activation: microRNAs can up-regulate translation, *Science* **2007**, *318*, 1931–1934.

[320] Vasudevan, S., Posttranscriptional upregulation by microRNAs, *Wiley interdisciplinary reviews. RNA* **2012**, *3*, 311–330.

[321] Banchereau, J. and Palucka, A., Dendritic cells as therapeutic vaccines against cancer, *Nature reviews* **2005**, *5*, 296–306.

[322] Huch, S. and Nissan, T., Interrelations between translation and general mRNA degradation in yeast, *Wiley interdisciplinary reviews. RNA* **2014**, *5*, 747–763.

[323] Simon, P., Omokoko, T.A., Breitkreuz, A. *et al.*, Functional TCR retrieval from single antigen-specific human T cells reveals multiple novel epitopes, *Cancer immunology research* **2014**, *2*, 1230–1244.

[324] Omokoko, T., Simon, P., Tureci, O. and Sahin, U., Retrieval of functional TCRs from single antigen-specific T cells: Toward individualized TCR-engineered therapies, *Oncoimmunology* **2015**, *4*, e1005523.

[325] Kranz, L.M. and Diken, M., Luciferase activity and immunstimulatory capacity of FI in BALB/c mice, *Internal communication* **2014**.

[326] Kawai, T. and Akira, S., Toll-like receptor and RIG-I-like receptor signaling, *Annals of the New York Academy of Sciences* **2008**, *1143*, 1–20.

List of Figures

List of Tables

A Appendix

Primers used for cold fusion cloning technology

Table A.1: Primers used for cold fusion cloning technology. Each chosen sequence element was combined with the other sequences in pair-wise combination (PWC-PP). Primerpairs (PP) used for PCR in preparation for cold fusion reaction are as follows: primer i was combined with primer iv and primer ii with primer iii. Tm refers to annealing temperature of the primer sequence, which binds to the template.

PWC-PP	Sequence (5' ⟶ 3')	Tm
II-i	GATCAATGTGTAAGGATCCGATCAAGCACGCAGCAATGCAG	68
II-ii	CAGCCACACCCAAGCACGCAGCAATGCAG	68
II-iii	TTGCCGTATCCCATCTTAGCGGCCGCGGTGTGGCTGGCACGAAATTGAC	72
II-iv	TGCGTGCTTGGGTGTGGCTGGCACGAAATTGAC	72
IG-i	GATCAATGTGTAAGGATCCGATCAAGCACGCAGCAATGCAG	68
IG-ii	CAGCCACACCCTGACAGCGTGGGCAACG	68
IG-iii	TTGCCGTATCCCATCTTAGCGGCCGCGTGGGGGTGGAGGTAGAG	60
IG-iv	ACGCTGTCAGGGTGTGGCTGGCACGAAATTGAC	72
IB-i	GATCAATGTGTAAGGATCCGATCAAGCACGCAGCAATGCAG	68
IB-ii	CAGCCACACCTGCCCGTCCTCACCAAG	65
IB-iii	TTGCCGTATCCCATCTTAGCGGCCGCGGTCACACCGGCAATGG	65
IB-iv	AGGACGGGCAGGTGTGGCTGGCACGAAATTGAC	72
ID-i	GATCAATGTGTAAGGATCCGATCAAGCACGCAGCAATGCAG	68
ID-ii	CAGCCACACCTTCCAGCCAGACACCCGC	68
ID-iii	TTGCCGTATCCCATCTTAGCGGCCGCGGGGTCAGAGAGTGGAAG	58
ID-iv	CTGGCTGGAAGGTGTGGCTGGCACGAAATTGAC	72
IJ-i	GATCAATGTGTAAGGATCCGATCAAGCACGCAGCAATGCAG	68
IJ-ii	CAGCCACACCCTTTGCAGGATGAAACACTTC	60
IJ-iii	TTGCCGTATCCCATCTTAGCGGCCGCGGAGGAGTACAGATGCATG	56
IJ-iv	TCCTGCAAAGGGTGTGGCTGGCACGAAATTGAC	72
IE-i	GATCAATGTGTAAGGATCCGATCAAGCACGCAGCAATGCAG	68
IE-ii	CAGCCACACCGCCTTGGCTCCTCCAGG	64
IE-iii	TTGCCGTATCCCATCTTAGCGGCCGCGGGGGGAGATGGCAGTG	65
IE-iv	GAGCCAAGGCGGTGTGGCTGGCACGAAATTGAC	72
IF-i	GATCAATGTGTAAGGATCCGATCAAGCACGCAGCAATGCAG	68
IF-ii	CAGCCACACCCTGGTACTGCATGCACGC	63
IF-iii	TTGCCGTATCCCATCTTAGCGGCCGCGGAGGTGTCTGGAACTAG	53
IF-iv	GCAGTACCAGGGTGTGGCTGGCACGAAATTGAC	72
IhBg-i	GATCAATGTGTAAGGATCCGATCAAGCACGCAGCAATGCAG	68
IhBg-ii	CAGCCACACCGAGAGCTCGCTTTCTTG	54
IhBg-iii	TTGCCGTATCCCATCTTAGCGGCCGCGACGCAGCAATGAAAATAAATGTT TTTTATTAGG	69
IhBg-iv	GCGAGCTCTCGGTGTGGCTGGCACGAAATTGAC	72
BB-i	GATCAATGTGTAAGGATCCGATTGCCCGTCCTCACCAAG	65
BB-ii	CGGTGTGACCTGCCCGTCCTCACCAAG	65
BB-iii	TTGCCGTATCCCATCTTAGCGGCCGCGGTCACACCGGCAATGG	65
BB-iv	AGGACGGGCAGGTCACACCGGCAATGG	65
BI-i	GATCAATGTGTAAGGATCCGATTGCCCGTCCTCACCAAG	65
BI-ii	CGGTGTGACCCAAGCACGCAGCAATGCAG	68
BI-iii	TTGCCGTATCCCATCTTAGCGGCCGCGGTGTGGCTGGCACGAAATTGAC	72
BI-iv	TGCGTGCTTGGGTCACACCGGCAATGG	65
BG-i	GATCAATGTGTAAGGATCCGATTGCCCGTCCTCACCAAG	65
BG-ii	CGGTGTGACCCTGACAGCGTGGGCAACG	68
BG-iii	TTGCCGTATCCCATCTTAGCGGCCGCGTGGGGGTGGAGGTAGAG	60
BG-iv	ACGCTGTCAGGGTCACACCGGCAATGG	65
BD-i	GATCAATGTGTAAGGATCCGATTGCCCGTCCTCACCAAG	65
BD-ii	CGGTGTGACCTTCCAGCCAGACACCCGC	68
BD-iii	TTGCCGTATCCCATCTTAGCGGCCGCGGGGTCAGAGAGTGGAAG	58

continues on next page

continues from previous page

BD-iv	CTGGCTGGAAGGTCACACCGGCAATGG	65
BJ-i	GATCAATGTGTAAGGATCCGATTGCCCGTCCTCACCAAG	65
BJ-ii	CGGTGTGACCCTTTGCAGGATGAAACACTTC	60
BJ-iii	TTGCCGTATCCCATCTTAGCGGCCGCGGAGGAGTACAGATGCATG	56
BJ-iv	TCCTGCAAAGGGTCACACCGGCAATGG	65
BE-i	GATCAATGTGTAAGGATCCGATTGCCCGTCCTCACCAAG	65
BE-ii	CGGTGTGACCGCCTTGGCTCCTCCAGG	64
BE-iii	TTGCCGTATCCCATCTTAGCGGCCGCGGGGGGAGATGGCAGTG	65
BE-iv	GAGCCAAGGCGGTCACACCGGCAATGG	65
BF-i	GATCAATGTGTAAGGATCCGATTGCCCGTCCTCACCAAG	65
BF-ii	CGGTGTGACCCTGGTACTGCATGCACGC	63
BF-iii	TTGCCGTATCCCATCTTAGCGGCCGCGGAGGTGTCTGGAACTAG	53
BF-iv	GCAGTACCAGGGTCACACCGGCAATGG	65
BhBg-i	GATCAATGTGTAAGGATCCGATTGCCCGTCCTCACCAAG	65
BhBg-ii	CGGTGTGACCGAGAGCTCGCTTTCTTG	54
BhBg-iii	TTGCCGTATCCCATCTTAGCGGCCGCGACGCAGCAATGAAAATAAATGTT TTTTATTAGG	69
BhBg-iv	GCGAGCTCTCGGTCACACCGGCAATGG	65
JJ-i	GATCAATGTGTAAGGATCCGATCTTTGCAGGATGAAACACTTC	60
JJ-ii	GTACTCCTCCCTTTGCAGGATGAAACACTTC	60
JJ-iii	TTGCCGTATCCCATCTTAGCGGCCGCGGAGGAGTACAGATGCATG	56
JJ-iv	TCCTGCAAAGGGAGGAGTACAGATGCATG	56
JI-i	GATCAATGTGTAAGGATCCGATCTTTGCAGGATGAAACACTTC	60
JI-ii	GTACTCCTCCCAAGCACGCAGCAATGCAG	68
JI-iii	TTGCCGTATCCCATCTTAGCGGCCGCGGTGTGGCTGGCACGAAATTGAC	72
JI-iv	TGCGTGCTTGGGAGGAGTACAGATGCATG	56
JG-i	GATCAATGTGTAAGGATCCGATCTTTGCAGGATGAAACACTTC	60
JG-ii	GTACTCCTCCCTGACAGCGTGGGCAACG	68
JG-iii	TTGCCGTATCCCATCTTAGCGGCCGCGTGGGGGTGGAGGTAGAG	60
JG-iv	ACGCTGTCAGGGAGGAGTACAGATGCATG	56
JB-i	GATCAATGTGTAAGGATCCGATCTTTGCAGGATGAAACACTTC	60
JB-ii	GTACTCCTCCTGCCCGTCCTCACCAAG	65
JB-iii	TTGCCGTATCCCATCTTAGCGGCCGCGGTCACACCGGCAATGG	65
JB-iv	AGGACGGGCAGGAGGAGTACAGATGCATG	56
JD-i	GATCAATGTGTAAGGATCCGATCTTTGCAGGATGAAACACTTC	60
JD-ii	GTACTCCTCCTTCCAGCCAGACACCCGC	68
JD-iii	TTGCCGTATCCCATCTTAGCGGCCGCGGGGTCAGAGAGTGGAAG	58
JD-iv	CTGGCTGGAAGGAGGAGTACAGATGCATG	56
JE-i	GATCAATGTGTAAGGATCCGATCTTTGCAGGATGAAACACTTC	60
JE-ii	GTACTCCTCCGCCTTGGCTCCTCCAGG	64
JE-iii	TTGCCGTATCCCATCTTAGCGGCCGCGGGGGGAGATGGCAGTG	65
JE-iv	GAGCCAAGGCGGAGGAGTACAGATGCATG	56
JF-i	GATCAATGTGTAAGGATCCGATCTTTGCAGGATGAAACACTTC	60
JF-ii	GTACTCCTCCCTGGTACTGCATGCACGC	63
JF-iii	TTGCCGTATCCCATCTTAGCGGCCGCGGAGGTGTCTGGAACTAG	53
JF-iv	GCAGTACCAGGGAGGAGTACAGATGCATG	56
JhBg-i	GATCAATGTGTAAGGATCCGATCTTTGCAGGATGAAACACTTC	60
JhBg-ii	GTACTCCTCCGAGAGCTCGCTTTCTTG	54
JhBg-iii	TTGCCGTATCCCATCTTAGCGGCCGCGACGCAGCAATGAAAATAAATGTT TTTTATTAGG	69
JhBg-iv	GCGAGCTCTCGGAGGAGTACAGATGCATG	56
FF-i	GATCAATGTGTAAGGATCCGATCTGGTACTGCATGCACGC	63
FF-ii	AGACACCTCCCTGGTACTGCATGCACGC	63
FF-iii	TTGCCGTATCCCATCTTAGCGGCCGCGGAGGTGTCTGGAACTAG	53
FF-iv	GCAGTACCAGGGAGGTGTCTGGAACTAG	53
FI-i	GATCAATGTGTAAGGATCCGATCTGGTACTGCATGCACGC	63

continues on next page

continues from previous page

FI-ii	AGACACCTCCCAAGCACGCAGCAATGCAG	68
FI-iii	TTGCCGTATCCCATCTTAGCGGCCGCGGTGTGGCTGGCACGAAATTGAC	72
FI-iv	TGCGTGCTTGGGAGGTGTCTGGAACTAG	53
FG-i	GATCAATGTGTAAGGATCCGATCTGGTACTGCATGCACGC	63
FG-ii	AGACACCTCCCTGACAGCGTGGGCAACG	68
FG-iii	TTGCCGTATCCCATCTTAGCGGCCGCGTGGGGGTGGAGGTAGAG	60
FG-iv	ACGCTGTCAGGGAGGTGTCTGGAACTAG	53
FB-i	GATCAATGTGTAAGGATCCGATCTGGTACTGCATGCACGC	63
FB-ii	AGACACCTCCTGCCCGTCCTCACCAAG	65
FB-iii	TTGCCGTATCCCATCTTAGCGGCCGCGGTCACACCGGCAATGG	65
FB-iv	AGGACGGGCAGGAGGTGTCTGGAACTAG	53
FD-i	GATCAATGTGTAAGGATCCGATCTGGTACTGCATGCACGC	63
FD-ii	AGACACCTCCTTCCAGCCAGACACCCGC	68
FD-iii	TTGCCGTATCCCATCTTAGCGGCCGCGGGGTCAGAGAGTGGAAG	58
FD-iv	CTGGCTGGAAGGAGGTGTCTGGAACTAG	53
FJ-i	GATCAATGTGTAAGGATCCGATCTGGTACTGCATGCACGC	63
FJ-ii	AGACACCTCCCTTTGCAGGATGAAACACTTC	60
FJ-iii	TTGCCGTATCCCATCTTAGCGGCCGCGGAGGAGTACAGATGCATG	56
FJ-iv	TCCTGCAAAGGGAGGTGTCTGGAACTAG	53
FE-i	GATCAATGTGTAAGGATCCGATCTGGTACTGCATGCACGC	63
FE-ii	AGACACCTCCGCCTTGGCTCCTCCAGG	64
FE-iii	TTGCCGTATCCCATCTTAGCGGCCGCGGGGGGGAGATGGCAGTG	65
FE-iv	GAGCCAAGGCGGAGGTGTCTGGAACTAG	53
FhBg-i	GATCAATGTGTAAGGATCCGATCTGGTACTGCATGCACGC	63
FhBg-ii	AGACACCTCCGAGAGCTCGCTTTCTTG	54
FhBg-iii	TTGCCGTATCCCATCTTAGCGGCCGCGACGCAGCAATGAAAATAAATGTT TTTTATTAGG	69
FhBg-iv	GCGAGCTCTCGGAGGTGTCTGGAACTAG	53
GG-i	GATCAATGTGTAAGGATCCGATCTGACAGCGTGGGCAACG	68
GG-ii	CCACCCCCACCTGACAGCGTGGGCAACG	68
GG-iii	TTGCCGTATCCCATCTTAGCGGCCGCGTGGGGGTGGAGGTAGAG	60
GG-iv	ACGCTGTCAGGTGGGGGTGGAGGTAGAG	60
GI-i	GATCAATGTGTAAGGATCCGATCTGACAGCGTGGGCAACG	68
GI-ii	CCACCCCCACCAAGCACGCAGCAATGCAG	68
GI-iii	TTGCCGTATCCCATCTTAGCGGCCGCGGTGTGGCTGGCACGAAATTGAC	72
GI-iv	TGCGTGCTTGGTGGGGGTGGAGGTAGAG	60
GB-i	GATCAATGTGTAAGGATCCGATCTGACAGCGTGGGCAACG	68
GB-ii	CCACCCCCACTGCCCGTCCTCACCAAG	65
GB-iii	TTGCCGTATCCCATCTTAGCGGCCGCGGTCACACCGGCAATGG	65
GB-iv	AGGACGGGCAGTGGGGGTGGAGGTAGAG	60
GD-i	GATCAATGTGTAAGGATCCGATCTGACAGCGTGGGCAACG	68
GD-ii	CCACCCCCACTTCCAGCCAGACACCCGC	68
GD-iii	TTGCCGTATCCCATCTTAGCGGCCGCGGGGTCAGAGAGTGGAAG	58
GD-iv	CTGGCTGGAAGTGGGGGTGGAGGTAGAG	60
GJ-i	GATCAATGTGTAAGGATCCGATCTGACAGCGTGGGCAACG	68
GJ-ii	CCACCCCCACCTTTGCAGGATGAAACACTTC	60
GJ-iii	TTGCCGTATCCCATCTTAGCGGCCGCGGAGGAGTACAGATGCATG	56
GJ-iv	TCCTGCAAAGGTGGGGGTGGAGGTAGAG	60
GE-i	GATCAATGTGTAAGGATCCGATCTGACAGCGTGGGCAACG	68
GE-ii	CCACCCCCACGCCTTGGCTCCTCCAGG	64
GE-iii	TTGCCGTATCCCATCTTAGCGGCCGCGGGGGGGAGATGGCAGTG	65
GE-iv	GAGCCAAGGCGTGGGGGTGGAGGTAGAG	60
GF-i	GATCAATGTGTAAGGATCCGATCTGACAGCGTGGGCAACG	68
GF-ii	CCACCCCCACCTGGTACTGCATGCACGC	63
GF-iii	TTGCCGTATCCCATCTTAGCGGCCGCGGAGGTGTCTGGAACTAG	53
GF-iv	GCAGTACCAGGTGGGGGTGGAGGTAGAG	60

continues on next page

continues from previous page

GhBg-i	GATCAATGTGTAAGGATCCGATCTGACAGCGTGGGCAACG	68
GhBg-ii	CCACCCCCACGAGAGCTCGCTTTCTTG	54
GhBg-iii	TTGCCGTATCCCATCTTAGCGGCCGCGACGCAGCAATGAAAATAAATGTT TTTTATTAGG	69
GhBg-iv	GCGAGCTCTCGTGGGGGTGGAGGTAGAG	60
DD-i	GATCAATGTGTAAGGATCCGATTTCCAGCCAGACACCCGC	68
DD-ii	CTCTGACCCCTTCCAGCCAGACACCCGC	68
DD-iii	TTGCCGTATCCCATCTTAGCGGCCGCGGGGTCAGAGAGTGGAAG	58
DD-iv	CTGGCTGGAAGGGGTCAGAGAGTGGAAG	58
DI-i	GATCAATGTGTAAGGATCCGATTTCCAGCCAGACACCCGC	68
DI-ii	CTCTGACCCCCAAGCACGCAGCAATGCAG	68
DI-iii	TTGCCGTATCCCATCTTAGCGGCCGCGGTGTGGCTGGCACGAAATTGAC	72
DI-iv	TGCGTGCTTGGGGGTCAGAGAGTGGAAG	58
DG-i	GATCAATGTGTAAGGATCCGATTTCCAGCCAGACACCCGC	68
DG-ii	CTCTGACCCCCTGACAGCGTGGGCAACG	68
DG-iii	TTGCCGTATCCCATCTTAGCGGCCGCGTGGGGGTGGAGGTAGAG	60
DG-iv	ACGCTGTCAGGGGGTCAGAGAGTGGAAG	58
DB-i	GATCAATGTGTAAGGATCCGATTTCCAGCCAGACACCCGC	68
DB-ii	CTCTGACCCCTGCCCGTCCTCACCAAG	65
DB-iii	TTGCCGTATCCCATCTTAGCGGCCGCGGTCACACCGGCAATGG	65
DB-iv	AGGACGGGCAGGGGTCAGAGAGTGGAAG	58
DJ-i	GATCAATGTGTAAGGATCCGATTTCCAGCCAGACACCCGC	68
DJ-ii	CTCTGACCCCCTTTGCAGGATGAAACACTTC	60
DJ-iii	TTGCCGTATCCCATCTTAGCGGCCGCGGAGGAGTACAGATGCATG	56
DJ-iv	TCCTGCAAAGGGGGTCAGAGAGTGGAAG	58
DE-i	GATCAATGTGTAAGGATCCGATTTCCAGCCAGACACCCGC	68
DE-ii	CTCTGACCCCGCCTTGGCTCCTCCAGG	64
DE-iii	TTGCCGTATCCCATCTTAGCGGCCGCGGGGGGAGATGGCAGTG	65
DE-iv	GAGCCAAGGCGGGGTCAGAGAGTGGAAG	58
DF-i	GATCAATGTGTAAGGATCCGATTTCCAGCCAGACACCCGC	68
DF-ii	CTCTGACCCCCTGGTACTGCATGCACGC	63
DF-iii	TTGCCGTATCCCATCTTAGCGGCCGCGGAGGTGTCTGGAACTAG	53
DF-iv	GCAGTACCAGGGGGTCAGAGAGTGGAAG	58
DhBg-i	GATCAATGTGTAAGGATCCGATTTCCAGCCAGACACCCGC	68
DhBg-ii	CTCTGACCCCGAGAGCTCGCTTTCTTG	54
DhBg-iii	TTGCCGTATCCCATCTTAGCGGCCGCGACGCAGCAATGAAAATAAATGTT TTTTATTAGG	69
DhBg-iv	GCGAGCTCTCGGGGTCAGAGAGTGGAAG	58
EE-i	GATCAATGTGTAAGGATCCGATGCCTTGGCTCCTCCAGG	64
EE-ii	ATCTCCCCCCCGCCTTGGCTCCTCCAGG	64
EE-iii	TTGCCGTATCCCATCTTAGCGGCCGCGGGGGGAGATGGCAGTG	65
EE-iv	GAGCCAAGGCGGGGGGAGATGGCAGTG	65
EI-i	GATCAATGTGTAAGGATCCGATGCCTTGGCTCCTCCAGG	64
EI-ii	ATCTCCCCCCCCAAGCACGCAGCAATGCAG	68
EI-iii	TTGCCGTATCCCATCTTAGCGGCCGCGGTGTGGCTGGCACGAAATTGAC	72
EI-iv	TGCGTGCTTGGGGGGGGAGATGGCAGTG	65
EG-i	GATCAATGTGTAAGGATCCGATGCCTTGGCTCCTCCAGG	64
EG-ii	ATCTCCCCCCCCTGACAGCGTGGGCAACG	68
EG-iii	TTGCCGTATCCCATCTTAGCGGCCGCGTGGGGGTGGAGGTAGAG	60
EG-iv	ACGCTGTCAGGGGGGGGAGATGGCAGTG	65
EB-i	GATCAATGTGTAAGGATCCGATGCCTTGGCTCCTCCAGG	64
EB-ii	ATCTCCCCCCCTGCCCGTCCTCACCAAG	65
EB-iii	TTGCCGTATCCCATCTTAGCGGCCGCGGTCACACCGGCAATGG	65
EB-iv	AGGACGGGCAGGGGGGGAGATGGCAGTG	65
ED-i	GATCAATGTGTAAGGATCCGATGCCTTGGCTCCTCCAGG	64
ED-ii	ATCTCCCCCCTTCCAGCCAGACACCCGC	68

continues on next page

continues from previous page

ED-iii	TTGCCGTATCCCATCTTAGCGGCCGCGGGGTCAGAGAGTGGAAG	58
ED-iv	CTGGCTGGAAGGGGGGAGATGGCAGTG	65
EJ-i	GATCAATGTGTAAGGATCCGATGCCTTGGCTCCTCCAGG	64
EJ-ii	ATCTCCCCCCCCTTTGCAGGATGAAACACTTC	60
EJ-iii	TTGCCGTATCCCATCTTAGCGGCCGCGGAGGAGTACAGATGCATG	56
EJ-iv	TCCTGCAAAGGGGGGGAGATGGCAGTG	65
EF-i	GATCAATGTGTAAGGATCCGATGCCTTGGCTCCTCCAGG	64
EF-ii	ATCTCCCCCCCCTGGTACTGCATGCACGC	63
EF-iii	TTGCCGTATCCCATCTTAGCGGCCGCGGAGGTGTCTGGAACTAG	53
EF-iv	GCAGTACCAGGGGGGGAGATGGCAGTG	65
EhBg-i	GATCAATGTGTAAGGATCCGATGCCTTGGCTCCTCCAGG	64
EhBg-ii	ATCTCCCCCCGAGAGCTCGCTTTCTTG	54
EhBg-iii	TTGCCGTATCCCATCTTAGCGGCCGCGACGCAGCAATGAAAATAAATGTT TTTTATTAGG	69
EhBg-iv	GCGAGCTCTCGGGGGGGAGATGGCAGTG	65
hBghBg-i	GATCAATGTGTAAGGATCCGATGAGAGCTCGCTTTCTTG	54
hBghBg-ii	TTGCTGCGTCGAGAGCTCGCTTTCTTG	54
hBghBg-iii	TTGCCGTATCCCATCTTAGCGGCCGCGACGCAGCAATGAAAATAAATGTT TTTTATTAGG	69
hBghBg-iv	GCGAGCTCTCGACGCAGCAATGAAAATAAATGTTTTTTTATTAGG	69
hBgI-i	GATCAATGTGTAAGGATCCGATGAGAGCTCGCTTTCTTG	54
hBgI-ii	TTGCTGCGTCCAAGCACGCAGCAATGCAG	68
hBgI-iii	TTGCCGTATCCCATCTTAGCGGCCGCGGTGTGGCTGGCACGAAATTGAC	72
hBgI-iv	TGCGTGCTTGGACGCAGCAATGAAAATAAATGTTTTTTTATTAGG	69
hBgG-i	GATCAATGTGTAAGGATCCGATGAGAGCTCGCTTTCTTG	54
hBgG-ii	TTGCTGCGTCCTGACAGCGTGGGCAACG	68
hBgG-iii	TTGCCGTATCCCATCTTAGCGGCCGCGTGGGGGTGGAGGTAGAG	60
hBgG-iv	ACGCTGTCAGGACGCAGCAATGAAAATAAATGTTTTTTTATTAGG	69
hBgB-i	GATCAATGTGTAAGGATCCGATGAGAGCTCGCTTTCTTG	54
hBgB-ii	TTGCTGCGTCTGCCCGTCCTCACCAAG	65
hBgB-iii	TTGCCGTATCCCATCTTAGCGGCCGCGGTCACACCGGCAATGG	65
hBgB-iv	AGGACGGGCAGACGCAGCAATGAAAATAAATGTTTTTTTATTAGG	69
hBgD-i	GATCAATGTGTAAGGATCCGATGAGAGCTCGCTTTCTTG	54
hBgD-ii	TTGCTGCGTCTTCCAGCCAGACACCCGC	68
hBgD-iii	TTGCCGTATCCCATCTTAGCGGCCGCGGGGTCAGAGAGTGGAAG	58
hBgD-iv	CTGGCTGGAAGACGCAGCAATGAAAATAAATGTTTTTTTATTAGG	69
hBgJ-i	GATCAATGTGTAAGGATCCGATGAGAGCTCGCTTTCTTG	54
hBgJ-ii	TTGCTGCGTCCTTTGCAGGATGAAACACTTC	60
hBgJ-iii	TTGCCGTATCCCATCTTAGCGGCCGCGGAGGAGTACAGATGCATG	56
hBgJ-iv	TCCTGCAAAGGACGCAGCAATGAAAATAAATGTTTTTTTATTAGG	69
hBgE-i	GATCAATGTGTAAGGATCCGATGAGAGCTCGCTTTCTTG	54
hBgE-ii	TTGCTGCGTCGCCTTGGCTCCTCCAGG	64
hBgE-iii	TTGCCGTATCCCATCTTAGCGGCCGCGGGGGGGAGATGGCAGTG	65
hBgE-iv	GAGCCAAGGCGACGCAGCAATGAAAATAAATGTTTTTTTATTAGG	69
hBgF-i	GATCAATGTGTAAGGATCCGATGAGAGCTCGCTTTCTTG	54
hBgF-ii	TTGCTGCGTCCTGGTACTGCATGCACGC	63
hBgF-iii	TTGCCGTATCCCATCTTAGCGGCCGCGGAGGTGTCTGGAACTAG	53
hBgF-iv	GCAGTACCAGGACGCAGCAATGAAAATAAATGTTTTTTTATTAGG	69

Functional analysis of selected 3′ UTRs in other cell types/lines

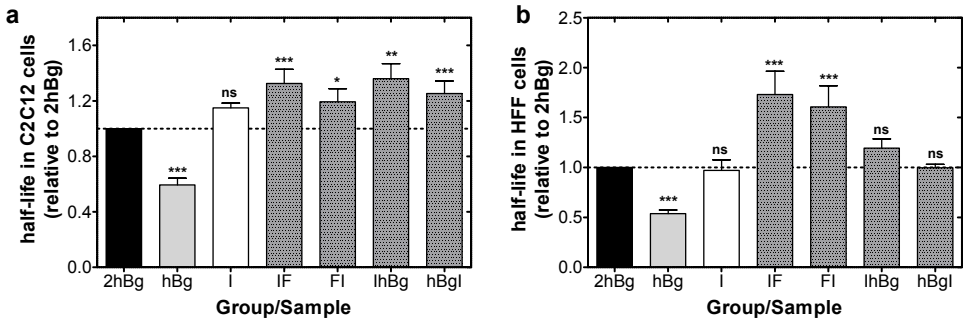

Figure A.1: RNA turnover with newly selected 3′ UTRs in (a) C2C12 and (b) HFF cells . Sequences were cloned as 3′ UTRs with luc2CPmut as reporter gene. Luciferase activity was measured over 72 h and half-life was calculated using R. Shown are results relative to internal reference 2hBg. Values are mean±SD of three independent experiments. (a, b) One-way ANOVA, Dunnett post-test, ***: $p<0.001$, **: $p<0.01$, *: $p<0.05$, ns: not significant ($p>0.05$).

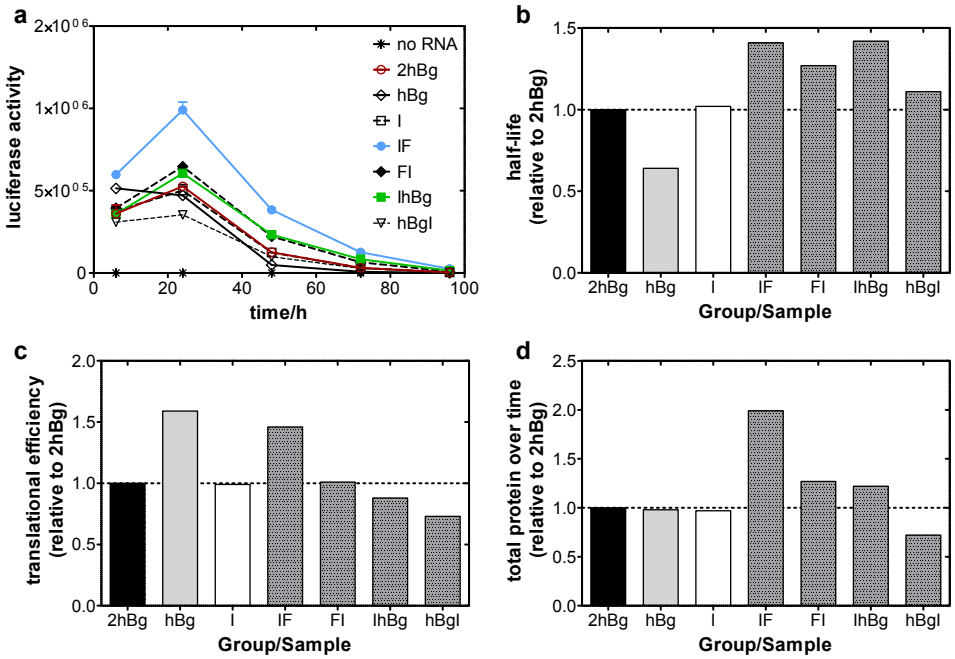

Figure A.2: RNA turnover with newly selected 3′ UTR in C2C12 cells. Sequences were cloned as 3′ UTRs with luc2mut as reporter gene. (a) Luciferase activity was measured over 96 h and (b) half-life, (c) translational efficiency and (d) total protein over time were calculated using R. Shown are results relative to internal reference 2hBg. (a) Representative curve diagram. Values are mean±SD of three measured samples.

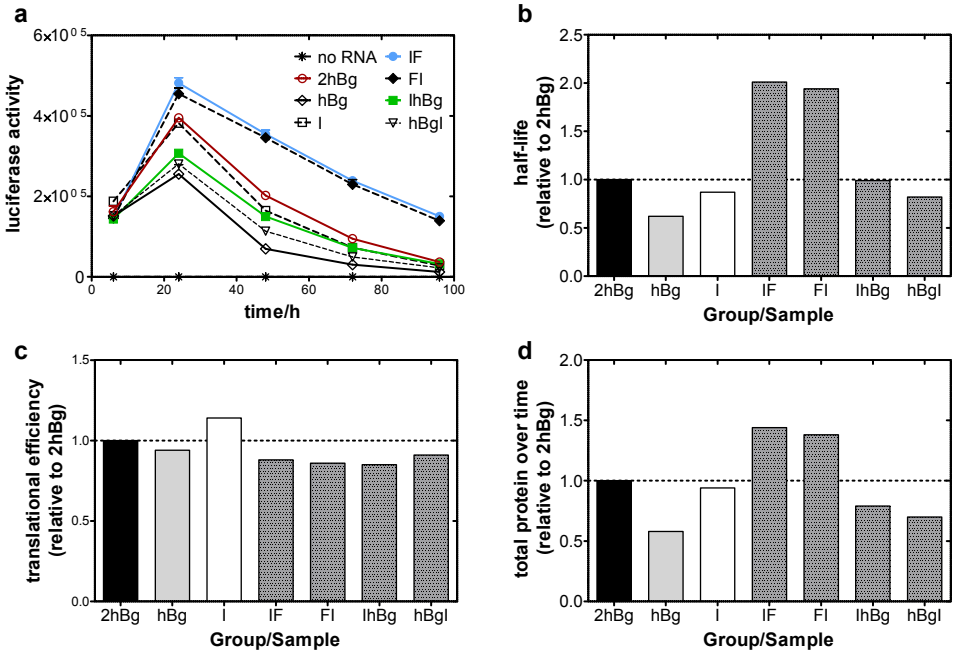

Figure A.3: RNA turnover with newly selected 3′ UTR in HFF cells. Sequences were cloned as 3′ UTRs with luc2mut as reporter gene. (a) Luciferase activity was measured over 96 h and (b) half-life, (c) translational efficiency and (d) total protein over time were calculated using R. Shown are results relative to internal reference 2hBg. (a) Representative curve diagram. Values are mean±SD of three measured samples.

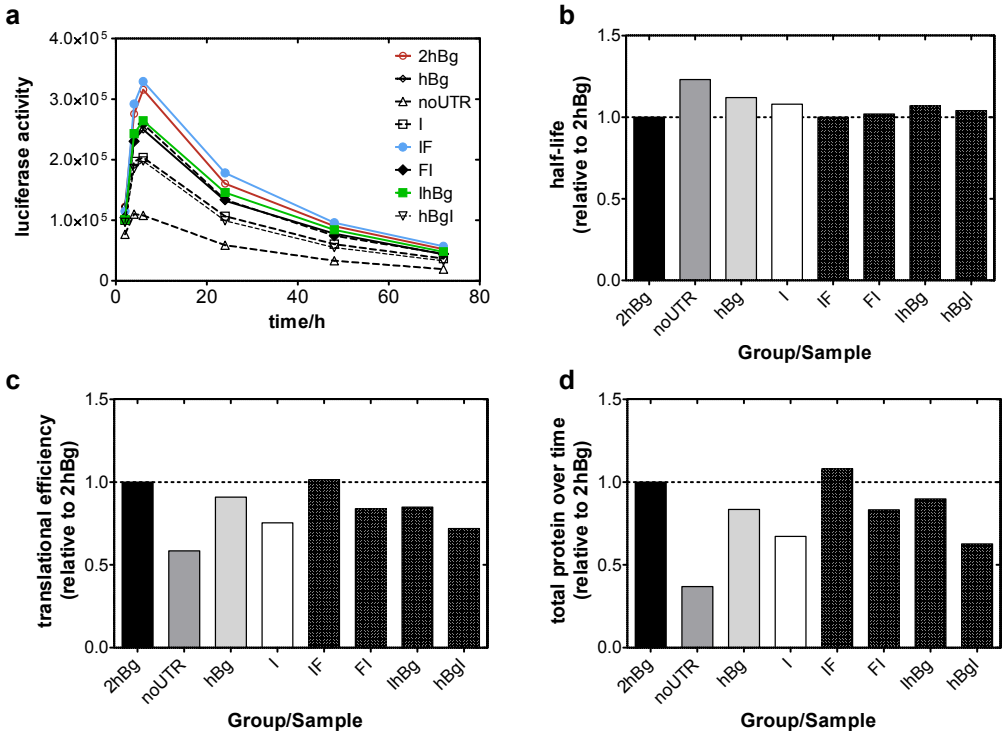

Figure A.4: RNA turnover with newly selected 3′ UTR in CD4$^+$ T cells. Sequences were cloned as 3′ UTRs with luc2mut as reporter gene. (a) Luciferase activity was measured over 72 h and (b) half-life, (c) translational efficiency and (d) total protein over time were calculated using R. Shown are results relative to internal reference 2hBg.

Used miRNA-sets and overview of results

Table A.2: miRNA-set used for prediction of RNA-RNA-interactions in unstimulated DCs combined from published data of Hashimi *et al.*[244] (▲) and Landgraf *et al.*[245] (✱).

miRNA	Sequence	copy number in hiDCs✱	p-value▲
hsa-let-7e	UGAGGUAGGAGGUUGUAUAGUU	0.833333	3.66109E-05
hsa-miR-17	CAAAGUGCUUACAGUGCAGGUAG	1	6.89538E-05
hsa-miR-21	UAGCUUAUCAGACUGAUGUUGA	1	0.000260416
hsa-miR-23b	AUCACAUUGCCAGGGAUUACC	1	0.103849766
hsa-miR-342-5p	5p AGGGGUGCUAUCUGUGAUUGA	1	-
hsa-let-7c	UGAGGUAGUAGGUUGUAUGGUU	1.5	0.055963737
hsa-miR-146a	UGAGAACUGAAUUCCAUGGGUU	2	0.009859239
hsa-miR-181a	AACAUUCAACGCUGUCGGUGAGU	2	0.375675915
hsa-miR-20a	UAAAGUGCUUAUAGUGCAGGUAG	2	0.001622631
hsa-miR-25	CAUUGCACUUGUCUCGGUCUGA	2	0.002523184
hsa-miR-93	CAAAGUGCUGUUCGUGCAGGUAG	2	7.81053E-05
hsa-miR-99b	CACCCGUAGAACCGACCUUGCG	2	4.6509E-06
hsa-miR-15b	UAGCAGCACAUCAUGGUUUACA	2.5	0.006058702
hsa-let-7i	UGAGGUAGUAGUUUGUGCUGUU	3	0.773660714
hsa-miR-103	AGCAGCAUUGUACAGGGCUAUGA	3	0.007731157
hsa-miR-132	UAACAGUCUACAGCCAUGGUCG	3	2.54555E-06
hsa-miR-155	UUAAUGCUAAUCGUGAUAGGGGU	3	0.000885463
hsa-miR-26a	UUCAAGUAAUCCAGGAUAGGCU	3	0.121488173
hsa-let-7d	AGAGGUAGUAGGUUGCAUAGUU	4	0.213855395
hsa-miR-19b	UGUGCAAAUCCAUGCAAAACUGA	4	0.025850685
hsa-miR-221	AGCUACAUUGUCUGCUGGGUUUC	4	0.707236332
hsa-miR-27b	UUCACAGUGGCUAAGUUCUGC	4	0.067998519
hsa-miR-34a	UGGCAGUGUCUUAGCUGGUUGU	4	4.79253E-05
hsa-miR-26b	UUCAAGUAAUUCAGGAUAGGU	6	0.702545063
hsa-miR-30b	UGUAAACAUCCUACACUCAGCU	6	0.07528109
hsa-miR-30c	UGUAAACAUCCUACACUCUCAGC	6	0.002152826
hsa-let-7g	UGAGGUAGUAGUUUGUACAGUU	7	0.457951639
hsa-miR-185	UGGAGAGAAAGGCAGUUCCUGA	7	0.081571637
hsa-miR-223	UGUCAGUUUGUCAAAUACCCCA	7	0.000312684
hsa-miR-342-3p	3p UCUCACACAGAAAUCGCACCCGU	9	0.004506455
hsa-miR-191	CAACGGAAUCCCAAAAGCAGCUG	10	0.045215458
hsa-miR-29a	UAGCACCAUCUGAAAUCGGUUA	11	0.023790499
hsa-miR-23a	AUCACAUUGCCAGGGAUUUCC	13	0.108114817
hsa-let-7b	UGAGGUAGUAGGUUGUGUGGUU	13.5	0.02689751
hsa-miR-30d	UGUAAACAUCCCCGACUGGAAG	14	0.556712511
hsa-miR-22	AAGCUGCCAGUUGAAGAACUGU	15	0.10719741
hsa-let-7f	UGAGGUAGUAGAUUGUAUAGUU	19.3333	0.658970893
hsa-let-7a	UGAGGUAGUAGGUUGUAUAGUU	19.8333	0.224037044
hsa-miR-24	UGGCUCAGUUCAGCAGGAACAG	24	0.029071151
hsa-miR-27a	UUCACAGUGGCUAAGUUCCGC	30	0.124546131
hsa-miR-15a	UAGCAGCACAUAAUGGUUUGUG	30,5	0.045513997
hsa-miR-142	5p CAUAAAGUAGAAAGCACUACU	95	0.039618335
hsa-miR-16	UAGCAGCACGUAAAUAUUGGCG	124	0.004524336

Table A.3: miRNA-set used for prediction of RNA-RNA-interactions in LPS-stimulated DCs combined from published data of Hashimi *et al.*[244] (▲) and Landgraf *et al.*[245] (❋).

miRNA	Sequence	copy number in hiDCs❋	p-value▲
hsa-let-7d	AGAGGUAGUAGGUUGCAUAGUU	1	0.213855395
hsa-let-7e	UGAGGUAGGAGGUUGUAUAGUU	1	3.66109E-05
hsa-miR-103	AGCAGCAUUGUACAGGGCUAUGA	1	0.007731157
hsa-miR-221	AGCUACAUUGUCUGCUGGGUUUC	1	0.707236332
hsa-miR-23b	AUCACAUUGCCAGGGAUUACC	1	0.103849766
hsa-miR-30b	UGUAAACAUCCUACACUCAGCU	1	0.07528109
hsa-miR-20a	UAAAGUGCUUAUAGUGCAGGUAG	2	0.001622631
hsa-miR-222	AGCUACAUCUGGCUACUGGGU	2	0.673845972
hsa-miR-30c	UGUAAACAUCCUACACUCUCAGC	2	0.002152826
hsa-miR-342	3p UCUCACACAGAAAUCGCACCCGU	2	0.004506455
hsa-miR-34a	UGGCAGUGUCUUAGCUGGUUGU	2	4.79253E-05
hsa-miR-92a	UAUUGCACUUGUCCCGGCCUGU	2	0.005275565
hsa-miR-342	5p AGGGGUGCUAUCUGUGAUUGA	2	0.004506455
hsa-let-7c	UGAGGUAGUAGGUUGUAUGGUU	2.5	0.055963737
hsa-miR-27b	UUCACAGUGGCUAAGUUCUGC	2.5	0.067998519
hsa-let-7g	UGAGGUAGUAGUUUGUACAGUU	3	0.457951639
hsa-miR-15b	UAGCAGCACAUCAUGGUUUACA	3	0.006058702
hsa-miR-25	CAUUGCACUUGUCUCGGUCUGA	3	0.002523184
hsa-miR-99b	CACCCGUAGAACCGACCUUGCG	3	4.6509E-06
hsa-miR-132	UAACAGUCUACAGCCAUGGUCG	4	2.54555E-06
hsa-miR-21	UAGCUUAUCAGACUGAUGUUGA	4	0.000260416
hsa-miR-185	UGGAGAGAAAGGCAGUUCCUGA	5	0.081571637
hsa-miR-21	UAGCUUAUCAGACUGAUGUUGA	4	0.000260416
hsa-miR-320	AAAAGCUGGGUUGAGAGGGCGA	5	0.016880854
hsa-miR-93	CAAAGUGCUGUUCGUGCAGGUAG	5	7.81053E-05
hsa-miR-155	UUAAUGCUAAUCGUGAUAGGGGU	7	0.000885463
hsa-miR-29a	UAGCACCAUCUGAAAUCGGUUA	7	0.023790499
hsa-miR-423	5p UGAGGGGCAGAGAGCGAGACUUU	8	0.072396595
hsa-miR-423	3p AGCUCGGUCUGAGGCCCCUCAGU	8	0.072396595
hsa-miR-26a	UUCAAGUAAUCCAGGAUAGGCU	8.5	0.121488173
hsa-miR-26b	UUCAAGUAAUUCAGGAUAGGU	9.5	0.702545063
hsa-let-7i	UGAGGUAGUAGUUUGUGCUGUU	11	0.773660714
hsa-miR-181a	AACAUUCAACGCUGUCGGUGAGU	13	0.375675915
hsa-miR-23a	AUCACAUUGCCAGGGAUUUCC	14	0.108114817
hsa-miR-223	UGUCAGUUUGUCAAAUACCCCA	16	0.000312684
hsa-miR-191	CAACGGAAUCCCAAAAGCAGCUG	17	0.045215458
hsa-miR-30e	UGUAAACAUCCUUGACUGGAAG	17	0.065812991
hsa-let-7b	UGAGGUAGUAGGUUGUGUGGUU	18	0.02689751
hsa-miR-146a	UGAGAACUGAAUUCCAUGGGUU	18	0.009859239
hsa-let-7f	UGAGGUAGUAGAUUGUAUAGUU	19	0.658970893
hsa-miR-30d	UGUAAACAUCCCCGACUGGAAG	20	0.556712511
hsa-miR-21	CAACACCAGUCGAUGGGCUGU	4	0.000260416
hsa-miR-22	AAGCUGCCAGUUGAAGAACUGU	43	0.10719741
hsa-miR-24	UGGCUCAGUUCAGCAGGAACAG	50	0.029071151
hsa-miR-27a	UUCACAGUGGCUAAGUUCCGC	67.5	0.124546131
hsa-miR-15a	UAGCAGCACAUAAUGGUUUGUG	75	0.045513997
hsa-miR-16	UAGCAGCACGUAAAUAUUGGCG	108	0.004524336
hsa-miR-142	5p CAUAAAGUAGAAAGCACUACU	153	0.039618335

Table A.4: Overview of miRNAs which bind to 3′ UTRs in unstimulated DCs. Shown are miRNAs, which bind to different 3′ UTRs and their respective hybridization energies (kcal/mol). Dark red: low energy; dark blue: high energy.

Group	3'-UTR	hsa-let-7a	hsa-let-7b	hsa-let-7c	hsa-let-7d	hsa-let-7e	hsa-let-7f	hsa-let-7g	hsa-let-7i	hsa-miR-103	hsa-miR-132	hsa-miR-142	hsa-miR-146a	hsa-miR-155	hsa-miR-15a	hsa-miR-15b	hsa-miR-16	hsa-miR-17	hsa-miR-181a	hsa-miR-185	hsa-miR-191	hsa-miR-19b	hsa-miR-20a	hsa-miR-21	hsa-miR-22	hsa-miR-221	hsa-miR-223	hsa-miR-23a	hsa-miR-23b	hsa-miR-24	hsa-miR-25	hsa-miR-26a	hsa-miR-26b	hsa-miR-27a	hsa-miR-27b	hsa-miR-29a	hsa-miR-30c	hsa-miR-30d	hsa-miR-342-3p	hsa-miR-342-5p	hsa-miR-34a	hsa-miR-93	hsa-miR-99b
	B	-21,6	-18,5	-17,4	-19,7	-19,1	-14,8	-19	-16,5	-13,4		-11,3	-12		-12,3	-14	-17,4	-14,1	-13,8	-16,9	-11,8		-14,1		-11,8	-13,5	-1,5	-16,8	-18	-18,6	-9,1				-16,1	-16,1				-11,2	-6,7	-21,4	-14,1	
	BB	-22,3	-2,9	-21	-2,4	-19,2	-16,2	-19,3	-16	-14,9		-11,4	-12		-12,3	-14	-17,4	-14,1	-11,9	-16,9	-11,8		-14,1		-11,8	-13,5	-1,5	-16,8	-18	-2,3	-12,4				-16,1	-16,1				-13,3	-6,8	-19,7	-16,3	
	BD	-22,3	-25,1	-22,5	-16,7	-17,5	-16,2	-18,2	-2,6	-13,4		-11,3	-12	-14,9	-1,4	-14,4	-17,4	-16,3	-8,9	-14,7	-12,5		-14,1	-5,1	-7,7	-13,5	-1,5	-16,8	-18	-17,8	-9,1	-13	-1,3	-14,8	-15,5			-1,7	-11,9	-8,9	-19,7	-16,3	
	BE	-22,3	-21	-21	-2,4	-19,8	-16,2	-19,3	-16	-16,7	-14,9	-11,4	-12	-13,3	-17,9	-14,4	-16,1	-16,3	-11,1	-2,1	-11,8		-14,1		-1,3	-13,5	-1,5	-16,8	-18	-2,3	-12,4	-12,5			-14,8	-15,5				-11,9	-17,3	-22,6	-16,3	
B	BF	-22,3	-21	-21	-2,4	-19,2	-16,2	-18,5	-15,7	-13,4		-11,4	-12	-8,2	-12,3	-14	-17,4	-16,3	-12	-17,5	-12,5		-14,1		-11,8	-13,5	-1,5	-15,3	-15,3	-18,6	-13,6	-16,8	-14,2	-16,1	-15,5				-15	-13,5	-19	-16,3	
	BG	-21,6	-18,5	-18,2	-16,4	-16,2	-11,9	-19	-14,4	-13,4	-9,6	-11,3	-12	-11,8	-12,3	-14	-17,4	-14,1	-13,3	-11,7	-11,8		-14,1		-11,8	-13,8	-1,5	-16,8	-18	-18,6	-18,7	-11,1	-11,3	-16,1	-15,5				-14,4	-16	-19,8	-14,1	
	BhBg	-22,3	-21	-21	-2,4	-19,8	-16,3	-18,5	-15,7	-14,9		-12	-12	-6,9	-12	-14,1	-16,1	-16,3	-11,2	-16,9	-12,5		-14,1			-13,5	-1,5	-16,8	-18	-19,5	-14	-1,4	-7,7	-14,8	-15,5	-8,6			-11,9	-9,7	-19	-16,3	
	BI	-21,6	-18,5	-17,4	-19,7	-19,1	-14,8	-19	-15,7	-13,4		-11,3	-12	-7,2	-12	-14	-17,4	-14,1	-8,9	-16,9	-11,8		-14,1	-7,3	-1	-12	-1,5	-16,6	-17,2	-18,6	-9,1			-16,1	-17				-11,9	-6,7	-19,8	-14,1	-15
	BJ	-22,3	-18,6	-19,6	-2,4	-22,2	-15,6	-19,3	-17	-13,1	-13,9	-11,3	-12	-1,9	-12,3	-14,4	-17,4	-16,3	-13,3	-16,9	-12,5	-8,4	-14,1	-7,1	-13,6	-13	-1,5	-16,8	-18	-18,6	-9,1	-11,1	-9	-14,8	-15,5	-8,3		-6,8	-11,9	-22,8	-21,4	-16,3	-3,7
	D	-17,1	-25,1	-22,5	-16,7	-17,5	-8,4	-7,9	-2,6	-21,8		-4,5		-14,2						-15,5	-13,4			-5,1	-7,7		-3,7	-15,7	-15,7	-17,4		-13	-1,3	-14,6	-11,5				-8,9	-17,3		
	DB	-21,6	-25,1	-22,5	-19,7	-19,2	-16,2	-19,3	-2,6	-13,4		-11,3	-12	-14,2	-12,3	-14	-17,4	-14,1	-1,8	-14,7	-11,8		-14,1	-5,1	-7,7	-13,5	-1,5	-15,7	-18	-19,4	-12,4	-13	-1,3	-16,1	-16,1				-11,2	-8,9	-19,8	-16,3	
	DD	-17,1	-25,1	-22,5	-16,7	-17,5	-9,5	-9,4	-2,6	-21,8		-4,5		-14,2						-14,7	-13,4			-5,1	-7,7		-3,7	-15,7	-15,7	-17,4		-13	-1,3	-14,6	-11,5			-1		-8,9	-16,1		
	DE	-17,4	-25,1	-22,5	-16,7	-17,2	-11	-11	-2,6	-16,7	-14,9		-11,1	-14,2	-17,9	-11,8	-15,5	-12,1		-2,1	-11,8		-12,4	-5,1	-8,3	-11,1	-5,8	-15,7	-15,7	-17,4		-12,5	-1,3	-12,2	-12,2				-17,3	-22,6	-14,3	
D	DF	-17,1	-25,1	-22,5	-16,7	-17,5	-11,7	-9,4	-2,6	-21,8		-4,5		-14,2			-5,2		-12	-17,5	-13,4			-5,1	-7,7	-7,6	-5,8	-15,1	-15,1	-17,4		-16,8	-14,2	-14,6	-11,5				-13,5	-15,4	-13	
	DG	-16,2	-25,1	-22,5	-16,4	-17,5	-11,9	-14,1	-2,6	-21,8	-9,6	-4,5		-14,2	-14,1			-15,9	-17,3	-14,7	-13,4		-14,7	-5,1	-6,7	-13,8	-8,3	-15,7	-15,7	-17,4	-18,7	-13	-11,3	-14,6	-11,5				-16	-17,3	-11,7	
	DhBg	-17,1	-25,1	-22,5	-16,7	-17,5	-9,6	-1,3	-2,6	-21,8		-9,3		-14,2		-4,6		-1,9	-11,2	-14,7	-1		-1,9	-5,1	-7,7	-3,1	-5,8	-15,7	-15,7	-17,4		-13	-7,7	-14,6	-11,5	-9,8			-8,9	-16,1		
	DI	-17,1	-25,1	-22,5	-16,7	-17,5	-8,4	-7,9	-2,6	-21,8		-4,5		-14,2	-5,8	-6				-15,5	-13,4			-7,3	-1	-12	-3,7	-15,7	-15,7	-17,4		-13	-1,3	-16,1	-17				-8,9	-17,3	-17,2	-15
	DJ	-17,1	-25,1	-19,6	-16,7	-22,2	-11,9	-13,3	-2,6	-18,5	-13,9	-4,5	-15,2	-14,2	-9,6	-9,6	-9,6	-1,9	-13,3	-14,7	-13,4	-8,4	-1,8	-7,1	-7,7	-13	-3,7	-16,9	-15,7	-17,4		-13	-1,3	-14,6	-11,5	-8,3		-6,8	-6,5	-22,8	-17,3	-1,4	-3,7
	E	-13,9	-13,9	-13,9	-14,1	-14,8	-11	-11	-1,4	-16,7	-14,9		-11,1	-14,1	-17,9	-12,9	-13,4	-12,1		-2,1	-11,8		-12,4			-13,5		-13	-13			-12,5		-12,2	-12,2				-17,3	-22,6	-14,3	
	EB	-21,6	-21	-18,3	-17,7	-19,2	-16,2	-19,3	-16	-16,7	-14,9	-11,3	-11,1	-14,1	-17,9	-14	-17,4	-14,1	-1,8	-2,1	-11,8		-14,1		-11,8	-13,5	-1,5	-13	-13	-19,4	-12,4	-12,5		-16,1	-16,1				-11,2	-17,3	-22,6	-14,1	
	ED	-17,1	-25,1	-22,5	-16,7	-17,5	-11	-11	-2,6	-16,7	-14,9	-4,5	-11,1	-13,3	-17,9	-12,9	-13,4	-12,1		-2,1	-11,8		-12,4	-5,1	-8,3	-13,5	-5,8	-13	-13	-13,4		-12,5	-1,3	-14,6	-11,5			-1,7		-17,3	-22,6	-14,3	
	EE	-13,9	-13,9	-13,9	-14,1	-14,5	-11	-11	-1,4	-16,7	-14,9		-11,1	-13,3	-17,9	-12,9	-15,5	-12,1		-2,1	-11,8		-12,4			-13,5		-13	-13			-12,5		-12,2	-12,2				-17,3	-22,6	-14,3	
E	EF	-13,9	-16,5	-13,9	-14,1	-14,5	-11	-11	-1,4	-16,7	-14,9		-11,1	-13,3	-17,9	-12,9	-15,5	-12,1	-12	-17,5	-11,8		-12,4			-11,1		-15,1	-15,1			-16,8	-14,2	-12,2	-12,2				-17,3	-22,6	-14,3	
	EG	-16,2	-18,3	-18,2	-16,4	-16,2	-11,9	-14,1	-14,4	-16,7	-14,6		-11,1	-13,3	-17,9	-12,9	-13,4	-12,1	-17,3	-2,1	-11,8	-11,2	-12,4			-17,6		-13	-13	-17,6	-18,7	-12,5	-11,3	-12,2	-12,2				-17,3	-22,6	-14,3	
	EhBg	-13,9	-13,9	-13,9	-14,1	-14,5	-11	-11	-1,4	-16,7	-14,9	-12	-11,1	-13,3	-17,9	-12,1	-15,5	-12,1	-11,2	-2,1	-11,8		-12,4			-11,1	-6,7	-13	-13	-14,4		-12,5	-7,7	-12,2	-12,2				-17,3	-22,6	-14,3	
	EI	-13,9	-13,9	-13,9	-14,1	-14,8	-11	-11	-15,7	-16,7	-15		-11,1	-13,6	-17,9	-12,9	-15,5	-12,1		-2,1	-11,8		-12,4	-7,3	-1	-12		-13	-13			-12,5		-16,1	-17				-17,3	-22,6	-14,3	-15
	EJ	-15,4	-18,6	-19,6	-18,2	-22,2	-11,9	-13,3	-1,4	-16,7	-14,9		-11,1	-13,3	-17,9	-12,9	-15,5	-1,9	-13,3	-2,1	-11,8	-8,4	-12,4	-7,1	-13,6	-13	-4,9	-16,9	-13	-11,1		-12,5	-9	-18,5	-12,2	-8,3		-6,8	-6,5	-17,3	-22,6	-14,3	-3,7
	F	-1,8	-16,5	-13	-11	-9,5	-11,7			-16,8				-8,2			-5,2		-12	-17,5	-12,5									-7,2				-16,8	-14,2	-8,3	-12,8				-13,5	-14,8	-13	
	FB	-21,6	-21	-18,3	-17,7	-19,8	-16,2	-19	-16	-13,4		-11,3	-12	-8,2	-12,3	-14	-17,4	-14,1	-12	-17,5	-11,8		-14,1		-11,8	-13,5	-1,5	-16,8	-18	-19,4	-12,4	-16,8	-14,2	-16,1	-16,1				-11,2	-13,5	-19,3	-14,1	
	FD	-17,1	-25,1	-22,5	-16,7	-17,5	-1,9	-9,4	-2,6	-16,8		-4,5		-14,3			-5,2		-12	-17,5	-12,5			-5,1	-8,3		-5,8	-15,7	-15,7	-17,4		-13	-1,3	-14,6	-11,5			-1,7		-12,8	-16,1	-13	
	FE	-13,9	-19,2	-13,5	-14,1	-14,5	-11,7	-11	-1,4	-16,7	-14,9		-11,1	-13,3	-17,9	-11,8	-15,5	-12,1	-12	-17,5	-11,8		-12			-11,1		-13,2	-13,2			-12,5	-14,2	-12,2	-12,2				-17,9	-22,6	-14,3	
F	FF	-1,8	-16,5	-13	-11	-11,8	-11,7			-16,8				-8,2			-5,2		-12	-17,5	-1,5							-16,3	-16,3			-16,8	-14,2	-8,3	-12,8				-13,5	-14,8	-13	
	FG	-16,2	-18,3	-18,2	-16,4	-16,2	-11,9	-14,1	-14,4	-16,8	-9,6			-11,8	-14,1		-5,2	-16,3	-21,3	-17,5	-12,5	-11,2	-15,1			-1,2		-11	-12,4	-17,6	-18,7	-11,1	-11,3	-11,8	-12,8				-16	-14,8	-14,1	
	FhBg	-1,2	-16,5	-13	-9,8	-12,1	-11,7	-1,3	-1,3	-16,8		-9,3		-8,2		-4,6	-5,2	-1,9	-12	-17,3	-12,5		-1,9			-3,1	-6,7	-3,7	-7,2	-14,4		-16,8	-7,7	-8,3	-12,8				-12,8	-14,8	-13	
	FI	-12,5	-16,5	-13	-11	-16,2	-11,7	-7,9	-15,7	-16,8				-8,2	-5,8	-6	-5,2		-12	-17,5	-12,5			-7,3	-1	-12		-13,2	-7,2			-16,8	-14,2	-16,1	-17				-12,8	-17,2	-17,2	-15
	FJ	-15,4	-18,6	-19,6	-18,2	-22,2	-11,9	-13,3	-1,4	-18,5	-13,9		-15,2	-1,9	-9,6	-9,6	-9,6	-1,9	-12	-17,5	-12,5	-8,4	-1,8	-7,1	-13,6	-13	-4,9	-16,9	-9	-11,1		-16,8	-14,2	-18,5	-12,8	-8,3		-6,5	-22,8	-16,8	-1,4	-3,7
	G	-16,2	-18,3	-18,2	-16,4	-16,2	-11,9	-14,1	-14,4	-9,2	-9,6			-11,8	-14,1			-12,4	-17	-11,7			-7,7			-1,2		-11	-12,4	-17,6	-18,7	-11,1	-11,3	-11,8	-11,8				-16	-7,2	-7,7	
	GB	-21,6	-21	-18,2	-16,4	-16,2	-16,2	-19,3	-14,4	-17,8	-9,6	-11,3	-12	-11,8	-12,3	-14	-17,4	-14,1	-17	-16,9	-11,8		-14,1		-11,8	-13,8	-1,5	-16,8	-18	-19,4	-18,7	-11,1	-11,3	-16,1	-16,1				-11,2	-16	-14,9	-14,1	
	GD	-16,2	-25,1	-22,5	-17,5	-17,5	-11,9	-14,4	-2,6	-14,5	-9,6	-4,5		-14,3	-14,4			-7,7	-17	-14,7	-13,4	-11,2	-7,7	-5,1	-7,7	-1,2	-3,7	-11	-12,4	-18,2	-18,5	-13	-11,3	-14,6	-11,5			-1,2		-16	-17,3	-7,7	
	GE	-16,9	-18,6	-18,2	-17,5	-16,9	-11,9	-14,4	-14,4	-16,7	-14,9		-11,1	-11,8	-17,9	-11,8	-15,5	-12,1	-17	-2,1	-11,8	-11,2	-12,4			-1,2		-13,2	-13,2	-17,6	-18,5	-11,1	-11,3	-12,2	-12,2				-2,5	-22,6	-14,3	
G	GF	-16,9	-18,6	-18,2	-17,5	-16,9	-11,9	-14,4	-14,4	-14,6	-9,6			-11,8	-14,4		-5,2	-7,7	-17	-17,5	-12,5	-11,2	-7,7			-1,2		-12,2	-12,4	-17,6	-18,7	-16,8	-11,3	-12,1	-12,8				-16	-14,8	-14,4	
	GG	-16,2	-18,6	-18,2	-16,4	-16,2	-12,2	-14,4	-14,4	-9,2	-9,6			-11,8	-14,1			-17,7	-2,5	-11,7			-16,5			-17,5		-11	-12,4	-17,6	-18,7	-11,1	-11,3	-11,8	-11,8				-16	-7,2	-16,9	
	GhBg	-16,2	-18,6	-18,2	-16,4	-16,2	-12,2	-14,4	-14,4	-9,3	-9,6	-12		-11,8	-14,4	-4,8		-7,7	-17	-11,7	-11,2	-11,2	-7,7			-1,2	-6,7	-11	-12,4	-14,4	-18,7	-11,1	-11,3	-12,1	-12,1				-16	-1,3	-7,7	
	GI	-16,2	-18,6	-18,2	-17,5	-16,2	-12,2	-14,4	-15,7	-12,2	-9,6			-11,8	-14,1	-6		-12,3	-17	-11,7	-5		-7,7	-7,3	-1	-12		-11	-12,4	-17,6	-18,7	-11,1	-11,3	-16,1	-17				-16	-7,2	-17,2	-15
	GJ	-16,2	-18,6	-19,6	-16,4	-22,2	-12,2	-12,4	-12,6	-18,5	-13,9		-15,2	-11,8	-14,4	-13,2	-9,6	-1,9	-17	-1,9	-13	-8,4	-1,8	-7,1	-13,6	-13	-4,9	-16,9	-12,4	-11,1	-18,7	-11,1	-11,3	-18,5	-16,3	-8,3		-6,8	-6,5	-16	-7,2	-1,4	-3,7
	hBg	-9,3	-9,3	-9,3	-9,5	-12,3	-9,3	-3	-11	-16,6		-9,3		-6,1			-4,6	-1,9	-11,4	-6,7	-12,8		-1,9				-6,7	-3,7	-4,3	-12,1		-13	-8,2	-8,4	-8,4		-9,8			-9,7	-1,3		
	hBgB	-21,6	-21	-2,3	-19,7	-19,2	-16,2	-19	-16,5	-13,4		-11,3	-11,3	-7	-12,3	-14	-17,4	-16,3	-11,2	-16,9	-11,8		-14,1		-11,8	-13,5	-1,5	-16,8	-18	-19,4	-12,4	-13	-7,7	-16,1	-16,1			-9,8	-11,2	-9,7	-21,4	-16,3	
	hBgD	-17,1	-25,1	-22,5	-16,7	-17,5	-1,8	-1,1	-2,6	-21,4		-12		-14,9	-4,8	-4,8		-1,8	-11,1	-14,6	-13,1		-1,8	-5,1	-7,7	-2,9	-3,7	-15,7	-15,7	-17,4		-13	-1,3	-14,6	-11,5	-9,8	-9,8		-8,9	-16,1		
	hBgE	-13,9	-13,5	-13,5	-14,1	-14,5	-11	-12	-1,4	-17	-14,9	-12	-11,1	-13,3	-17,9	-11,8	-15,5	-12,1	-11,2	-2,1	-11,8		-12,4			-8,1	-7,1	-11	-11	-14,4	-7,1	-12,5	-2,7	-12,2	-12,2		-9,8			-17,9	-22,6	-14,3	
hBg	hBgF	-11,2	-16,5	-13	-13,6	-1,9	-11,7	-8,4	-11	-13,7		-9,3		-8,2	-4,8	-5,8	-7,1	-1,8	-12	-17,5	-12,5		-1,8	-3,7		-7,3	-7	-11,7	-11,7	-14,4	-7,1	-16,7	-14,1	-8,3	-8,3		-9,8			-12,8	-14,8	-1,7	
	hBgG	-16,2	-18,3	-18,2	-16,4	-16,2	-11,9	-14,1	-14,4	-16,6	-9,6	-9,3		-11,8	-14,1	-7,1		-12,4	-17	-11,7	-12,8	-11,2	-11,5	-9		-1,2	-6,6	-11	-12,4	-14,4	-18,7	-13	-11,3	-11,8	-11,8		-9,8			-16	-11,5	-14,9	
	hBghBg	-11,2	-14,9	-11,2	-13,6	-12,1	-9,6	-1,3	-1,3	-12,8		-12		-6,1	-4,5	-4,6		-1,8	-11,2	-15,6	-11,2		-1,8			-5,2	-7	-3,7	-4,3	-14,4	-7,1	-13	-7,7	-8,7	-9,9		-9,8			-9,7	-15		
	hBgI	-12,5	-15,2	-12,4	-13,3	-16,2	-1,1	-8,4	-15,7	-17,5		-9,3		-11	-4,8	-5,8		-1,9	-11,4	-6,7	-12,4		-11,7	-9,4	-1	-11,5	-6,6	-3,7	-4,3	-12,1	-7,1	-13	-8,2	-16,1	-17		-9,8			-9,7	-11,5	-17,2	-15
	hBgJ	-15,4	-18,6	-19,6	-18,2	-22,2	-11,9	-13,3	-1,4	-13,1	-13,9	-9,3	-8,4	-1,9	-15	-13,2	-9,6	-1,9	-8,5	-11,9	-11,2	-8,4	-1,8	-7,1	-13,6	-13	-6,7	-16,9	-9	-11,1	-7,1	-15,5	-8,2	-18,2	-16	-8,3	-9,8	-6,8	-6,5	-22,8	-15	-1,4	-3,7
	I	-12,5	-18,2	-12,2	-1,2	-16,2	-8	-7,9	-15,7	-16				-7,2	-5,8	-6				-5				-7,3	-1	-12								-13,8	-17					-1,7		-17,2	-15
	IB	-21,6	-21	-18,3	-17,7	-19,2	-14,8	-19,3	-15,7	-13,4		-11,3	-12	-7,2	-12,3	-14	-17,4	-14,1	-1,8	-16,9	-11,8		-14,1	-7,3	-1	-12	-1,5	-16,8	-18	-19,4	-12,4			-16,1	-16,1				-11,2	-6,8	-19,8	-14,1	-14,9
	ID	-17,1	-25,1	-22,5	-16,5	-17,5	-8	-7,9	-2,6	-16		-4,5		-14,3	-5,8	-6				-14,7	-13,4			-12,6	-1	-11,5	-5,8	-15,7	-15,7	-12,4		-13	-1,3	-16,1	-17			-1,7		-8,8	-17,3	-17,2	-14,9
	IE	-13,9	-25,5	-13,9	-16,8	-15,4	-1,7	-1,7	-15,7	-16,7	-14,9		-11,1	-13,3	-17,9	-11,8	-15,5	-12,1		-2,1	-11,8		-12,4	-7,3	-1	-11,5		-1,9	-1,9			-12,5		-16,1	-17				-17,3	-22,6	-14,3	-14,9
I	IF	-1,8	-16,5	-13	-11	-14,1	-11,7	-7,9	-15,7	-15,4				-8,2	-5,8	-6	-5,2		-12	-17,5	-12,5			-7,3	-1	-11,5		-15,3	-15,3			-16,8	-14,2	-16,1	-17				-13,5	-14,8	-17,6	-14,9
	IG	-16,2	-18,3	-18,2	-16,4	-16,2	-11,9	-14,1	-15,7	-16	-9,6			-11,8	-14,1	-6		-15,9	-19,3	-11,7	-5,7	-11,2	-14,7	-7,3	-1	-17,6		-11	-12,4	-17,6	-18,7	-11,1	-11,3	-13,8	-17				-16	-7,2	-17,2	-14,9
	hBg	-12,5	-18,2	-12,2	-9,8	-16,2	-9,6	-1,3	-15,7	-12,2		-12		-7,2	-5,8	-6			-11,2	-16,5	-11,2			-7,3	-1	-12,2	-6,7	-6,3	-4,3	-14,2	-13	-1,4	-7,7	-16,1	-17		-9,8			-9	-1,3	-17,2	-14,9
	II	-12,5	-13,1	-12,2	-1,2	-16,2	-8	-7,9	-15,7	-16				-7,2	-5,8	-6				-5				-7,3	-1	-12								-16,1	-17					-11,6		-17,2	-15
	IJ	-15,4	-18,6	-19,6	-18,2	-22,2	-11,9	-13,3	-15,7	-18,5	-13,9		-15,2	-1,9	-9,6	-9,6	-9,6	-1,9	-13,3	-15,5	-9,4	-8,4	-1,8	-7,3	-1	-13	-4,9	-16,9	-9	-11,1		-11,1	-9	-16,1	-17	-8,3			-6,5	-22,8	-4,5	-17,2	-14,9
	J	-15,4	-18,6	-19,6	-18,2	-22,2	-14,4	-17,1	-11,7	-18,2	-13,9		-15,2	-15,4	-9,6	-9,6	-9,6	-1,9	-13,3	-15,5	-9,4	-8,4	-1,8	-7,1	-13,6	-15,6	-4,6	-16,9	-9	-11,2		-11,1	-9	-11,8	-11,8	-11,2			-6,5	-23,1	-14,9	-1,4	
	JB	-21,6	-21	-19,6	-17,7	-24,4	-16,2	-19	-16	-18,3	-13,9	-11,4	-15,2	-15,4	-12,3	-14	-17,4	-16,3	-13,3	-16,7	-11,8	-8,4	-14,1	-6,4	-13,6	-13	-1,5	-16,9	-18	-19,4	-12,4	-11,1	-9	-16,1	-16,1	-11,2			-11,2	-23,1	-19,8	-16,3	
	JD	-17,1	-25,1	-22,5	-16,7	-22,2	-11,9	-13,3	-2,6	-13,1	-13,9	-4,5	-8,4	-14,9	-9,6	-9,6	-9,6	-1,9	-13,1	-14,7	-13,4	-8	-1,8	-6,7	-13,6	-13	-5,8	-16,9	-15,7	-13,4		-13	-1,3	-14,6	-11,5	-8,3		-1,7	-6,5	-23,1	-16,1	-1,4	
	JE	-15,4	-18,6	-19,6	-18,2	-22,2	-11,9	-13,3	-1,4	-16,7	-14,9		-11,1	-1,9	-17,9	-12,9	-15,5	-1,9	-13,1	-2,1	-11,8	-8,4	-12,4	-6,7	-13,6	-13		-16,9	-13,2	-11,1		-12,5	-9	-12,2	-12,2	-8,3			-6,5	-23,1	-22,6	-14,3	
J	JF	-15,4	-18,6	-19,6	-18,2	-22,2	-11,7	-13,3	-1,4	-14,3	-13,9		-8,4	-1,9	-9,6	-9,6	-9,6	-1,8	-12	-17,3	-12,5	-8,4	-1,7	-6,7	-13,9	-13		-16,9	-16,3	-11,1		-16,8	-14,2	-18,5	-12,5	-8,3			-6,5	-23,1	-14,8	-16	
	JG	-16,2	-18,3	-19,6	-16,4	-22,2	-11,9	-14,1	-14,4	-18,2	-13,9		-15,2	-11,8	-14,1	-9,6	-9,6	-1,9	-21,3	-11,7	-9,4	-8,4	-1,8	-7,1	-13,6	-13	-4,6	-16,9	-12,4	-17,6	-18,7	-11,1	-11,3	-11,8	-11,8	-11,2			-6,3	-23,1	-14,9	-15,6	
	JhBg	-15,4	-18,6	-19,6	-18,2	-22,2	-11,9	-13,3	-1,4	-13,1	-13,9	-11,7	-8,4	-1,9	-9,6	-9,6	-9,6	-1,9	-11,2	-11,9	-11,2	-8	-1,8	-7,4	-13,6	-13	-6,7	-16,9	-9,8	-14,4		-1,4	-7,7	-18,5	-12,6	-8,3			-6,5	-23,1	-1,3	-16,7	
	JI	-15,4	-18,6	-19,6	-18,2	-22,2	-14,4	-17,1	-15,7	-18,2	-13,9		-15,2	-15,4	-9,6	-9,6	-9,6	-17,9	-13,3	-15,5	-9,4	-8	-17,9	-7,3	-13,9	-13	-4,6	-16,9	-9,8	-11,1		-11,1	-9	-16,1	-17	-11,2			-6,3	-23,1	-14,9	-16,3	-15
	JJ	-15,4	-18,6	-19,6	-18,2	-22,2	-11,9	-13,3	-1,4	-13,1	-13,9		-15,2	-1,9	-9,6	-9,6	-9,6	-1,9	-13,1	-11,9	-13	-8,4	-1,8	-6,7	-13,9	-13	-4,9	-16,9	-9	-11,1		-11,1	-9	-18,5	-12,6	-8,3		-6,8	-6,5	-23,1	-4,5	-16	-3,7

Table A.5: Overview of miRNAs which bind to 3′ UTRs in LPS-stimulated DCs. Shown are miRNAs, which bind to different 3′ UTRs and their respective hybridization energies (kcal/mol). Dark red: low energy; dark blue: high energy.

	3'-UTR	hsa-let-7a	hsa-let-7b	hsa-let-7c	hsa-let-7d	hsa-let-7e	hsa-let-7f	hsa-let-7g	hsa-let-7i	hsa-miR-103	hsa-miR-132	hsa-miR-142	hsa-miR-146a	hsa-miR-155	hsa-miR-15a	hsa-miR-15b	hsa-miR-16	hsa-miR-181a	hsa-miR-185	hsa-miR-191	hsa-miR-19a	hsa-mir-19b	hsa-miR-20a
	B	-21,6	-18,5	-17,4	-19,7	-19,1	-14,8	-19	-16,5	-13,4		-11,3	-12		-12,3	-14	-17,4	-1,8	-16,9	-11,8			-14,1
	BB	-22,3	-2,9	-21	-2,4	-19,2	-16,2	-19,3	-16	-14,9		-11,4	-12		-12,3	-14	-17,4	-11,9	-16,9	-11,8			-14,1
	BD	-21,6	-25,1	-22,5	-16,7	-17,5	-16,2	-18,2	-2,6	-13,4		-11,3	-12	-14,9	-1,4	-14,4	-17,4	-8,9	-14,7	-12,5			-14,1
	BE	-21,6	-21	-21	-2,4	-19,8	-16,2	-19,3	-16	-16,7	-14,9	-11,4	-12	-13,3	-17,9	-14,4	-16,1	-11,1	-2,1	-11,8			-14,1
B	BF	-21,6	-21	-21	-2,4	-19,2	-16,2	-18,5	-15,7	-13,4		-11,4	-12	-8,2	-12,3	-14	-17,4	-12	-17,5	-12,5			-14,1
	BG	-21,6	-18,5	-18,2	-16,4	-16,2	-11,9	-19	-14,4	-13,4	-9,6	-11,3	-12	-11,8	-12,3	-14	-17,4	-13,3	-11,7	-11,8			-14,1
	BhBg	-21,6	-21	-21	-2,4	-19,8	-16,3	-18,5	-15,7	-14,9		-12	-12	-6,9	-12	-14,1	-16,1	-11,2	-16,9	-12,5			-14,1
	BI	-21,6	-18,5	-17,4	-19,7	-19,1	-14,8	-19	-15,7	-13,4		-11,3	-12	-7,2	-12	-14	-17,4	-8,9	-16,9	-11,8			-14,1
	BJ	-21,6	-18,6	-19,6	-2,4	-22,2	-15,6	-19,3	-17	-13,1	-13,9	-11,3	-12	-1,9	-12,3	-14,4	-17,4	-13,3	-16,9	-12,5	-8,4	-8,4	-14,1
	D	-17,1	-25,1	-22,5	-16,7	-17,5	-8,4	-7,9	-2,6	-21,8		-4,5		-14,2					-15,5	-13,4			
	DB	-21,6	-25,1	-22,5	-19,7	-19,2	-16,2	-19,3	-2,6	-13,4		-11,3	-12	-14,2	-12,3	-14	-17,4	-1,8	-14,7	-11,8			-14,1
	DD	-17,1	-25,1	-22,5	-16,7	-17,5	-9,5	-9,4	-2,6	-21,8		-4,5		-14,2					-14,7	-13,4			
	DE	-17,1	-25,1	-22,5	-16,7	-17,2	-11	-11	-2,6	-16,7	-14,9		-11,1	-14,2	-17,9	-11,8	-15,5		-2,1	-11,8			-12,4
D	DF	-17,1	-25,1	-22,5	-16,7	-17,5	-11,7	-9,4	-2,6	-21,8		-4,5		-14,2			-5,2	-12	-17,5	-13,4			
	DG	-16,2	-25,1	-22,5	-16,4	-17,5	-11,9	-14,1	-2,6	-21,8	-9,6	-4,5		-14,2	-14,1			-17,3	-14,7	-13,4			-14,7
	DhBg	-17,1	-25,1	-22,5	-16,7	-17,5	-9,6	-1,3	-2,6	-21,8		-9,3		-14,2		-4,6		-11,2	-14,7	-1			-1,9
	DI	-17,1	-25,1	-22,5	-16,7	-17,5	-8,4	-7,9	-2,6	-21,8		-4,5		-14,2	-5,8	-6			-15,5	-13,4			
	DJ	-17,1	-25,1	-19,6	-16,7	-22,2	-11,9	-13,3	-2,6	-18,5	-13,9	-4,5	-15,2	-14,2	-9,6	-9,6	-9,6	-13,3	-14,7	-13,4	-8,4	-8,4	-1,8
	E	-13,9	-13,9	-13,9	-14,1	-14,8	-11	-11	-1,4	-16,7	-14,9		-11,1	-14,1	-17,9	-12,9	-13,4		-2,1	-11,8			-12,4
	EB	-21,6	-21	-18,3	-17,7	-19,2	-16,2	-19,3	-16	-16,7	-14,9	-11,3	-11,1	-14,1	-17,9	-14	-17,4	-1,8	-2,1	-11,8			-14,1
	ED	-17,1	-25,1	-22,5	-16,7	-17,5	-11	-11	-2,6	-16,7	-14,9	-4,5	-11,1	-13,3	-17,9	-12,9	-13,4		-2,1	-11,8			-12,4
	EE	-13,9	-13,9	-13,9	-14,1	-14,5	-11	-11	-1,4	-16,7	-14,9		-11,1	-13,3	-17,9	-12,9	-15,5		-2,1	-11,8			-12,4
E	EF	-13,9	-16,5	-13,9	-14,1	-14,5	-11	-11	-1,4	-16,7	-14,9		-11,1	-13,3	-17,9	-12,9	-15,5	-12	-17,5	-11,8			-12,4
	EG	-16,2	-18,3	-18,2	-16,4	-16,2	-11,9	-14,1	-14,4	-16,7	-14,6		-11,1	-13,3	-17,9	-12,9	-13,4	-17,3	-2,1	-11,8		-11,2	-12,4
	EhBg	-13,9	-13,9	-13,9	-14,1	-14,5	-11	-11	-1,4	-16,7	-14,9	-12	-11,1	-13,3	-17,9	-12,1	-15,5	-11,2	-2,1	-11,8			-12,4
	EI	-13,9	-13,9	-13,9	-14,1	-14,8	-11	-11	-15,7	-16,7	-15		-11,1	-13,6	-17,9	-12,9	-15,5		-2,1	-11,8			-12,4
	EJ	-15,4	-18,6	-19,6	-18,2	-22,2	-11,9	-13,3	-1,4	-16,7	-14,9		-11,1	-13,3	-17,9	-12,9	-15,5	-13,3	-2,1	-11,8	-8,4	-8,4	-12,4
	F	-1,8	-16,5	-13	-11	-9,5	-11,7			-16,8				-8,2			-5,2	-12	-17,5	-12,5			
	FB	-21,6	-21	-18,3	-17,7	-19,8	-16,2	-19	-16	-13,4		-11,3	-12	-8,2	-12,3	-14	-17,4	-12	-17,5	-11,8			-14,1
	FD	-17,1	-25,1	-22,5	-16,7	-17,5	-1,9	-9,4	-2,6	-16,8		-4,5		-14,3			-5,2	-12	-17,5	-12,5			
	FE	-13,9	-19,2	-13,5	-14,1	-14,5	-11,7	-11	-1,4	-16,7	-14,9		-11,1	-13,3	-17,9	-11,8	-15,5	-12	-17,5	-11,8			-12
F	FF	-1,8	-16,5	-13	-11	-11,8	-11,7			-16,8				-8,2			-5,2	-12	-17,5	-1,5			
	FG	-16,2	-18,3	-18,2	-16,4	-16,2	-11,9	-14,1	-14,4	-16,8	-9,6			-11,8	-14,1		-5,2	-21,3	-17,5	-12,5		-11,2	-15,1
	FhBg	-1,8	-16,5	-13	-9,8	-12,1	-11,7	-1,3	-1,3	-16,8		-9,3		-8,2		-4,6	-5,2	-12	-17,3	-12,5			-1,9
	FI	-12,5	-16,5	-13	-11	-16,2	-11,7	-7,9	-15,7	-16,8				-8,2	-5,8	-6	-5,2	-12	-17,5	-12,5			
	FJ	-15,4	-18,6	-19,6	-18,2	-22,2	-11,9	-13,3	-1,4	-18,5	-13,9		-15,2	-1,9	-9,6	-9,6	-9,6	-12	-17,5	-12,5	-8,4	-8,4	-1,8
	G	-16,2	-18,3	-18,2	-16,4	-16,2	-11,9	-14,1	-14,4	-9,2	-9,6			-11,8	-14,1			-17	-11,7				-7,7
	GB	-21,6	-21	-18,2	-16,4	-16,2	-16,2	-19,3	-14,4	-17,8	-9,6	-11,3	-12	-11,8	-12,3	-14	-17,4	-17	-16,9	-11,8			-14,1
	GD	-16,2	-25,1	-22,5	-17,5	-17,5	-11,9	-14,4	-2,6	-14,5	-9,6	-4,5		-14,3	-14,4			-17	-14,7	-13,4			-7,7
	GE	-16,2	-18,6	-18,2	-17,5	-16,9	-11,9	-14,4	-14,4	-16,7	-14,9		-11,1	-11,8	-17,9	-11,8	-15,5	-17	-2,1	-11,8			-12,4
G	GF	-16,2	-18,6	-18,2	-17,5	-16,9	-11,9	-14,4	-14,4	-14,6	-9,6			-11,8	-14,4		-5,2	-17	-17,5	-12,5			-7,7
	GG	-16,2	-18,6	-18,2	-16,4	-16,2	-12,2	-14,4	-14,4	-9,2	-9,6			-11,8	-14,1			-2,5	-11,7				-16,5
	GhBg	-16,2	-18,6	-18,2	-16,4	-16,2	-12,2	-14,4	-14,4	-9,3	-9,6	-12		-11,8	-14,4	-4,8		-17	-11,7	-11,2			-7,7
	GI	-16,2	-18,6	-18,2	-17,5	-16,2	-12,2	-14,4	-15,7	-12,2	-9,6			-11,8	-14,1	-6		-17	-11,7	-5			-7,7
	GJ	-16,2	-18,6	-19,6	-16,4	-22,2	-12,2	-12,4	-12,6	-18,5	-13,9		-15,2	-11,8	-14,4	-13,2	-9,6	-17	-1,9	-13	-8,4	-8,4	-1,8
	hBg	-9,3	-9,3	-9,3	-9,5	-12,3	-9,3	-1	-11	-16,6		-9,3		-6,1		-4,6		-11,4	-6,7	-12,8			-1,9
	hBgB	-21,6	-21	-2,3	-19,7	-19,2	-16,2	-19	-16,5	-13,4		-11,3	-11,3	-7	-12,3	-14	-17,4	-11,2	-16,9	-11,8			-14,1
	hBgD	-17,1	-25,1	-22,5	-16,7	-17,5	-1,8	-1,1	-2,6	-21,4		-12		-14,9	-4,8	-4,8		-11,1	-14,6	-13,1			-1,8
	hBgE	-13,9	-13,5	-13,5	-14,1	-14,5	-11	-12	-1,4	-17	-14,9	-12	-11,1	-13,3	-17,9	-11,8	-15,5	-11,2	-2,1	-11,8			-12,4
hBg	hBgF	-1,8	-16,5	-13	-13,6	-1,9	-11,7	-8,4	-11	-13,7		-9,3		-8,2	-4,8	-5,8	-7,1	-12	-17,5	-12,5			-1,8
	hBgG	-16,2	-18,3	-18,2	-16,4	-16,2	-11,9	-14,1	-14,4	-16,6	-9,6	-9,3		-11,8	-14,1	-7,1		-17	-11,7	-12,8		-11,2	-11,5
	hBghBg	-9,3	-9,3	-9,3	-13,3	-12,3	-9,3	-1	-11	-16,6		-9,3		-1,7	-4,5	-6,9		-11,4	-17,2	-12,8			-1,9
	hBgI	-12,5	-15,2	-12,4	-13,3	-16,2	-1,1	-8,4	-15,7	-17,5		-9,3		-11	-4,8	-5,8		-11,4	-6,7	-12,4			-11,7
	hBgJ	-15,4	-18,6	-19,6	-18,2	-22,2	-11,9	-13,3	-1,4	-13,1	-13,9	-9,3	-8,4	-1,9	-15	-13,2	-9,6	-8,5	-11,9	-11,2	-8,4	-8,4	-1,8
	I	-12,5	-18,2	-12,2	-1,2	-16,2	-8	-7,9	-15,7	-16				-7,2	-5,8	-6				-5			
	IB	-21,6	-21	-18,3	-17,7	-19,2	-14,8	-19,3	-15,7	-13,4		-11,3	-12	-7,2	-12,3	-14	-17,4	-1,8	-16,9	-11,8			-14,1
	ID	-17,1	-25,1	-22,5	-16,5	-17,5	-8	-7,9	-2,6	-16		-4,5		-14,3	-5,8	-6			-14,7	-13,4			
	IE	-13,9	-25,5	-13,9	-16,8	-15,4	-1,7	-1,7	-15,7	-16,7	-14,9		-11,1	-13,3	-17,9	-11,8	-15,5		-2,1	-11,8			-12,4
I	IF	-1,8	-16,5	-13	-11	-14,1	-11,7	-7,9	-15,7	-15,4				-8,2	-5,8	-6	-5,2	-12	-17,5	-12,5			
	IG	-16,2	-18,3	-18,2	-16,4	-16,2	-11,9	-14,1	-15,7	-16	-9,6			-11,8	-14,1	-6		-19,3	-11,7	-5,7		-11,2	-14,7
	IhBg	-12,5	-18,2	-12,2	-9,8	-16,2	-9,6	-1,3	-15,7	-12,2		-12		-7,2	-5,8	-6		-11,2	-16,5	-11,2			
	II	-12,5	-13,1	-12,2	-1,2	-16,2	-8	-7,9	-15,7	-16				-7,2	-5,8	-6				-5			
	IJ	-15,4	-18,6	-19,6	-18,2	-22,2	-11,9	-13,3	-15,7	-18,5	-13,9		-15,2	-1,9	-9,6	-9,6	-9,6	-13,3	-15,5	-9,4	-8,4	-8,4	-1,8
	J	-15,4	-18,6	-19,6	-18,2	-22,2	-14,4	-17,1	-11,7	-18,2	-13,9		-15,2	-15,4	-9,6	-9,6	-9,6	-13,3	-15,5	-9,4	-8,4	-8,4	-1,8
	JB	-21,6	-21	-19,6	-17,7	-24,4	-16,2	-19	-16	-18,3	-13,9	-11,4	-15,2	-15,4	-12,3	-14	-17,4	-13,3	-16,7	-11,8	-8,4	-8,4	-14,1
	JD	-17,1	-25,1	-22,5	-16,7	-22,2	-11,9	-13,3	-2,6	-13,1	-13,9	-4,5	-8,4	-14,9	-9,6	-9,6	-9,6	-13,1	-14,7	-13,4	-8	-8	-1,8
	JE	-15,4	-18,6	-19,6	-18,2	-22,2	-11,9	-13,3	-1,4	-16,7	-14,9		-11,1	-1,9	-17,9	-12,9	-15,5	-13,1	-2,1	-11,8	-8,4	-7,7	-12,4
J	JF	-15,4	-18,6	-19,6	-18,2	-22,2	-11,7	-13,3	-1,4	-14,3	-13,9		-8,4	-1,9	-9,6	-9,6	-9,6	-12	-17,3	-12,5	-8,4	-8,4	-1,7
	JG	-16,2	-18,3	-19,6	-16,4	-22,2	-11,9	-14,1	-14,4	-18,2	-13,9		-15,2	-11,8	-14,1	-9,6	-9,6	-21,3	-11,7	-9,4	-8,4	-8,4	-1,8
	JhBg	-15,4	-18,6	-19,6	-18,2	-22,2	-11,9	-13,3	-1,4	-13,1	-13,9	-11,7	-8,4	-1,9	-9,6	-9,6	-9,6	-11,2	-11,9	-11,2	-8	-8,4	-1,8
	JI	-15,4	-18,6	-19,6	-18,2	-22,2	-14,4	-17,1	-15,7	-18,2	-13,9		-15,2	-15,4	-9,6	-9,6	-9,6	-13,3	-15,5	-9,4	-8	-8	-17,9
	JJ	-15,4	-18,6	-19,6	-18,2	-22,2	-11,9	-13,3	-1,4	-13,1	-13,9		-15,2	-1,9	-9,6	-9,6	-9,6	-13,1	-11,9	-13	-8,4	-8,4	-1,8

	3'-UTR	hsa-miR-21	hsa-miR-22	hsa-miR-221	hsa-miR-222	hsa-miR-223	hsa-miR-23a	hsa-miR-23b	hsa-miR-24	hsa-miR-25	hsa-miR-26a	hsa-miR-26b	hsa-miR-27a	hsa-miR-27b	hsa-miR-29a	hsa-miR-30c	hsa-miR-30d	hsa-miR-30e	hsa-miR-320	hsa-miR-342-3p	hsa-miR-342-5p	hsa-miR-34a	hsa-miR-423-3p	hsa-miR-423-5p	hsa-miR-92a	hsa-miR-93	hsa-miR-99b
	B		-11,8	-13,5		-1,5	-16,8	-18	-18,6	-9,1			-16,1	-16,1					-15	-11,2	-6,7	-21,4	-22,8	-24,4	-8,7	-14,1	
	BB		-11,8	-13,5		-1,5	-16,8	-18	-2,3	-12,4			-16,1	-16,1					-15	-13,3	-6,8	-19,7	-22,8	-24,4	-8,7	-16,3	
	BD	-5,1	-7,7	-13,5	-16	-1,5	-16,8	-18	-17,8	-9,1	-13	-1,3	-14,8	-15,5			-1,7	-11,7	-16,6	-11,9	-8,9	-19,7	-22,8	-26,5	-8,7	-16,3	
	BE		-1,3	-13,5	-13,5	-1,5	-16,8	-18	-2,3	-12,4	-12,5		-14,8	-15,5				-5,5	-15	-11,9	-17,3	-22,6	-22,8	-24,4	-8,7	-16,3	
B	BF		-11,8	-13,5	-7,5	-1,5	-15,3	-15,3	-18,6	-13,6	-16,8	-14,2	-16,1	-15,5					-15	-15	-13,5	-19	-22,8	-24,4	-8,7	-16,3	
	BG		-11,8	-13,8	-8,6	-1,5	-16,8	-18	-18,6	-18,7	-11,1	-11,3	-16,1	-15,5					-22,4	-14,4	-16	-19,8	-22,8	-24,1	-17,9	-14,1	
	BhBg			-13,5		-1,5	-16,8	-18	-19,5	-14	-1,4	-7,7	-14,8	-15,5	-8,6				-15,4	-11,9	-9,7	-19	-22,8	-24,4	-8,7	-16,3	
	BI	-7,3	-1	-12		-1,5	-16,6	-17,2	-18,6	-9,1			-16,1	-17					-21,6	-11,9	-6,7	-19,8	-22,8	-24,1	-15,2	-14,1	-15
	BJ	-7,1	-13,6	-13	-13,6	-1,5	-16,8	-18	-18,6	-9,1	-11,1	-9	-14,8	-15,5	-8,3		-6,8		-2	-11,9	-22,8	-21,4	-22,8	-22,8	-8,7	-16,3	-3,7
	D	-5,1	-7,7		-13	-3,7	-15,7	-15,7	-17,4		-13	-1,3	-14,6	-11,5					-16,6		-8,9	-17,3		-26,5			
	DB	-5,1	-7,7	-13,5	-13	-1,5	-15,7	-18	-19,4	-12,4	-13	-1,3	-16,1	-16,1					-18,9	-11,2	-8,9	-19,8	-22,8	-25,4	-8,7	-16,3	
	DD	-5,1	-7,7		-16,4	-3,7	-15,7	-15,7	-17,4		-13	-1,3	-14,6	-11,5			-1	-1	-16,6		-8,9	-16,1		-25,4			
	DE	-5,1	-8,3	-11,1	-13	-5,8	-15,7	-15,7	-17,4		-12,5	-1,3	-12,2	-12,2					-19,8		-17,3	-22,6	-15,2	-26,5		-14,3	
D	DF	-5,1	-7,7	-7,6	-13	-5,8	-15,1	-15,1	-17,4		-16,8	-14,2	-14,6	-11,5					-16,6		-13,5	-15,4		-26,5		-13	
	DG	-5,1	-6,7	-13,8	-16,9	-8,3	-15,7	-15,7	-17,4	-18,7	-13	-11,3	-14,6	-11,5					-22,4		-16	-17,3	-2,3	-26,5	-17,9	-11,7	
	DhBg	-5,1	-7,7	-3,1	-13	-5,8	-15,7	-15,7	-17,4		-13	-7,7	-14,6	-11,5		-9,8			-16,5		-8,9	-16,1	-21,9	-26,3			
	DI	-7,3	-1	-12	-13	-3,7	-15,7	-15,7	-17,4		-13	-1,3	-16,1	-17					-21,6		-8,9	-17,3		-26,5	-15,2	-17,2	-15
	DJ	-7,1	-7,7	-13	-13	-3,7	-16,9	-15,7	-17,4		-13	-1,3	-14,6	-11,5	-8,3		-6,8		-16,6	-6,5	-22,8	-17,3	-21,9	-25,4		-1,4	-3,7
	E			-13,5	-13,5		-13	-13			-12,5		-12,2	-12,2					-7,8		-17,3	-22,6	-12,1	-18,8		-14,3	
	EB		-11,8	-13,5	-14,2	-1,5	-13	-13	-19,4	-12,4	-12,5		-16,1	-16,1					-15	-11,2	-17,3	-22,6	-22,8	-24,4		-14,1	
	ED	-5,1	-8,3	-13,5	-16,4	-5,8	-13	-13	-13,4		-12,5	-1,3	-14,6	-11,5			-1,7	-1	-16,6		-17,3	-22,6	-12,1	-25,4		-14,3	
	EE			-13,5	-13,5		-13	-13			-12,5		-12,2	-12,2					-15		-17,3	-22,6	-12,1	-19,5		-14,3	
E	EF			-11,1	-14,1		-15,1	-15,1			-16,8	-14,2	-12,2	-12,2				-5,5	-13,2		-17,3	-22,6	-12,1	-24,4		-14,3	
	EG			-17,6	-8,6		-13	-13	-17,6	-18,7	-12,5	-11,3	-12,2	-12,2				-5,5	-22,4		-17,3	-22,6	-2,3	-24,1	-17,9	-14,3	
	EhBg			-11,1	-13,5	-6,7	-13	-13	-14,4		-12,5	-7,7	-12,2	-12,2					-15,4		-17,3	-22,6	-16,3	-21,5		-14,3	
	EI	-7,3	-1	-12	-13,5		-13	-13			-12,5		-16,1	-17				-5,5	-21,6		-17,3	-22,6	-12,1	-19,5	-15,2	-14,3	-15
	EJ	-7,1	-13,6	-13	-13,5	-4,9	-16,9	-13	-11,1		-12,5	-9	-18,5	-12,2	-8,3		-6,8		-2	-6,5	-17,3	-22,6	-21,9	-22,8		-14,3	-3,7
	F							-7,2			-16,8	-14,2	-8,3	-12,8					-11,5		-13,5	-14,8		-24,4		-13	
	FB		-11,8	-13,5		-1,5	-16,8	-18	-19,4	-12,4	-16,8	-14,2	-16,1	-16,1					-15	-11,2	-13,5	-19,3	-22,8	-24,4	-8,7	-14,1	
	FD	-5,1	-8,3		-15	-5,8	-15,7	-15,7	-17,4		-13	-1,3	-14,6	-11,5			-1,7	-11,7	-16,6		-12,8	-16,1		-26,5		-13	
	FE			-11,1	-14,2		-13,2	-13,2			-12,5	-14,2	-12,2	-12,2					-12,4		-17,9	-22,6	-12,4	-24,4		-14,3	
F	FF				-7,5		-16,3	-16,3			-16,8	-14,2	-8,3	-12,8					-12,4		-13,5	-14,8		-24,4		-13	
	FG			-1,2	-8,6		-11	-12,4	-17,6	-18,7	-11,1	-11,3	-11,8	-12,8					-22,4		-16	-14,8	-2,3	-24,1	-17,9	-14,1	
	FhBg			-3,1		-6,7	-3,7	-7,2	-14,4		-16,8	-7,7	-8,3	-12,8					-12,4		-12,8	-14,8	-19,2	-24,4		-13	
	FI	-7,3	-1	-12			-13,2	-7,2			-16,8	-14,2	-16,1	-17					-21,6		-12,8	-17,2		-24,4	-15,2	-17,2	-15
	FJ	-7,1	-13,6	-13	-13,6	-4,9	-16,9	-9	-11,1		-16,8	-14,2	-18,5	-12,8	-8,3				-2	-6,5	-22,8	-16,8	-21,9	-24,4		-1,4	-3,7
	G			-1,2	-8,6		-11	-12,4	-17,6	-18,7	-11,1	-11,3	-11,8	-11,8					-22,4		-16	-7,2	-2,3	-24,1	-17,9	-7,7	
	GB		-11,8	-13,8	-8,6	-1,5	-16,8	-18	-19,4	-18,7	-11,1	-11,3	-16,1	-16,1					-22,4	-11,2	-16	-14,9	-22,8	-24,1	-17,9	-14,1	
	GD	-5,1	-7,7	-1,2	-16,1	-3,7	-11	-12,4	-18,2	-18,5	-13	-11,3	-14,6	-11,5			-1,2	-1,2	-22,4		-16	-17,3	-2,4	-25,4	-17,9	-7,7	
	GE			-1,2	-7,9		-13,2	-13,2	-17,6	-18,5	-11,1	-11,3	-12,2	-12,2					-22,4		-2,5	-22,6	-2,4	-24,1	-17,9	-14,3	
G	GF			-1,2	-7,9		-12,2	-12,4	-17,6	-18,7	-16,8	-11,3	-12,1	-12,8					-22,4		-16	-14,8	-2,4	-24,1	-17,9	-14,4	
	GG			-17,5	-8,6		-11	-12,4	-17,6	-18,7	-11,1	-11,3	-11,8	-11,8					-22,4		-16	-7,2	-2,3	-24,1	-17,9	-16,9	
	GhBg			-1,2	-7,9	-6,7	-11	-12,4	-14,4	-18,7	-11,1	-11,3	-12,1	-12,1					-22,4		-16	-1,3	-2,3	-24,1	-17,9	-7,7	
	GI	-7,3	-1	-12	-8,6		-11	-12,4	-17,6	-18,7	-11,1	-11,3	-16,1	-17					-22,4		-16	-7,2	-2,4	-24,1	-17,9	-17,2	-15
	GJ	-7,1	-13,6	-13	-7,9	-4,9	-16,9	-12,4	-11,1	-18,7	-11,1	-11,3	-18,5	-16,3	-8,3		-6,8		-22,4	-6,5	-16	-7,2	-21,9	-22,8	-14,1	-1,4	-3,7
	hBg					-6,7	-3,7	-4,3	-12,1		-13	-8,2	-8,4	-8,4		-9,8			-12,1		-9,7	-1,3	-21,9	-18,7			
	hBgB		-11,8	-13,5		-1,5	-16,8	-18	-19,4	-12,4	-13	-7,7	-16,1	-16,1		-9,8			-15	-11,2	-9,7	-21,4	-21,9	-24,4	-8,7	-16,3	
	hBgD	-5,1	-7,7	-2,9	-13	-3,7	-15,7	-15,7	-17,4		-13	-1,3	-14,6	-11,5		-9,8	-9,8	-9,8	-16,6		-8,9	-16,1	-21,9	-26,5			
	hBgE			-8,1	-14,2	-7,1	-11	-11	-14,4	-7,1	-12,5	-7,7	-12,2	-12,2		-9,8		-5,5	-15,4		-17,9	-22,6	-13,7	-21,5		-14,3	
hBg	hBgF	-3,7		-7,3	-7,2	-7	-11,7	-11,7	-14,4	-7,1	-16,7	-14,1	-8,3	-8,3		-9,8			-15,5		-12,8	-14,8	-13,7	-24,1		-1,7	
	hBgG	-9		-1,2	-16,9	-6,6	-11	-12,4	-14,4	-18,7	-13	-11,3	-11,8	-11,8		-9,8			-22,4		-16	-11,5	-21,9	-24,1	-17,9	-14,9	
	hBghBg	-9,4		-3,1		-7	-6,4	-6,4	-14,4	-7,1	-13	-8,2	-8,4	-8,4		-9,8			-12,1		-9,7	-11,5	-21,9	-18,7			
	hBgI	-9,4	-1	-11,5		-6,6	-3,7	-4,3	-12,1	-7,1	-13	-8,2	-16,1	-17		-9,8			-21,6		-9,7	-11,5	-21,9	-18,7	-15,2	-17,2	-15
	hBgJ	-7,1	-13,6	-13	-13,6	-6,7	-16,9	-9	-11,1	-7,1	-15,5	-8,2	-18,2	-16	-8,3	-9,8	-6,8		-13,9	-6,5	-22,8	-15	-21,9	-22,8		-1,4	-3,7
	I	-7,3	-1	-12									-13,8	-17					-21,6		-1,7			-15	-15,2	-17,2	-15
	IB	-7,3	-1	-12		-1,5	-16,8	-18	-19,4	-12,4			-16,1	-16,1					-21,6	-11,2	-6,8	-19,8	-22,8	-24,4	-15,2	-14,1	-14,9
	ID	-12,6	-1	-11,5	-16	-5,8	-15,7	-15,7	-12,4		-13	-1,3	-16,1	-17			-1,7	-11,7	-21,6		-8,8	-17,3		-26,5	-15,2	-17,2	-14,9
	IE	-7,3	-1	-11,5	-13,5		-1,9	-1,9			-12,5		-16,1	-17					-21,6		-17,3	-22,6	-12,4	-19,5	-15,2	-14,3	-14,9
I	IF	-7,3	-1	-11,5	-7,5		-15,3	-15,3			-16,8	-14,2	-16,1	-17					-21,6		-13,5	-14,8		-24,4	-15,2	-17,6	-14,9
	IG	-7,3	-1	-17,6	-8,6		-11	-12,4	-17,6	-18,7	-11,1	-11,3	-13,8	-17					-22,4		-16	-7,2	-2,3	-24,1	-17,9	-17,2	-14,9
	IhBg	-7,3	-1	-12,2		-6,7	-6,3	-4,3	-14,2	-13	-1,4	-7,7	-16,1	-17		-9,8			-21,6		-9	-1,3	-19,2	-23,9	-15,2	-17,2	-14,9
	II	-7,3	-1	-12									-16,1	-17					-21,6		-11,6			-15	-15,2	-17,2	-15
	IJ	-7,3	-1	-13	-13,6	-4,9	-16,9	-9	-11,1		-11,1	-9	-16,1	-17	-8,3				-21,6	-6,5	-22,8	-4,5	-21,9	-22,8	-15,2	-17,2	-14,9
	J	-7,1	-13,6	-15,6	-13,3	-4,6	-16,9	-9	-11,2		-11,1	-9	-11,8	-11,8	-11,2				-2	-6,5	-23,1	-14,9	-16,2	-2,6		-1,4	
	JB	-6,4	-13,6	-13	-13,3	-1,5	-16,9	-18	-19,4	-12,4	-11,1	-9	-16,1	-16,1	-11,2				-2	-11,2	-23,1	-19,8	-22,8	-24,4	-8,7	-16,3	
	JD	-6,7	-13,6	-13	-15	-5,8	-16,9	-15,7	-13,4		-13	-1,3	-14,6	-11,5	-8,3		-1,7	-11,7	-16,6	-6,5	-23,1	-16,1	-2,3	-25,4		-1,4	
	JE	-6,7	-13,6	-13	-14,2		-16,9	-13,2	-11,1		-12,5	-9	-12,2	-12,2	-8,3				-15,1	-6,5	-23,1	-22,6	-2,3	-22,8		-14,3	
J	JF	-6,7	-13,9	-13	-16,6		-16,9	-16,3	-11,1		-16,8	-14,2	-18,5	-12,5	-8,3				-15,1	-6,5	-23,1	-14,8	-2,3	-24,4		-16	
	JG	-7,1	-13,6	-13	-8,6	-4,6	-16,9	-12,4	-17,6	-18,7	-11,1	-11,3	-11,8	-11,8	-11,2				-22,4	-6,3	-23,1	-14,9	-16,2	-24,1	-17,9	-15,6	
	JhBg	-7,4	-13,6	-13	-16,6	-6,7	-16,9	-9,8	-14,4		-1,4	-7,7	-18,5	-12,6	-8,3				-15,1	-6,5	-23,1	-1,3	-19,2	-22,8		-16,7	
	JI	-7,3	-13,9	-13	-13,3	-4,6	-16,9	-9,8	-11,1		-11,1	-9	-16,1	-17	-11,2				-21,6	-6,5	-23,1	-14,9	-16,2	-22,8	-15,2	-16,3	-15
	JJ	-6,7	-13,9	-13	-16,6	-4,9	-16,9	-9	-11,1		-11,1	-9	-18,5	-12,6	-8,3		-6,8		-15,1	-6,5	-23,1	-4,5	-21,9	-22,8		-16	-3,7

Table A.6: Analysis of miRNA-binding in unstimulated DCs. Each 3′ UTR as single or as pair-wise combination was compared to each other 3′ UTR regarding hybridization energy (kcal/mol) and RNA-stability via One-way ANOVA (Tukey post test; ***: p<0.001, **: p<0.01, *: p<0.05, ns: not significant wit p> 0.05).

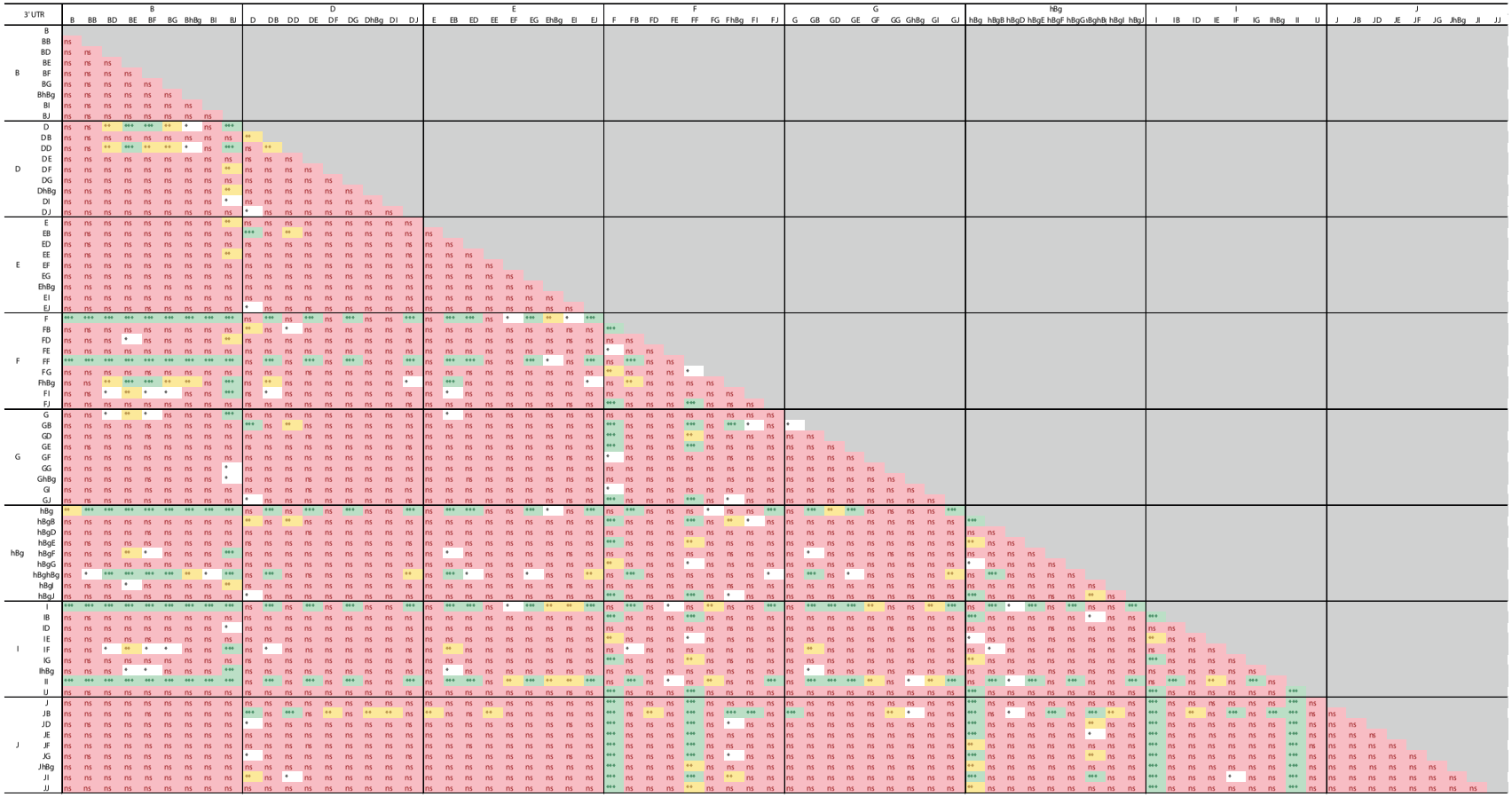

Table A.7: Analysis of miRNA-binding in LPS-stimulated DCs. Each 3′ UTR as single or as pair-wise combination was compared to each other 3′ UTR regarding hybridization energy (kcal/mol) and RNA-stability via One-way ANOVA (Tukey post test; ***: p<0.001, **: p<0.01, *: p<0.05, ns: not significant wit p> 0.05).

Danksagung

Posters

A.G. Orlandini von Niessen, S. Burghardt, N. Piganeau, Application of vitamin-binding nucleic acids as sensors for food analytics, *2. Treffen der Norddeutschen Biophysiker, Borstel, Germany* **2009.**

A.G. Orlandini von Niessen, B. Vallazza, A.N. Kuhn, Ö. Türeci, U. Sahin, Optimisation of RNA vaccines using 3′ UTR-sequences selected for stabilisation of RNA, *BSI Summerschool, UK* **2011.**

A.G. Orlandini von Niessen, A.N. Kuhn, V. Boisguérin, B. Vallazza, M. Löwer, T. Bukur, J. de Graaf, J. Castle, Ö. Türeci, U. Sahin, Investigation of mRNA stability by transcriptome profiling of Actinomycin D treated human immature dendritic cells via Next-Generation-Sequencing, *1st TRON Postersession, Mainz, Germany* **2011**.

A.G. Orlandini von Niessen, A.N. Kuhn, V. Boisguérin, U. Sahin, Development of a Selection Process within human immature Dendritic Cells to find naturally occurring RNA elements, which stabilize RNA for Improvement of RNA-based Cancer Vaccines, *2nd TRON Postersession, Mainz, Germany* **2012**.

Oral presentations

A.G. Orlandini von Niessen, S. Burghardt, N. Piganeau, Application of vitamin-binding nucleic acids as sensors for food analytics, *2. Treffen der Norddeutschen Biophysiker, Borstel, Germany* **2009**.

A.G. Orlandini von Niessen, A.N. Kuhn, V. Boisguérin, U. Sahin, Characterization of naturally occurring stabilizing 3′ UTRs selected via a newly-developed in vivo selection process in hiDCs for improvement of RNA-based cancer vaccines., *1st TRON Retreat, Mainz, Germany* **2013**.

A.G. Orlandini von Niessen, A.N. Kuhn, V. Bukur, L.M. Kranz, U. Sahin, Improvement of mRNA therapeutics by selecting 3′-untranslated regions for cell type-specific mRNA stabilization., *5th TRON Retreat, Mainz, Germany* **2016**.

Patent

A.G. Orlandini von Niessen, S. Fesser, B. Vallazza, T. Beissert, M. Poleganov, A.N. Kuhn, U. Sahin, 3′ UTR Sequences for Stabilization of RNA., *Registration number: PCT/EP2015/073180* **2015**.

Publication

A.G. Orlandini von Niessen, A.N. Kuhn, V. Bukur, L.M. Kranz, S. Fesser, K.C. Reuter, M. Löwer, B. Vallazza, T. Beissert, P. Simon, J. de Graaf, Ö. Türeci, U. Sahin, Improvement of mRNA therapeutics by selecting 3′-untranslated regions for cell type-specific mRNA stabilization, *manuscript in preparation*.

Graphic contribution to other publications

J.O. Orlandini, J.N. Schaper, J.H. Petersen, N.H. Bings, Development and characterization of a thermal inkjet-based aerosol generator for micro-volume sample introduction in analytical atomic spectrometry, *J. Anal. Atom. Spectrom.* **2011**, *26*, 1781-1789.

J.O. Orlandini, J.H. Petersen, J.N. Schaper, N.H. Bings, Comparison of novel and conventional calibration techniques for the analysis of urine samples using plasma source mass spectrometry combined with a new dual-drop-on-demand aerosol generator, *J. Anal. Atom. Spectrom.* **2012**, *26*, 1781-1789.

A.G. Orlandini, J.O. Orlandini, Cover Invite, *J. Anal. Atom. Spectrom.* **2012**, *27*, 1160-1160.

J. Diekmann, M. Löwer, J.C. Castle, S. Kreiter, Ö. Türeci, U. Sahin, The T Cell Druggable Genome, *European Pharmaceutical Review* **2012**, *17*

S. Kreiter, M. Vormehr, N. van de Roemer, M. Diken, M. Löwer, J. Diekmann, S. Boegel, B. Schrörs, F. Vascotto, J.C. Castle, A.D. Tadmor, S.P. Schoenberger, C. Huber, Ö. Türeci, U. Sahin, Mutant MHC class II epitopes drive therapeutic immune responses to cancer, *Nature* **2015**, *520*, 692-696.

Eidesstattliche Erklärung

Ich versichere, dass ich die von mir vorgelegte Dissertation selbstständig angefertig, die benutzten Quellen und Hilfsmittel angegeben und die Stellen der Arbeit, einschließlich der Tabellen und Abbildungen, die anderen Werken im Wortlaut oder dem Sinn nach entnommen sind, in jedem Einzelfall als Entlehnung kenntlich gemacht habe; dass ich diese Dissertation noch keiner anderen Fakultät oder Universität zur Prüfung vorgelegt habe; dass sie, abgesehen von angegebener Teilpublikation, noch nicht veröffentlicht worden ist, sowie, dass ich eine solche Veröffentlichung vor Abschluss des Promotionsverfahrens nicht vornehmen werde. Die Bestimmungen der Promotionsordnung der Fachbereiche 17-22 der Johannes Gutenberg-Universität Mainz in der Fassung vom 28. September 2004 sind mir bekannt.

Mainz, September 5, 2016

Alexandra Orlandini von Niessen

Curriculum vitae - Alexandra Orlandini von Niessen